Zeitschrift: IABSE reports = Rapports AIPC = IVBH Berichte
Band: 79 (1998)

Rubrik: Working session: Case studies of bridges. Papers and posters

Working Session

Case Studies of Bridges

Papers and Posters

Leere Seite
Blank page
Page vide

Study on Wind Resistant Design of Super Long-Span Bridges

Hiroshi SATO
Head, Structure Div.
Public Work Research Inst.
Tsukuba, Japan

Nobuaki FURUYA
Mgr, First Design Div.
Honshu-Shikoku Bridge Authority
Kobe, Japan

Katsuya OGIHARA
Senior Research Eng.
Public Work Research Inst.
Tsukuba, Japan

Ryuichi TORIUMI
Dep. Mgr, First Design Div.
Honshu-Shikoku Bridge Authority
Kobe, Japan

Summary

Wind Resistance is one of the most important themes in the design of super long-span bridges. To improve their wind resistance, a series of wind tunnel studies and analytical studies were conducted. According to the test results and analytical results, it was found that slot at the center of girder and cross hangers were effective to improve the aerodynamic stability. By reviewing the wind tunnel studies for the Akashi Kaikyo Bridge conducted at the Large Boundary Layer Wind Tunnel, wind resistant design methods for super long-span bridges are discussed and proposed.

1. Introduction

The Akashi Kaikyo Bridge has the world-longest span length of 1990m. In the world and in Japan, there are several plans or ideas to construct bridges longer than the Akashi Kaikyo Bridge. In the design of such super long-span bridges, wind resistance is one of the most important themes. The approaches to improve aerodynamic stability can be classified into structural one and aerodynamic one. In this paper described first is the study on improvement of wind resistance of super long-span bridges.

As was found from the full model wind tunnel studies for the Akashi Kaikyo Bridge, special cares should be taken when we predict wind-induced vibrations of super long-span bridges. In this paper follows discussion and proposal on the wind resistant design methods for super long-span bridges.

2. Improvement of Wind Resistance by Aerodynamic Approach

2.1 Flutter Characteristics of Slotted Box Girders

The effect of location and size of slot on aerodynamic characteristics was examined through section model wind tunnel tests [1]. Considering a super long-span bridge which has center span length of 3,000m with two side spans of 1,500m, the structural conditions were assumed. Reduced mass μ (=m/(ρ B^2), m: mass per unit length, ρ : air density, B: girder width), reduced polar moment of inertia ν (=I/(ρ B^4), I: polar moment of inertia per unit length), and natural frequency ratio ε (=f_θ/fz, f_θ: torsional natural frequency, fz: vertical bending natural frequency) were 16, 2.1, and 2.1, respectively. The cross section of the model is shown in Fig.1. From the test results, it was found that the slot at the center increased the flutter onset wind speed. It was

also found that the flutter onset wind speed was increased with the width of slot at the center of the girder (Fig.2).

In order to understand the effect of slot at the center of girder, preliminary analysis was conducted. For the analysis, aerodynamic forces acting on the each box of the girder were calculated using the Theodorsen's function. The aerodynamic interference between the 2 boxes was neglected. Using these aerodynamic forces, two degree-of-freedom flutter analysis was conducted by U-g method [2]. The result of the flutter analysis (Fig.2) indicates that the flutter onset wind speed increases with size of slot. The differences between the analysis and the experiment seems to be caused by aerodynamic interference between the 2 boxes.

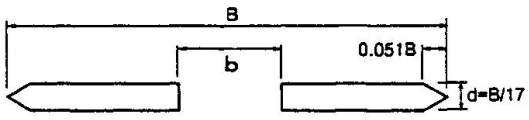

Fig.1 Cross section of girder

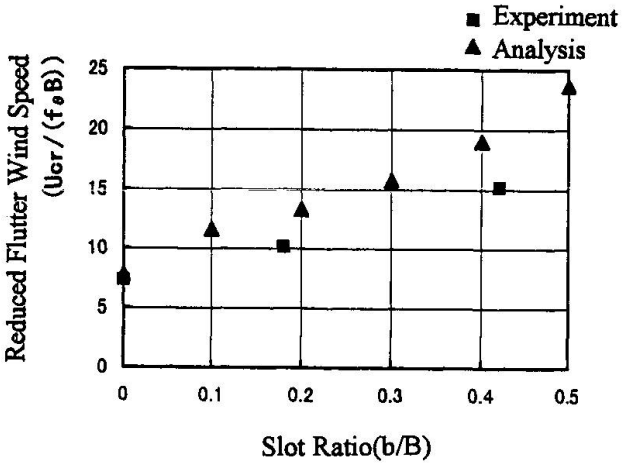

Fig.2 Flutter onset speed and slot ratio

Although wide slot at the center of the girder improves flutter characteristics, narrower slot would be preferable from the viewpoint of construction cost of towers and foundations. To improve aerodynamic characteristics, the effect of some devices was studied by section model tests [1]. The tested devices are illustrated in Fig.3. The results showed that the center barrier and guide vanes improved flutter characteristics very well. However, the flutter speed was not so high when angle of attack was -3 deg. It was found that the guard rails at the bottom deck increased the flutter speed considerably at this angle of attack.

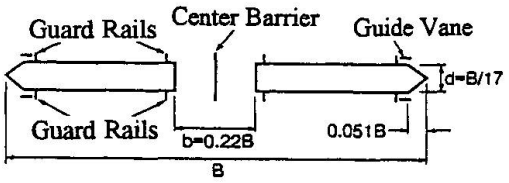

Fig.3 Slotted box girder with devices

2.2 Unsteady Aerodynamic Forces of Slotted Box Girders

In order to understand the aerodynamic characteristics of the slotted box girder more precisely, unsteady aerodynamic forces were measured for three models: model A (single box girder, b=0 in Fig.1), model B (slotted box girder, b=0.22B in Fig.1) and model C (slotted box girder with devices, Fig.3). The measurement was made by forced oscillation method [3]. Coefficients of the unsteady aerodynamic forces were defined as follows:

$$L=\pi\rho\{B^2[L_{ZR}\omega^2 z+L_{ZI}\omega z']+B^3[L_{\theta R}\omega^2\theta+L_{\theta I}\omega\theta']\} \quad (1.1)$$

$$M=\pi\rho\{B^3[M_{ZR}\omega^2 z+M_{ZI}\omega z']+B^4[M_{\theta R}\omega^2\theta+M_{\theta I}\omega\theta']\} \quad (1.2)$$

where, L: lift (upward positive), M: aerodynamic moment (head up positive), z: vertical displacement (upward positive), θ : torsional displacement (head up positive), ω: circular frequency, ( )': d( )/dt, L_{xx} or M_{xx}: coefficients of unsteady aerodynamic forces ($_R$: in phase with displacement, $_I$: in phase with velocity).

In general, it is difficult to predict coupled flutter characteristics directly from these coefficients. For 2-degrees of freedom system, Nakamura[4] showed approximate relationship between unsteady aerodynamic coefficients M_{ZI}, $M_{\theta I}$, $L_{\theta R}$ and $M_{\theta R}$ and some flutter properties as follows:

$$\delta a \fallingdotseq -\pi^2 M_{ZI} X/\nu - \pi^2 M_{\theta I}/\nu \quad (2.1)$$

$$X \equiv z_0/\theta_0/B \fallingdotseq \pi L_{\theta R}/(-1+(f_z/f_\theta)^2\sigma^2)/\mu \quad (2.2)$$

$$\sigma^2 \equiv (f_\theta/f)^2 \fallingdotseq 1+\pi M_{\theta R}/\nu \quad (2.3)$$

where, δa: aerodynamic damping in logarithmic decrement. They were derived by assuming that absolute value of aerodynamic damping and phase angle are small, and that absolute value of the amplitude ratio X is small. As is shown here, $M_{\theta R}$ affects the frequency ratio σ. $L_{\theta R}$ and σ affect the amplitude ratio X. M_{ZI}, $M_{\theta I}$ and X affect the aerodynamic damping.

If onset of flutter is defined as $\delta a \leqq 0$, simpler inequality for onset of flutter can be derived from (2.1)-(2.3) as follows:

$$\alpha M_{ZI} L_{\theta R}/M_{\theta I} + \beta M_{\theta R} \geqq 1 \quad (3.1)$$

$$\alpha \equiv (\varepsilon^2/(\varepsilon^2-1))(\pi/\mu) \quad (3.2)$$

$$\beta \equiv (1/(\varepsilon^2-1))(\pi/\nu) \quad (3.3)$$

The left hand side of equation (3.1) was calculated for the Models A, B and C using measured unsteady aerodynamic forces, as well as for single plate and slotted plate using the Theodorsen's function. μ, ν and ε were assumed as 15, 2.0 and 2.0, respectively. The results are shown in Fig.4, where they are plotted with $f_\theta B/U$. The slotted box girders and slotted plate show higher flutter speed than the single box girder or single plate. Since the first term of the left hand side of equation (3.1) was much larger than the second term, it can be said that this higher flutter speed was caused mainly by property of $M_{ZI} L_{\theta R}/M_{\theta I}$. In Fig.4, flutter speed of slotted box girder with devices is higher than that without devices. When the left hand side of equation (3.1) was plotted with fB/U (where f is apparent frequency in wind) rather than $f_\theta B/U$, reduced flutter speed U/(fB) of slotted box girder with devices was almost identical with that of slotted box girder. It means that the effect of devices comes from small value of $M_{\theta R}$, which affects apparent frequency in wind.

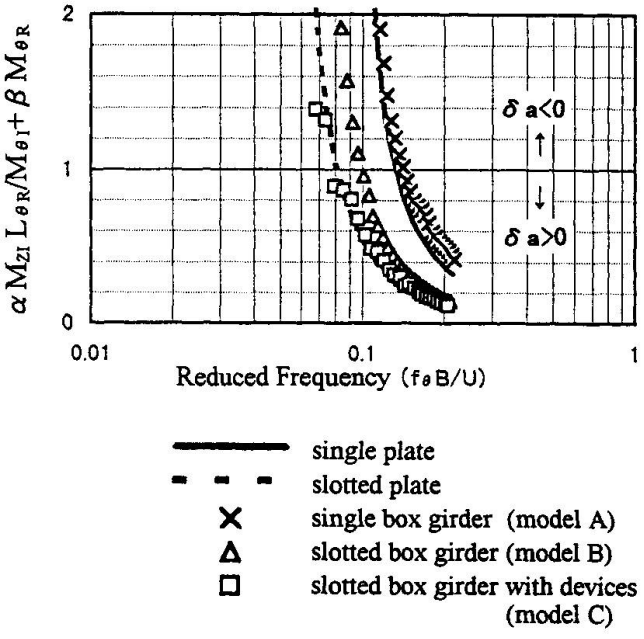

Fig.4 Prediction of flutter speed

2.3 Flutter Analysis for a Super Long-Span Bridge

Using all the measured coefficients of unsteady aerodynamic forces of model C, flutter analysis of a super long-span bridge was conducted. The main span length of the super long-span bridge was 2,500 m, and the side span was 1,250 m. μ, ν and ε were assumed as 14, 1.8, and 1.8, respectively. For comparison, flutter analysis was also conducted using

unsteady aerodynamic forces of the single plate derived from Theodorsen's function. The structural conditions for both cases were same. Flutter speed for the slotted box girder was as high as about 80 m/s. On the other hand, the critical wind speed for single flat plate was as low as about 40 m/s.

3. Improvement of Wind Resistance by Structural Approach

In order to improve aerodynamic stability of a super long-span bridge, cross hanger systems were examined. Cross hangers are hangers which connect main cables to stiffening girder crossing over the deck. Cross hanger systems changed natural frequencies, mode shapes and modal masses of the bridge. Natural frequencies, mode shapes and modal masses of the bridge have close relation with flutter onset wind speed of it. Two types of the system were tried, shown in fig.5. One was a system used cables as cross hangers. This system is not effective for compression force. The other is a system used steel members as cross hangers, effective for compression force. Four sets of cross hangers were used in a super long-span bridge, one set at the center of each side span and two sets in the center span (Fig.6). The main span of the bridge was 2,500m, and side spans were 1,250m each. μ, ν and ε were assumed as 21, 2.5, and 2.7, respectively. The type of stiffening girder was a box girder without slot. Flutter analysis of the bridge was conducted. From analysis results, the cable cross hanger system increased the flutter onset wind speed about 10 m/s from that of the bridge without the system, about 60 m/s. The steel member cross hanger system increased 20 m/s.

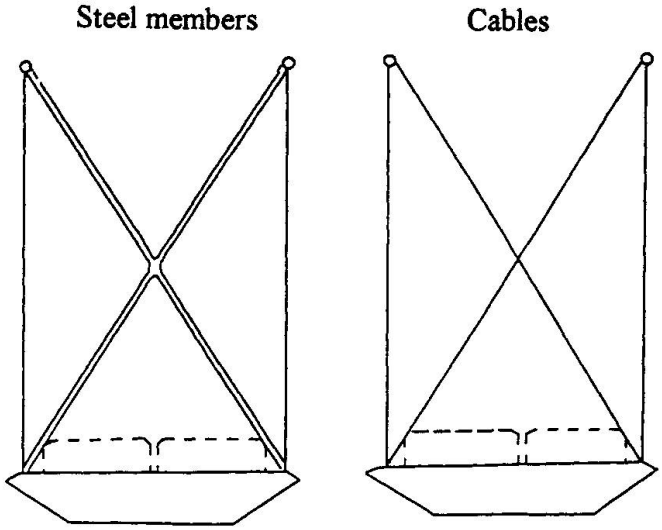

Fig.5 Cross hanger system

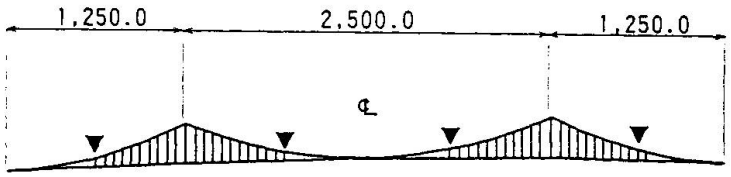

Fig.6 Locations cross hangers set (▼)

4. Wind Resistant Design Methods for Super Long-Span Bridges

4.1 Findings from the Wind Tunnel Study for the Akashi Kaikyo Bridge

Wind tunnel study for the Akashi Kaikyo Bridge was conducted at the Large Boundary Layer Wind Tunnel in Tsukuba using 1/100 full aeroelastic model. The model was designed so that the

similarity requirements of shape, mass distribution and stiffness distribution might be satisfied. In the smooth flow test [5], remarkable static torsional displacement was observed. Coupled flutter was observed at the wind speed of 8.5m/s (85m/s for real bridge). The rotation center lay on the windward side at the midspan, on the leeward side at quarter point of center span, and on the windward side again at the middle of side spans. During the flutter, its vertical bending vibrational mode was not similar to any of natural modes, while its torsional vibrational mode was similar to the first symmetric natural mode. Therefore it does not seem that aerodynamic stability of super long-span suspension bridges can be predicted directly from spring-mounted rigid model test. From comparison between wind tunnel tests and flutter analyses, it was found that aerodynamic derivatives such as Drag due to Heaving motion, Drag due to Torsional motion, Lift due to Along-wind motion, and Pitching moment due to Along-wind motion should be included in addition to the conventional aerodynamic derivatives.

In the turbulent flow test [5], gust responses were observed, and the responses were compared with the calculated ones. As for vertical bending and torsional responses, the agreement was fairly good, however, the observed horizontal bending responses were much smaller than calculated ones. One of the causes of this discrepancy was thought to be the spatial correlation which was assumed as the exponential function of $fb \mid x1-x2 \mid /B$. Since the measured spatial correlation of wind speed did not tend to unity as frequency became 0 when separation of measurement points were large, the calculation might lead to an overestimation as was pointed out in ref.[6] and [7]. Using the measured aerodynamic admittance and the spatial correlation based on the turbulent flow of the wind tunnel, gust responses were calculated again. Although there still remains some discrepancy, accuracy of the calculation has been improved.

4.2 Design Tools for Super Long-Span Bridges

In general, there are three kinds of tools for wind resistant design. They are:
a) Section model test (spring mounted rigid model test, measurement of aerodynamic forces, and so on),
b) Analysis based on aerodynamic forces measured from section model tests, and
c) Full aeroelastic model test.

Section model test is the simplest method. If aerodynamic instability of interest can be assumed as one-degree of freedom (eg. Vortex-induced vibration, galloping, and torsional flutter) or two-degree of freedom, and if torsional deformation of the bridge deck due to steady aerodynamic forces is negligibly small, we can predict critical wind speed of the instability directly from the section model test. As was shown in the experiment for the Akashi Kaikyo Bridge, however, we could not predict the critical wind speed of flutter directly from the section model test, because the torsional deformation was not negligibly small, and because flutter mode consisted of higher vibrational modes as well as fundamental modes. For the wind resistant design of super long-span bridges, therefore, we may well regard the section model test as a tool for eliminating aerodynamically unfavorable cross section of bridge deck or a tool for obtaining aerodynamic data that will be used in the detailed analysis.

As was demonstrated in the wind tunnel studies for the Akashi Kaikyo Bridge, and as was pointed out by Irwin [8], full aeroelastic models give important and unexpected insights into the bridge response. In the full aeroelastic model test, turbulence effects can be well simulated; three-dimensional and local topographical effects can be studied; and influences of various modes and mode shape can be included. Disadvantages of full aeroelastic models are greater cost and time for building and testing them.

If the accuracy of an analytical method is verified by comparing with a full aeroelastic model test, we can use the analytical method instead of the full aeroelastic model test. Comparison with a full model wind tunnel test suggests how to improve analytical methods. To predict flutter of the Akashi Kaikyo Bridge, for instance, the effect of the static torsional displacement and higher natural modes had to be considered, and several aerodynamic derivatives had to be included in addition to the conventional ones. To predict gust responses of the Akashi Kaikyo Bridge, more accurate spatial correlation model was required. Although the present analytical method has been improved by comparing with the full aeroelastic model tests of the Akashi Kaikyo Bridge, the

verification of the method is necessary if the method is applied to super long-span bridges that have longer span, inexperienced bridge deck configuration or inexperienced cable system.

4.3 Design Procedures for Super Long-Span Bridges

The procedure of wind resistant design for super long-span bridges can be proposed as follows:
a) Selection of bridge deck cross section by section model tests
b) Prediction and evaluation of wind-induced deformation and vibration by the analytical method that is the most reliable at that time
c) Verification and improvement of the analytical method by comparing with a full aeroelastic model test
d) (in case of slight change of bridge design) Prediction and evaluation of wind-induced deformation and vibration by the verified analytical method
e) (if the accuracy of the analytical model is not enough) Verification of the finalized bridge design by a full aeroelastic model test

5. Concluding Remarks

(1) It was found that box girder with slot at the center had good flutter characteristics, and that it could be improved by some devices like center barrier and guide vane. It seems that the slotted box girder would be one of the possible stiffening girders for super long-span bridges. It was also found that cross-hangers were effective to increase flutter speed of super long-span bridges.

(2) Since super long-span bridges will have inexperienced span length, inexperienced bridge deck cross section or cable systems, full aeroelastic model tests will play an important roll in wind resistant design of super long-span bridges. To overcome its disadvantage, namely greater cost and time, section model tests can be used to select aerodynamically favorable cross section, and analytical methods verified by the full aeroelastic model tests can be applied to predict and evaluate wind-induced response.

References

[1] Sato H., Toriumi R. and Kusakabe T., Aerodynamic characteristics of slotted box girders, Proceedings of Bridges into the 21st Century, 1995
[2] Bisplinghoff R. L., Ashley H., and Halfman R. L., Aeroelasticity, Addison Wesley.
[3] Okubo, T., Narita N. and Yokoyama K., Some approaches for improving wind stability of cable-stayed girder bridges, Proc. of the 4th International Conference on Wind Effects on Buildings and Structures, 1975
[4] Nakamura, Y., An analysis of binary flutter of bridge deck sections, J. of Sound and Vibration, 57(4), 1978
[5] Sumiyoshi Y., Endo T., Miyata T., Sato H. and Kitagawa M., Experiments for the Akashi Kaikyo Bridge in a Large Boundary Layer Wind Tunnel, Proc. of International Seminar on Utilization of Large Boundary Layer Wind Tunnel, Tsukuba, Japan, 1993
[6] ESDU, Characteristics of atmospheric turbulence near the ground, Part Ⅲ: variations in space and time for strong winds (neutral atmosphere), 1975
[7] Irwin H.P.A.H., Wind tunnel and analytical investigations of the response of Lions' Gate Bridge to a turbulent wind, Laboratory Technical Report LTR-LA-210, National Research Council Canada, 1977
[9] Irwin P. A., Full aeroelastic tests, Aerodynamics of Large Bridges, A. A. Balkema, Rotterdam, Brookfield, 1992

Cable Supported Bridge under Movement of Foundation due to Earthquake

Yasutsugu YAMASAKI
Bridge Eng.
Chodai Co. Ltd
Tsukuba, Japan

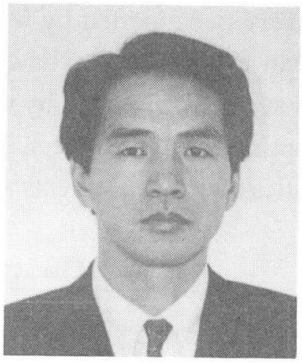

Yasutsugu Yamasaki, born 1951, MSc in Structural Eng. from the Nagoya Univ. Since 1975, he had been working in heavy industry co. for 16 years, and joined Chodai Co., Ltd 1991 and is working as responsible engineer for major bridges.

Torahiko IKEDA
Bridge Eng.
Chodai Co. Ltd
Tsukuba, Japan

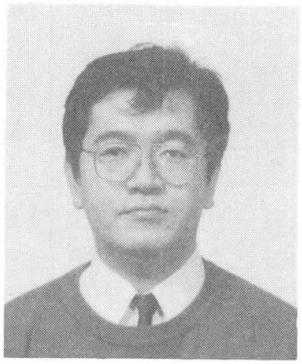

Torahiko Ikeda, born 1959, MSc in Structural Eng. from the Nagasaki Univ. Since 1985, he has been working as bridge engineer in Chodai Co. Ltd.

Summary

The experience of the Akashi Kaikyo Bridge hit by the earthquake indicates that a suspension bridge is such bridge as not seriously effected by movement of foundation as compared with a cable stayed bridge. If the bridge was cable stayed bridge, much more damages would be observed. This paper describes the magnitude of stress of suspension bridge and cable stayed bridge having the same span length caused by movement of foundation due to earthquake.

1. Introduction

After the earthquake hit Kobe area including the Akashi kaikyo Bridge located very near the epicenter, where the compacting work was under way, some small damages by the shock were observed on the temporary work, but no serious influence was found on the permanent structure of the Akashi kaikyo Bridge.

This was because the earthquake had happened before the suspended truss was constructed, the magnitude of the movements were relatively small as compared with the span length and fortunately the Akashi Kaikyo Bridge was suspension bridge (not complex structure).It is easily imagined that some part of permanent structure would be damaged or overstressed if the earthquake happened after the completion and furthermore if the span length was not so long, and that another behavior of structure would be observed if the bridge was cable stayed bridge.

In this circumference, we have computed the behavior of suspension bridge and cable stayed bridge after the completion under the similar scale of movements of the foundations. The bridges for computation are suspension bridge with a main span of 1,000m having un-continuous suspended girder vertically supported by links and transversely supported by wind shoes at the towers and the anchorages, and cable stayed bridge with a main span of 1,000m having continuous suspended girder vertically supported by bearings and links, transversely supported by wind shoes at the towers and the anchorages, and longitudinally supported by spring from the towers. The general arrangements of the bridges are shown in Fig 1. and the characteristics of bridge elements are shown in Table 1.

Table 1. Characteristics of bridge elements

Suspension bridge	
Girder	A=1.378 m2
	Iz= 2.43 m4 Iy=162.24 m4
Tower	A=2.362 m2
	Iz= 21.97 m4 Iy=12.18 m4
Cable	A=0.195 m2
Cable stayed bridge	
Girder	A=1.567 m2
	Iz=2.58 m4 Iy=172.76 m4
Tower	A=2.362 m2
	Iz= 21.97 m4 Iy=12.18 m4
Cable	A=0.009~0.015 m2

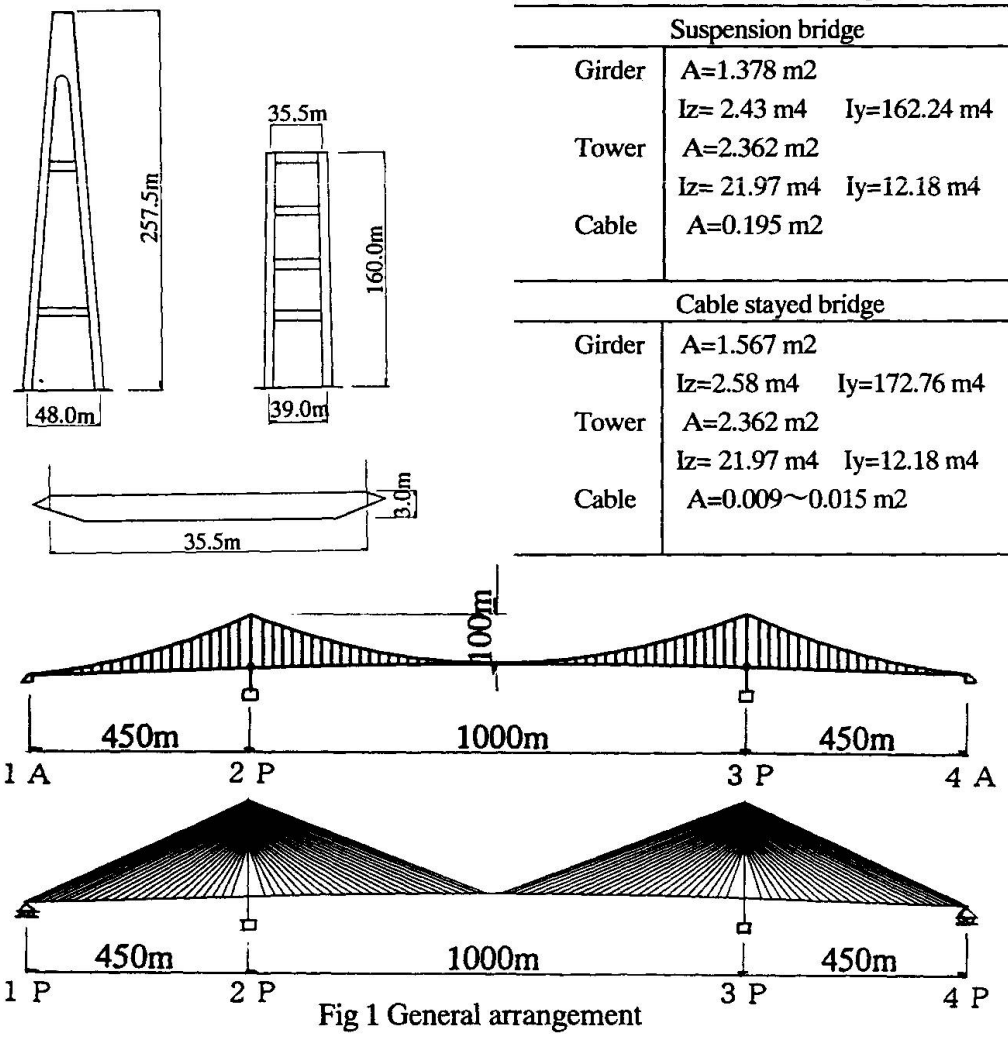

Fig 1 General arrangement

2. Longitudinal Movement

We assumed two cases. One is a tower foundation and an anchorage (or a pier) in the same side move longitudinally outward by the same distance (main span extension), which simulates that fault located in the main span slides, and the other is only an anchorage (or a pier) moves longitudinally outward (side span extension), which simulates that fault located in the side span slides, as shown in Fig 2.

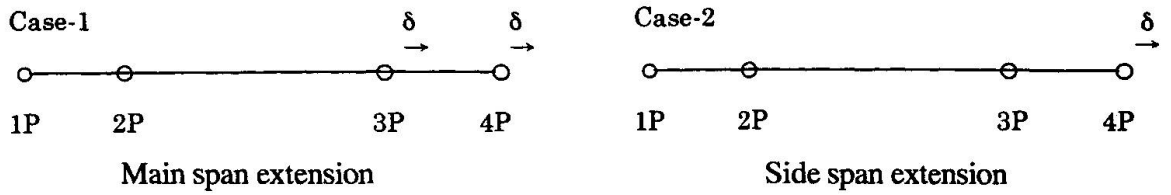

Fig 2. Longitudinal movement

2.1 Main Span Extension

Fig 3. shows the deformation of two bridges for the main span extension of 1.0m, and Fig 4. & 5 show the extra stresses occur in the tower and in the cable of the two bridges by the main span extension ranging from 0.5m to 1.0m . Suspension bridge is able to absorb a extension of main span easily by a change of cable sag (1.4m for extension of 1.0m), which doesn't make tower top displacement much (0.09m each) to balance cable forces of main span and side span at tower top and increase a stress of main cable (13Mpa). By this behavior, suspension bridge is not much overstressed by main span extension. While, cable stayed bridge absorbs a extension of main span by displacement of tower tops (0.52m each for extension 1.0m) inward pulled straight by stay cables. By this behavior, cable stayed bridge is much stressed by main span extension, and the extra stress occurs at the tower base comes up to17% of its allowable stress by a extension of 1.0m.

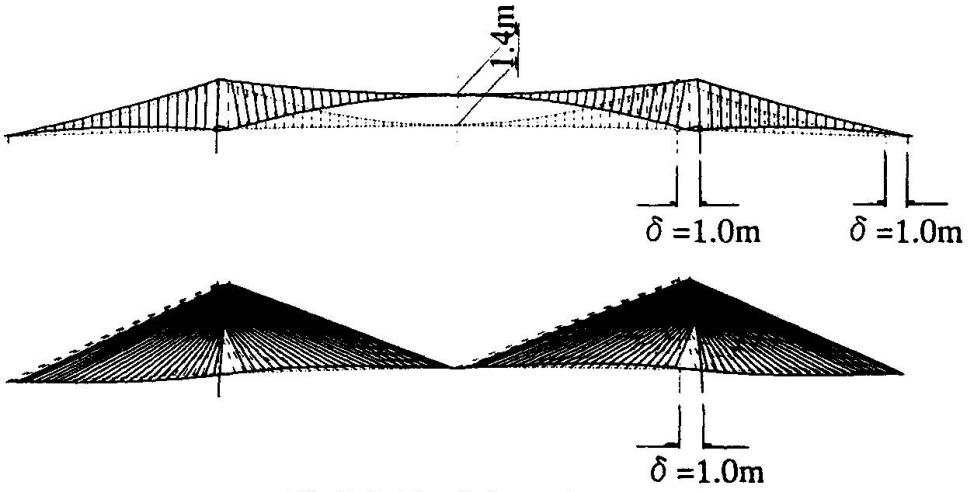

Fig 3. Bridge deformation

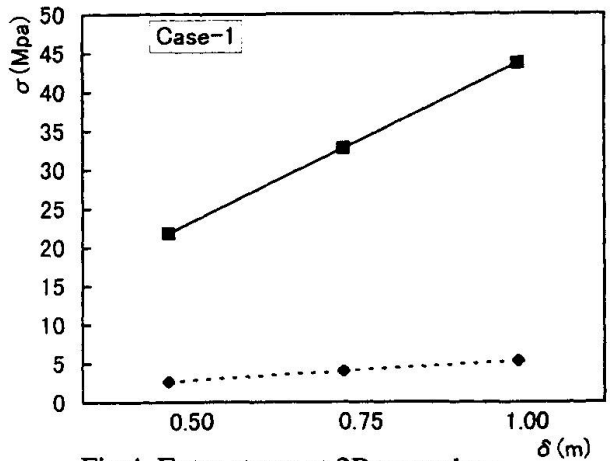

Fig 4. Extra stress at 3P tower base

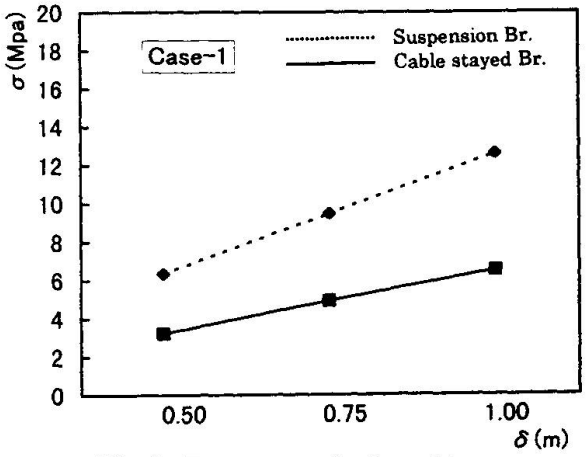

Fig 5. .Extra stress in the cable

2.2 Side Span Extension

Fig 6. and 7. show the extra stresses occur in the tower and in the cable of the suspension bridge by the side span extension ranging from 0.5m to 1.0m. Suspension bridge is much effected by a extension of side span. The tower top moves by nearly the same scale as that of the movement of anchorage (0.86m for extension of 1.0m), which doesn't produce much extra stress in main cable (16Mpa), but produces, depend on the stiffness of tower, some stress at the tower base. Cable stayed bridge is not effected by a extension of side span, because a damage of bearing at the end pier absorbs most of such extension.

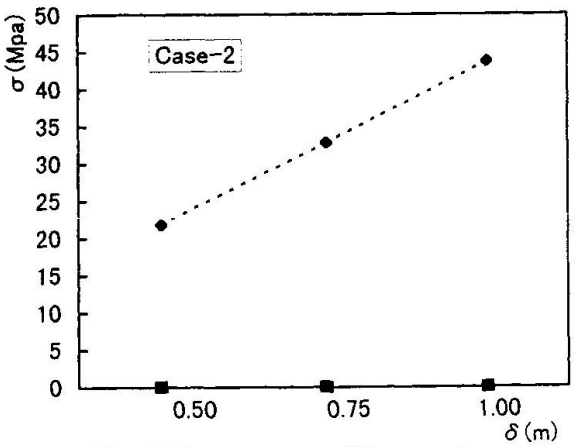

Fig 6. Extra stress at 3P tower base

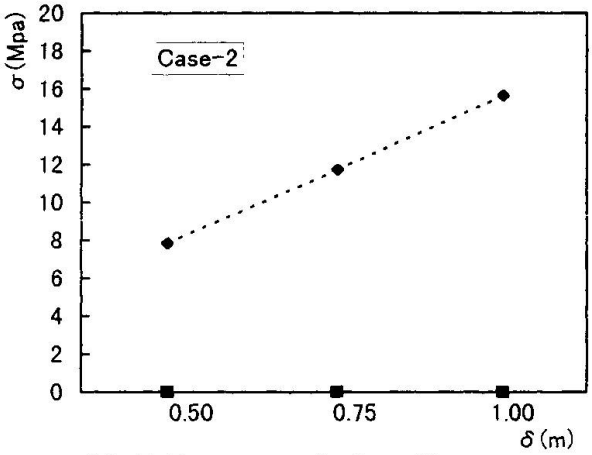

Fig 7. Extra stress in the cable

3. Transverse Movement

We assumed two cases. One is a tower foundation and an anchorage (or a pier) in the same side move transversely by the same distance (transverse shift in main span), which simulates that fault located in the main span slides, and the other is only an anchorage (or a pier) moves transversely (transverse shift in side span), which simulates that fault located in the side span slides, as shown in Fig 8.

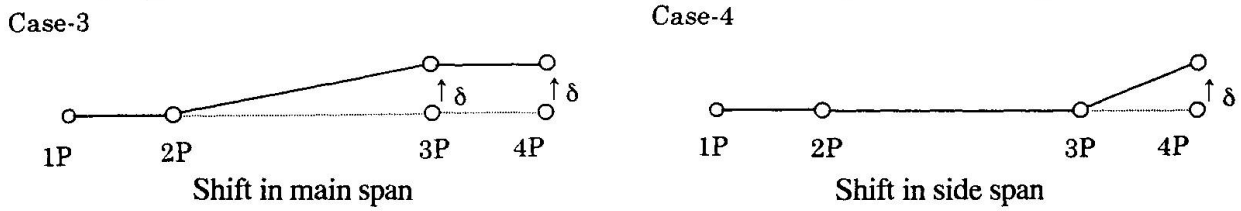

Fig 8. Transverse movement

3.1 Transverse Shift in Main Span

Fig 9. and 10. show the extra stresses occur in the suspended girder and in the tower of the two bridges for the transverse shift in main span ranging from 0.5m to 1.0m. The governing factor to produce the extra stresses in the suspended girder is a continuity of the suspended girder. Suspension bridge with un-continuous girder, which is normally applied to Japanese suspension bridges, is not effected by transverse movement of foundation. The tower tops of suspension bridge move

transversely much (0.39m each for shift of 1.0m) because a big force is applied at the tower top by the main cable. While, cable stayed bridge, for which continuous girder is necessarily applied, is much effected by transverse movement of foundation, and the extra stress occurs in the suspended girder at the tower comes up to 6% of its allowable stress. The tower tops of cable stayed bridge moves transversely, but not much (0.27m for shift of 1.0m).

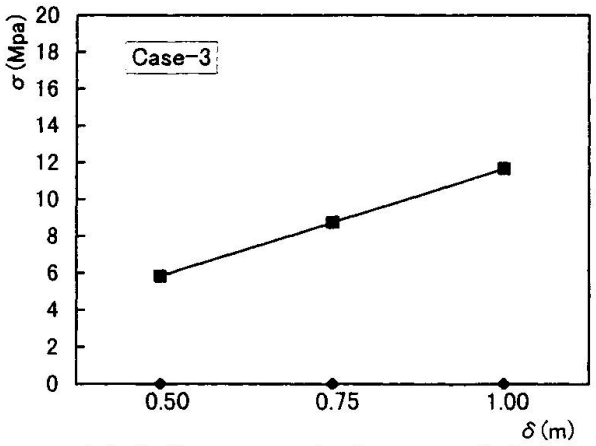

Fig 9. Extra stress in the suspended girder

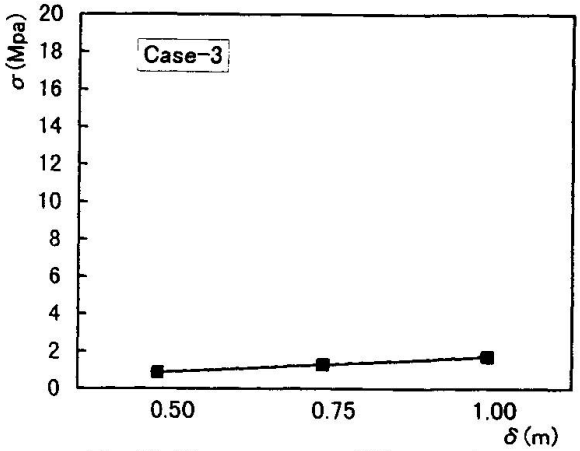

Fig 10. Extra stress at 3P tower base

3.2 Transverse Shift in Side Span

Fig 11 and 12. show the extra stresses occur in the suspended girder and in the tower of the two bridges for the transverse shift in side span ranging from 0.5m to 1.0m. Cable stayed bridge is much more stressed by the transverse shift in side span than by the transverse shift in main span. The extra stress occurs in the suspended girder at the tower is 10% of its allowable stress. The top of 3P tower moves transversely by 0.54m, but doesn't produce much extra stresses at the tower base because A-shape tower change the in-plane bending moment due to the tower top displacement to the axial forces in the tower section. Suspension bridge with un-continuous girder is not effected by transverse movement of foundation.

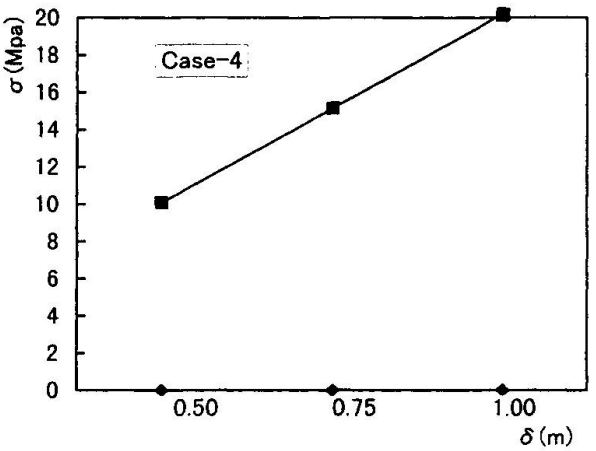

Fig 11. Extra stress in the suspended girder

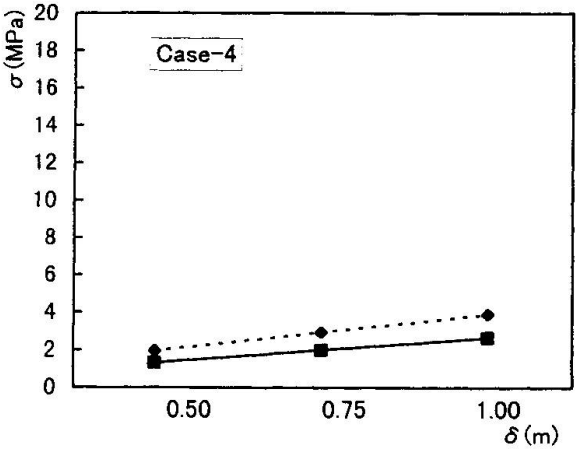

Fig 12. Extra stress at 3P tower base

4. Concluding Remarks

From the above case studies, the followings are obtained for selection of bridge type to be constructed in a seismic area.

- Suspension bridge is preferred bridge type if bridge is constructed in a seismic area, in particular near faults, and shall be constructed so that the fault is located in the main span. Un-continuous girder is to be applied not to be effected much by transverse shift.
- Cable stayed bridge requires necessarily continuous girder, which is effected much by transverse shift, and is overstressed at the tower base when the tower foundation is moved longitudinally.

It is also founded that a increase of span length doesn't reduce the extra stress of suspension bridge much. The extra stress occurs at the tower base of the suspension bridge of 900-2000-900 for the side span extension of 1.0m is 41 Mpa for 44Mpa of the suspension bridge of 450-1000-450.

Reference

K. Tada and others, "Effect of the Southern Hyogo Earthquake on the Akashi-Kaikyo Bridge", Structural Engineering International, January 1995

The Ting Kau Bridge in Hong Kong

Rudolf BERGERMANN
Consulting Eng.
Schlaich Bergermann und Partner
Stuttgart, Germany

Michael SCHLAICH
Consulting Eng.
Schlaich Bergermann und Partner
Stuttgart, Germany

Summary

The Ting Kau bridge is one of the trio of long span bridges which connect Hong Kong's new Chep Lak Kok airport, located on Lan Tau island some 30km away from Hong Kong, to the city and the main land. It is a multispan cable stayed bridge with 1177m of cable supported deck. The unusual features of the bridge are its two adjacent main spans with stabilising cables for the central main tower which run diagonally from its top towards the deck of the side towers. With further stabilising cables in the transverse direction, the towers of the bridge appear like masts of a sailing boat. The „Design and Build" contract for the Ting Kau bridge was awarded in August 1994 and the bridge was opened to traffic in April 1998. The design of the structure will be introduced here and the process of deck erection and analysis will be described.

1. Introduction - Conceptual design

The bridge crosses the 900m wide Rambler channel, one of the main water ways to Hong Kong's container port. Therefore the number of supports in the water, which require costly ship impact protection was to be minimised. While generally the level of bed rock in the channel is about 40m below water, approximately in the middle of the channel there is an underwater „hill" of less than 30m depth. This fortunate fact offered the opportunity to design a bridge with a central tower in the channel and two lateral ones on land (see elevation in fig. 1).

Further boundary conditions for the design were the extremely strong winds in Hong Kong and the short construction time. To offer the least resistance to typhoon winds (up to 95m/s according to the specifications) monoleg towers with aerodynamically favourable shapes were chosen. The towers separate the deck into two carriageways with a central gap. The slender deck with a width to height ratio of 25 also follows the design criteria of reduction of wind resistance. The towers and the deck were designed for fast construction. The towers are composed of three segments with constant cross sections to permit slipforming. The composite deck made of prefabricated steel grids and precast concrete panels was trial assembled on the ground which allowed deck erection in record time.

The basic challenge of a multispan cable stayed bridge is the stabilisiation of the central main tower, which contrary to the towers of a conventional cable stayed bridge cannot be connected by backstays to a fixed point such as an abutment. This is especially problematic during balanced cantilevering erection of the deck. Longitudinal stabilising cables which diagonally connect the top of the main tower to the deck at the side towers were introduced already during construction. They fulfill the function of backstay cables, by reducing the displacements of the main tower due to unsymmetric live loads and wind induced oscillations.

2. Structural design

Ting Kau bridge has a deck of 1177m length consisting of four spans of 127, 448, 475 and 127m length respectively.

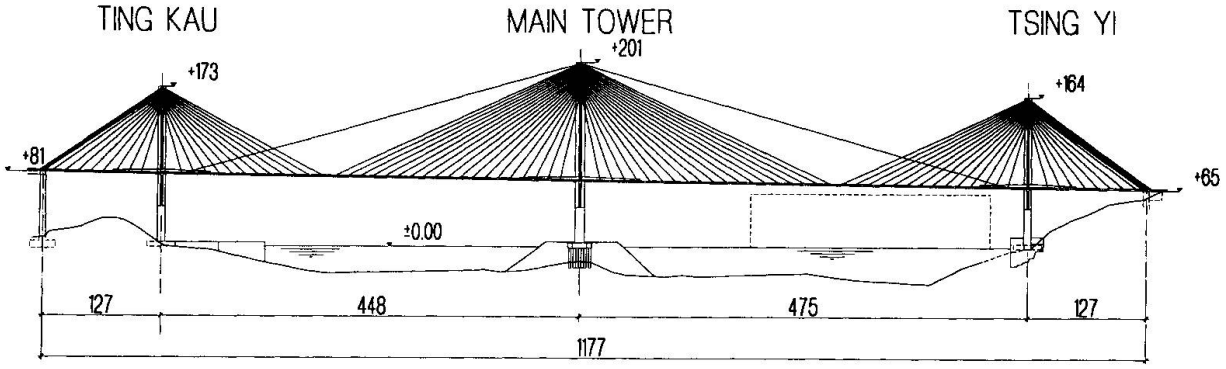

Fig. 1 Elevation

The three towers of concrete grade 60 reach heights of up to 201m and consist of three segments, each of constant cross section. The very slender segment above the deck, which is minimised for reasons of wind resistance and also to keep the gap between the carriageways within reasonable limits, is stabilised by transverse cables. These cables are spread by steel struts which are connected to the middle segment underneath the deck. This segment has to carry additional horizontal loads introduced by the deck and is therefore increased in size. Since for reasons of ship clearance no stabilising cables could be connected to the bottom of the tower, the lowest segment is the strongest. While the two lateral towers are supported directly on rock by pad foundations, the main tower is supported by 52 bored piles each with a diametre of 2.5m. To give stability to the piles and and to protect the tower from ship impact, an artificial island was designed.

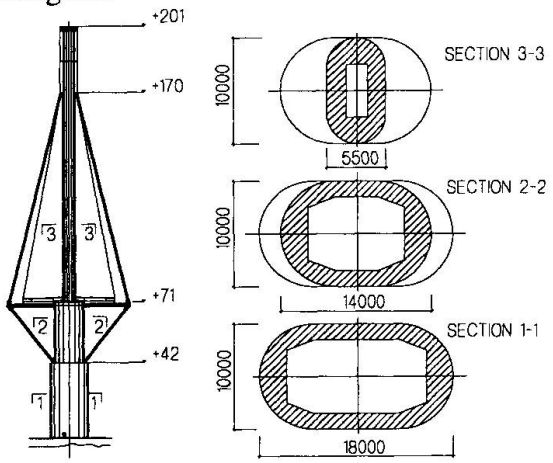

Four cable planes support the carriageways of the deck. The cables consist of bundles of 17 to 58 monostrands. They are anchored in steel boxes which are connected to the sides of the tower tops. Theses boxes, up to 30m long and weighing up to 200 tons, connect the horizontal components of the cables and introduce their vertical components via steel brackets and posttensioned bars and loop tendons into the concrete ot the towers.

Fig. 2 Main Tower

The two carriageways of the composite deck are separated by a gap of 5.2m width. They are generally 18.77m wide and each carry 3 traffic lanes and a hardshoulder. Every 13.5m, the distance between cables, they are connected by steel cross girders. The steel grids, made of steel grade S355JO, which carry the deck slab, consist of L-shaped longitudinal main girders and I-shaped cross girders which are spaced 4.5m. Usually grids of 13.5m length were prefabricated on the ground by welding and connected to the existing deck by spliced connections with high strength friction grip bolts (M30, grade 8.8). The deck slab consists of precast panels of concrete

grade 60 which span the 4.5m from cross girder to cross girder. Their thickness is normally 24cm and increases to 30cm around the main tower. Such a composite deck for a cable stayed bridge permits fast and easy assembly, since the use of formwork and reinforcement on site is reduced to a minimum. Another advantage is that the concrete can be used to carry the horizontal components of the cables, which at the same time prestress the concrete. Also it should be noted that the use of „old" precast panels can greatly reduce the effects of creep and shrinkage.

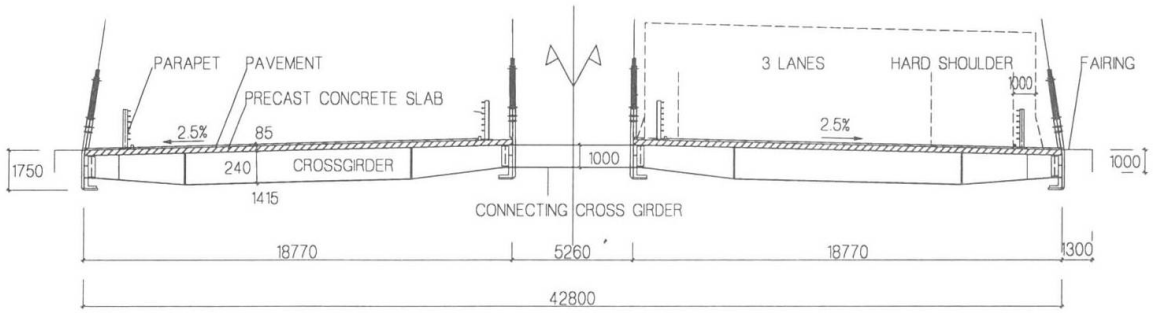

Fig. 3 Deck, typical cross section

For further details of the conceptual and structural design of the Ting Kau bridge, please refer to [1], [2] and [3].

3. Deck Erection

The deck of the Ting Kau bridge was erected by the balanced free cantilever method. Firstly, heavy lifting equipment was hoisted to the tower tops and the steel tower heads were positioned. Then at each tower deck erection began with the positioning of the starter grids, which are about 50% longer than the standard grids. They were manoeuvered into a vertical position at the tower foot, hoisted, attached and then lowered into their horizontal position (see fig. 4). After the precast concrete slabs were placed and cast in, stiff leg derrick cranes were assembled on the starter grids and the standard deck erection cycle began.

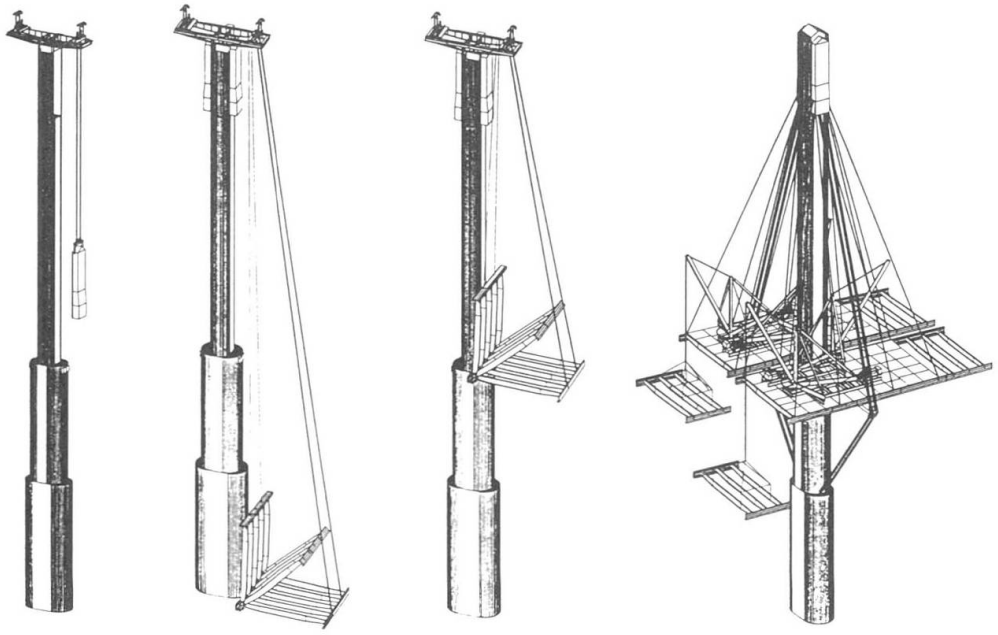

Fig. 4 Deck erection sequence (taken from [3])

The typical erection cycle for a grid was defined by four stages:

1. steel stage: two prefabricated welded steel grids each consisting of 2 longitudinal main girders with a cable anchorage at their tips and 3 cross girders were lifted by the derrick cranes from barges and bolted to the deck. Diagonal bracing in the grids consisting of 20mm bars were used to orient these very flexible grids correctly in plan. Along the longitudinal girders a row of concrete panels were placed to gain access to the cable anchorages. Finally the steel cross girders which connect the two grids at the location of the inner cable anchorages were installed. In elevation the correct tangential connection of the new grids to the existing deck was guaranteed by drifts in block drilled bolt holes placed during trail assembly.
2. panel stage: the steel grids were designed to bear the loads of the steel stage and before any further slabs could be placed, cable installation had to start. Strands were stressed to a first stressing stage and the remaining concrete slabs were placed in parallel.
3. freeze stage: after all panels and strands were in place, the grid geometry and the cable forces were checked again and after approval of the results the joints of the concrete slabs were cast, thus making the new grid act compositely.
4. final stage: when the concrete in the joints had reached a strength of 20MPa, in a second stressing stage the cables were stressed to their final length and with a concrete strength of 30MPa the derrick cranes were advanced onto the new grid to start the cycle again.

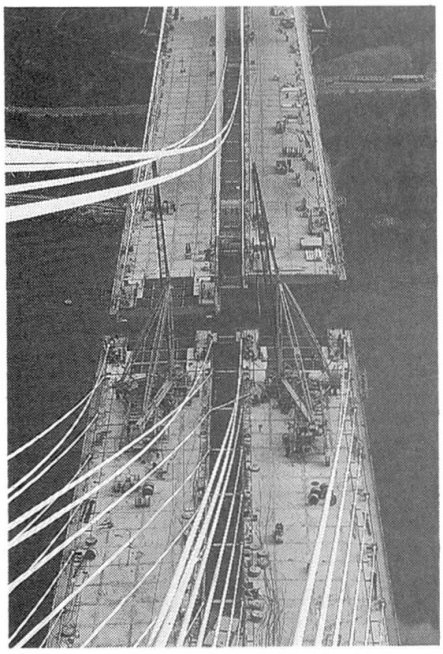

Fig. 5 Deck Erection

For the composite deck of the Ting Kau bridge stressing the cables was a two step procedure. In the first step at the panel stage the cables were stressed „to force" and in the second step at the final stage the cables were stressed „to length". At the panel stage the cable forces and the dead weight of the new grid act on the steel sections only. The cable forces of the first step were determined so that zero overall curvature was introduced into the steel, i.e. when the section was made composite at the freeze stage neither upwards nor downward curvature was „frozen" into the deck sections. Only in the second step at the final stage the cable were stressed to their final length which for the completed structure under permanent loads would guarantee bending moments in the deck equal to those of a continuous beam on rigid supports.

For the stages described above the deck geometry and cable forces were controlled exhaustively. Local surveys of the grid geometry in plan, elevation and in the cross direction were done at the steel and panel stages. For each freeze stage a global geometric survey of the entire cantilever was produced. Cable forces were surveyed at the panel and at the final stage. The designers were present on site to compare the survey results with the theoretical values on a day to day basis. Each of the cantilever stages was modeled with a computer model which could exactly represent the ever varying loads at each stage as well as effects of creep, shrinkage and temperature. Any measures of correction such as adjustments of the grids in plan at the steel stage or restressing of cables at the panel stage, which fortunately were rarely necessary, could thus be executed immediately and evaluated.

While in the beginning construction of the towers and fabrication of the steel work had some slow periods, deck erection was executed at record speed. Initially a deck erection cycle as described above took almost 2 weeks but after experience was gained the cycle time reduced to 4 days. A mayor part of the deck was built in three month. In October and November 1997 the deck „grew" at a speed of almost 100m per week. In November alone, 1000 tons of cable steel were installed and in December the main cantilevers reached the impressive length of 275m each (see fig. 6 and 7).

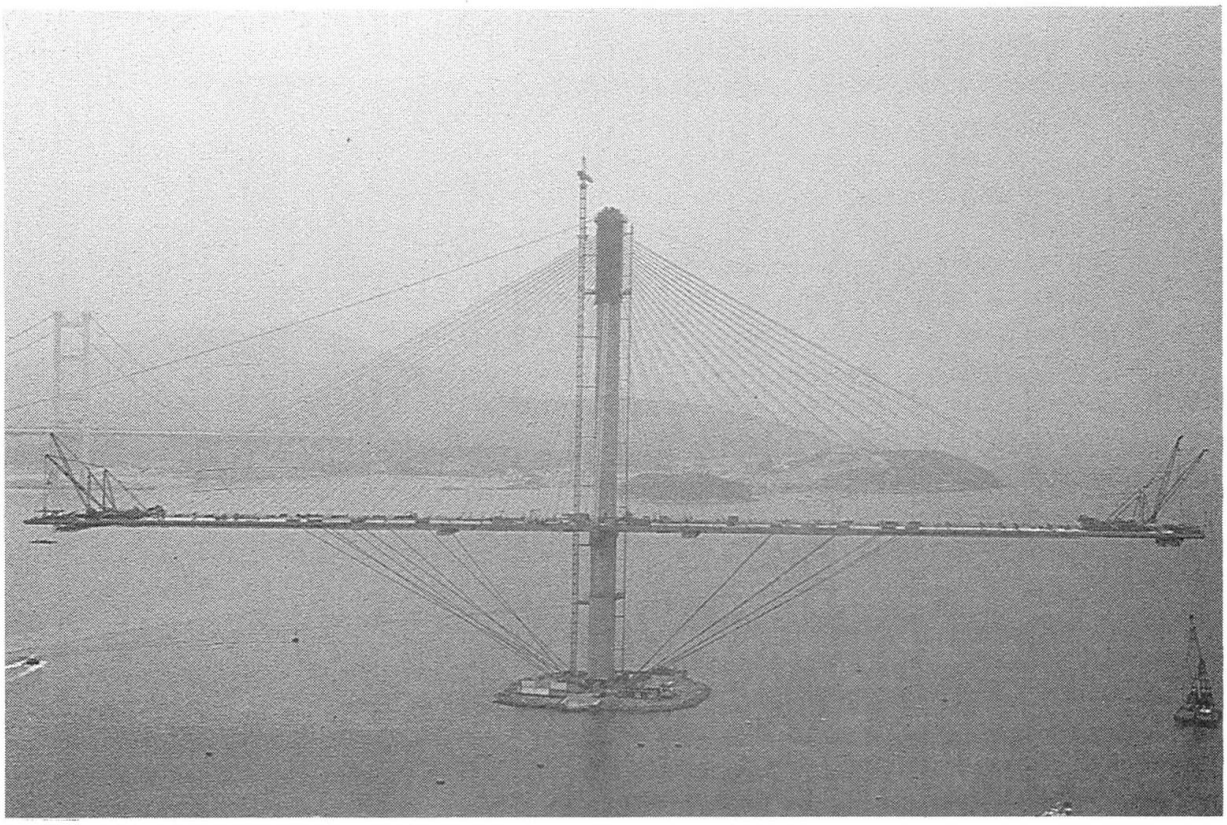

Fig. 6 Main cantilever

Regarding wind loads the design philosophy for the Ting Kau bridge was to dimension the towers for the completed structure and to reduce all unacceptable forces and displacment due to wind during erection by introducing additional temporary cables. A full aeroelastic model, which was used to prove the aerodynamic stability of the completed structure in the wind tunnel, had been designed so that portions of the deck could be removed to test erection stages (see also [4]). Thus all critical cantilever stages were tested in the wind tunnel. For the main tower the longitudinal stabilising cables were installed at an early stage in order to reduce wind induced oscillations (rocking) of the tower in elevation. In order to reduce torsional rotation of the deck around the tower in plan under typhoon conditions, three types of temporary measures were envisaged. For a cantilever length up to 70m the deck was torsionally fixed to the tower by temporary steel brackets and up to a cantilever length of 170m cross wise installed tie down cables connected the deck to the pile cap of the tower foundation (see fig. 6). For longer cantilever lengths two pairs of cross cables would have connected the cantilever tips to the tips of the adjacent lateral spans. The latter, however, which would have been cumbersome to install, eventually did not become necessary because the cantilevers reached their critical lengths out of the typhoon season and for reduced wind speeds the tie down cable were sufficient.

4. Conclusion

The Ting Kau bridge in Hong Kong, with 1177m of cable supported deck one of the longest cable stayed bridges in the world, and the process of deck erection and analysis has been described here. A multispan deck, separate carriageways and longitudinal and transverse stabilising cables on monoleg towers have led to a design that tries to combine, beauty and economy, slenderness and stability.

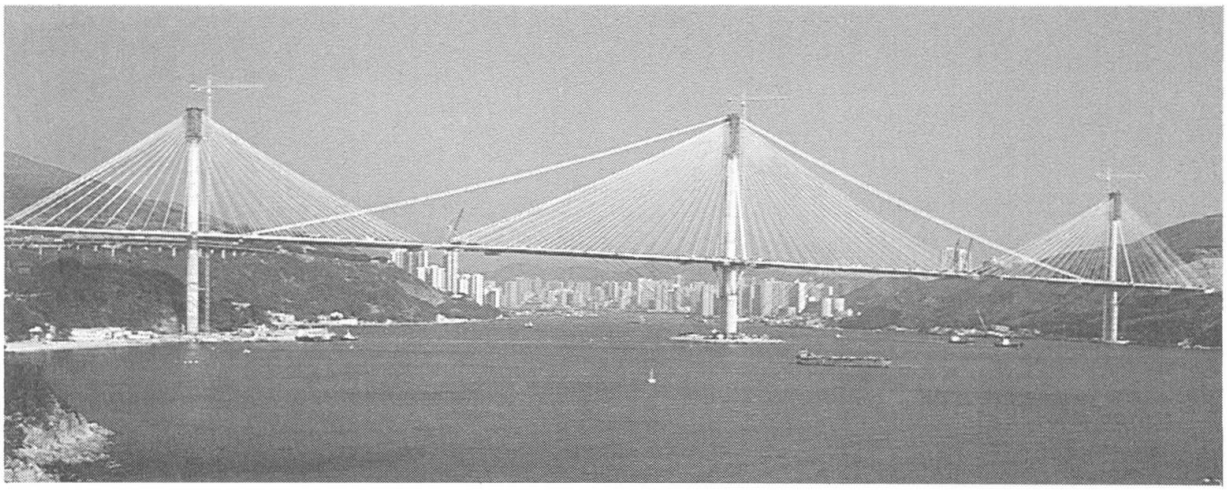

Fig. 7 Ting Kau Bridge in January 1998

References

[1] R. Bergermann, M. Schlaich, „Ting Kau Bridge Hong Kong", IABSE SEI 3/96.

[2] R. Bergermann, M. Schlaich, „Variety in Cable Stayed Bridge Design (The Conceptual Design of the Ting Kau Bridge)", Proceedings of IASS Syposium Conceptual Design of Structures, Stuttgart, Germany, 1996.

[3] R. Swan, „The real landmark", Bridge Design & Engineering, issue August 1997, p. 43.

[4] P. King, A. Davenport, M. Schlaich, „Wind Engineering Studies for the Ting Kau Bridge Hong Kong", ASCE congress 1997, USA.

Very Long Suspension Bridges Using the Temporary Mass Method

Shunzo NAKAZAKI
Mgr
Nippon Eng. Consultants Co. Ltd
Tokyo, Japan

Hiroki YAMAGUCHI
Prof. Dr
Saitama Univ.
Urawa, Japan

Summary

This paper deals with the method to enhance the aerodynamic stability by adding a mass temporarily into the box girder of a suspension bridge. Studies were carried out for both single and twin deck suspension bridges. For a single deck suspension bridge, the most effective longitudinal position of such a mass to improve the aerodynamic stability was first determined, then suspension bridges were roughly designed using this method. As a result, this method could reduce much structural material in comparison with the conventional design method. It was found that this method was also effective for a twin deck suspension bridge.

1. Introduction

Very long suspension bridges with more than 2000m span length are being planned in the world . If the conventional design method is used in order to achieve the required aerodynamic stability, the construction cost of such suspension bridges will be prohibitively expensive. Therefore, some new design methods (ex. mono-duo cable system and cross hanger system [1], active control system [2] and others) are being developed.

This paper deals with the method to enhance the aerodynamic stability by adding a mass such as sea water temporarily into the girder of a suspension bridge during a storm. This method is expected to give the suspension bridge the mass effect, the increase of cable stiffness and the mode control, and consequently enhances the aerodynamic stability.

Studies were carried out for single and twin deck suspension bridges. For a single deck suspension bridge, the most effective longitudinal position for such a mass to improve the aerodynamic stability was first determined, then suspension bridges were roughly designed in order to compare with the conventional design method. Since this study needed many natural vibration modes, the extended Bleich theory [3] and a numerical integration method [4] were employed. In the case of twin deck suspension bridge, since constant added mass was fully applied along the bridge, the suspension bridge was analyzed as a 2-D (vertical and torsional) problem.

2. Single Deck Suspension Bridges

2.1 Suspension Bridges Studied

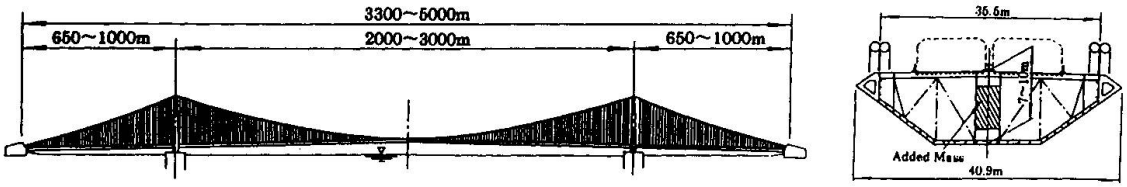

Fig1. Single deck suspension bridge

Three suspension bridges with center span of 2000m, 2500m and 3000m were investigated in order to study the relation between the span and the effect of mass (Fig.1). As shown in Fig.1, the mass such as sea water was added at the center of box girder section, so that the added mass hardly changed the polar moment of inertia and the torsional frequency. The following conditions were assumed:

- The Theodorsen's unsteady aerodynamic force is acting on the girder.
- The required critical wind speed of the coupled flutter is 85m/s.

2.2 Selection of the Longitudinal Position for Added Mass

Seventeen loading cases shown in Fig.2 were analyzed to determine the most effective position of the added mass from the aerodynamic stability point of view. Case-0 has no added mass. Cases-1~9 have 0~100% mass length in the center span and full mass length in both side spans. Cases-10~17 are the same conditions as Cases-2~9 without the mass in side spans.

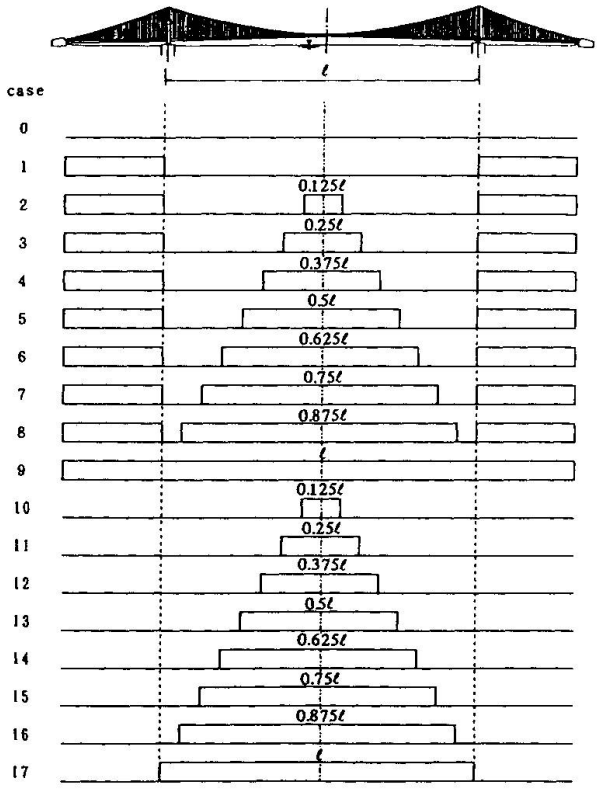

Fig.2 Added mass loading cases

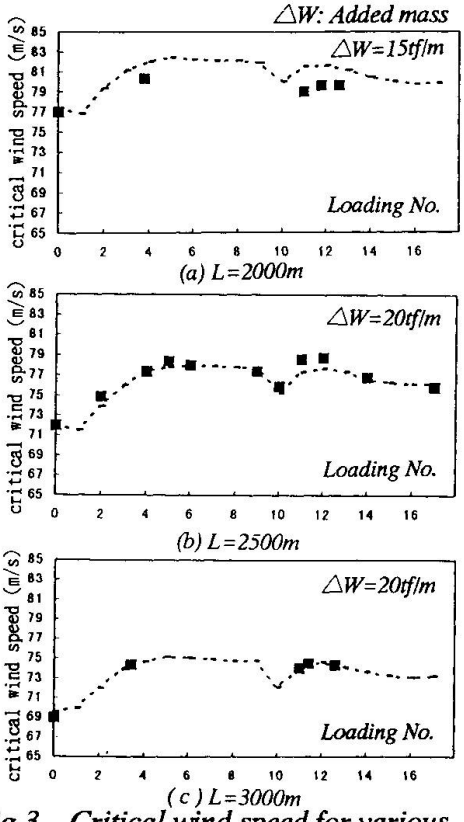

Fig.3 Critical wind speed for various loading conditions

The critical wind speeds of the coupled flutter were analyzed for the 17 cases shown in Fig.2. In the analysis of the flutter of a bridge, the extended Bleich theory and a numerical integration method were employed, as stated in introduction. In Fig.3, all cases were analyzed by the former and some cases were analyzed by the latter method. From Fig.3, the following trends were found:
- Results of both analytical methods show good agreement.
- The maximum increase of the critical wind speed due to the added mass is 6 to 7m/s.
- Cases-4 and 5 and Cases-10 through 13 are configurations with better locations for the added mass, because their critical wind speed are higher and their added mass are less than others.

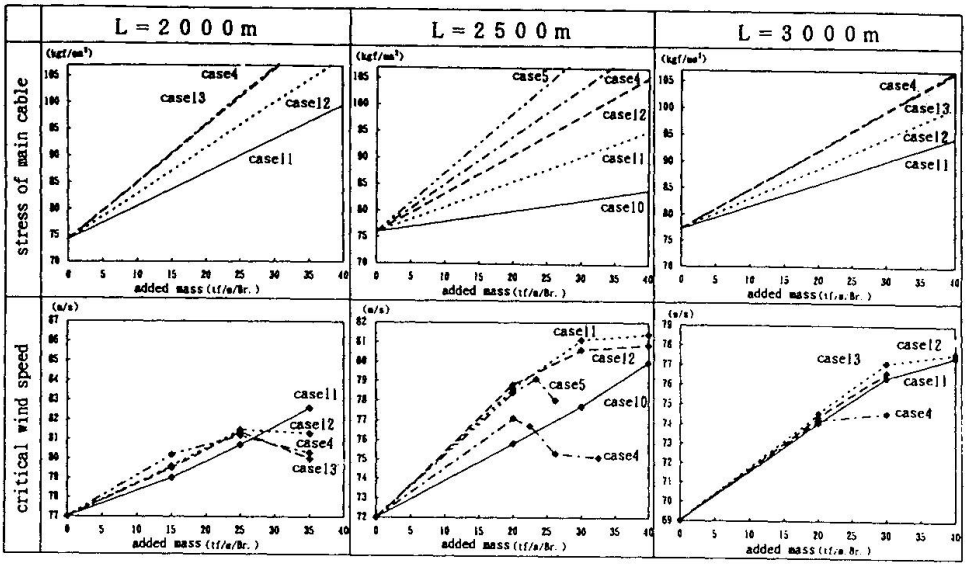

Fig.4 The effect of added mass intensity on the main cable stress and the critical wind speed

The mass intensity of Cases-4 and 5 and Cases-10 through 13 can be increased, because the main cable stresses in these cases are much lower than the allowable stress of Case-9. Then, the effect of increasing added mass intensity on the critical wind speed was investigated, and at the same time, the stress in the main cable was studied(Fig.4). For the analysis, a numerical integration method was used. Reviewing Fig.4, the following results can be noted:
- The increase of added mass intensity doesn't always increase the critical wind speed. For example, the critical wind speed of Cases-4 and 5 for L=2500m tends to decrease from 20tf/m.
- It seems that Case-11 (25% of center span) is the best configuration, because its aerodynamic stability is high and the main cable stress is low.

Based on Fig.4, loading position Case-11 and added mass intensity shown in Table 1 were selected.

2.3 Preliminary Design

After determining the position and intensity of the added mass, the conventional type and the added mass type suspension bridge were designed to find the economic consequences of the added mass method. Table 1 summarizes the results of design investigated. The increase in the critical wind speed was 6~9m/s. And, the decrease in the steel weight of a suspended structure was 9~12%.

L	Added Mass	△V※1	△W※2
2000m	38tf/m/Br.	6.0m/s	-9%
2500m	30tf/m/Br.	9.0m/s	-12%
3000m	40tf/m/Br.	8.6m/s	-11%

※1: Increase of the critical wind speed
※2: Decrease of the steel weight of a suspended structure

Table 1 Main results of design

3. Twin Deck Suspension Bridges

3.1 Suspension Bridges Studied

A suspension bridge with 2500m center span and two 1250m side spans was investigated in order to study the effect of added mass (Fig.5a). Four cables system (Fig.5b) and two cables system (Fig.5 c) were assumed as cable support systems for twin deck. The twin deck serves four lanes.

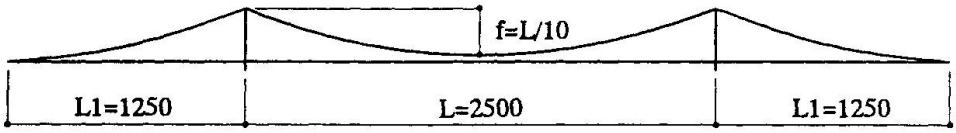

Fig.5a Twin deck suspension bridge (Unit:m)

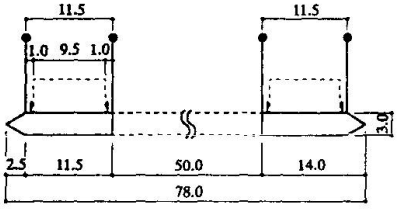

Fig.5b Four cables system

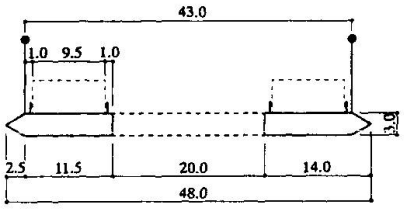

Fig.5c Two cables system

3.2 Analytical Methods

For the calculation of the coupled flutter, the following analytical methods were employed.

METHOD-1 (M-1): This method is quoted from reference [5] which is based on the quasi-steady theory. This theory gives a smaller critical wind speed than the unsteady theory. Air forces are assumed to act on a flat plate.

METHOD-2 (M-2): This method is based on the equation (1) considering Theodorsen's air forces on a flat plate. An underlined term in the equation (1) is the effect of the air force dumping due to pitching.

Unit Dead Load	Cable	tf/m	13.6
	Girder	tf/m	14.0
	Pavement, etc.	tf/m	6.0
	Total	tf/m	33.6
Section Properties	Cable Area A_C	m^2	1.5
	Girder I_X	m^4	1.4
	Girder J	m^4	4.0
Polar Moment of Inertia		$tf \cdot m \cdot s^2/m$	1177

Table 2 Structural condition(/Bridge)

If the aerodynamic interference between the two boxes is completely neglected, the coefficient c equals 1. But, in this case, even though a equals b, namely, D equals zero, an underlined term remains. Accordingly, we give the coefficient c which becomes zero when $D=0$.

$$L = -2sv^2\left[f_1\left(\alpha+\frac{\dot{h}}{v}\right)+f_2\cdot\frac{b}{2v}\cdot\dot{\alpha}\right]$$

$$M = sbv^2\left[f_1\left(\alpha+\frac{\dot{h}}{v}\right)-\left(f_3\cdot\frac{b}{2v}+\underline{f_1\cdot\frac{2a^2}{bv}\cdot c}\right)\dot{\alpha}\right] \quad (1)$$

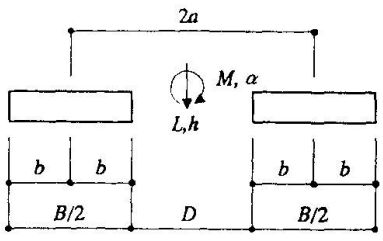

Fig.6 Idealized twin deck

where, L, M: unsteady aerodynamic lift and pitching moment, $f_1=C(k)$, $f_2=1+C(k)$, $f_3=-C(k)$, $C(k)$: Theodorsen function, $s=2\pi\rho b$, ρ: air density, b: semi-chord of a deck, a: semi-distance between deck centers, v: wind speed, h and α: vertical and torsional displacements, c: coefficient for the aerodynamic interference between two boxes ($1-(b/a)^2$ or $1-b/a$).

METHOD-3 (M-3): This method uses the equation (2) quoted from reference[6]. This equation was obtained from the wind tunnel test of twin deck with wind screen.

$$V_F = \left[1+1.2438\cdot\left(\frac{D}{B}\right)^{1.4712}\right]\cdot V_{sel} \qquad (2)$$

where, V_F : the critical wind speed of flutter, V_{sel} : the flat plate critical wind speed obtained from the Selberg formula, D : slot width, B : solid deck width.

In order to find the differences among above methods, calculations were carried out for the two cables system (Fig.5c), using datum shown in Table 2. Fig.7 shows the results of analyses **M-2** and **M-3** about the relationship between D/B and V_F/V_{scl}. Moreover, **M-2.1** and **M-2.2** use [1-(b/a)^2] and [1- (b/a)] for the coefficient c, respectively. Fig.7 shows that **M-2.2** and **M-3** agree well with each other. On the other hand, **M-2.1** shows the excessive value of V_F/V_{scl}, compared with other methods.

For the calculation of the divergence speed, the equation (3) quoted from reference [5] was used.

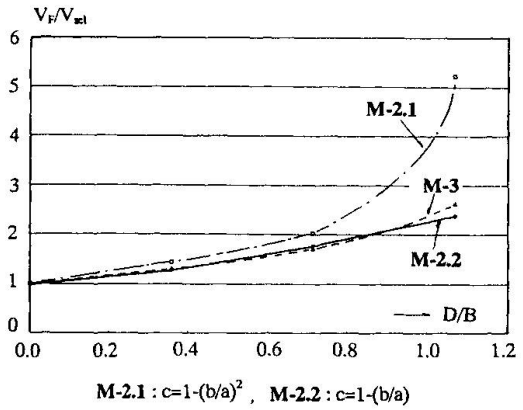

Fig.7 Comparison of flutter analytical methods for two cables system

$$V_D = \omega_t r\sqrt{\mu} \qquad (3)$$

where, V_D : the divergence speed, ω_t : torsion frequency, r : radius of gyration of bridge,

$\mu = \dfrac{m}{4\pi\rho b^2}$, m : mass / unit span.

3.3 Four Cables System

In this system, the bending frequency ω_b nearly equals to the torsion frequency ω_t. It is known that the flutter is eliminated in this case. Fig.8 shows V- δ (wind speed - logarithmic decrement) curves analyzed by **M-1** and **M-2.1**. Both methods never show the flutter and the logarithmic decrement of **M-1** shows smaller values than that of **M-2.1**.

The divergence speed V_D is calculated from the equation (3). V_D of a bridge shown in Fig.5b increases from 63m/s to 77m/s by adding a mass of 16tf/m/Bridge. If V_D of 77m/s is to be accomplished by increasing the length of cross beam, it's length must be increased from 50m to 62m. In this system, A-shaped rigid tower can also increase the bending frequency, and consequently enhance the divergence speed.

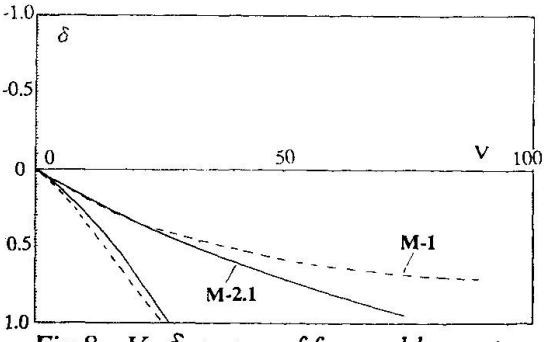

Fig.8 V- δ curves of four cables system

3.4 Two Cables System

In this system (Fig.5 c), the torsion frequency is larger than the bending frequency, because the radius of gyration of bridge r is much smaller than the semi-distance between two main cables. In order to find out the most effective position of added mass in deck for the wind resistant design, V_D and V_F are calculated in 3 cases of added mass position. The changes of V_D and V_F by adding temporary mass (16tf/m) are shown in Table 3. V_F is calculated using **M-3** method. From Table 3, the following results can be noted.

- Added mass affects not only V_D but also V_F unlike four cables system.
- Added mass increases V_D, but the added mass position hardly affects V_D.
- The position of added mass changes V_F, and the value of V_F is the maximum for the Case 1.

Items	Case-0	Case-1	Case-2	Case-3
f_b (Hz)	0.0541	0.0532	0.0532	0.0532
f_t (Hz)	0.0891	0.0912	0.0872	0.0759
f_t / f_b	1.647	1.714	1.639	1.427
V_D (m/s)	70.5	77.3	77.1	77.0
V_F (m/s)	63.5	75.6	72.1	60.7

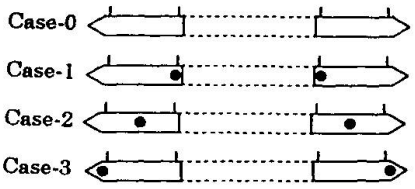

Table 3 Added mass effects for two cables system

4. Conclusion

For single deck suspension bridges, it could be concluded, that

- the middle 25% part of the center span was the most effective position for the temporary mass from the aerodynamic stability point of view.
- this method increased the coupled flutter speed by 6~9m/s for a given condition.
- this method reduced the steel weight of a suspended structure by approximately 9~12%, compared with the conventional method.

For twin deck suspension bridges, it could be concluded, that

- the coupled flutter speeds predicted by the methods **M-2.2** and **M-3** showed good agreement.
- in the case of four cables system, added mass was effective to increase the divergence speed.
- in the case of two cables system, added mass was effective to increase not only the divergence speed but also the coupled flutter speed.

References

[1] Astiz,M.Z. and Andersen, E.Y., On wind stability of very long spans in connection with a bridge across the Strait of Gibraltar, Strait crossing, Ed. J.Krokeborg, Balkema, 1990, pp.257-264.

[2] Ostenfeld, K.H., Innovative structural systems for the Gibraltar strait crossing project, IASS-CSCE International Congress, Toronto, July, 1992, pp.231-242.

[3] Bleich,et al.., The mathematical theory of vibration suspension bridges, Dept. of U.S.Gov.Print Office, 1950.

[4] Bell,A.J. and Brotton,D.M., A numerical integration method for the determination of flutter speeds, Int.J.Mech.Sci.15, 1973, pp.473-483.

[5] Richardson, J.R., The development of the concept of the twin suspension bridge, National Maritime Institute, NMI R125, 1981.

[6] Larsen,A.,Ostenfeld, K.H. and Antiz,M.A., Aeroelastic stability study for the Gibraltar Bridge feasibility phase, 4th Int'l Colloquium on the Gibraltar Strait Fixed Link, May 1995, pp.99-108.

Aerodynamic Stabilisation for Super Long-Span Suspension Bridges

Toshio UEDA
Techn. Supervisor
Hitachi Zosen Co.
Osaka, Japan

Hiroshi TANAKA
Chief Bridge Designer
Hitachi Zosen Co.
Osaka, Japan

Yasuhiro MATSUSHITA
Bridge Designer
Hitachi Zosen Co.
Osaka, Japan

Summary

As the post projects of the Akashi-Kaikyo Bridge, some new projects have been planned to cross straits in Japan by the application of super-long-span suspension bridges. Their center spans will be far above 2000m and a streamlined box deck is thought to be proper for its economy.
In this paper the aerodynamic stabilization of the suspension bridges with streamlined box deck is discussed and it is realized by using the configurations of so called flat box deck (i.e. shallow box deck) with vertical and horizontal stabilizers. The assessment is conducted by the wind tunnel tests and the three dimensional multi-mode flutter analysis. The vertical stabilizer is installed in the center slot of the deck and the horizontal stabilizers are also attached on both upper, lower of leading and rear edges of the deck. Then the deck is aerodynamically stable up to the proposed design wind speed at the deck height (i.e.,80m/s).

1. Introduction

Generally speaking bridge decks are classified into two types; truss and streamlined box ones. Since the well known collapse of the Original Tacoma Narrows Bridge in 1940, the truss decks have been applied to almost suspension bridges mainly in the United States and Japan. On the contrary, the streamlined box decks have been prevailed in England and so on. In Japan these two choices have been assessed in feasible studies in almost cases executing wind tunnel tests. Akashi-Kaikyo Bridge was determined to have the truss deck with a vertical-stabilizer installed at the center of the deck in the center span. Thus the bridge is stable in Akashi-Straits where the locations are susceptible to typhoon winds and the design wind speed (i.e.,V_{10}=43m/s) is relatively higher in Japan. The application of a streamlined box deck was also examined however an appropriate one could not be found to reach the design speed without any aeronautical problems (e.g., flutter, buffeting and vortex induced vibrations).

For the post Akashi-Kaikyo Bridge project, super-long-span suspension bridges are being proposed and their center span will be longer than about 2,250m. The application of streamlined box decks is predominant to these projects for their economy: the labor cost of workers and the financial condition of the government compel this choice.

This paper presents the aerodynamic stabilization for super-long-span suspension bridges by using vertical and horizontal stabilizers. The research was carried out by the wind tunnel experiments and the multi-mode flutter analysis.

2. Application of Stabilizers

A vertical stabilizer (i.e., V.S.) is the effective device to enhance the flutter speed. Therefore Akashi-Kaikyo Bridge has installed it in the center span as shown in Fig.1. The stabilizing mechanism of the vertical stabilizer for the truss deck is as follows[1]:

1) According to the flow visualization and the pressure distribution measurement around the deck at rest, the separated flow at the leading edge of the deck re-separates at the bottom edge of the V.S. and the upward flow is increased by the existence of the V.S. As a result of them, the negative pressure becomes large at the deck in the downstream. The pressure recovery is also observed at the trailing edge of the top surface of the deck in the

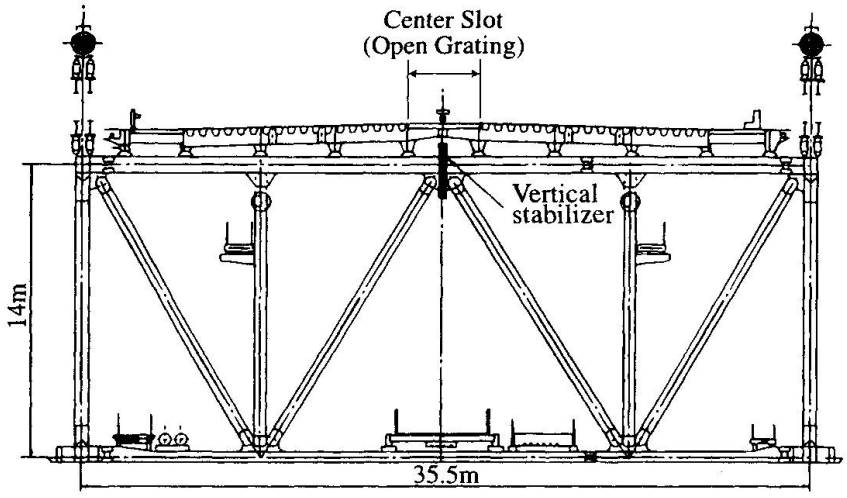

Fig. 1 The Vertical Stabilizer of the Akashi-Kaikyo Bridge in the center span

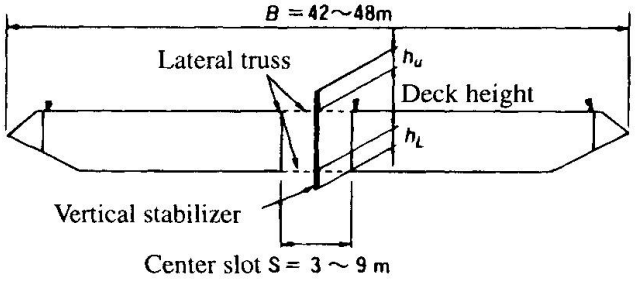

Fig. 2 Investigeted flat box girder

downstream. These phenomena become the stronger as the angle of attack becomes the larger. The absolute values of the lift coefficient with the V.S. become smaller than those without the V.S.

2) According to the flow visualization and the pressure distribution measurement around the deck in motion, the flow under the deck re-separates at the bottom edge of the V.S. and the upward flow is increased in the center slot at the middle of the deck. Then the damping force is created at the bottom surface in the downstream.
3) It is emphasized that the center slot in the middle of the deck plays the significant role for the improvement of the aerodynamic stability.

The authors proposed the application of the V.S. for a tapered box deck [2]. The center slot was made in the middle of the deck and the V.S. and lateral truss were installed there. The lateral truss retains the torsional rigidity of the deck (Fig.2). This method has been extended for the aerodynamic stabilization of the proposed super-long-span suspension bridge in this study.

3. Aerodynamic Stabilization

3.1 Objected Models

The proposed super-long-span suspension bridges namely the objects of this study are shown in Fig.3. The dynamic properties of the objected suspension bridges are shown in Table 1 and they were used for the section model tests.

3.2 Test Results

As the preliminary tests, deck height of 3, 5 and 7m were examined with changing a center slot

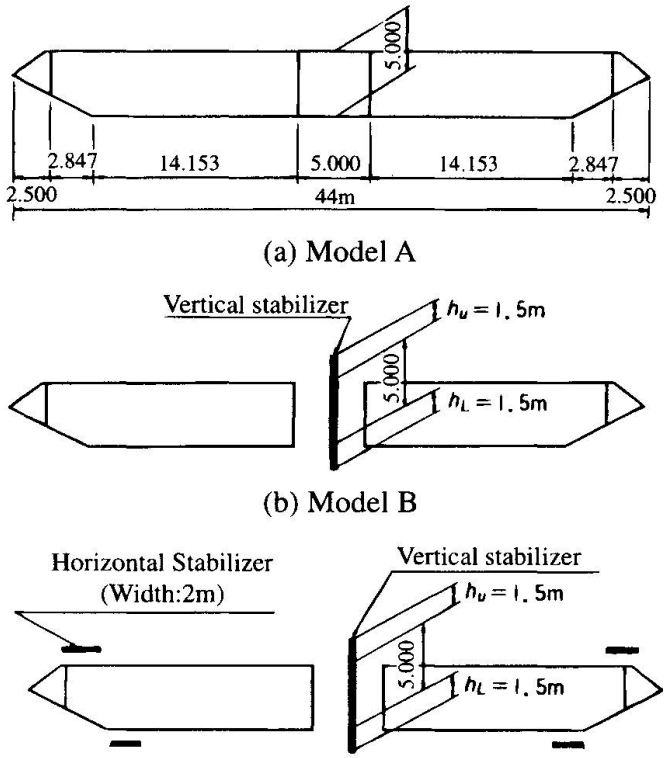

Fig. 3 Flat box girder with 5m depth and 5m center slot width

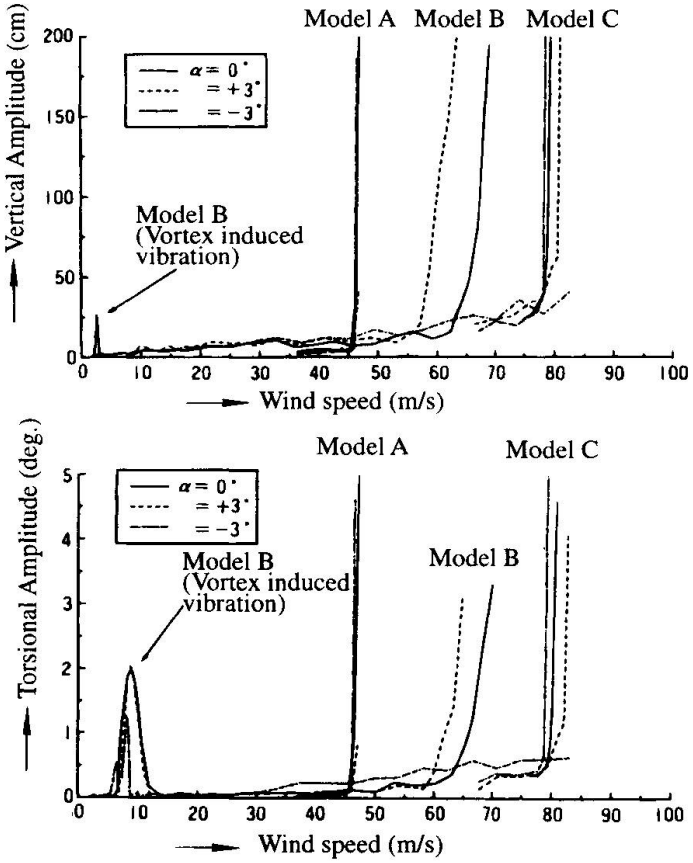

Fig. 4 Comparison of aerodynamic responses among model A, B and C

width from 3 to 5,7,9m. At the same time the height of h_U and h_L shown in Fig.2 were changed. It was found that the model B is the most aerodynamically stable when the deck height of 5m with a center slot width 5m and the V.S.($h_U = h_L$=1.5m) in Fig.3 The aerodynamic responses of the model B is shown in Fig.4 where the coupled flutter speeds of α (i.e., angle of attack) = 0 and 3 degree are 66 and 62m/s respectively. The flutter did not occurred below the wind speed of 82.5 m/s at α = -3 degree. Though the vortex induced vibrations occurred at 2~3 m/s in vertical bending vibration and at 7~9 m/s in torsional one in the laminar flow tests, they disappeared in the turbulent flow with the 10% intensity of turbulence. These vibrations seem to be due to the existence of the V.S. however the test result indicates that the amplitudes of them will be very small in natural winds.

Table.1 Dynamic Properties of the Studied Suspension Bridges

The objected bridges / Deck Types / Dimensions		The objected suspension bridge (1250m+2500m +1250m)	The proposed suspenson bridges for Akashi-kaikyo project (960m+1,990m+960m)		
		Flat box deck (44m×5m)	Truss deck	Flat box deck	
			33.5m×14m	46m×7m	46m×5m
Mass(tf/m) (Cable+hanger+deck)		38.2	43.5	44.7	42.8
Mass moment(tf.m.s^2/m) (Cable+hanger+deck)		869	1,199	1,128	1,103
Frequency (Hz)	Vertical freq.	0.0523	0.0606	0.0608	0.0606
	Torsional freq.	0.133	0.152	0.176	0.150
Frequecy ratio		2.55	2.51	2.90	2.48

3.3 Application of Horizontal Stabilizer

The flat plate corner vane which we call "horizontal stabilizer" was introduced in addition to the vertical stabilizer to enhance the flutter speed as shown in Fig.3 (Model C). This device was originally invented by Sato et.al [3]. However the simultaneous application of vertical and horizontal stabilizers was the first trial and the results of the section model tests seem to be almost satisfactory as shown in Fig.4: The flutter speeds are almost 80m/s at α = -3, 0, +3 degree respectively without vortex induced vibrations.

3.4 Multi-Mode Coupled Flutter Analysis

The result of the section model tests does not always guarantee the aerodynamic stability of the long-span bridges. Therefore the multi-mode coupled flutter analysis is indispensable to its assessment[4]. In applying this analysis, the position shift of the bridge axis (i.e., bridge camber) was considered because under strong winds the bridge axis of long span bridges will have relatively large lateral displacements and torsional ones in the deck and cables. These incidents change not only the natural frequency but also the angle of attack to winds. These shifts were named "camber change" here and were taken into account for the flutter analysis. The derivatives which are defined as the following Eq.1 were measured and used for the analysis in accordance with the angle of attack by the camber change.

$$\left.\begin{aligned} L &= 1/2\,\rho\,V^2B\,[k\cdot H_0^*\cdot \dot{s}/V + k\cdot H_1^*\cdot \dot{h}/V + k\cdot H_2^*\cdot B\cdot \dot{\alpha}/V + k^2\cdot H_3^*\cdot \alpha + k^2\cdot H_4^*\cdot h/B + k^2\cdot H_5^*\cdot s/B] \\ M &= 1/2\,\rho\,V^2B^2\,[k\cdot A_0^*\cdot \dot{s}/V + k\cdot A_1^*\cdot \dot{h}/V + k\cdot A_2^*\cdot B\cdot \dot{\alpha}/V + k^2\cdot A_3^*\cdot \alpha + k^2\cdot A_4^*\cdot h/B + k^2\cdot A_5^*\cdot s/B] \\ D &= 1/2\,\rho\,V^2A\,[k\cdot P_0^*\cdot \dot{h}/V + k\cdot P_1^*\cdot \dot{s}/V + k\cdot P_2^*\cdot B\cdot \dot{\alpha}/V + k^2\cdot P_3^*\cdot \alpha + k^2\cdot P_4^*\cdot h/B + k^2\cdot P_5^*\cdot s/B] \end{aligned}\right\} \cdots (1)$$

Where,

L, M, D : Unsteady lift, moment and drag force

ρ : Air density

V : Wind velocity, $k = 2\pi f B/V$

B : Deck width

f : Frequency of forced vibration

$h \cdot \alpha \cdot s$: Amplitude of heave, rotation and sway motion in forced vibration

The forced vibration method was applied to measure the above-mentioned eighteen flutter derivatives by using a newly devised machine. The examples of the measured flutter derivatives are compared with the ones expressed by Theodorsen's function in Fig.5. The Model A in Fig.3 has no center slot (i.e., the closed section) and the flutter derivatives are resemble to those obtained by the Theodorsen's function as shown in Fig.5. Fig.6 shows the result of the analysis with/without the camber change. Though these differences between with/without the camber change were not large among both cases, the flutter speeds of Model C are almost 80m/s and

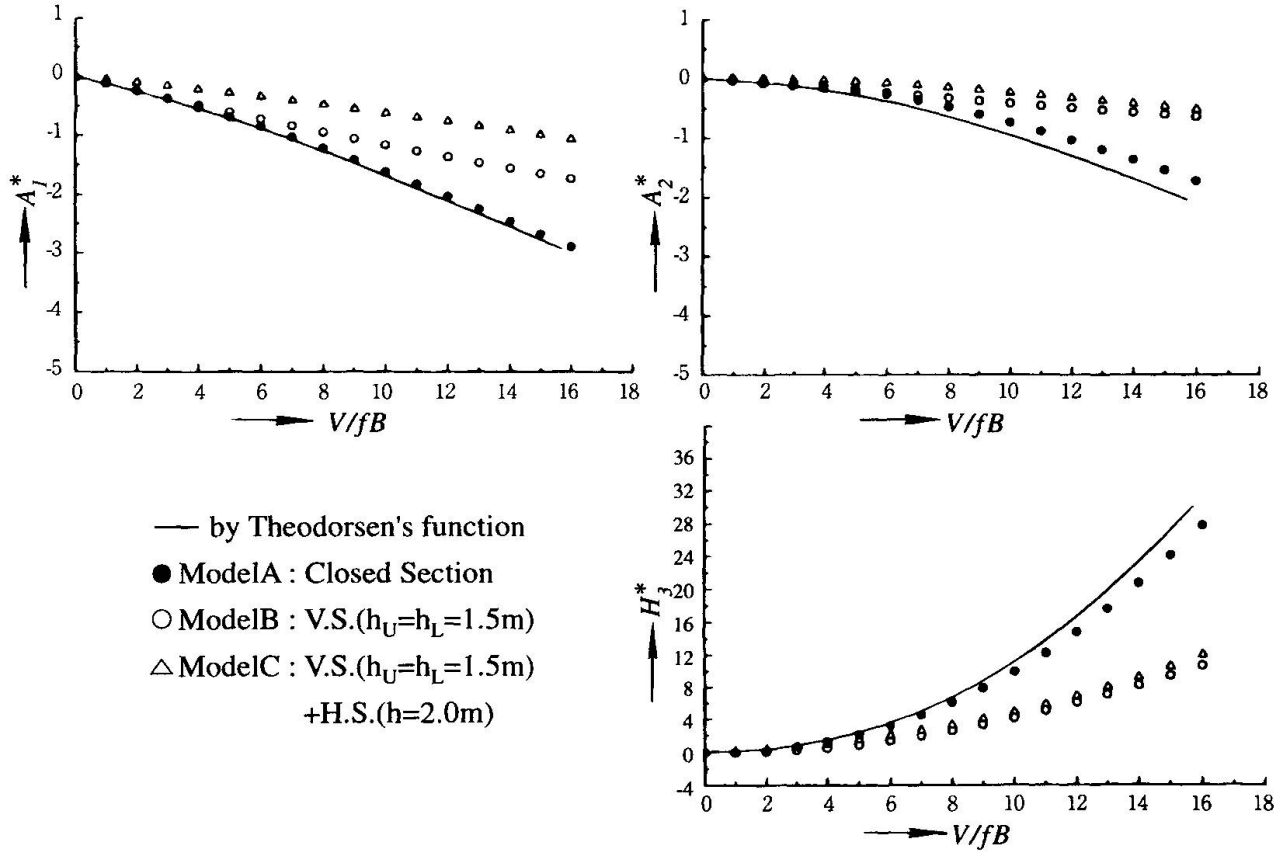

Fig. 5 Examples of Flutter Derivatives (Model A, B, C)

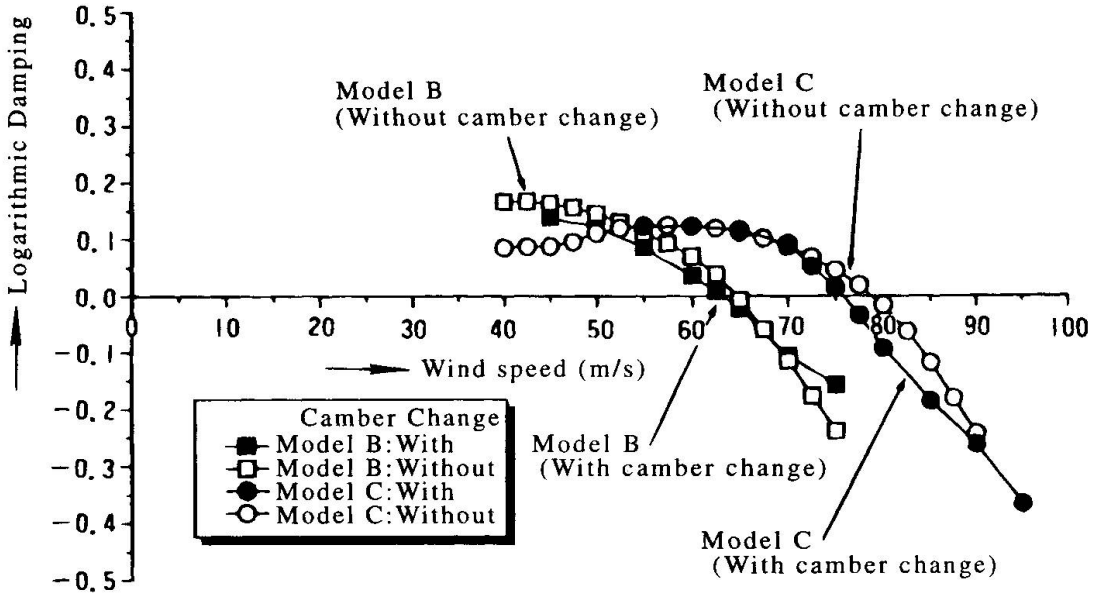

Fig. 6 3-D multi-mode coupled flutter analysis in case of section B and C

fulfill the design goal.

4. Conclusions

The aerodynamic stability of the super-long-span suspension bridges with the center span of 2,500m were assessed. The configuration of the deck is the flat box with six traffic lanes. The installation of the vertical stabilizer in the center slot and that of the horizontal stabilizer on both upper, lower leading and rear edges of the deck are very effective to enhance the flutter speed. It is ensured by the wind tunnel tests and multi-mode coupled flutter analysis.

This study was conducted as the cooperative research for the committee of "Joint Research on Development of Wind-Resistant and Economical Design of Super-Long-Span Bridges." Authors express their sincere appreciations to the members of the committee for their valuable discussions.

References

[1] Ueda, T., Yasuda, M. and Nakagaki, R., "Mechanism of Aerodynamic Stabilization for Long-Span Suspension Bridge with Stiffening Truss-Girder, " *J. of Wind Engineering*, No.37, JWE, pp.477-484, October 1988

[2] Tanaka, H., Yamamura, N. and Ueda,T., "Design of Super-Long-Span Suspension Bridge Based on Aerodynamics," *Bridges into the 21st Century*, October 1995, Hong Kong

[3] Sato, H., Toriumi, R. and Kusakabe, T. et al., "Flutter Characteristics of Box Decks with Slot Holes," *No. 50th Annual Convention of JSCE*, I-681, September 1995

[4] Tanaka, H., Yamamura, N. and Shiraishi, N., "Multi-Mode Flutter Analysis and Two & Three Dimensional Model Tests on Bridge with Non-Analogous Modal Shapes," *J. Struct. Mech. Earthquake Eng.*, No.471/I-24, JSCE, pp.71-82, July 1993

Stochastic Modelling of Traffic Loads for Long-Span Bridges

Pietro CROCE
Assist. Prof.
Dept of Structural Eng.
Pisa, Italy

Pietro Croce, born in 1957, got his PhD degree in 1989. He is assist. prof. of Structural Eng. at the Univ. of Pisa. He is involved in several researches on bridges, fatigue and damage, reliability, fire resistance and vibration control.

Walter SALVATORE
Res. Eng.
Dept of Structural Eng.
Pisa, Italy

Walter Salvatore, born 1966, got PhD degree in 1997. He is involved in several researches regarding bridges, fatigue, safety of civil structures, damage in reinforced concrete structures, vibration control.

Summary

Load traffic models usually given in the Codes cannot be used for the design of long-span bridges, because they result too much severe when the span length is bigger than 200 m. For this reason the evaluation of traffic loads on long span bridges requires special studies, based on probabilistic concepts, leading to suitable numerical procedures. In the paper a theoretical stochastic traffic model, based on special vehicles (super-vehicles), representing convoys crossing simultaneously the bridge, is illustrated. Numerical examples, illustrating the application of the model to a cable-stayed long-span bridge, show the potentiality of the model to describe effects induced by traffic running on one or in several lanes.

1. Introduction

The design of long-span bridges requires special preliminary studies devoted to define suitable load traffic models. In fact, the load traffic models usually given in the modern Codes, intended to be used properly for the most common bridge types, whose span length is lesser than 200 or 300 m, result too much severe for long span bridges, which are highly sensitive to the magnitude of traffic loads.

The evaluation of traffic loads on long span bridges is generally based on probabilistic concepts, leading to numerical procedures, in which traffic samples, representing as well as possible the expected traffic on the bridge, are suitably handled according to reasonable deterministic traffic scenarios, in order to obtain the characteristic values of the relevant effects. Obviously, this procedure becomes more and more unsatisfactorily when, rather than the effects induced by the traffic running on one single lane, multi-lane traffics or combination of traffic loads with other action of different nature, for example, wind or temperature, must be taken into account, mainly because it is very difficult to foresee reasonable traffic scenarios, including jammed and flowing vehicle convoys of considerable length. Beside that, when geometric non-linearity effects become significant, further difficulties occur, as the effects cannot be superimposed and the whole set of vehicles running simultaneously on the bridge must be considered.

To solve the problem, a new theoretical stochastic traffic model is proposed, which allows to represent in a very general way traffic scenarios on one or several lanes, using the general results

of the stochastic process theory.
The model illustrated in the following is a further development of the one, based on an equilibrium renewal process of vehicle arrivals, previously proposed by the Authors [1] for pre-normative research studies. The theoretical method has been already validated [1] through an analytical-numerical procedure, starting from the traffic data recorded in Auxerre, used for the calibration of load models of EC1-part 3 [2], comparing the extreme values obtained with the proposed model with the target ones, for a wide set of different bridge schemes, spanning up to 200 m.
The traffic model needs some improvement to be extended to long span bridges, in particular to surmount the difficulties concerning the vehicle distribution and the treatment of second order effects.
At present, the problem has been completely solved as illustrated in the following, for all cases in which second order effects can be disregarded, introducing some kind of special vehicles (super-vehicles), representing convoys crossing simultaneously the bridge, while solution for bridges sensitive to geometric non-linearity requires further studies.
The solution has been found by means of a two step method, very similar to those described in [1] for span length up to 200 m. Provided that in long span bridges the traffic effects depend on the equivalent uniformly distributed load, the first step of the method consists in the set up, according to the aforesaid procedure, of some kind of super-vehicles, each one representing one long convoy (up to 200 m long), associated with the suitable PDF of its length and of its uniformly distributed weight. The super-vehicles so determined are then used in the second step to assemble super-convoys, which substitute convoys for long span bridge analysis. In this way the sensitivity of the results on the assumption concerning the intervehicle distance is strongly reduced: in fact, because intervehicle distance concerns only very long vehicles (the super-vehicles), its effect on the EUDL is practically insignificant, even if it varies in a wide range.
Numerical examples, illustrating the application of the model to a cable-stayed long span bridge, show the potentiality of the method.

2. The Theoretical Traffic Model

To represent reliably the traffic, satisfying at the same time the physical condition that the distance between two consecutive vehicles cannot be smaller than a limit value, depending on the vehicles themselves, the theoretical traffic model [1] has been derived assuming a stationary ergodic arrival process of vehicles, each one characterised by its own probabilistic distribution of length and total weight, described by a suitably modified equilibrium renewal process, so that the time interval between two consecutive arrivals is given by

$$f(x) = \int_{l_{min}}^{l_{max}} t(l) \cdot \sum_i (p_i \cdot b_i(l)) dl \qquad (1)$$

in which t(l) is the truncated distribution of the intervehicle distance, $b_i(l)$ is the truncated distribution of the length of the i-th standard vehicle, whose frequency is p_i, and l_{min} and l_{max} are the extreme values of the vehicle lengths.
Clearly, the geometry and the main statistical properties of each standard vehicle depend on the expected traffic and they should be chosen to fit at the best the real traffic.
The probability $P_n(l_c, L)$ that a lonely n-vehicles convoy of length l_c is travelling on the bridge length L (see fig. 1) is then given by

$$P_n(l_c, L) = \int_0^{L-l_c} \frac{\Im(y)}{\mu} \cdot \int_0^{l_c} f_n(x) \cdot \Im(L-x) \cdot dx \cdot dy + \int_{L-l_c}^{L} \frac{\Im(y)}{\mu} \cdot \int_0^{L-y} f_n(x) \cdot \Im(L-x) \cdot dx \cdot dy \qquad (2)$$

being $f_n(x)$ the n-th convolution of (1), $\Im(x)$ the survival function and μ the mean arrival rate. On the other hand, from the mechanical point of view, because the bridge behaves like a filter, converting the traffic process in the extreme effects process, each part of the time history of the

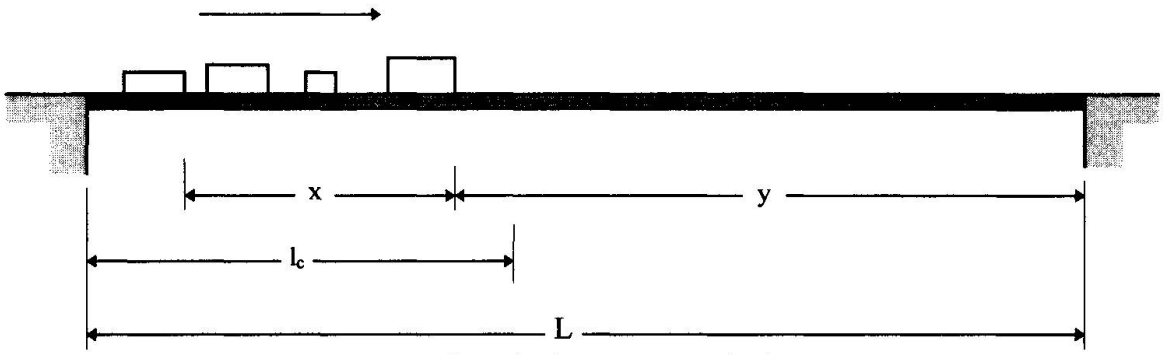

Fig.1 - Transit of a vehicle convoy on the bridge

actions on the structure can be considered as the consequence of the transit of an appropriate convoy, composed by one or several standard type vehicles, characterised by its length and its composition, in such a way that each convoy can be associated to the maximum value of the part of the history related to it. As the length L_e of the relevant loaded area of the bridge increases, the effects are governed mainly by the uniformly distributed weight of the convoy, being quite independent on the individual axle load values; so that the transfer function T, which relies the maximum effect induced by the convoy to its the uniformly distributed weights, depends only on the total length l_c of the convoy and on the total length L of the bridge. In particular, when second order effects can be disregarded, $T(L,l_c)$ can be derived from the knowledge of the ordinates $\eta(x)$ of the relevant influence line,

$$T(L,l_c)=\max_{0\le t<L-l_c}\left(\int_t^{t+l_c}\eta(x)\,dx\right),\quad l_c\le L. \tag{3}$$

On the other hand, the distribution of the total weight of an n-vehicles convoy can be determined through the convolution of the PDFs of the total weight of each individual vehicle of the convoy itself. Being m the total number of vehicles of the standard set and $\rho_i(W)$ the PDF of the total weight of the i-th standard vehicle, the PDF $\rho^{(1)}(W)$ of the total weight W of one vehicle results

$$\rho^{(1)}(W)=\sum_{i=1}^{m}p_i\cdot\rho_i(W), \tag{4}$$

while the PDF $\rho^{(n)}(W)$ of the total weight of an n-vehicles convoy is expressed by

$$\rho^{(n)}(W)=\sum_{\omega_i\in\Omega^n}\left[\frac{\prod_{s=1}^{n}p_{i_s}}{\sum_{\omega_j\in\Omega^n}\prod_{k=1}^{n}p_{j_k}}\cdot\rho_{\omega_i}(W)\right],\qquad \omega_i=(i_1,i_2,.....,i_n), \tag{5}$$

where the sums are extended to all the possible choices of n vehicles in a set of m, the products are extended to all the n vehicles of the convoy and $\rho_{\omega_i}(W)$ is the convolution of the PDFs $\rho_{i_s}(W)$.

Obviously, this procedure is independent on the length L, but it becomes very cumbersome and time expensive, as the number of vehicles or the length of the convoy, i.e. the number of convolutions, increases. Nevertheless, the procedure can be considerably simplified introducing some kind of super-vehicle, representing convoys whose length is lesser than an assigned value l^*, for example 100 m or 200 m, which is a convenient fraction of the relevant length L. The

significant parameters concerning the super-vehicle can be then easily derived, using the formulae given above, pointing out that the distribution $w_{sv}(W)$ of the total weigth W of the super-vehicle itself is given by

$$w_{sv}(W) = \frac{\sum_{i=1}^{r} \int_0^{l^*} P_i(l_c, l^*) \cdot dl_c \cdot \rho^{(i)}(W)}{\sum_{i=1}^{r} \int_0^{l^*} P_i(l_c, l^*) \cdot dl_c}, \tag{6}$$

where $\int_0^{l^*} P_i(l_c, l^*) \cdot dl_c$ represents the CDF, evaluated according (2), of the transit of a lonely i-vehicles convoy on the given length l^* and $\rho^{(i)}(W)$ is the PDF (5) of its weight, while r is the maximum number of vehicles in l^*.

Obviously, in this way all the convoys whose length is lesser than l^* are considered as a single fictitious vehicle, the *super-vehicle*, characterised by the length l^* and the weight distribution $w_{sv}(W)$. The supervehicle can be then introduced in the standard vehicle set, provided that the annual flows of the standard vehicles are suitably rearranged in order to maintain unchanged the annual traffic flow. The general procedure can be then applied, considering the significant length of the influence surface L, to the so modified standard vehicle set, in such a way that, using properly formulae (1), (2), (4) and (5), the characteristic parameters of new convoys, the *super-convoys*, are obtained.

The PDF $f_m(\xi)$ of the maximum value ξ of the considered effect, induced by the given traffic running on one lane, is so

$$f_m(\xi) = \sum_{i=1}^{s} \int_0^{L} \left[\overline{P}_i^*(L, l_c) \cdot \overline{\rho}^{(i)}(W) \cdot \frac{l_c}{T(L, l_c)} \right] \cdot dl_c, \qquad W = \frac{\xi \cdot l_c}{T(L, l_c)}, \tag{7}$$

where $\overline{P}_i^*(L, l_c)$ is the probability that an l_c-long lonely i-vehicles super-convoy is on L, $\overline{\rho}^{(i)}(W)$ is the PDF of the total weight of the i-vehicle super-convoy and $T(L, l_c)$ is the transfer function, expressed by (3).

At this point, it must be emphasised that appropriate input traffic data should take into account various scenarios, including both flowing and jammed traffics. Since flowing traffics only can be directly derived from traffic measurements, jam situations, characterised by reduced intervehicle distances and even by the rise of the percentage of the heavy vehicles, are artificially modelled, introducing reasonable a priori hypotheses and manipulating the data records accordingly [2], [3], so that a general representation of the actual traffic can be obtained, mixing suitable percentages of flowing and jammed traffic.

Said q_1 and $q_2=(1-q_1)$, respectively, the probabilities of the flowing and jammed reference traffics and $f_{m1}(\xi)$ and $f_{m2}(\xi)$ the PDFs of their extreme effects, the general PDF $f_{gm}(\xi)$ of the maxima induced by traffic running on one lane results

$$f_{gm}(\xi) = q_1 \cdot f_{m1}(\xi) + q_2 \cdot f_{m2}(\xi), \tag{8}$$

and the CDF of the maxima $F_\tau(\xi)$ in an assigned return period τ is then obtained, starting from the CDF of $f_{gm}(\xi)$, $F_{gm}(\xi)$, using the usual formula of the statistics of extreme

$$F_\tau(\xi) = [F_{gm}(\xi)]^{N(\tau)}, \tag{9}$$

in which $N(\tau)$ represents the total number of lonely super-convoys crossing the bridge on the given lane, in the time interval τ.

The general PDF $f_{gm}(\xi)$ represents the theoretical solution of the problem, even if it can be

evaluated only numerically. In fact, the PDFs of the maxima induced by traffic on several lanes as well as those concerning the combinations of the traffic actions with actions of different nature can be evaluated, as soon as the relevant PDF $f_{gm}^{(i)}(\xi)$ for each lane is known. Of course, the evaluation of the PDFs pertaining to traffic combinations on two or more lanes can be evaluated through the convolutions of the relevant $f_{gm}^{(i)}(\xi)$, provided that the number of super-convoys travelling simultaneously on the considered lanes can be determined, for example using the formulae derived in previous studies [4].

3. Numerical Application of the Model

The theoretical procedure described above has been used to determine the characteristic values of traffic effects in several relevant cross sections of the long span cable-stayed concrete bridge, illustrated in fig. 2. The four lane bridge is characterised by a total length of about 575 m, a central span of about 440 m and a total width of the cross section of about 26 m, while the 130 m height Y-shaped pylon is made in concrete, except the upper part, which is made in steel. The static behaviour of the bridge subject to the traffic loads is sensibly linear.
The analysis has been carried out using the Auxerre traffic, previously assumed as reference traffic for the calibration of load models of EC1.3 [2], [5] by reason of its very aggressive composition: in fact, on the basis of the present trends, Auxerre traffic represents the natural evolution of the long-distance commercial traffic in continental Europe.

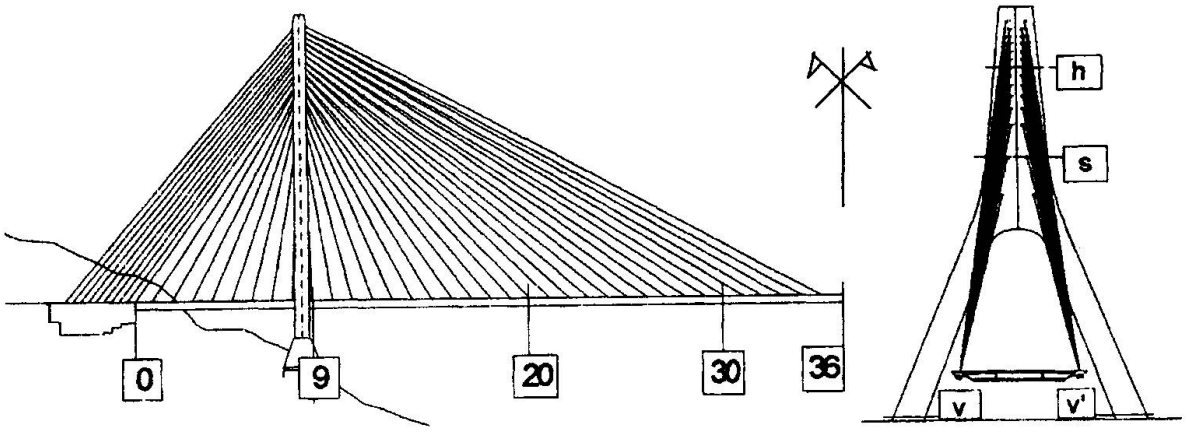

Fig. 2 – Cable stayed bridge

The effects which has been considered in the simulation refer to axial forces S in stays n. 5, 9, 15, 20, 25, 30 and 35 and in the anchor stays n. 1 and 10, as well as axial forces N, bending moments M, shear forces V and torque T in the relevant section 0, 9, 20, 30, 36 (the number correspond to the stay ordering) of the girder and in the relevant sections h, s, v and v' of the pylon, as indicated in fig. 2, considering one or two loaded lanes, with a jammed traffic percentage of 20%. Of course, effects characterised by base length of the influence surface lesser than 200 m has been disregarded, because they are just covered by the model proposed in [1].
In the figures 3÷8 are reported some significant influence surfaces, concerning, in particular, the axial forces N in the stay n. 35 (fig. 3) and in the anchor stay n. 1 (fig. 4), the bending moments M in the box girder at the midspan (fig. 5) and at the support (fig. 6), as well as the torque T at the support of the box girder, (fig. 7), and the axial force N in the cross section s of the pylon (fig. 8).
In order to present in a comprehensible way the whole set of the theoretical results, it has been decided to determine the equivalent uniformly distributed load (EUDL) to be considered on the

notional lane, 3 m width, together with the corresponding axle loads of the EC1.3, to reproduce the characteristic effects, characterised by a return period of 1000 years, determined with the proposed method.
The EUDL so determined are shortly summarised, depending on the base length of the influence surface, in figures 9 and 10, concerning the first and the second lane, respectively. It must be noted however, that the second lane effects are evaluated as difference between the total effects induced by two-lane traffics and the effects induced by the traffic on the main lane.

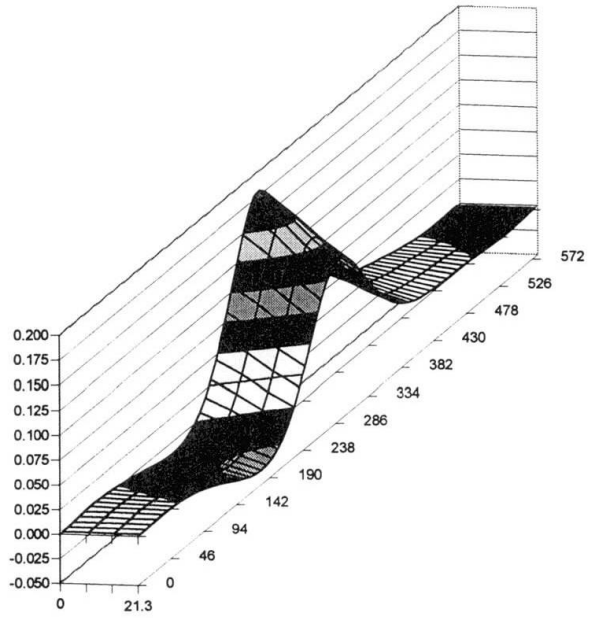

Fig. 3 – Influence surface of axial force N in the stay n. 35

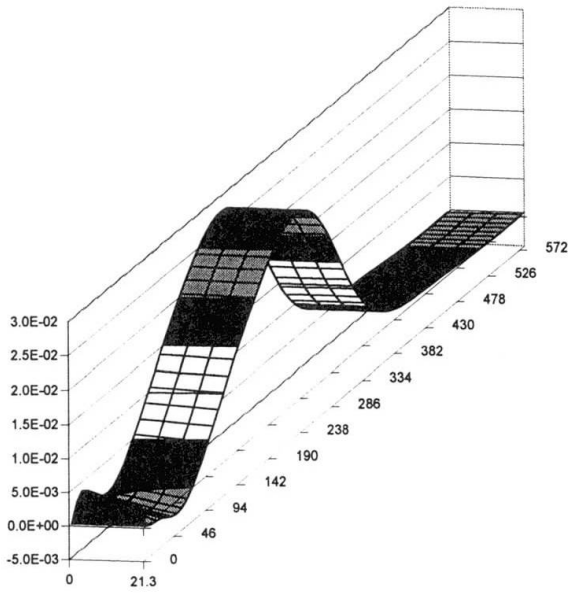

Fig. 4 – Influence surface of axial force N in the anchor stay n. 1

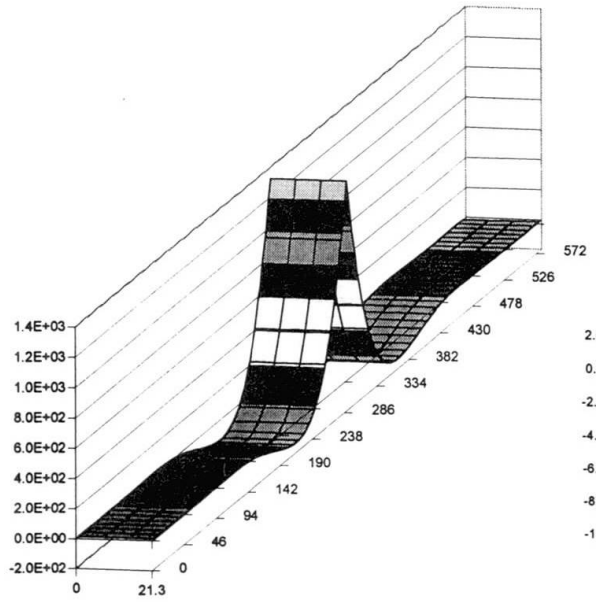

Fig. 5 – Influence surface of bending moment M at midspan (section n. 36)

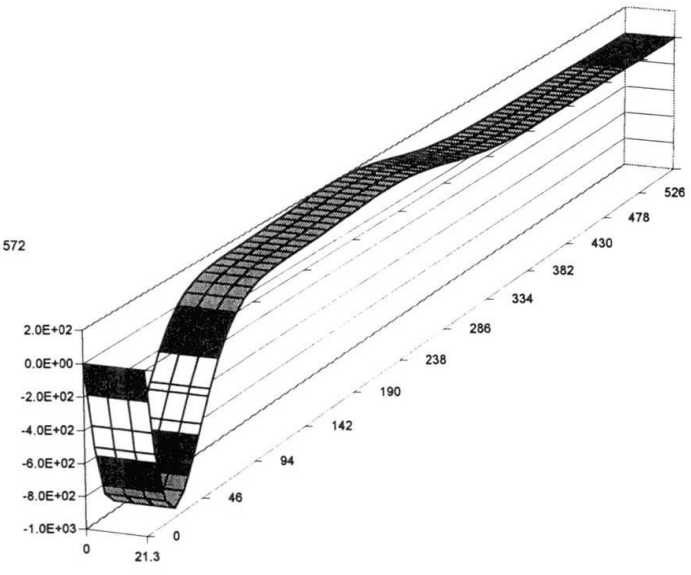

Fig. 6 – Influence surface of bending moment M at the support (section n. 0)

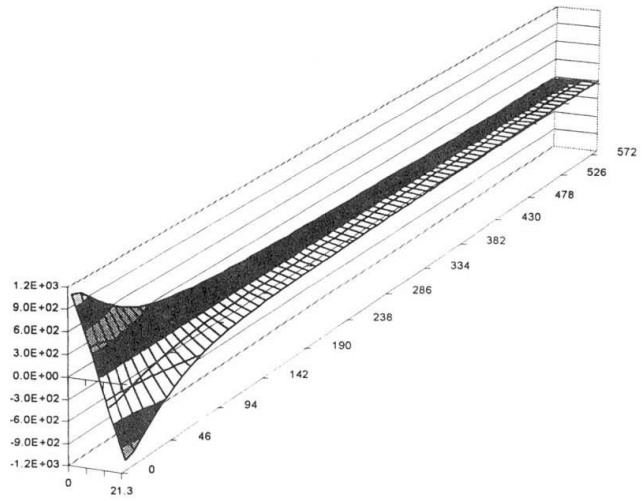

Fig. 7 – Influence surface of torque T at the support (section n. 0)

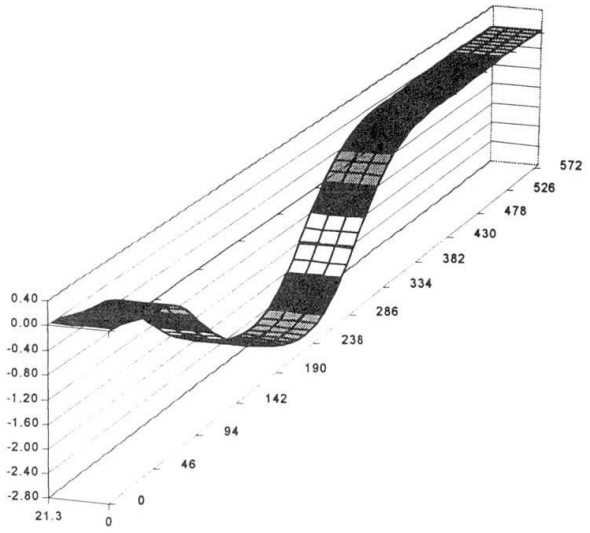

Fig. 8 – Influence surface of the axial force in the pylon (section s)

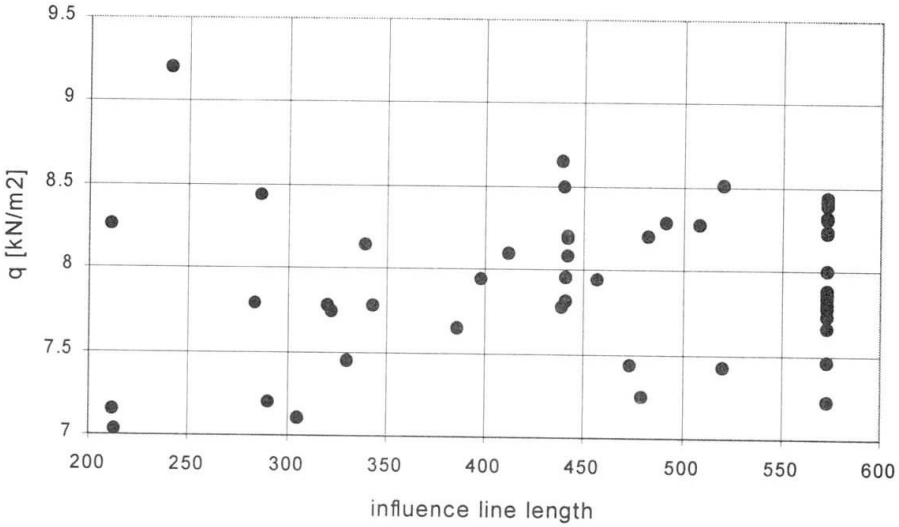

Fig. 9 – EUDL on the first lane vs base length of the influence lines

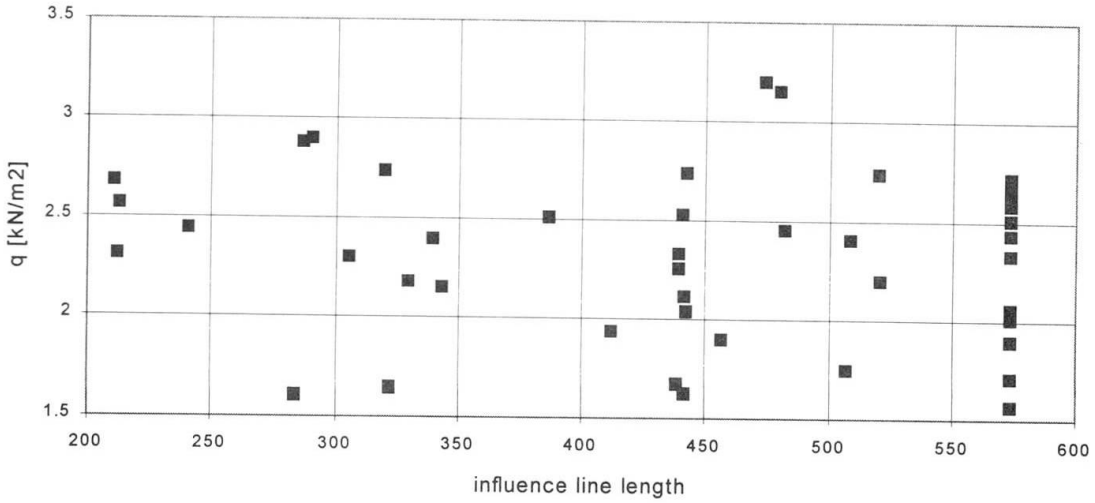

Fig. 10 – EUDL on the second lane vs base length of the influence lines

Obviously, as expected, the EUDL values are scattered, since a big number of effects, N, M, T and V, characterised by different shapes of the influence surfaces are simultaneously considered in the diagrams, so that the definition of some kind of target values requires further analyses, which are out of the scope of the present paper, to optimise the EUDL versus influence line length functions. Nevertheless, it clearly appears that the EUDL values tend to reduce increasing the base length.

5. Conclusions

A refined stochastic model to evaluate theoretically the probability distribution function of the extreme values of the traffic induced multilane effects in long span bridges has been presented. The procedure, which is based on the stochastic process theory, is a considerable improvement of the previous one concerning short and medium span bridges, proposed by the Authors in [1].
The main feature of the method consists in the introduction of special vehicles (super-vehicles) and special convoys (super-convoys), allowing to reproduce very easily probabilistic traffic scenarios including free flowing as well as jammed traffic, which can happen during the bridge life, under arbitrarily assigned traffics.
The fully developed numerical example, concerning a long span cable stayed concrete bridge, emphasise the possibilities of the method.
At present, the method cannot be applied to bridges which are sensitive to second order effects, further developments are still in progress to consider these cases too.

References

[1] Croce, P., Salvatore, W,: Stochastic Modelling of Traffic Loads for Multilane Effects Evaluation, *Proceedings of the ESREL '97*, Lisbon, 1997.
[2] Bruls, A., Croce, P., Sanpaolesi, L., Sedlacek, G., ENV 1991 - Part 3: Traffic loads on bridges. Calibration of road load models for road bridges, *IABSE Colloquium, Basis of Design and Actions on Structures*, Delft, 1996.
[3] Bruls, A., Mathieu, A., Calgaro, J., Prat, M., ENV 1991 Part 3: The main models of traffic loads on road bridges - Background studies, *IABSE Colloquium, Basis of Design and Actions on Structures*, Delft, 1996.
[4] Croce, P., Vehicle interactions and fatigue assessment of bridges, *Iabse Colloquium, Basis of Design and Actions on Structures*, Delft, 1996.
[5] CEN, European Committee for Standardisation, *ENV1991-3:1994 - Eurocode 1: Basis of design and action on structures - Part 3: Traffic loads on bridges*, 1994.

Höga Kusten Bridge: Main Cable Anchorages and Pylon Foundations

Lars PETTERSSON
Sen. Mgr
Skanska Teknik AB
Stockholm, Sweden

Lars Pettersson, born 1959, received his civil eng. degree 1984. He was until 1997 Head of Bridge Dept at Kjessler & Mannerstrale AB (KM). KM was appointed by the Swedish National Road Administration as main consultants for the detailed design of the Höga Kusten Bridge.

Summary

The newly finished Höga Kusten Bridge (opened to traffic on the 1st of December 1997) in the northern part of Sweden is with its 1210 m main span one of the largest suspension bridges in the world. The bridge carries the road E4 over the mouth of the river Ångermanälven which is more than 1 km wide and 90 m deep at the bridge site. Ground rock conditions at the bridge site has made it possible to use rock as counter weights for the large pulling forces from the main cables. Also, rock is used to found the towers in excavations 13 - 18 m below river surface. In the following, a presentation of the various design aspects for the main cable anchorages and the tower foundations along with some of the construction methods chosen are presented.

1 Introduction

The Höga Kusten Bridge in the northern part of Sweden some 500 km north of Stockholm is designed as a suspension bridge with a main span of 1210 m and an overall length of over 1800 m. The bridge is designed to carry a dual-lane highway and has a minimum clearance under the main span of 40 m. The overall width of the aerodynamically formed bridge girder is 22 m as shown in Fig. 2.

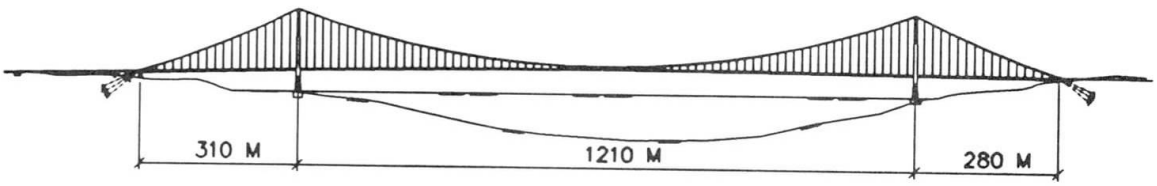

Fig. 1. Elevation of the bridge. The total length exceeds 1800 m with the three suspended spans being 310 m, 1210 m and 280 m respectively.

Water depth at the bridge site being 90 m made a suspension bridge concept the only feasible bridge alternative. Rock ground conditions at the bridge site has made it possible to both found the towers on rock and to anchor back the very large pulling forces from the main cables using rock as counter weights.

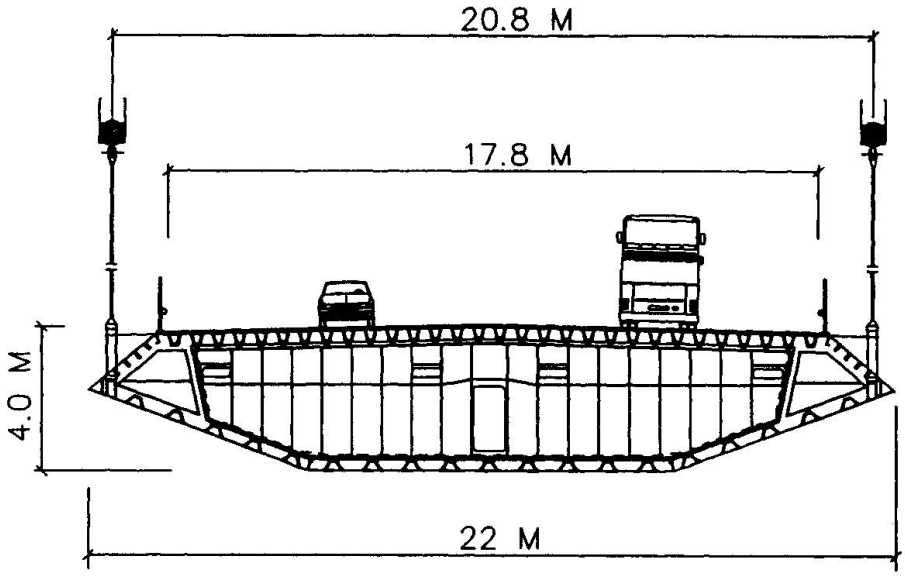

Fig. 2. Cross section of bridge girder. Overall width 22 m, effective width 17.8 m, height 4.0 m and distance between main cables 20.8 m.

The Swedish National Road Administration (SNRA) appointed the Swedish company Kjessler & Mannerstråle AB, (KM) as main consultants for the design and detailed design of the bridge. In the all-nordic design team the following companies were represented: Ahlgren Edblom Architects AB, Sweden, COWI AS, Denmark, The Geotechnical Institute of Norway, Danish Maritime Institute, Denmark, Haug and Blom-Bakke AS and SINTEF, both from Norway and VTT Finland.

Chief Engineer for the total Höga Kusten Project is Karl-Erik Ekesund for the Swedish National Road Administration. Chief Engineer for the Design Team is Gerner Rörsö Jörgensen for KM with Lars Pettersson as deputy Chief Engineer.

The Höga Kusten Bridge was built by a joint venture called Scandinavian Bridge Joint Venture (SBJV) consisting of Skanska AB (Sweden), Monberg og Thorsen AS (Denmark) and Alfred Andersen AS (Norway). As subcontractor for the fabrication the 1800 m long steel superstructure SBJV choose the Finnish company Finnyards OY.

2 Articulation of the bridge

The Höga Kusten Bridge is designed according to Swedish design codes and standards although codes for aerodynamic wind design had to be developed as part of the design of the bridge.

The articulation of the bridge is shown in Fig. 3. The two aerial spun main cables are anchored in rock on each side of the river. The superstructure is continuos between the two abutments. The length of the superstructure is therefore 1800 m.

Temperature variations and main cable deformations caused by live load leads to very large longitudinal movements at the abutments. These longitudinal movements are therefore blocked by large hydraulic dampers at each end of the superstructure, compare Fig. 4.

The limitation of longitudinal movements will result in restraining forces, however, these are absorbed by the abutments.

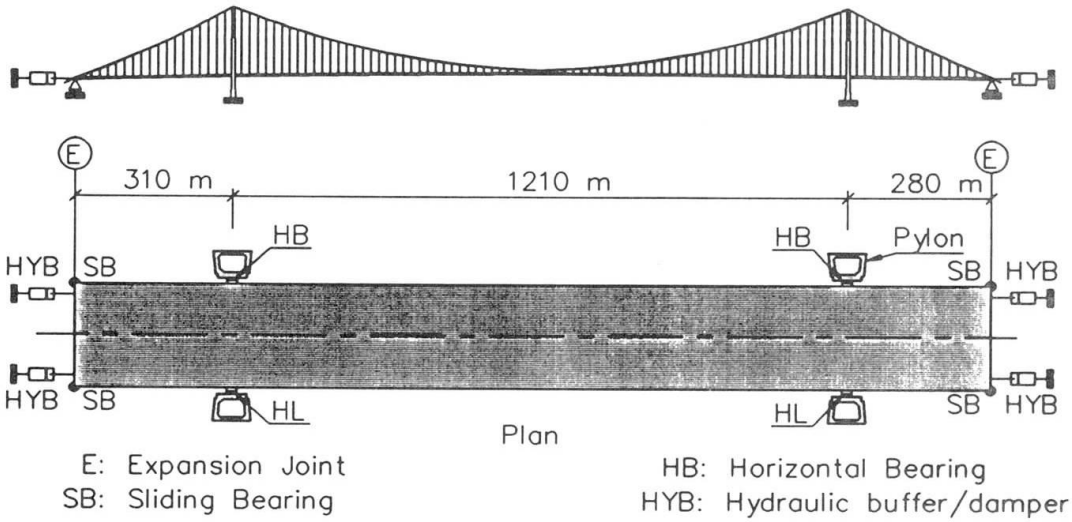

Fig. 3. Articulation of the bridge

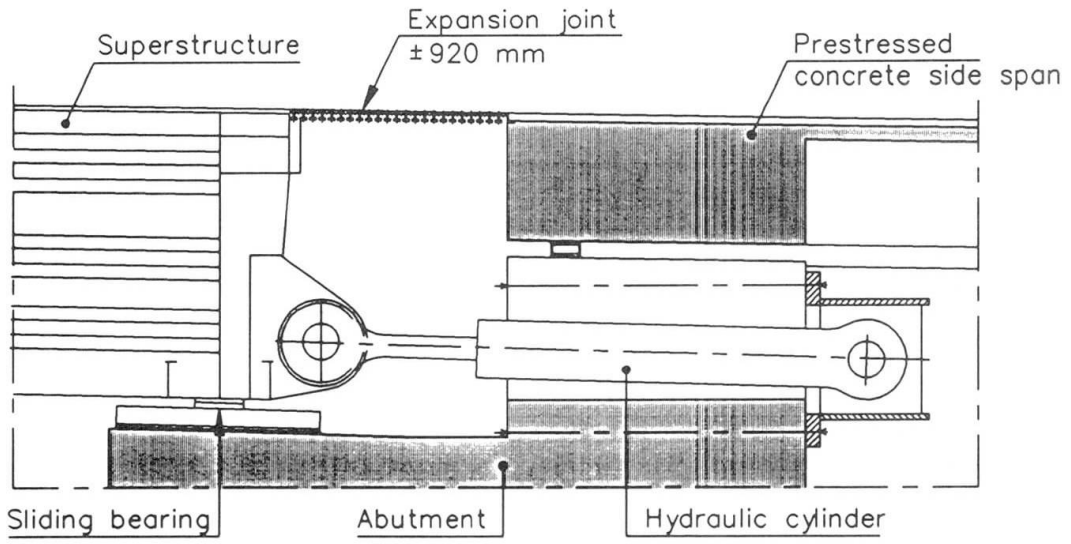

Fig. 4. Hydraulic dampers at bridge abutments reducing longitudinal movements to ±0.85 m.

3 Main cable anchorages and abutments

The design of the Höga Kusten Bridge with its two side spans over land has made an integrated and compact design of the abutments and main cable anchorages possible. This integrated design has lead to comparatively small abutments.

In the splay chamber, the main cable is spread out and deflected over a steel splay saddle as shown in Fig. 5. The splay chamber is equipped with a dehumidification system in order to minimise maintenance requirements. The main cable strands are anchored to steel bars threaded in anchor plates cast into a concrete slab.

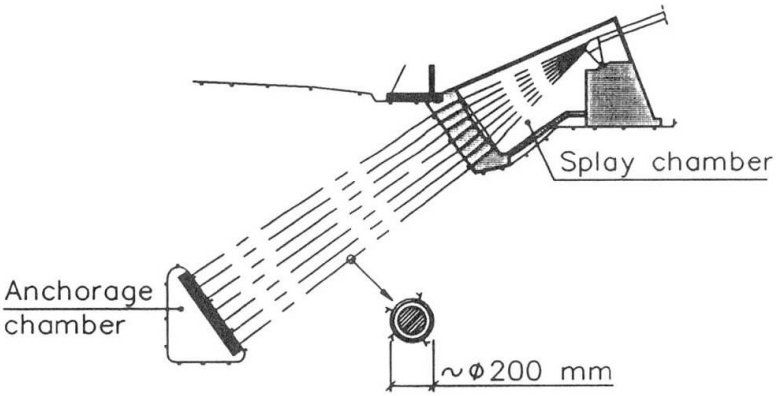

Fig. 5. Main cable anchorage.

The splay saddles rests on massive, 450 m^3 concrete block structures which form part of the forward part of the abutment. These concrete blocks are founded directly on rock reducing the necessary foundation area to a minimum. The force from the splay saddle is used to partly balance the large horizontal forces (18 MN, ultimate limit state) from the hydraulic buffers.

Between the splay chamber and the anchorage chamber, for each main cable, 39 prestressing strands placed in approximately 38 m rock drilled holes with 200 mm diameter. The drilling equipment was specially developed for this purpose.

The 39 strands were prestressed against two large concrete slabs, one in the splay chamber and one in the anchorage chamber. These concrete slabs with concrete volumes up to 400 m^3 were cast directly onto rock resulting in relatively large restraining forces during hardening of the concrete. Thus, at the concreting process cooling efforts by water and air minimised the risk for concrete cracking due to temperature and restraining effects.

The prestressing strands are protected from corrosion by PEH-tubes. Grouting with cement mortar were carried out both between the PEH-tubes and the rock (before installation of the prestressing strands) as well as between prestressing strands and PEH-tubes following prestressing operations. The grouting between rock and PEH-tubes is critical. Therefore the PEH-tubes were filled with water to outbalance the pressure from the grouting mortar.
The prestressing tendons (VSL-type) consisting of 32 each 0.6 inch strands giving each tendon a breaking load of 8.5 MN. Totally the tendons for each main cables have a ultimate load capacity of approximately 330 MN. The partial coefficient of 1.75 for the forces in the prestressing tendons is used in the ultimate limit state.

The front part of the abutments has been used for many purposes, the most important being:

- base for the splay saddles
- support for the suspended side spans
- support for the hydraulic cylinders
- support for the prestressed 23 m side spans bridging over the splay chambers
- providing space for telecommunication and electrical installations

Dominating forces acting on the abutments are splay saddle reactions and reactions from the hydraulic cylinders. Reactions from the hydraulic cylinders being relatively small in serviceability limit state increase in ultimate limit state to approximately 18 MN on each

cylinder. To balance this very large force both the vertical reaction from the splay saddle and the weight of the concrete side spans are used.

4 Pylons

The pylons are given a very special architectural treatment, compare Fig. 6. From aesthetical reasons both pylons are placed in the river close to the shore line. The total height of the pylons are 196 m of which approximately 179 extends over water surface. With over 12 m high steel and glass spires places on the pylon tops the total height of the pylons is over 200 m. The pylons are designed as plane frame reinforced concrete structures with transversely inclined legs with two transverse prestressed beams. The pylons are founded on solid rock on full (solid) cross section foundations cast in dryness. To reach solid rock for the southern pylon excavation of about 5 m bad rock was necessary before foundation works were carried out. On the northern pylon foundation could be carried out directly on solid rock at a water depth of about 17 m. The pylons are designed to withstand ship-collision impact from vessels up to 40,000 tons displacement.

The pylon concrete was chosen with relatively low strength in compression (grade K40 according to Swedish standards). The reason being the large dimensions and the wish from the designers to keep heat release during the concrete hardening process as low as possible.

The water cement ratio has been varied in the different parts of the pylons. Especially in the very large solid block foundations a low cement content was important. In the inner parts of the foundations a water cement ratio was therefore chosen to 0.52 while in the splash zone of the pylon legs a water cement ratio of 0.40 was chosen. Concrete cover, both for foundations as well as pylon legs, is 70 mm.

For the pylons approximately 32000 m³ of concrete, 3000 tons of reinforcement and 80 tons of prestressing tendons are used.

The pylons where built by climbing formwork, the climbing steps being approximately 4 m.

The pylons are both founded on rock. The foundation levels are between 13 and 18 m below river surface. In spite of the large water depth the foundations are cast in dryness, compare Fig. 7. Foundation work has been carried out inside large sheet pile walls. The sheet piles where made tight to the rock by under water cast concrete beams at the inside of the sheet pile. These beams where in turn supplemented by grouted vertical cut-off walls directly under the sheet pile walls.

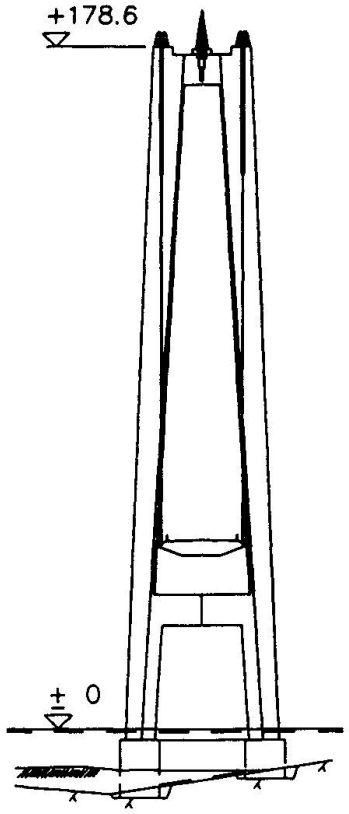

Fig. 6. Pylon elevation.

The foundations have been made relatively long in the direction of the bridge axis to ensure stability without rock anchors even in the critical free standing condition. In spite this, due to the high quality of the rock the length of the foundations could be limited to 15 m, the width being 9.5 m.

The four foundations where all cast without construction joints leading to approximately 2000 m^3 castings. The time used for casting one of the foundations were approximately 36 hours.

To control the large heat release the concrete was cooled with river water running in steel pipes mounted on the horizontal reinforcement. The distance between the pipes was approximately 800 mm horizontally and 1000 mm vertically.

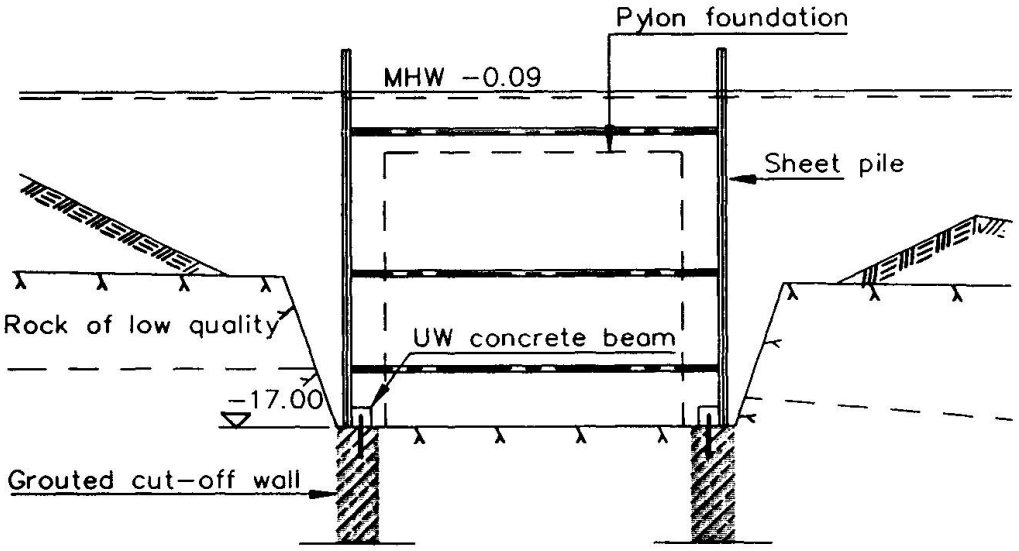

Fig. 7. Pylon foundations. Temporary sheet piling shown.

The total vertical reaction on the rock foundation is approximately 500 MN from dead load only resulting in a ground pressure of 2 MPa. In the ultimate limit state the ground pressure was allowed to increase to 3.5 MPa. In the accidental limit state combinations of vertical and shear stress were checked against rock failure envelopes.

5 Concluding remarks

The Höga Kusten Bridge is with its 1210 m main span the largest bridge in Sweden. This complicated bridge project has been successfully completed at the end of November 1997. The high quality rock at the bridge site has been used to minimise structure dimensions, especially the main cable anchorages and pylon foundations.

6 References

/1/ Pettersson, L., "Höga Kusten-bron", Proceedings at the Nordic Concrete Conference and Nordic Concrete Industries Meeting, Odense, June 1995.

In Service Modelling of the Humber Bridge

R. KARUNA
Civil Eng.
Brunel Univ.
Uxbridge, UK

R. Karuna, born 1964, received his first degree in Civil Eng. from the Univ. of Peradeniya in Sri Lanka in 1990, and MSc in Civil Eng., structures from City Univ., UK in 1996. He is currently a Research Student in the Dept of Mechanical Eng. at Brunel Univ.

Ming S. YAO
Dr
Brunel Univ.
Uxbridge, UK

Ming Yao, born 1957, received his first degree in Aeronautical Eng. form NUAA, China in 1982, and his PhD from Imperial College, UK in 1989. He worked as a Lecturer in the School of Eng., Univ. of Humberside before joining the Dept of Mechanical Eng. at Brunel Univ. in 19956.

Chris J. BROWN
Civil Eng.
Brunel Univ.
Uxbridge, UK

Chris Brown, born 1949, received his degree in civil Eng. form the Univ, of Leeds in 1971. He worked as a Lecturer in the Dept of Building Technology at Brunel Univ. from 1974, and transferred to the Dept of Mech. Eng. in 1984. He is now a Senior Lecturer, and Head of the Struct. Mechanics Res. Group.

R.A. EVANS
Bridgemaster
Humber Bridge Board
Hessle, UK

Roger Evans, born 1945, received his degree in Civil Eng. from the Univ. of Leeds in 1967. He worked as an engineer specialising in heavy foundations, a planning engineer, and subsequently as a bridge designer. He is now responsible for the operation and maintenance of the Humber Bridge, having worked there since 1981.

Summary

The Humber Bridge, until recently the world's longest span suspension bridge, has been carefully maintained and monitored during its 17 year life. As part of the monitoring programme, the Humber Bridge Board commissioned the development of a Finite Element computer model which has been validated against existing engineering data and which gives a good description of actual behaviour. The model has been used to investigate the effects of modified or updated bridge loading and can also be used to give a rapid structural assessment in unexpected conditions. Other potential uses of such a tool are outlined.

1. Introduction

The Humber Bridge is a suspension bridge which was completed and opened in 1981, and has remained in good working order throughout its life. The Humber estuary is in the north-east of England, and the bridge runs north (Hessle) - south (Barton). The main span is 1410 m. The Hessle side span is 280 m. and the Barton side span is 530 m. (Figure 1). The two towers, each 155.5 m. high, are concrete, while the main deck is a slim, streamlined, steel box suspended from inclined hanger ropes. The aerial-spun main cables (14948 wires each) terminate in concrete gravity anchorages founded on the Kimmeridge clay of Barton, and the chalk rock at Hessle. The deck is discontinuous at the towers, with deck movements accommodated by a system of rolling-leaf expansion joints and A-frames. The A-frames also provide restraint against vertical, lateral and torsional loads.

Consultants Freeman Fox and Partners designed the bridge on the basis of their experience gained on the first crossings of the Severn (England) and the Bosphorus (Turkey), both of which were conceptually similar. Humber Bridge incorporates the innovative features of concrete towers, A-frame arrangements and special welding details in the box deck, as well as inclined hangers. These have all performed very well in service.
The site is an exposed marine location and significant temperature variations can be expected. The box deck is de-humidified to minimise maintenance painting. The inspection regime includes formal inspections every two years, and Principal Inspections every six years.
The construction cost was £98m (US$155m) but capitalisation of interest caused the bridge debt to grow to £435m (US$690m) by 1993 and necessitated the restructuring of the Bridge Board's finances. Operation of the bridge (toll collection, traffic safety, security) costs £1.6m (US$2.5m) per annum, and maintenance costs £1.0m (US$1.6m) per annum. In the financial year 1997/98 the toll income from 6.2m vehicles was £13.9m (US$22.0m).

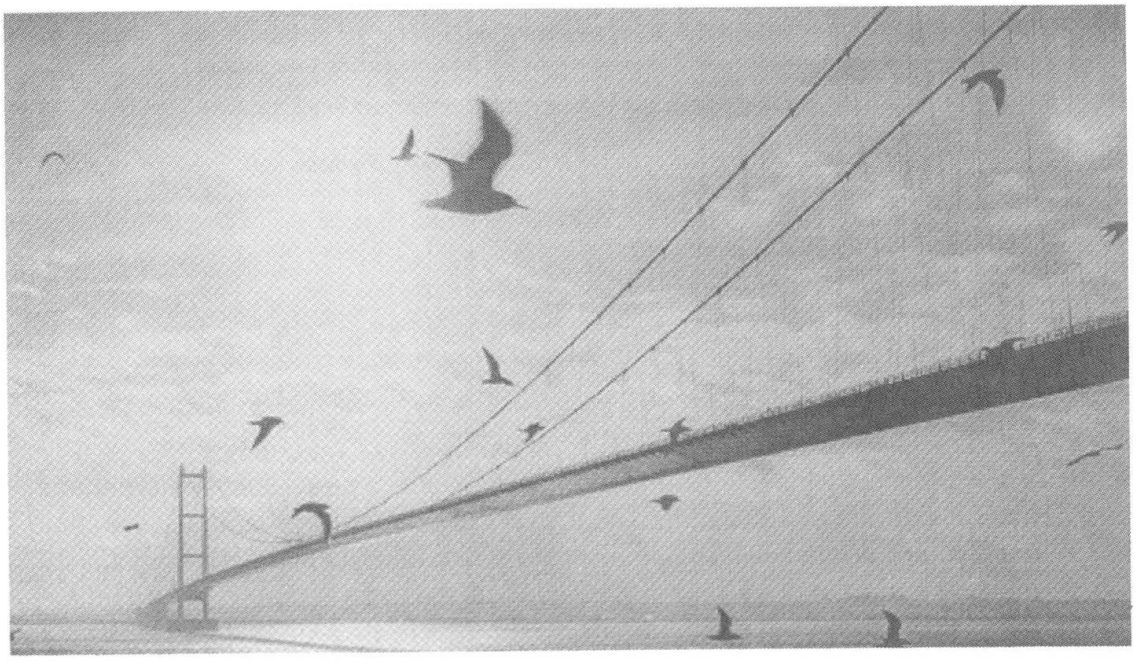

Figure 1 - Humber Bridge showing slender box and inclined hangers

2. Why should the Humber Bridge Board commission a Finite Element model?

The Humber Bridge Board is responsible for the operational safety of the bridge. Its staff inspect and maintain the bridge either directly or by using contractors or consultants. The original design calculations are used as a maintenance tool but, having been prepared at a time when computer-based design was in its infancy, they consists mainly of hand calculations. Consequently they can be unwieldy to use, are of limited value for investigating the consequences of revised Highway Loading Standards and are not suitable for assessing the effects either of unforeseen service loads or of structural damage. Computer models can now be prepared at reasonable cost, run efficiently on a PC and are relatively user-friendly. Such a model facilitates rapid structural appraisal after accidents, allows investigation of various "what if" scenarios and assists with decisions regarding traffic management in unusual circumstances, as well as being an important maintenance tool.

3. Finite Element Modelling

The finite element method applied to structural analysis is well known. To fulfil the brief, the model has to be validated against known in-service performance criteria. It is not initially predictive, but must be fully descriptive. This is a different challenge to that faced when designing *ab initio*.

The finite element model was built to run on a P.C. using a commercially available version of ANSYS [5]. In developing a descriptive model, assumptions made in the original design may not be acceptable (e.g. rotation capacity at connections or supports may have been simplified), and care must be taken to identify the effect of such assumptions in modelling. During development, different levels of sophistication have been built into a number of models, but only two models are used for calculations presented here. They are referred to as the *full model* and the *plate model*, the difference being the extent of detailed representation of the deck. They are run as both linear elastic and geometrically non-linear analysis. The use of a non-linear elastic model is essential for large span structures. While the major design forces change very little, deformations can be significantly modified, and 5% changes on non-trivial values can be expected. On such large deformations, this can give values up to 0.1m and these are clearly measurable quantities.

The *full model* has 68924 degrees of freedom, and mainly uses link, plate and beam elements. The cable is modelled as a series of link elements, and they connect the nodal points at which hangers are supported. The hanger elements have the "birth and death" capability which ensures they carry tension only. The towers are modelled as a series of beam elements, while the deck consists of inter-connected plate elements. The material of construction for deck, cables and hangers is steel, while the towers are in-situ reinforced concrete. The *plate model* simplifies the deck to a two-dimensional flat plate system with equivalent flexural properties. Simplification of the deck reduces the total degrees of freedom to 22760, and reduces run times with virtually no change in predicted hanger or cable forces.

There is clearly no unstrained position for the bridge, as the self-weight is such a significant proportion of the total load. In order to represent this feature which is important in modelling the non-linear response, the designer's original initial strain values were applied. Subsequent application of gravity loading gave a deflected form under dead load which must match that given by the initial strain data. There were few inaccuracies which required minor adjustment of initial strain values to give a smooth deflected form. This process cannot be validated, except that the geometry of the final as-built structure is known and follows smooth lines.

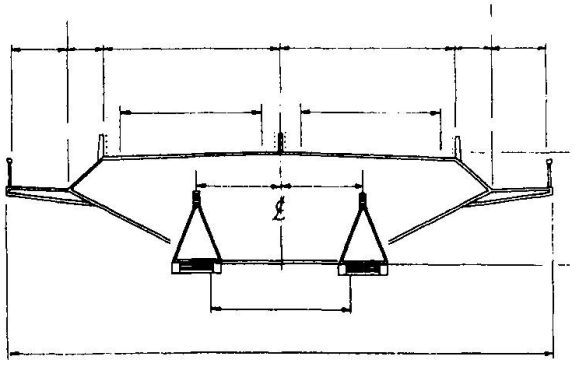

Figure 2 - General cross-section of deck and A-frames (all dimensions in m.)

A-frames support the deck at two transverse positions at each end of the side and main spans. Their primary function is to prevent both vertical and lateral movement from both symmetric and

asymmetric loading. The inclined hangers also provide significant longitudinal stiffness in this respect. A detail showing the deck cross-section and A-frames is given in Figure 2.

In order to validate the model, it was essential to compare predicted behaviour to measured data. Partly because it was the world's longest span suspension bridge, it has already been the subject of several investigations.
Reliable and extensive data are available from dynamic studies carried out by a group from Bristol University[1]. They used ambient vibration testing from several locations on the bridge to determine natural vibration frequencies and associated modes. Natural frequencies of the deck section had also been determined for design purposes from (unpublished) wind tunnel tests carried out at the National Physical Laboratory.
Data from tests involving a single heavy lorry crossing have also been obtained [2,3] although these data are slightly less reliable as the load is not *precisely* known. Haulier's records suggest their estimate of the load at 172t, but this is doubted from observations made at the time.
More recently GPS data have been reported[4], although these are yet to be calibrated against known loads.

Measured and predicted natural frequencies are given in Table 1, while a comparison of deflections under the action of the travelling load is given in Figure 3. More detail of the calibration process has been given elsewhere [6].

	Vertical				Lateral			Torsional	
Mode No.	1	2	3	4	1	2	3	1	2
F.E. Model (Hz)	0.108	0.116	0.169	0.207	0.054	0.119	0.178	0.318	0.524
Measured (Hz)	0.116 (0.104)	0.154 (0.107)	0.177	0.218	0.056	0.143	0.218	0.311 (0.300)	0.482 (0.519)

Table 1. Natural frequency values from F.E. analysis and measurements
Figures in brackets are data provided by the National Physical Laboratory, UK.

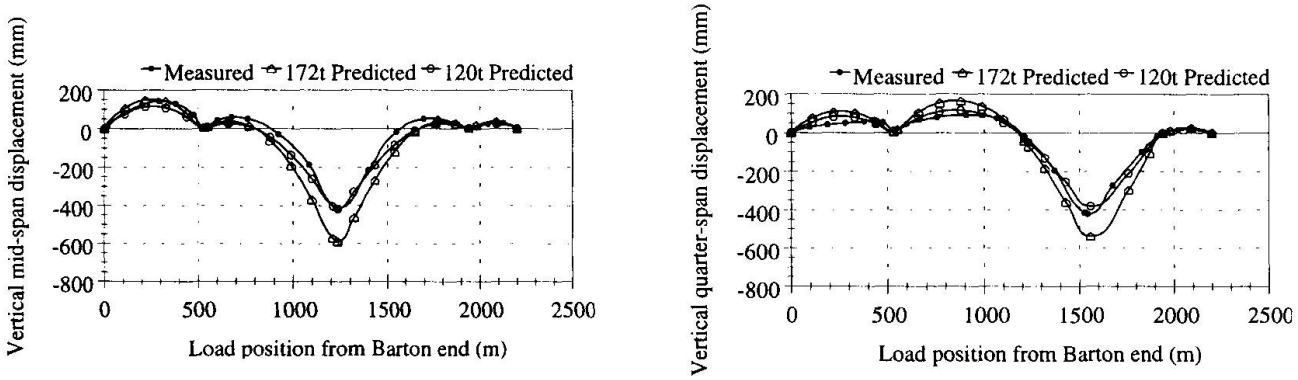

Figure 3 - Single Heavy Lorry Crossing - Comparison of Measured and Predicted Vertical Displacements at a) Midspan b) Quarter Point of Centre Span

It is shown from Table 1 that good agreement is obtained between predicted values and the best available measured data. It may also be noted that some modes predicted by the current computer model have not been reported in Reference 1. The quasi-static tests of the single heavy lorry, as shown in Figure 3, also give excellent qualitative agreement.

4. Applications

There are many possible uses to which such a model may be put, including:

- Assessment in connection with revised Loading Codes
- Assessing special or abnormal vehicles
- Structural assessment after accidents
- Investigating the viability of maintenance or repair procedures
- Assisting with the development of traffic management procedures
- Assessing the consequences of foundation movements

By way of example, removal of a hanger in the model (chosen at random - not highest or least loaded) indicated in Figure 4 leads to the change in hanger forces shown in Figure 5. The loading used has been a case from BSALL - Bridge Specific Assessment Live Loading (used to assess the bridge in line with national UK guidelines), and subsequently a Special Vehicle Load of 180t. The bridge operator is able to assess the integrity of the structure under possible combinations of maintenance and exceptional load conditions, and in the case shown, the hanger loads remain within design values (1450kN).

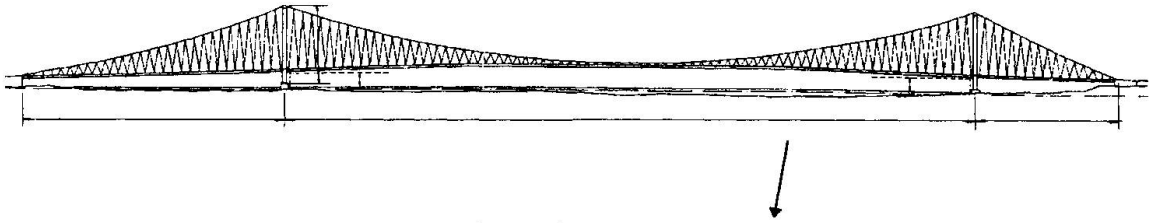

Figure 4 - Bridge Elevation

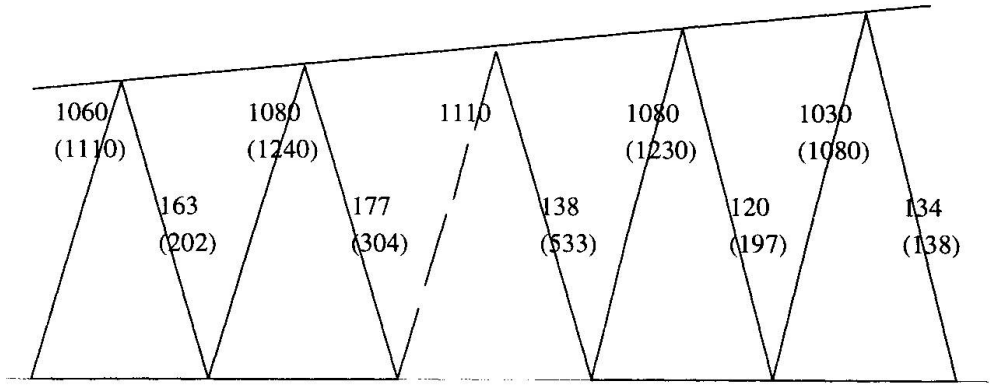

Figure 5 - Hanger Forces (kN) under BSALL and Special Vehicle loading (figures in brackets with Hanger removed)

An alternative example could involve the determination of maximum wind speeds in which the bridge may continue to be used, again combined with BSALL loads and loss of a hanger. For the removal of the same hanger, the bridge may operate in winds up to 33 m/sec at deck level without exceeding the permitted working load in the hangers. The design wind speed (i.e.with no hanger removed) is 48m/sec.

Other structural elements can be considered in the same way under this, or any other loading.

5. Concluding comments

There is a need for bridge operators to have ready access to tools which help ensure safe operation of bridges. Technology change (particularly with respect to computational capability) over the last decade or so has made this process more attractive and achievable. Improved understanding of real loads and their characteristics leads to a need to be constantly reassessing safety and structural response.

This paper has demonstrated how a finite element model has been developed which describes the behaviour of a long-span suspension bridge as-built. The model has been used for an assessment of the bridge under revised loading requirements, and with the possible loss of structural elements.

Future uses might include an increased potential for on-line control systems, enhanced condition monitoring, and more accurate determination of any actual traffic and wind loads that are present.

The authors would conclude that for many major bridge structures it would be advantageous for a model to be supplied to the bridge operators by the designers, along with the design calculations.

References

1. Brownjohn, J.M.W., Dumanoglu, A.A., Severn, R.T. and Taylor, C.A. (1986), Ambient vibration survey of the Humber Suspension Bridge, Research Report UBCE-EE-86-2, Civil Engineering Department, Bristol University, U.K

2. Brownjohn, J.M.W., Bocciolone, M., Curami, A., Falco, M. and Zasso, A. (1994), Humber Bridge full-scale measurement campaigns 1990-1991, J Wind Eng. Ind. Aerodyn. Vol. 52 pp185-218.

3. Zasso, A., Vergani, M., Bocciolone, M., and Evans, R. (1993), Use of a newly designed optometric instrument for long-term, long distance monitoring of structures, with an example of its application on the Humber Bridge, 2nd Int. Conf. on Bridge Management, 18-21 April 1993, University of Surrey, U.K.

4. Ashkenazi, V. and Roberts, G.W. (1997), Experimental monitoring of the Humber bridge using GPS, Paper 11296, Proc. Instn Civ. Engrs, Civ. Engng, Vol 120, pp177-182

5. ANSYS (Revision 5.3), Swanson Analysis Systems, 1993

6. Karuna, R., Yao M.S., Brown C.J.and Evans R.A., "Modelling and Analysis of the Humber Bridge" IASS International Colloquium on Computation of Shell and Spatial Structures (ICCSS'97), Taiwan, November 1997

Comparative Investigations of Suspension Bridges and Cable-Stayed Bridges for Spans Exceeding 1000 m

Mehdi ASCHRAFI
Senior Eng.
DSD GmbH
Saarlouis, Germany

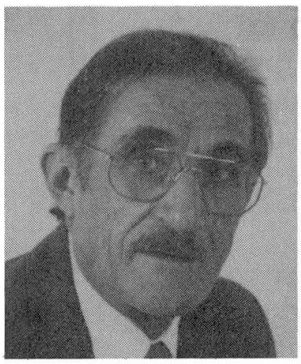

Mehedi Aschrafi, born 1941, received his structural eng. degree from Techn. Univ. Aachen in 1969. From 1969 to 1983 he worked in the Bridge Constr. Dept as structural eng. and since 1984 he is Senior Eng. for Bridge and Heavy Industries with the company DSD Germany.

Summary

The author has studied the possibility of building long-span cable-stayed bridges with spans of 1000 m and more. This is possible based on the present high standard of theory and calculation methods and additionally due to the tendency to use lightweight structures (super-structure, orthotropic plates) including optimum welding techniques as well as high admissible stresses in cables. The use of lightweight structures is also important in seismic areas. Finally, the vibration of complex long cables is controllable.

1. Introduction

As F. Leonhardt (1972) showed , cable-stayed bridges with a maximum span of approximately 400 m are possible. From the engineering point of view, only the erection stage is critical due to wind excitations [1].
In 1972, this problem was investigated by full-scale tests on the cable-stayed motorway bridge over the Rhine near Speyer, Germany.The paper deals with the results and the conclusions of passive control. Furthermore, the passive control of cable vibrations, especially rain-induced oscillations, is illustrated.
First results regarding long-span cable-stayed bridges were presented by the author in the International Wind-Engineering Congress in 1983 Australia [2] and the International Conference IABSE, FIP in Deauville, France.[3], where he pointed out that even with long spans, cable-stayed bridges are by far superior to other bridge types not only technically and economically but particularly with regard to aerodynamic stability. Meanwhile, numerous cable-stayed bridges with spans up to 856 m (Normandy bridge) have been built all over the world. At present, the Tatara bridge with a span of 890 m is under construction. The most common opinion is that the conventional suspension bridge is still the best solution for long-span bridges. In specialist literature one can also read that the so-called Hybrid [4] or the bi-stayed bridges [5] are the bridge types of the future.
This paper presents comparisons of the behaviour of suspension and cable-stayed bridges under critical conditions.
This paper will discuss the optimum shape of the superstructure selected for pylons, the type of cable suspensions and details of cable connections including passive control, temporary control of vibration during erection stages and studies of active control devices.

2. Comparative Investigation of Suspension and Cable-Stayed Bridges

Fig. 1 shows the development of the suspension and cable-stayed bridges. It illustrates the rapid development of the spans of cable-stayed bridges over the past few years. Since the 1980s, the cable-stayed bridge has become a standard system for spans up to 600 m.

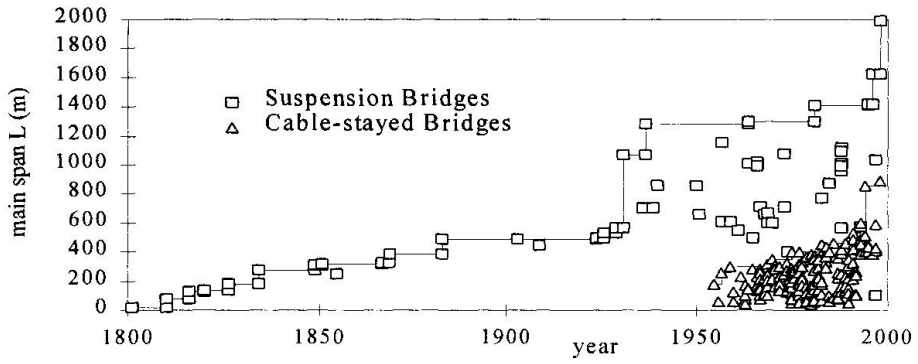

Fig. 1 : Development of the construction of suspension and cable-stayed bridges

To find out the optimum solution for bridges with spans between 1000 m and 2000 m, various 3D systems were calculated - in intervals of 200 m - acc. to the 2nd order theory. These calculations were carried out for the bridge widths 22.0 m, 30.0 m, 38.0 m. (Fig. 2).

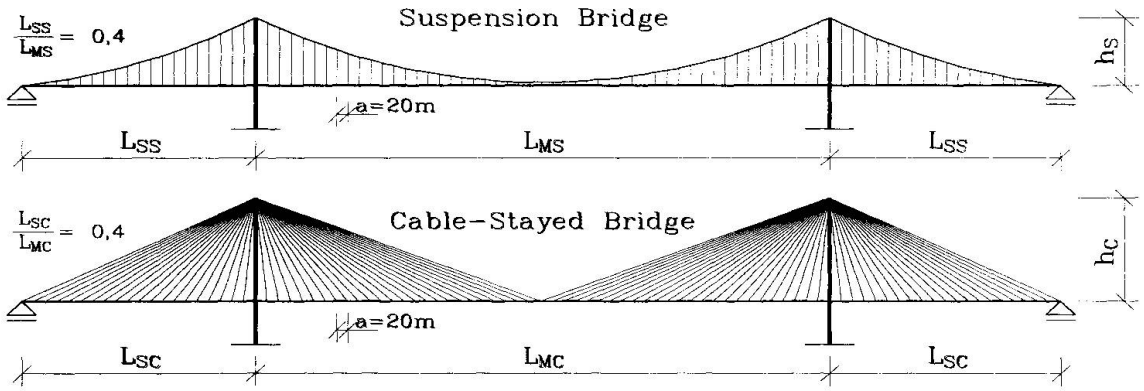

Fig. 2 : Suspension and cable-stayed bridge systems with fan-shaped cables

2.1 Bridge Deck Cross-Sections

Meanwhile, numerous wind tunnel tests and practical experience have shown which cross-section designs of the bridge deck must be chosen in order to avoid the occurrence of wind vortices. Furthermore, lift and pitching moment should to be reduced to a minimum to avoid flutter- and torsion-induced vibrations.

The development of the cross-section design of the bridge deck shows that the conventional truss design to achieve stability against wind is out-dated. The flat cross-section design as shown in Fig. 2 will replace the truss-type cross-sections in future. In the intervening period, several bridges have been built with these new cross-section types.

It has been proved by now that aerodynamic stability can be achieved even in suspension bridges which are susceptible to vibrations by using these aerodynamically shaped cross-sections, if the bridge deck is sufficiently wide in relation to the span and is continuous at the pylons.

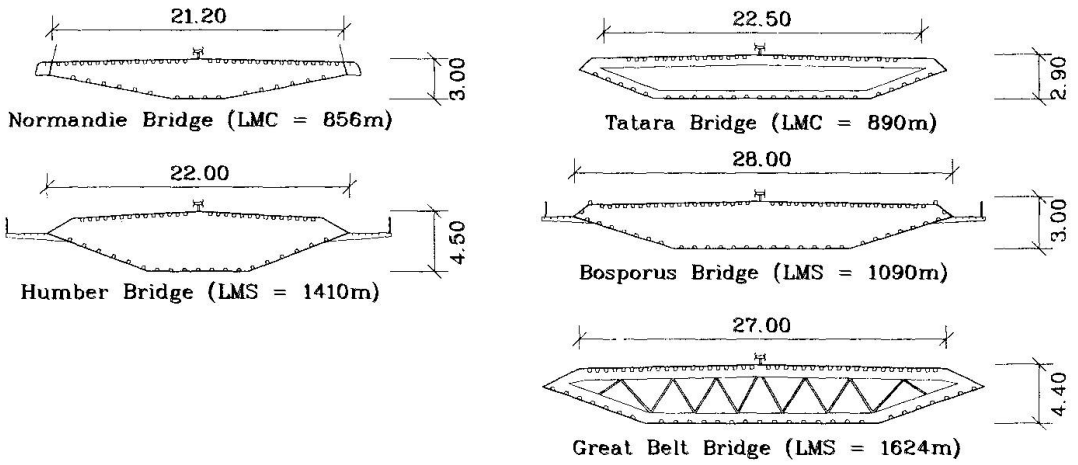

Fig. 3 : Cross-sections of bridge decks

The aerostatic coefficients measured for these cross-sections show that the coefficient is low both for lift and for pitching moment, so that the forces inducing bending and torsional vibrations remain very small, but the coefficient for the horizontal wind resistance is also exceptionally small, too [3], [6], [7].
The investigation shows that for spans of more than 1000 m, an overall construction height of such flat bridge cross-sections of 3.0 to 3.6 m is sufficient for cable-stayed bridges.
If we consider the quantity of steel required for the superstructure, we see firstly that the orthotropic plate is the same in both cases. The suspension bridge needs a bridge deck with higher bending strength and torsional stiffness than the cable-stayed bridges, on the other hand, the latter requires additional steel to resist the axial compression forces which result from the cables anchored in the deck. The resulting requirement of steel is however. relatvely small.

2.2 Pylons

The investigation shows that the cable forces and also the required steel quantities for the cables are influenced by the height of the pylons above the road in relation to the span (Fig. 4).

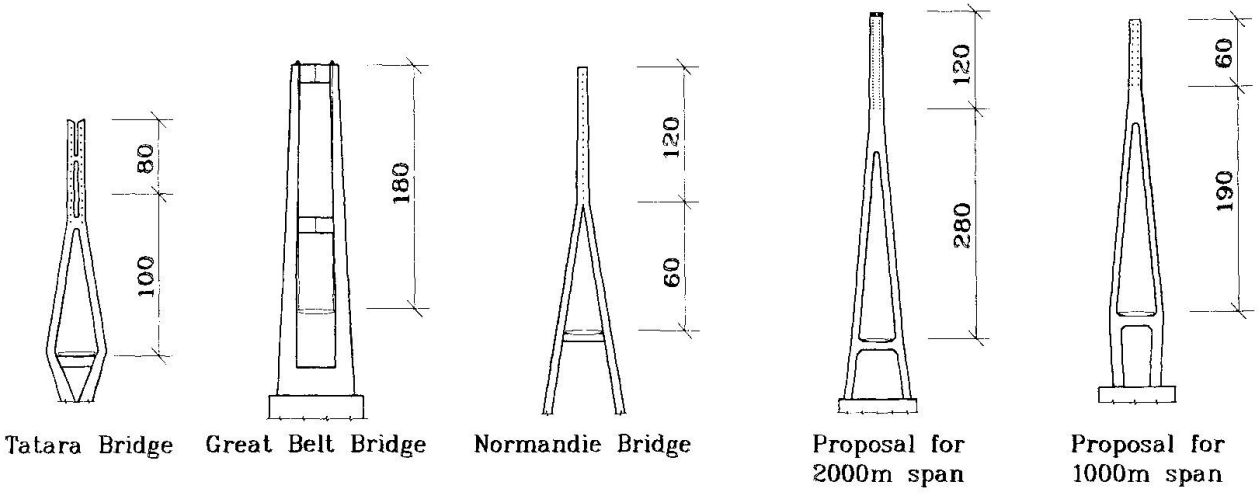

Fig. 4 Types of pylons

Regarding the steel required for the pylons (cable-stayed bridge in composite construction), the bridge deck and the fact that for a sufficient stiffness of the bridge, the pylons must not be too high, a good relation for cable-stayed bridges (fan-shaped cable arrangement) would be h/l = 1/5 and for suspension bridges h/l = 1/9. Furthermore the investigations show that bringing the cables together in a pylon saddle above the bridge axis on an A-shaped pylon is an excellent solution for spans up to 2000 m.

2.3 Cables

The deflections of cable-stayed bridges depend to a great extent on the changes in the length of the cables under increasing loads. The changes in length depend on the change in the sagging of the cables, which occurs with the 3rd power of the stresses.
This shows to what extent it is necessary, especially with long spans, to use cables which can bear great stresses, with the strength of the cable anchorage playing an important role.
Of course it is possible to reduce the sagging changes of very long cables by means of bracing cables, so that the loss of stiffness of the cables due to sagging changes can be limited to 20 % of horizontal cable lengths of more than 1000 m.
The cable-stayed bridges with fan-shaped cable arrangement require about 50 % less steel for the cables than suspension bridges (1000 m span) under the same admissible stresses.
With long spans, the cables already have a considerable dead weight with a span of 1000 m, i.e. 15 %, compared to only 4 % for the fan-shape solution. With a span of 2000 m, a suspension bridge requires nearly half the weight of the cables to support itself.
In contrast to the cables and hangers of suspension bridges, the vibrations of the stay cables of cable-stayed bridges are significant in particular. Because of the potentially large amplitudes of cables, there is a risk of fatigue failures, and the ensuing possible traffic risk (Bangkok bridge for example) due to excessive deck vibrations. Although the cable vibrations will not cause failures of cable-stayed bridges immediately, the capacity or fatigue resistance will be diminished, leading finally to a reduction in service life and the occurrence of failures.
At present, the passive control method is most commonly applied in the control of cable vibrations [3], [8].
As we know, the cable damping is very small. The logarithmic decrement of structural damping will be approximately 0.003. Using a simple damper (e.g. hydraulic or rubber damper), the generalized equivalent damping ratio can be increased considerably. Thus, vortex-induced oscillations, galloping, rain-induced vibrations and also parameter instability (caused by bridge deck and / or pylon movement) may be controlled completely.
Aerodynamic control methods are uneconomical in comparison to simple mechanical devices.

3. Erection Stages, Temporary Control of Vibrations

The investigations show that under construction with a 1000 m long cantilever, the width of the bridge should be 38 m minimum.
During erection stages, the detached pylons of cable-stayed and suspension bridges present a special kind of tower structure. Steel pylons are low-damped and therefore particulary susceptible to vibrations.
The nature of vibrations depends on the form of the pylon. Apart from their response to stochastic gust effects, bridge pylons show a tendency both to forced vibrations due to vortex excitation and also to self-induced movements (galloping).
In the first place, optimum tuned vibration absorbers should be considered. Figure 5 shows a sketch of such a system in use.

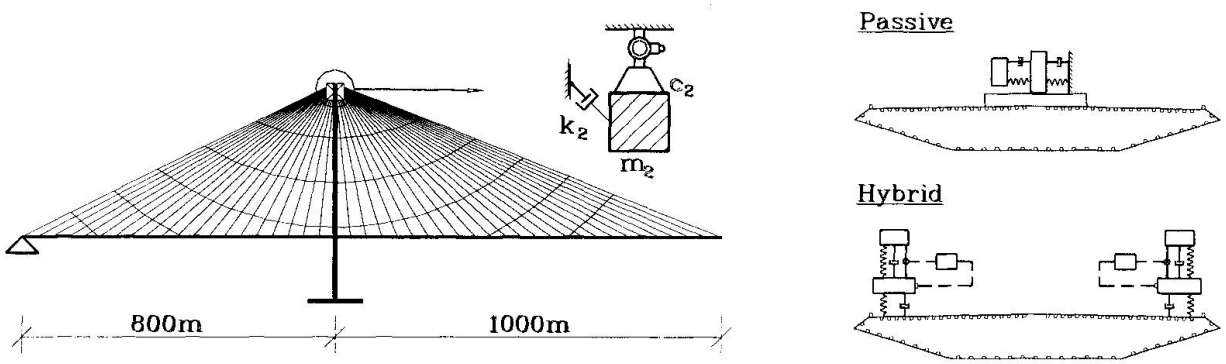

Fig. 5 : Cable-stayed bridge under construction (main span 2000m)

If the natural frequencies in both principal directions are different, the pendulum system could also have different natural frequencies in the two directions by means of connections in series of torsional-springs pendulum suspensions. After completion of the bridge, the damping system can be alive but tuned to the changed natural frequencies.
Tuned mass dampers (Fig. 6) should be considered also to avoid vibrations of the bridge deck in the erection stage [9], [11].

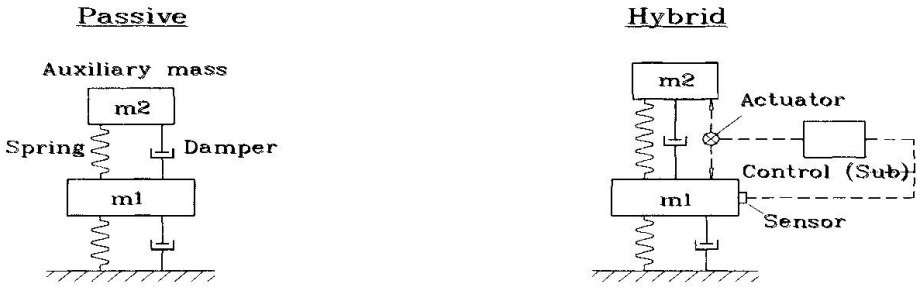

Fig. 6 : Tuned mass dampers

4. Studies of Active Control Devices

For ultra-long-span bridges, other means than maximizing the torsional stiffness and possible redistribution of the torsional inertia may be achieved. If properly arranged, additional damping will reduce the amplitudes of response due to wind (buffeting, vortex shedding, galloping and wake-galloping). However, by means of passive devices, the critical flutter speed (separated flow torsional flutter) cannot be increasead considerably. Active control measures will be necessary for this. The active control can be carried out by means of aerodynamic and/or mechanical systems. From an economical point of view the mechanical hybrid system (combination of passive and active control) will be the best. As the governing equation shows [11] by means of active/passive control both an increasing of the total damping and or stiffness will be attainable. In the case of a bridge, the control of the acceleration (mass influence) will be unrealistic.
To avoid forced and self-induced vibrations, including bending and/or torsional vibrations, both in the erection stage and after completion of the bridge, mechanical hybrid systems at the bridge deck corners are proposed as follows.
Active control systems acc. to [10] are - though very interesting technically - not economical. Since traffic induced vibrations will act on the bridge, in addition to the wind, those mechanical control systems will not be able to fully control the vibrations.
This phenomenon was experienced during the reconstruction of the Lisbon Tagus bridge [12].

5. Conclusions

The comparative investigations showed that the cable-stayed bridge with fan-type cables is superior to the suspension bridge both technically and economically and with regard to aerodynamic stability despite taller pylons. That applies also to spans up to 2000 m.
The structural and aerodynamic stability will also be safe during construction with a 1000 m cantilever. The cross-section of the bridge deck should be flat and wide and of slender box girder type. Preferably, an A-shaped pylon with inclined cable ends should be used.
Further investigations should deal with particular solutions concerning hybrid dampers.
For total bridge length of 3600m or more, the multispan cable-stayed bridge should be used.

References

[1] LEONHARDT, F.-ZELLNER , W.: Comparative Investigations Between Suspension Bridges and Cable-Stayed Bridges for Spans Exceeding 600 m, Publications 32-1, 1972 IABSE, p.126-165.
[2] ASCHRAFI, M.-HIRSCH,G. : Control of Wind-Induced Vibrations of Cable-Stayed Bridges. J. of Wind Eng. and Ind. Aerodyn., 1983, Vol 14 , P. 235-246
[3] ASCHRAFI, M. : Control of Wind-Induced Vibrations of Cable-Stayed Bridges International Conference A.I.P.C.-F.I.P. Deauville, France, Oct. 1994, Volume 2, p. 45-52
[4] WALTHER, R.-AMSLER, D.: Hybrid Suspension System for Very Long-Span Bridges: Aerodynamic Analysis and Cost Estimates Cable-Stayed and Suspension Bridges. International Conference A.I.P.C.-F.I.P. Deauville, France, Oct. 1994, Volume 1, p. 529-536
[5] MULLER, J.: The Bi-Stayed Bridge Concept : Overview of Wind Engineering Problems. Aerodynamics of Large Bridges, A. A. Balkema / Rotterdam / Brokfield / 1992 p. 237-245
[6] VIRLOGEUX, M.: Wind Design and Analysis for the Normandy Bridge. Aerodynamics of Large Bridges, A. A. Balkema / Rotterdam / Brokfield / 1992p. 183-216
[7] LARSEN, A.-JACOBSEN, A.-S.: Aerodynamic Design of Great Belt East Bridge. Aerodynamics of Large Bridges , A. A. Balkema / Rotterdam / Brokfield / 1992 p. 269-283
[8] HIRSCH, G. : Cable Vibration Overview. International Conference A.I.P.C.-F.I.P. Deauville, France, Oct. 1994 Volume 2, p. 453-464
[9] CONTI, E. - GRILLAUD, G. - JACOB, J.- COHEN, N.: Wind Effects on the Normandy Cable-Stayed Bridge: Comparison between Full Aeroelastic Model Test and Quasi-Steady Analytical Approach. International Conference A.I.P.C.-F.I.P. Deauville, France, Oct. 1994 Volume 2, p. 81-90
[10] OSTENFELD, K.H. - LARSEN,A. : Elements of Active Flutter Control of Bridges. New Technologies in Structural Engineering, 1997. Lisbon, Portugal, p. 683-694 volume 2
[11] ASCHRAFI, M. - HIRSCH, G.:Vibration Control of Assembly Stands during Bridge Extension. Technologies in Structural Engineering, 1997, Lisbon. Portugal, p. 543-550
[12] ASCHRAFI, M. - HIRSCH, G.:Vibration Control of Tejo Bridge during Extension - to be published shortly

Comparison of Numerical and Physical Models for Bridge Deck Aeroelasticity

Jannette FRANDSEN
PH.D. Student
Cambridge Univ.
Cambridge, UK

Jannette Frandesen, born 1967, obtained her degree in structural eng. in 1991. After working for five years, at first as an offshore structural eng. and then as a bridge designer, she returned to research by first obtaining a degree in structural steel design and is at present a PhD student pursuing research within the field of bridge aerodynamics.

Allan McROBIE
Lecturer
Cambridge Univ.
Cambridge, UK

Allan McRobie, born 1958, obtained degrees in Physics in 1979 and Structural Eng. in 1985. After working for five years as a bridge designer in Australia, he returned to pursue research in nonlinerar structural dynamics and is now a Lecturer in Structural Eng. in Cambridge.

Summary

A finite element approach to the fluid-structure interaction of long-span bridges is described. Using an Arbitrary Lagrangian-Eulerian formulation for the fluid around a spring-supported section model, self-excited oscillations of bridge cross-sections can be modelled in the time-domain. The eventual aim is to verify or otherwise the validity of the approach. If verified, the method could provide additional insight into the effects of minor changes of cross-section geometry on the various aeroelastic phenomena and so provide an aid to design evolution. Two case studies are presented, both involving the Great Belt East project in Denmark. In the first we consider the vortex-induced oscillations of the approach spans and in the second we consider the coupled flutter of the main suspension span. The initial results are interesting.

1. Introduction

There has been much research into the application of computational fluid dynamics (CFD) to long-span bridge cross-sections. In this paper we describe some initial results of an Arbitrary Lagrangian-Eulerian code applied to two-dimensional section models. The bridge sections are spring-supported and self-excitation of the combined fluid-structure systems occurs naturally as the field equations are integrated forward in time. The first objective of the research is to ascertain whether or not this approach can accurately model the various aeroelastic instabilities, and if so, to see how such a facility may best be used to guide design evolution.

The code, a transient fully-coupled CFD/FEA code, is *Spectrum* [2] of Centric Engineering Systems Inc., based on the work of T.J.R. Hughes and coworkers to whose papers [1, 5, 6] the reader is referred for the finite element theory. Two case studies involving the Great Belt East project are described.

2. Computational Method

Spectrum is a fully three-dimensional code, but all analyses presented here are essentially two dimensional. The fluid is modelled by the isothermal incompressible Navier-Stokes equations. Although a number of turbulence modelling capabilities (such as Large Eddy Simulation) are available within *Spectrum*, no turbulence modelling is included in the preliminary analyses presented here. The fluid equations are obtained by a Streamline-Upwind Petrov-Galerkin formulation on unstructured meshes. In the Arbitrary Lagrangian-Eulerian formulation, the mesh is endowed with fictitious elastic properties such that the mesh evolution can be tracked in response to the moving fluid-structure boundaries. Automatic mesh adjustment is achieved by forward integration of the fictitious elasticity field equations, with the mesh velocity feeding into the convective term of the fluid equations at each time step. The structure, essentially a rigid body in the studies here, is modelled using stiff shell elements supported on springs and dashpots. *Spectrum* uses an implicit Hilber-Hughes-Taylor integrator. Typical boundary conditions here include a constant pressure outflow, an incident wind speed and zero normal velocity on the upper and lower boundaries (see Fig. 1c). At the fluid-structure interface, a no-slip condition is prescribed since viscous flow is being modelled. Further boundary conditions associated with the fictitious mesh elasticity problem are also specified to keep the fluid mesh in contact with the structure. A complete set of initial conditions is also required. These typically involve zero structural motion and a fluid velocity comparable to the incident wind speed everywhere. A variety of aeroelastic phenomena then naturally emerge as the field equations are integrated forward in time.

3. Case Study: Great Belt East Bridges

The CFD/FEA program *Spectrum* [2] was used in two case studies of bridge aeroelasticity, both involving the Great Belt East project in Denmark. In the first case study, the vortex-induced oscillations of the approach bridges were considered whilst the second focused on the flexural-torsional coupled flutter of the main suspension bridge.

3.1 Approach bridges - vortex-induced oscillations

From the original wind tunnel tests carried out by others at the Danish Maritime Institute [4], the 193 metre span approach bridges were known to be susceptible to vertical, vortex-induced oscillations at low wind speeds. A system of Tuned Mass Dampers (TMDs) were subsequently designed and fitted to alleviate this problem. In our initial numerical analyses we attempt to simulate the response without TMDs, leaving the complex problem of modelling the effects of TMDs on a continuous viaduct for future research. The two-dimensional full-scale numerical model of the approach bridge is illustrated in Fig. 1. The box-girder deck section is 25.8m wide and 7m high. It was modelled using four-noded isoparametric quadrilateral plate elements sufficiently stiff to create an essentially rigid structure. A 1m slice of the deck was supported on linear springs as shown in Fig.1b. The section mass ascribed was the actual mass per unit length of the real bridge and the spring stiffnesses were proportioned to provide the correct natural frequencies. Owing to the high torsional rigidity of the box section, only the vertical motions are of significant interest in this study. Structural damping (corresponding to 1% logarithmic decrement) was applied via a pair of dashpots attached to the top of the middle flange. The surrounding fluid mesh has 1752 nodes and 854 eight-noded hexahedral elements. The control volume has a total size of 100×200m with unit thickness. Each simulation took approximately 6 hours on an HP C180, using a time increment of 0.05 seconds.

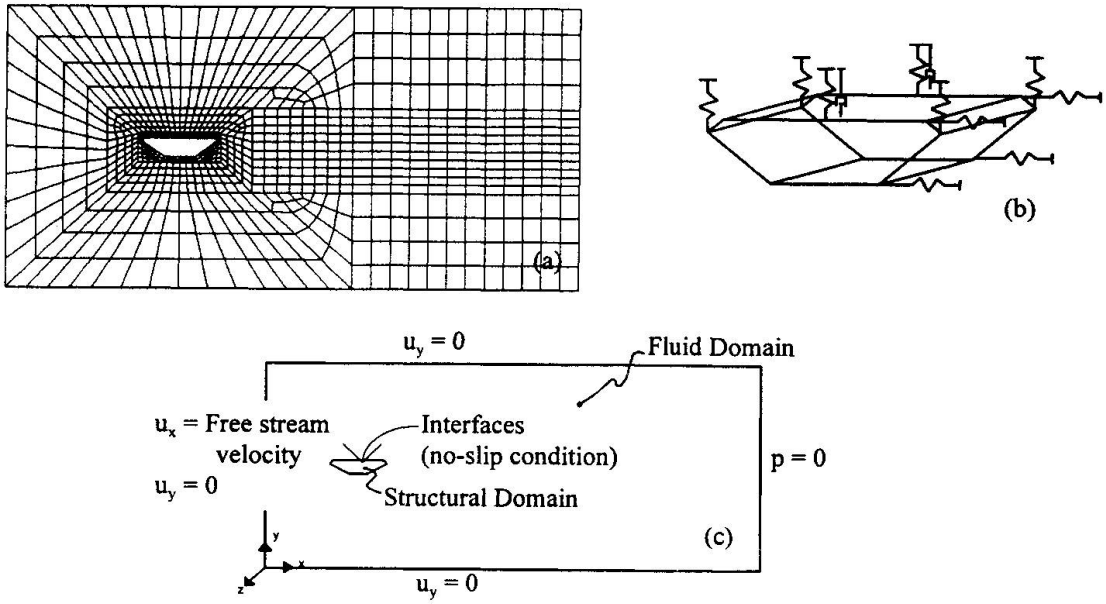

Fig. 1. *Computational model of the approach bridge. (a) Finite element mesh. (b) Location of springs and dashpots in the deck model. (c) Boundary conditions.*

Starting from initial conditions with no structural motion and the full inflow wind speed, the model self-excites into a vortex-induced oscillatory response. At the wind speed corresponding to resonance conditions the structure undergoes some transient motion before stabilising onto a large-amplitude periodic response. Fig. 2 shows two snapshots of the mesh movement (with displacements magnified) during a simulation at resonance. Fig. 3 shows the pressure contours at two similar instants, and a large-scale coherent vortex street is clearly visible downwind.

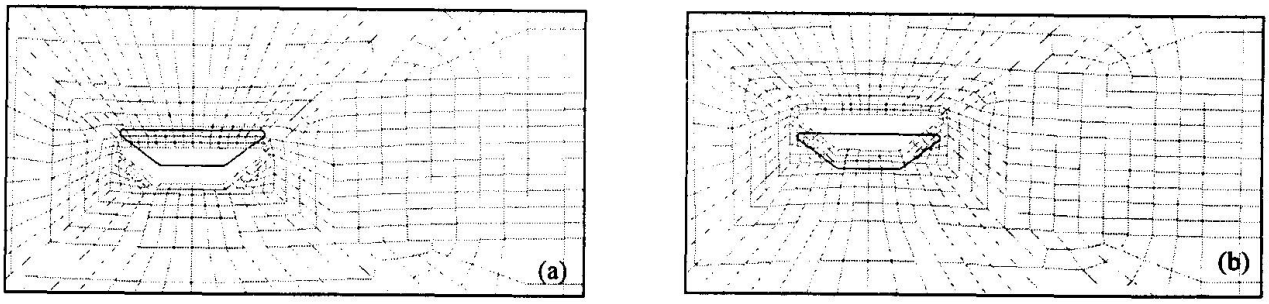

Fig. 2. *Mesh movement at resonance (vertical displacement magnified 5 times). (a) Maximum downwards movement. (b) Maximum upwards movement. Note: original position of bridge deck shown in black.*

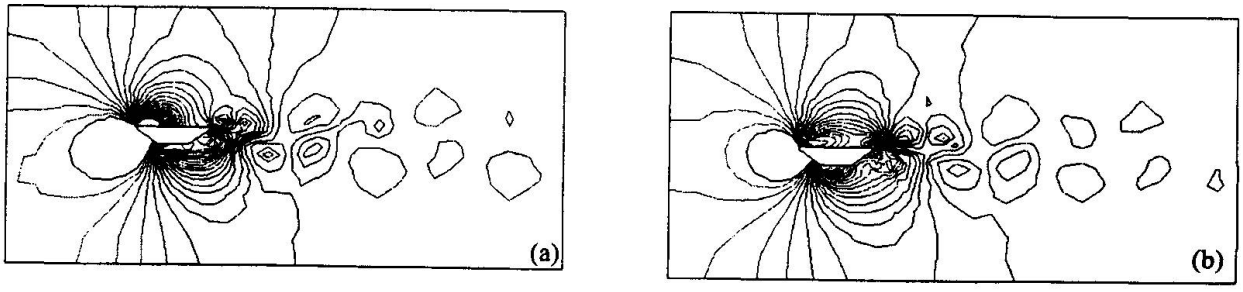

Fig.3. *Pressure contours at resonance. A vortex street is evident downwind. (a) Maximum upwards movement. (b) Maximum downwards movement.*

Fig. 4 shows some typical displacement histories at and off resonance. Maximum displacements were extracted from a set of such histories and are plotted against wind speed in Fig. 5, together with the corresponding results taken from the original experimental investigations at the Danish Maritime Institute [4].

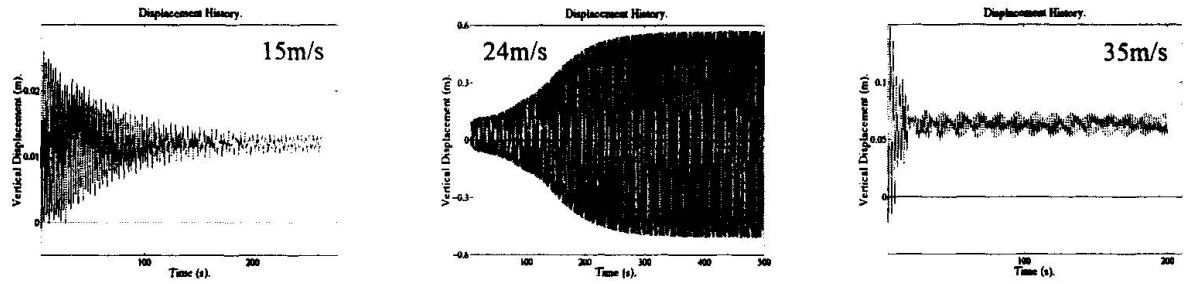

Fig. 4. Displacement histories at and off lock-in.

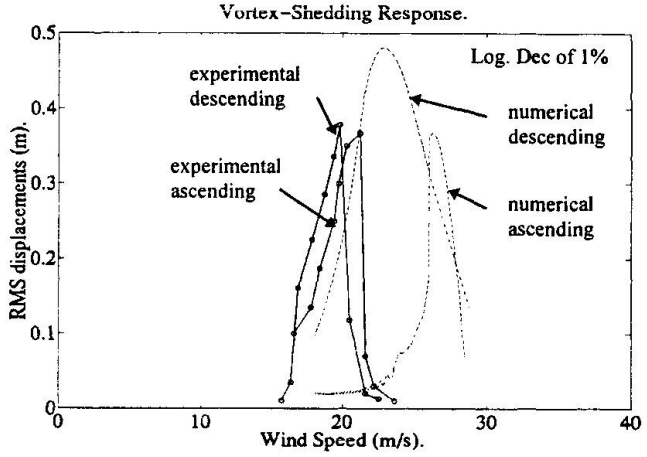

Fig.5. Comparison of numerical (----) and experimental (o-o) RMS displacements.

The first conclusion is that, qualitatively at least, the ability of the computational model to self-excite vortex-induced oscillations has been demonstrated. Quantitatively, although there is some degree of agreement between the predicted resonant response amplitudes there is an evident disparity in the predictions of the critical wind speed at which resonance occurs. The cross-section is comparatively bluff and although separation points are largely dictated by the various sharp corners of the section the fluid processes at these locations are complex. It is thus suspected that the crudeness of the mesh used in these preliminary investigations could be a major factor in this disagreement. Further research is required, needing additional physical modelling to provide detailed flow-visualisation data at and around the separation points during an oscillation cycle for comparison with the initial and improved numerical simulations.

3.2 Suspension bridge - coupled flutter analysis

The case study presented here describes a preliminary investigation into the stability of the 1624m main span of the Great Belt East suspension bridge. A full-scale two-dimensional cross-section with unit thickness is constructed from plate elements and supported on springs and dashpots. The model is given the mass and mass moment of inertia per unit length of the actual structure, and the spring stiffnesses and dampers are then ascribed to give the correct natural frequencies and damping ratios in the flexural and torsional modes. The torsional rigidity of the deck is sufficiently high that this required the vertical springs to be placed on 'out-riggers' outside the cross-section (see Fig. 6b). (Note that these outriggers do not interfere with the fluid flow: the fluid-structure interface is the boundary of the deck). Horizontal motion was restrained by a horizontal spring attached at the intersection of four stiff, massless struts

meeting at the shear centre. The fluid mesh is illustrated in Fig. 6a and involved 7176 nodes and 3508 hexahedron elements. Preliminary analyses showed that the sudden application of the full wind speed to a stationary structure led to large transient disturbances from which, for much computational expense, it was difficult to extract definitive conclusions about the stability of small oscillations. Therefore, for the first few seconds real-time, the level of structural damping was increased to near-critical values, and after the structure had settled into a stable stationary onfiguration under the full wind-speed, the damping values were then set to their correct values. The subsequent motion under further forward integration could then be observed to see if self-excited oscillatory behaviour of the structure occurred.

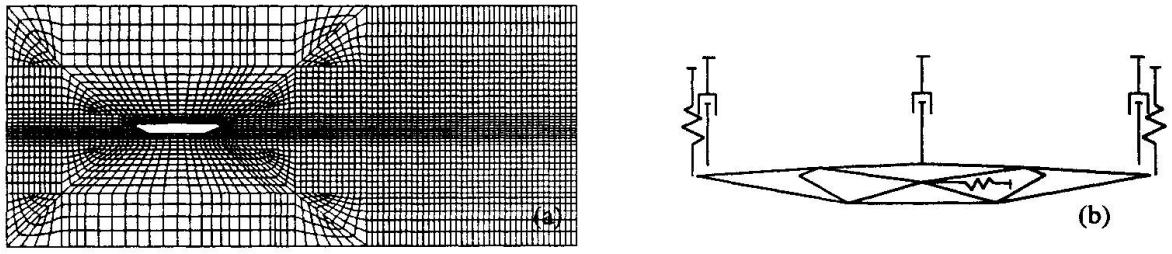

Fig. 6. Computational model of the suspension bridge.(a) Finite element mesh. (b) Location of springs and dashpots.

Fig. 7 shows typical mesh deformations and pressure contours in the vicinity of the bridge at an instant when significant oscillatory motion had occurred. (Displacements have been magnified for clarity). It is interesting to observe the pattern of vortices evident in the pressure contours downwind. By aeronautical standards the deck is comparatively bluff and has a number of sharp corners where separation can occur. Such vortex-shedding is thus to be expected at all wind speeds, even though most theories of flutter make no mention of its existence.

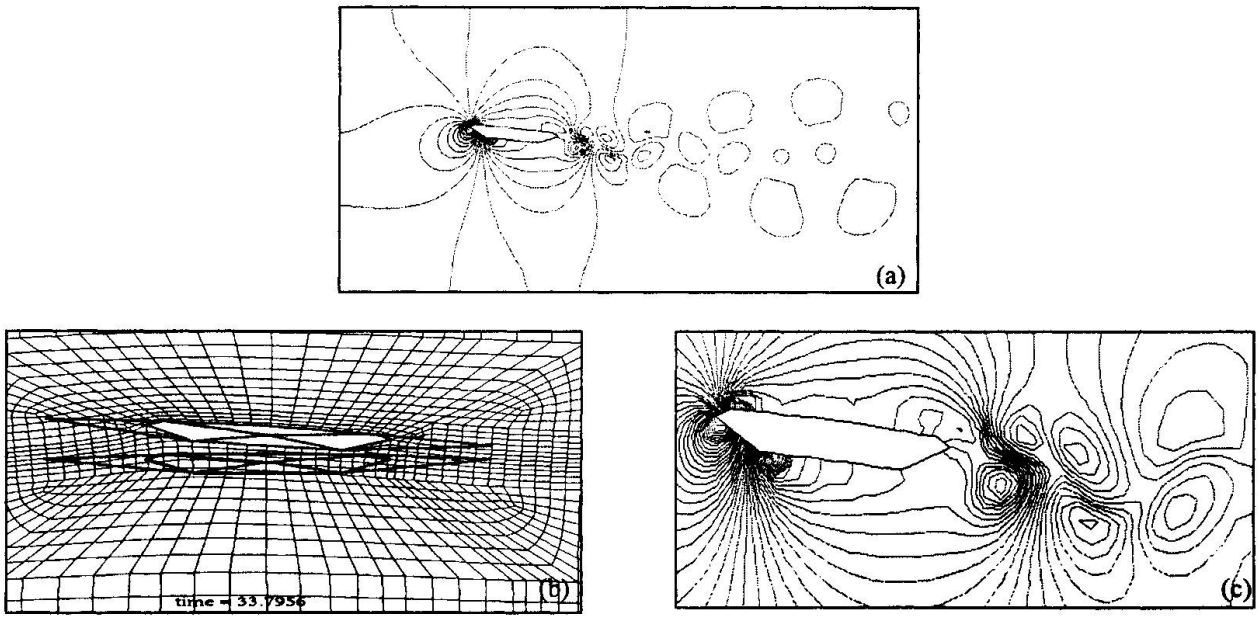

Fig. 7. Coupled flutter at 60 m/s. (a) Pressure contours in whole domain. (b) Mesh deformation (c) Pressure contours near deck. (displacements magnified 5 times).

Fig. 8 shows two displacement histories at 50m/s and 60m/s wind speed. The histories show the vertical displacement of the downwind out-rigger after the artificially-high structural damping has been switched to its correct values (1% and 0.6% logarithmic decrement for vertical and torsional modes respectively, in this case). At 60m/s, flexural-torsional oscillations self-excite at a frequency of about 0.24Hz, this comparing with 0.27Hz and 0.097Hz for the frequencies (still air) of the uncoupled torsional and flexural modes respectively. Each 35 second simulation took approximately 9 hours on an HP C200,

using a time-step of 0.05 seconds. These preliminary results suggest a flutter velocity of around 50m/s, which is at some variance with the flutter limit of 73m/s predicted by the original wind tunnel tests conducted on the section models without windscreens at the Danish Maritime Institute [3]. Conclusions at this stage can only be tentative. In the first instance, the numerical method has demonstrated that under increasing wind speed it is capable of predicting self-excited flexural-torsional oscillations at a frequency close to that expected. However, the cause of the disparity in predicted flutter velocities between the physical and numerical experiments remains to be determined. An obvious source of concern is the poor mesh. Ascribing the no-slip boundary condition to the fluid at the structural interface implies that an attempt is being made to model the substantial wind-shear across the boundary layer, and yet the element dimensions in this region are clearly too large to accomplish this accurately. Future studies will aim to improve the meshing.

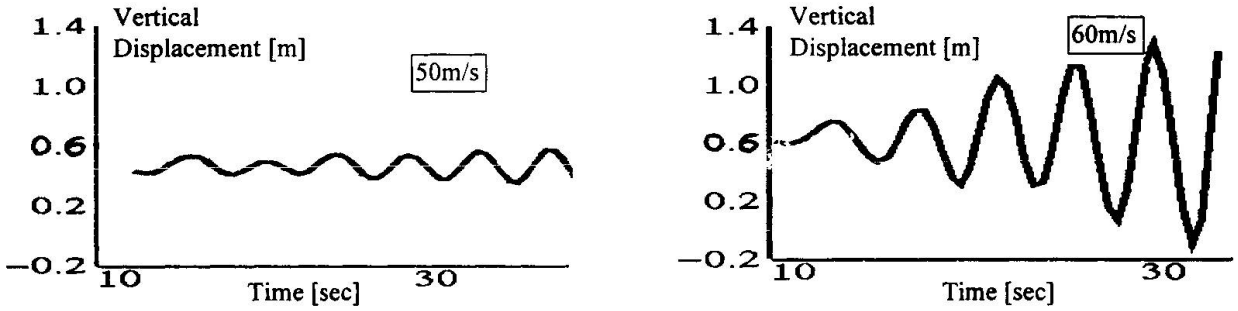

Fig. 8. Histories of vertical displacements at the downwind outrigger.

4. Conclusions and future work

The results of a preliminary investigation into the suitability of a finite element approach to bridge aeroelasticity have been presented. The ability of the numerical models to self-excite into vortex-induced vertical oscillations and flexural-torsional flutter were demonstrated on two case studies based around the Great Belt East project. Although a number of interesting qualitative phenomena were displayed, important quantitative predictions of critical wind speeds are somewhat at variance with the results of the original wind tunnel experiments. Further research is intended to discern the causes of these disagreements. If reliable quantitative predictions can subsequently be obtained by this method, then in tandem with the established physical testing procedures, it could provide a useful tool to aid the evolution of long-span bridge design.

5. References

[1] Brooks, A.N. and Hughes, T.J.R., Streamline upwind/Petrov-Galerkin formulations for convection dominated flows with particular emphasis on the incompressible Navier-Stokes equations. Comp. Meth. Appl. Mech. Eng., Vol. 32: 199-259, 1982.

[2] Centric Engineering Systems Inc., Sunnyvale, California. Spectrum Solver (ver. 2.0) Command reference and Theory Manual, May 1993. (Spectrum is the Registered Trademark of Centric Engineering Systems, Inc.)

[3] DMI report no. 90108.40.01: Section Model Tests to Determine Aerodynamic Derivatives, Vol. 1: Text, Storebælt East Bridge, August 1991.

[4] DMI report no. 92194.01: Detailed Design, Approach Bridges, Section Model Tests III, Storebælt East Bridge, March 1993.

[5] Hughes, T.J.R., Liu W.K. and Zimmerman T.K., Lagrangian-Eulerian Finite Element Method for incompressible viscous flows. Computer Methods Appl. Mech. Eng., Vol. 29, No. 1: 329-349, 1981.

[6] Nomura, T. and Hughes, T.J.R., An arbitrary Lagrangian-Eulerian Finite Element Method for interaction of fluid and a rigid body. Comp. Meth. Appl. Mech. Eng., Vol. 95, No. 1: 115-138, 1992.

The Oeresund Bridge

Örjan LARSSON
Contract Director
Oeresundskonsortiet
Malmö, Sweden

Örjan Larsson is responsible for the Oeresund Bridge contract. He joined Oeresundskonsortiert in 1993. Oeresundskonsortiert is the Owner of the Oeresund Link between Denmark and Sweden.

Klaus FALBE-HANSEN
Project Director
ASO Group
Copenhagen, Denmark

Klaus Falbe-Hansen is a Director of Ove Arup & Partners. He is responsible for the activities of the ASO Group, the group responsible for the bridge concept and the construction monitoring.

Anders H. JANSSON
Production Dir.
Sundlink Contractors
Malmö, Sweden

Anders Jansson is responsible for production and is Deputy Project Director of Sundlink Contractors, the Joint Venture construction the bridge. He is employed by Skanska SB, Sweden.

Summary

The Øresund Bridge is part of the Øresund Link currently under construction across the Sound between Copenhagen, Denmark and Malmö, Sweden. The Link, scheduled to open in the year 2000, is a toll-funded motorway and railway crossing. The 16km coast-to-coast part of the Link consists of a 4km immersed concrete tunnel, a 4km artificial island and an 8km bridge. The 490m main span will be the longest cable-stayed span in the world carrying both road and rail traffic. Minimum headroom in the main span is 57m. Øresundskonsortiet, owned 50/50 by the Danish and Swedish governments, is the Owner of the Link. ASO Group is Consultant responsible for the bridge concept, the construction monitoring and the quality auditing. The Contractor for the bridge is Sundlink Contractors HB.

1. Introduction

On 23rd March 1991 the Danish and Swedish governments finally entered into a binding treaty to establish a fixed connection between Copenhagen and Malmö. The Link would accommodate two tracks for high-speed passenger trains and heavy goods trains together with a dual two-lane motorway. There would be a tunnel under the Drogden channel adjacent to Copenhagen Airport, an artificial island 1km south of the island nature reserve Saltholm, and a high-level bridge crossing the navigation channel Flintrännan.

Øresundskonsortiet is owned jointly by the two governments and is responsible for financing, planning, construction and subsequent operation and maintenance of the Link. The finance is raised on the international markets, with the two states acting as guarantors, ensuring the most favourable borrowing terms. The money will be paid back through user payments over a period estimated currently to be about 27 years.

Five groups of engineers and architects were invited to take part in a design competition for the Link in the early part of 1993. Two groups, ASO and ØLC were chosen to develop their bridge designs further. In the following only ASO's design is described as this turned out to be the economically most advantageous to the Owner and is the design currently being built. ASO Group is led by Ove Arup & Partners (UK) with SETEC (F), Gimsing & Madsen (DK) and ISC (DK). Georg Rotne (DK) is the group's architect.

The tender documents were issued in November 1994 and the bids returned in June 1995. After tender evaluation, the contract was awarded to Sundlink Contractors HB in November 1995. Sundlink Contractors is led by Skanska (S) with Hochtief (D), Monberg & Thorsen (DK) and Højgaard & Schultz (DK). CV Joint Venture consisting of COWI (DK) and VVB (S) carry out the detailed design for the Contractor.

2. The Bridge

The bridge carries the traffic at two levels with the road at the upper level and the railway below. This arrangement was chosen for its safety, operational and visual advantages. An important safety aspect is that the high-speed trains, which will be travelling at up to 200kph do not disturb and interfere with the road traffic. The operational flexibility is increased; during lane closures caused by road accidents or maintenance works traffic can anywhere along the bridge be directed on to the other carriageway. It is an important aesthetic and visual advantage, in particular to the road user that the view during the journey is unimpaired by the installations and fencing associated with an electrified railway. A curved alignment was chosen for the bridge to further enhance the experience of crossing the Sound.

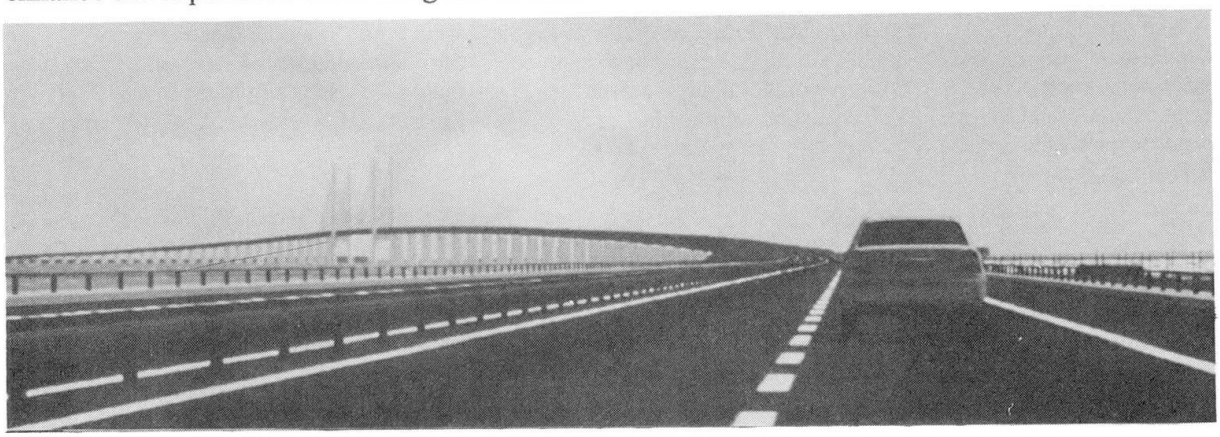

Fig. 1 View when driving towards Sweden

2.1 The Approach Spans

The approach spans make up 85% of the length of the bridge and it was therefore important that an economical deck solution was found for this part. To ensure a unified design for the whole bridge the solution should also be able to act as girder in a cable supported span over the navigation channel. The most economical solution for the two-level deck was found to be a double composite solution consisting of a concrete road deck supported on two parallel steel trusses placed on either side of the concrete railway deck.

The Warren type trusses are designed with a more open bracing than is generally used in existing steel truss bridges. With an inclination of the diagonals of 45° instead of 60° the number of nodes in the trusses is almost halved offsetting the extra cost of the longer span of the chords. Truss bay length is 20m, members are closed boxes, corners at nodes are rounded and all connections are welded. The bridge appears lighter and is more transparent so railway passengers also enjoy better views of the Sound.

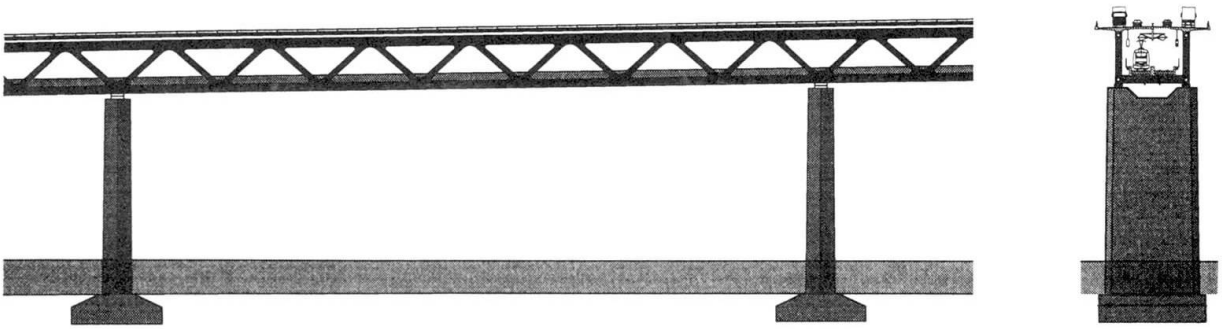

Fig. 2 Typical 140m approach span

The pairs of trusses are connected at the lower level at each node position through transverse steel box beams 3m wide, which in turn carry the railway. The railway deck consists of twin concrete troughs spanning between the transverse beams. The webs of the troughs contain the ballast for the railway tracks, act as containment barriers in case of derailment and reduce noise emission. The deep girder leads to longer spans, with both visual and environmental advantages. Span lengths vary from 120m near the shore to 140m further out.

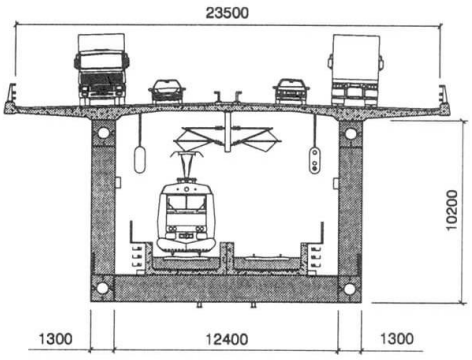

Fig. 3 Approach spans – Cross-section

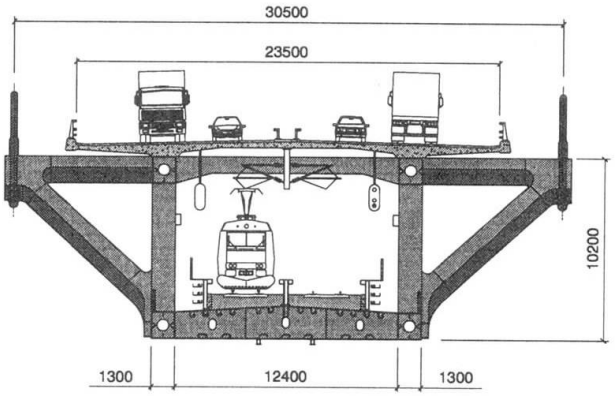

Fig. 4 Cable-stayed spans – Cross-section

2.2 The Cable-Stayed Spans

The basic girder cross-section for the cable-stayed spans is similar to the approach spans except for the lower railway deck. In order to save weight the railway is carried on a continuous steel box acting as part of the lower chords of the trusses. Longitudinal steel parapets provide containment in case of derailment.

The inherent stiffness of the deep girder was a factor in the choice of cable configuration. The bridge is subjected to considerable live loading which normally would suggest a fan configuration to control moments and deflections; however, this does not apply to the same degree with a deep stiffening girder. By optimising the position of the side span anchor piers adequate stiffness of the system is readily achieved with a harp configuration. An important reason for choosing this configuration is the natural affinity of the harp with the repeating geometry of the truss. The affinity is emphasised by modifying the inclination of the diagonals in the cable-stayed spans so that every other diagonal has the same inclination as the cables.

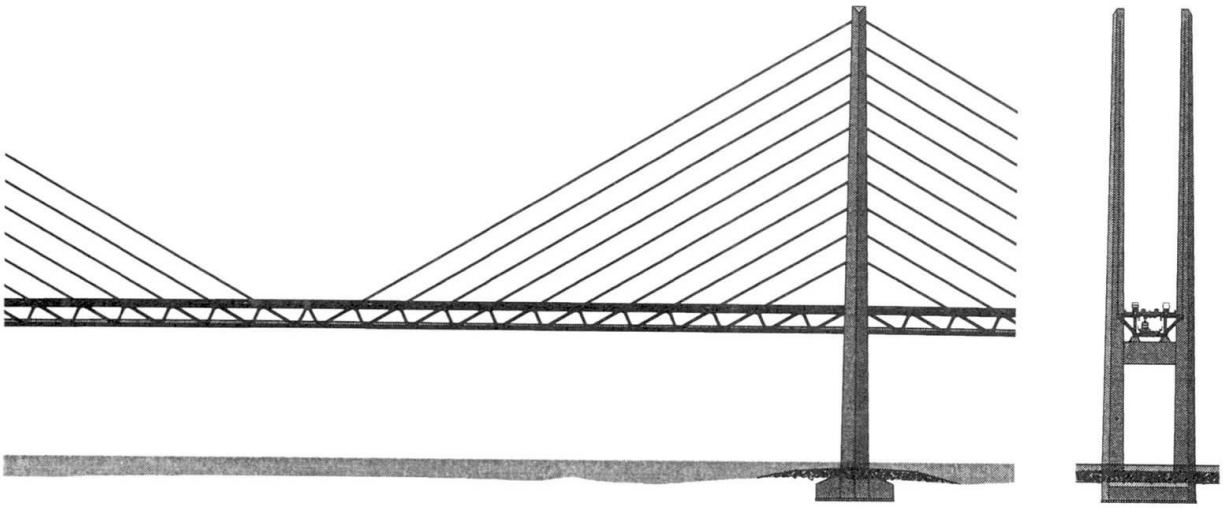

Fig. 5 Part of 490m main span with pylon reaching level 203.5m

The visual formality of the harp is particularly apparent when the cable planes are vertical. The effect is further enhanced here because independent free-standing towers above deck level support each cable plane. To achieve this the cable plane must coincide with the centroidal axis of the tower in order to avoid permanent transverse bending in the towers due to vertical loads on the deck. The deck passes between the concrete towers with the cable planes at a safe distance from the roadway, well protected from damage due to accidents on the road. The stay-cables are anchored to inclined triangular frames attached to the outside of the truss.

Fig. 6 Drivers' view

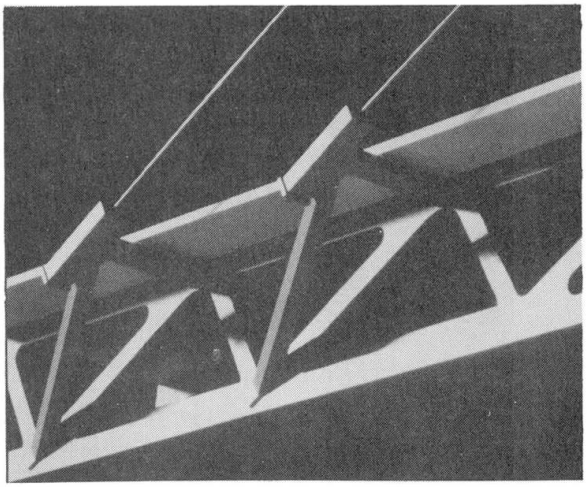

Fig. 7 Anchoring of stay-cables

2.4 Definition Drawings

Prior to tender, extensive consultations were held with authorities in the two countries on matters like aesthetics, environment, road and railway operation, navigation, safety, etc, and risk analyses were carried out to identify major risks and measures to alleviate them. The design was markedly influenced by these activities and included many features over which the client wished to maintain control. Some of these could be expressed as functional requirements but some important design features could not. The tender documentation for the 'design and construct' contract therefore included not only the usual design and construction requirements but also Definition Drawings describing those design features, geometry and materials that had to be retained in the successful contractor's design. The documents also included for the contractors' information an Illustrative Design as an example of a comprehensive design that fulfilled the Owner's requirements.

3. Detailed Design

The basis for the detailed design is the Eurocodes extended with the Owner's Project Application Document and Design and Construction Requirements. The aim is to produce a robust structure with a service life of 100 years using established and environmental-friendly techniques,

The Contractor is responsible for the detailed design, which has been carried out by his designer. This has the advantage that, as long as the Design Requirements including the Definition Drawings are adhered to, the design can be refined and optimised to suit the precise construction methods used. The erection concept includes prefabricating and handling of a large number of heavy structural elements, caissons, pier shafts and whole span elements, much design effort has gone into optimising dimensions and weight of these elements.

4. Construction

Erection based on extensive prefabrication of very large elements is nowadays used on most long bridges being constructed offshore. Some important advantages using this concept are, that the

influence of the climate on the construction programme is reduced, elements are produced under factory conditions and adverse environmental impact of the works is easier to control. There is less risk of delays and therefore also less risk of the cost of the project escalating.

4.1 Substructure Construction

Prefabrication of caissons and pier shafts for the approach spans is carried out in a purpose-built yard in Malmö North Harbour, close to the bridge line. The caisson bases vary in plan size from 18m x 20m to 22m x 24m. The central top part of the caisson, being the bottom part of the shaft is constructed to 'installed level' +4m. However, for the pier positions closest to the shore the complete pier, caisson and shaft are prefabricated in one piece. A high degree of prefabrication of reinforcement cages is used in a station system along two production lines in the yard. Each line ends in a load-out jetty, where the Heavy Lift Vessel Svanen can collect the caissons that are finished and ready for transportation and placing in the bridge line. The weight of the caissons at load-out varies from 2500 tons up to 4700 tons. Production started towards the end of 1996.

The caissons for the two pylons (35m x 37m) weighing 19,000 tons each were too heavy for HLV Svanen, which has a lifting capacity of 9,000 tons. The pylon caissons were therefore constructed in a nearby dry dock in Malmö Central Harbour. A purpose-built catamaran barge was used, after flooding of the dock to lift, transport and place the two caissons during April 1997.

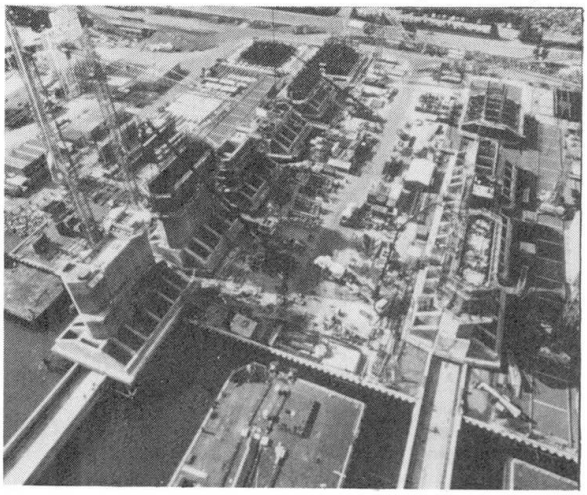

Fig. 8 Caisson production lines

Fig. 9 First pier at load-out jetty

Seabed levels at pier positions vary from -3m to -9m and foundation levels from -8,5m to-18.5m. Foundation pits are excavated by backhoe dredgers. After cleaning and inspection of the pit the caisson is placed on three pre-positioned concrete pads. The space between the limestone and the underside of the caisson is grouted with a special mortar and the caisson ballasted. Backfilling up to seabed level and scour protection complete the foundation.

Prefabrication of pier shafts takes place at a separate area in the yard. The shafts, from 'installed level' +4m to the top, are produced fully finished in one position, before being moved to the load-out jetty. Also here a high degree of prefabrication of reinforcement is used. Each pier shaft is cast in 4m lifts. The pier shafts vary from 13m to 51m in height and from 900 tons to 3300 tons in load-out weight. Pier shaft production started early 1997.

HLV Svanen takes the shafts to the bridge line and places them on the top part of the already positioned caisson at level +4m. The lower 2m of the shaft is recessed to accommodate the construction of an in-situ joint between shaft and caisson. The pier shafts are to a varying degree ballasted in accordance with the detailed design.

The 203.5m pylons are the only major element of the bridge to be constructed in-situ.
A traditional climbing form, each lift being 4m, is used in constructing the towers. Construction began July 1997 and will be completed during the second half of 1998. Protective reefs are

constructed around the pylon footings. Reefs are also constructed at the three piers each side of the pylons. The pylons will be completed in parallel with the erection of the cable-stayed deck.

4.2 Superstructure Construction

The approach span deck girders are being prefabricated in Cádiz in southern Spain. Here 49 deck elements, 7 nos. 120m and 42 nos. 140m are produced. The two steel trusses, joined by the lower transverse steel box beams and the transversely prestressed top concrete road deck, form a deck element. Fully painted, these elements are transported in pairs on ocean-going barges from Cadiz to the yard in Malmö North Harbour where the prefabricated lower railway troughs are installed. Erection in the bridge line is by HLV Svanen. At load-out, deck elements weigh from 5500 tons to 6900 tons, close to the lifting capacity of HLV Svanen considering its purpose-built 1800 tons lifting gear. Production started in Cadiz early 1997 and final delivery in Malmö will be during the second half of 1999.

The cable-stayed deck girder is produced in Karlskrona, Sweden, some 200km from the site. Steel sections 120m and 140m long are transported on barges to Malmö North Harbour where the upper roadway deck is cast. The section is then transported out and put in place by HLV Svanen. The shallow waters of Øresund, and the fact that the navigation channel Flintrännan is being realigned as part of the construction of the Link, give a special advantage when erecting the cable-stayed bridge. The main span can be erected in four sections supported by temporary towers founded on the seabed at level -8m to -10m. This speeds up the deck erection, and greatly reduces the construction risk compared to the common cantilever construction of cable-stayed bridges. After completion of the main span the shipping traffic is moved to its new channel. The cable-stayed bridge will be erected during 1998.

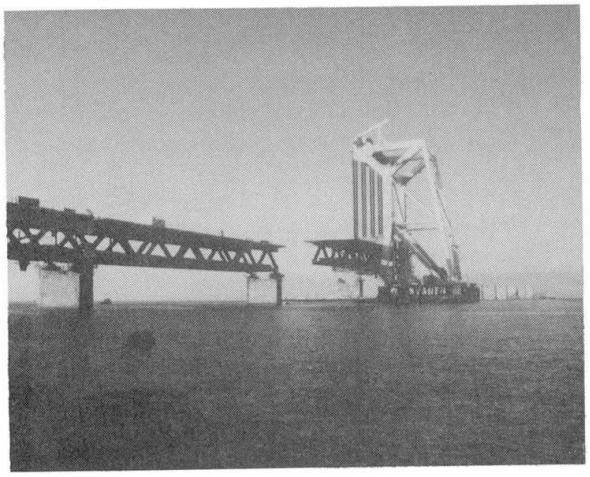

Fig. 10 Svanen positions 120m span

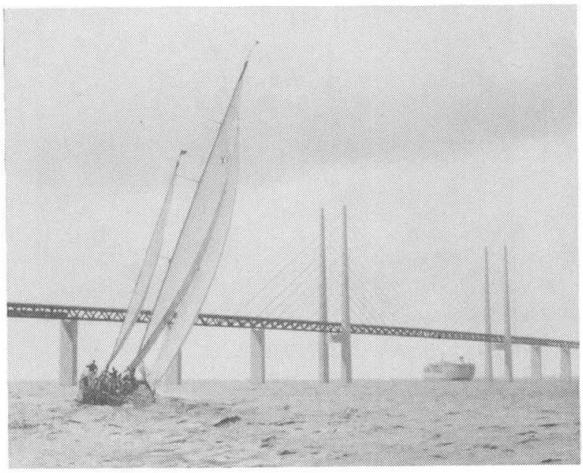

Fig. 11 Sailors' view year 2000

5. Conclusion

The form of contract developed for the bridge has worked successfully. The Contractor is responsible for delivering the quality assured construction works in accordance with the Owner's requirements. He is also responsible for the detailed design, which can be tailored to the precise construction method. By including comprehensive Definition Drawings, as part of the Contract Documents the Owner will receive a bridge that not only fulfils his quality requirements on materials and workmanship but also looks aesthetically like the bridge he envisaged before he signed the contract.

When the Link is opened in the year 2000 the Øresund Bridge will, with its main span of 490m rank as joint number 9 among the cable-stayed bridges around the world. However, the bridge will at that time be the only cable-stayed bridge with both road and rail traffic among the world's twenty longest cable-stayed spans. The bridge will also be the longest railway-bridge in Europe.

Sunningesund Cable-Stayed Bridge

Carl HANSVOLD
Techn. Dir.
Johs. Holt AS
Oslo, Norway

Project leader for the design of the cable-stayed main bridge and the superstructures of the approach bridges.

Helge NILSSON
Civil Eng.
Skanska Teknik AB
Stockholm, Sweden

Senior Engineer of bridge design at Skanska Teknik, responsible for design co-ordination and quality assurance of the final design.

Summary

The Sunningesund bridge, today named the Uddevallabridge from the town Uddevalla located on the Swedish west coast, is part of the motorway E6 between Gothenburg and Oslo. Construction of the bridge started in mid 1997 and is scheduled completion during summer 2000. This paper gives a description of the bridge, the early design considerations, the wind investigations and the construction methods.

1 Introduction

The Uddevalla bridge consists of three parts, the south approach bridge, the cable-stayed main bridge crossing the navigation channel to Uddevalla and the north approach bridge. The total length is 1712 m. This section of the E6 passes through a very beautiful province of Sweden, thus the motorway is constructed with considerable emphasis concerning the surroundings with all sections of the bridge being detailed carefully and given high quality with regard to the aestethic. A design-built contract was awarded to Skanska and the contract was signed with the Swedish Road and Bridge Administration in the early 1997. The detailed design is carried out for the contractor Skanska by Skanska Teknik AB, a subsidiary of Skanska AB and Johs Holt A.S in Norway.

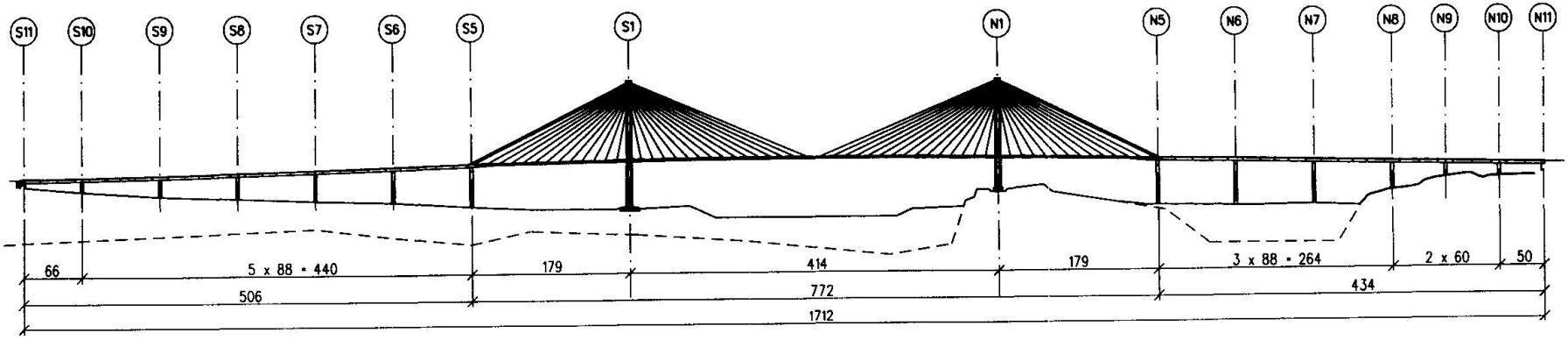

Figure 1

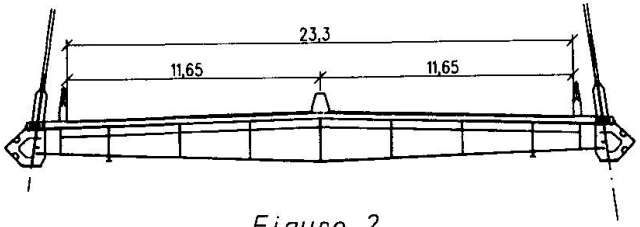

Figure 2

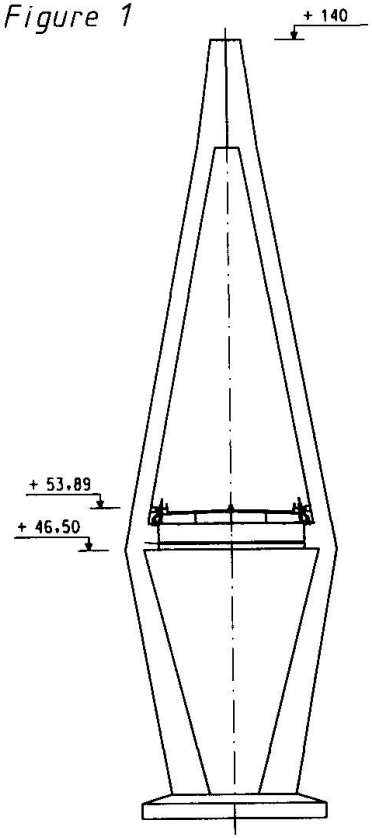

South tower

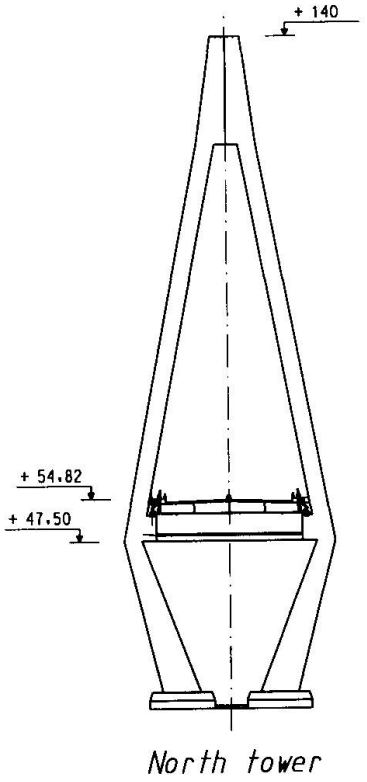

North tower

Figure 3

2 Description of the Bridge

2.1 Overall configuration

The bridge is a high-level bridge of total length 1712 m carrying 4 traffic lanes, ***figure 1***. The central cable-stayed section provides a navigation clearance 190 m wide and 52 m high over the Sunninge Sund. The approach bridges to either side of the cable-stayed section at the centre, have a total length of 506 m at the south side and 434 m at the north side. The spans increase from 50 m at the north abutment to typical 88 m towards the centre. The cross-section of the superstructure is constructed using two separate steel box girders with concrete deck cast in situ. The design is conventional and not further described in this paper. The central cable-stayed bridge is made up of a 414 m main span and two 179 m spans either side. The cables supporting the bridge are arranged in slightly inclined cable planes nearly parallel to the tower legs. They are anchored at equidistant intervals along the bridge deck of 13,32 m except for the outer 3 back stays which are concentrated at the anchor piers N5 and S5, ***figure 1.***
The entire structure is continuous with expansion joints only at the abutments. Continuity between the approach bridges and the cable-stayed bridge is provided by a heavy concrete transition structure. The six piers at axes N5-N7 and S5-S7 are hinged to the bridge superstructure and contributes to the stability of the bridge in the longitudinal direction. All other piers are equipped with sliding bearings.

2.2 Bridge superstructure

The bridge cross-section in the stayed spans, ***figure 2***, is a composite structure of an open steel grid and prefabricated concrete slab elements. The wind nose, connected to the outer longitudinal I-beam, is a load bearing thin walled shell structure. The stay cables are directly connected to the web of the 1,7 m high longitudinal girders.
The slab elements are spanning longitudinally and are connected by loop reinforcement in the cast in place joints. The thickness of the concrete elements is 240 mm and longitudinal reinforcement of 20 mm bars at spacing 160 mm is generally provided to achieve satisfactory strength and limitation of crack widths to 0,20 mm.
The bridge-cross section accommodates 6 traffic lanes.

2.3 Towers

The towers are made of concrete grade K55 according to the Swedish Standard BBK 94.
They are diamond shaped and rise to elevation 140, **figure 3**. At the tower top the stay cables are anchored inside steel boxes fixed to the concrete by shear studs. The tie-beam between the tower legs is fully post-tensioned for the outward thrust from the tower legs.
According to the project specifications no cracking of the tower is allowed during the construction period. This criterion imposes strict limitations on the erection procedure for the bridge superstructure and temporary struts between the tower legs are required. Also temporary supports of the superstructure are necessary.

2.4 Stay cables

The stay cables consists of 22 to 77 strands (15,7 mm), individually galvanised, waxed and sheathed. The bundle of strands is covered by an external HDPE pipe.

The void between the strands and the external pipe is maintained empty. The stay cables and the anchorage system is delivered and installed by VSL.
The structure has been designed to allow for exchange of any stay cable for a situation with a reduction in live loads to three opposite lanes. In addition any stay cable can be accidentally removed under full traffic load without structural instability or inelastic deformations.
Cable vibrations have been a problem on several cable-stayed bridges. To our knowledge, no well documented theory exists for evaluating the risk for such vibrations. Thus the following precautions have been taken:
- The external HDPE pipes have ribs to prevent so called "rain-wind vibrations".
- The longest cables will be equipped with dampers, probably hydraulic dampers outside the anchorage. The damping system is currently being evaluated.
- The cable system shall allow for future installation of transverse stiffening ropes if deemed necessary.

3 Design Development

3.1 Conceptual Design

Due to strict limitations in the project specifications the main span could at an early stage be fixed to 400-420 m. The remaining but rather challenging task was to select suitable shapes and dimensions of the bridge cross-section and the towers.
Three alternative cross-sections, all composite, were evaluated:

a) An orthotropic steel box girder with concrete deck. Two cable planes.
b) As a), but with a single, central cable plane
c) An open steelgrid with bridge deck cast in place or made up of pre-fabricated slab elements

Alternative c) was found to be the most economical and also aestethically acceptable. The structural adequacy of this type of cross-section has been clearly demonstrated by several long span bridges completed during the last decade. Alternative c) was thus selected for the final design.
Two tower shapes were investigated: Diamond and H-shapes. The lower cost of the H-tower legs was to some extent balanced by higher foundation cost due to separate footings for the H-tower. Finally, the diamond shape was found to be the most suitable, combining aspects of economy, aestethics and structural behaviour.

3.2 Wind effect investigations

The wind climate at the bridge site is not particularly severe. The 10-minutes average wind speed at the bridge deck level is 32, 8 m/s and the turbulence intensity 14,7%. Above values refer to a return period of 100 years, relevant for the completed bridge. For the construction phase, a return period of 10 years applies.
Wind tunnel tests on sectional models were performed to determine the aerodynamic stability, the sensibility to vortex shedding and the aerodynamic force coefficients. The tests comprised three model configurations:

1. The completed bridge without traffic
2. The completed bridge with traffic
3. Construction stage

The sectional model was tested both in low turbulent and high turbulent flow. The test results confirmed that the stability criterion of 53 m/s was achieved with an ample margin.
According to the project specification for traffic comfort, the RMS of the vertical acceleration should be less than 0,3 m/s^2 for frequencies lower than 1Hz at a 10-minute wind speed of 25 m/s at bridge deck level. Also this criterion was fulfilled.
The wind tunnel investigations were carried out by the Norwegian University of Science and Technology, Trondheim in co-operation with Svend Ole Hansen ApS, Copenhagen, **(I).**
The results of the wind tunnel testing have been used as basis for a series of buffeting response analyses. These analyses cover the completed bridge with and without traffic and critical stages during construction. The buffeting analyses have been carried out with the SVING program developed by Hans Björge, **(II)**

3.3 Static analysis and design

A step by step analysis including all structural systems during the various erection stages until completion of the bridge has been performed. Time dependent strain from creep and shrinkage is included, also amplification of bending moments due to second order effects. Non-linear influences from cable sag showed to be limited. The stay-cables have therefore been modelled as linear elements with an effective modulus of elasticity. The analysis has been performed with the RM-spaceframe programme. **(III)**
ULS-criteria govern in most cases the design of structural elements. An exception is the stay cables where the SLS-criteria is governing.

4 Foundation Structures

The geological presumptions and geotechnical conditions at the bridge site vary considerably, typical for the Swedish west coast. All types of foundations have been used for the bridge. The south approaches and the south pylon are placed on or close to an edge from the inland ice with layers of moraine, gravel and sand formed during a period of 200 years, 12000 years ago. In the north the rock level is varying from 100 m below sea level to 35 m above.
The south abutment S11 and the three next piers S10-S8 are founded on well natural compacted material from the inland ice. The piers S7-S5 are founded on driven precast concrete piles having lengths varying between 14 m to 25 m, 350 mm square and bearing capacity of 1600 kN. The loads are carried combined by surface friction and by pile tip. The south pylon S1 is placed in the sea close to the shore and founded on driven sheet piles to the rock with a diameter of 700 mm. After having checked the straightness the piles are filled with concrete cast in dry and partly reinforced. With a bearing capacity of 4700 kN the loads are carried by a composite structure, steeltube-concrete, taking into account the corrosion in the surface of the steel sheet, the lengths are 25-28 m.
The north pylon N1 is founded on a rock base 20 m above sea level.
The anchor pier N5 is founded on piles of drilled steel cores with diameter 210 mm and 150 mm and length of 6 m to 15 m due to the excessive big slope of the rock. Bearing capacities are 3600 kN respectively 2500 kN. The next two piers N6, N7 are founded on driven sheet piles to the rock, diameter 500 mm and maximum length 30 m to 80 m. Concrete fill and composite structure similar to pylon S1 and a bearing capacity of 2400 kN. The rest of the piers N8-N10 and abutment N11 are founded on rock.

5 Construction

Towers and piers are built by climbing formwork in sections of approx. 4 metres, and reinforced to a large extent by prefabricated nets or cages lifted into place. The superstructure of the main bridge will be erected by free cantilevering from the towers outwards. Stability of the bridge system during erection is ensured by 3 auxiliary towers, supporting the bridge superstructure. Pre-assembled steel grid sections of 13,32 m length will be lifted up and welded to the previous section. The cables are then installed and stressed, the precast slabs are positioned and the joints between them casted. After final tensioning of the stays the next section will follow.
The steel box girders of the approach bridges will be welded to continuous girders behind the abutments and launched to right position. After that the concrete slab is reinforced and casted in situ on a travelling scaffolding.

6 Concluding remarks

The construction work is now well under way with the exception of the tower S1 where the foundation work is almost completed. Launching of the steel box girders of the approaches will commence in March 1998. Erection of the steel superstructure in the main span is planned to commence in August this year. The bridge is scheduled for completion during summer 2000.

ACKNOWLEDGEMENTS

Owner:	Swedish Road and Bridge Administration, Region West
Contractor:	Skanska Civil Engineering AB, Bridge Department
Stay cables:	VSL International Ltd
Structural design:	Skanska Teknik AB in co-operation with Johs. Holt A.S.

REFERENCES

(I) NTNU and Svend Ole Hansen ApS:
Sunningesund Cable-stayed Bridge
Investigation of Wind Effects:
Part A: Static tests
Part B: Dynamic tests
Part C: Full scale response predictions

(II) Hans Björge: SVING-A "Finite Element Program for Wind and Earthquake Analysis of Frame Structures", Reinertsen Engineering 1997

(III) TDV: RM-Spaceframe Users Manual, rev. 5.80-09/96

Great Belt East Bridge: Aerial Spinning of the Main Cables

O. Rud HANSEN
Civil Eng.
COWI
Copenhagen, Denmark

Ole Rud Hansen, born 1944, received his civil engineering degree from the Danish Eng. Academy in 1968. He is currently Techn. Mgr heading Techn. Sercives on the Great Belt East Bridge.

F. ROUVILLAIN
Civil Eng.
COWI
Copenhagen, Denmark

Francis Rouvillain, Born 1933, received his civil engineering degree from Ecole Central de Lille in 1956. Post graduated form the Welding Institute in Paris 1957. He is currently working as senior Technical Advisor on cable works for the Great Belt East Bridge.

Dan OLSEN
Civil Eng.
COWI
Copenhagen, Denmark

Dan Olsen, born 1945, M.Sc. C.E. 1970, and Ph.D. 1973 from the Techn. Univ,. of Denmark. In COWI since 1977 he has been working with risk analysis in civil engineering, including construction risk analysis.

Summary

The East Bridge forms a major part of the Great Belt link which connects Denmark's two largest islands, Sjælland (Zealand) and Fyn (Funen). The total length of the link is 17.5 km and it is separated in the middle of the Belt by a small island, Sprogø. The East Bridge comprises a suspension bridge and two approach bridges with a length of 2592 m and 1567 m, respectively. The total length of the suspension bridge is 2694 m with a main span of 1624 m, the second largest span in the world. This paper represents the designer's point of views concerning activities related to the erection of the main cables and experiences gained from this work, especially as regards unbalanced spinning and down-time due to adverse weather conditions.

1. Method Statement for Cable Spinning

The spinning of the main cables is normally on the critical path of the working schedule when constructing suspension bridges. The start of many other activities depends on the completion of the spinning works (compacting of cables, erection of clamps, erection of hangers followed by erection of the main girder). Two options for constructing the main cables were given in the tender documents: Traditional aerial spinning or prefabricated parallel wire strands (PPWS). Due to higher construction costs for the PPWS option a traditional aerial spinning method was chosen, but modified by adopting "The Low Tension Control" principle. This modification gave several advantages being less time consuming and less sensible for adverse wind conditions compared to the traditional free hanging wire method. The cables were spun alternating the north and south cable. At the same time 2 strands were spun on the same cable. Two independent tramway systems were erected, one on each cable and each with 2 spinning wheels able to transfer 4 loops of wires at each trip. All installations were located on one anchorblock only. The use of "The Low

Tension Control" principle (80% of the free hanging tension) required installation of sag control cables to correct the lowering of the catwalk caused by the partial (20%) weight of the strand.

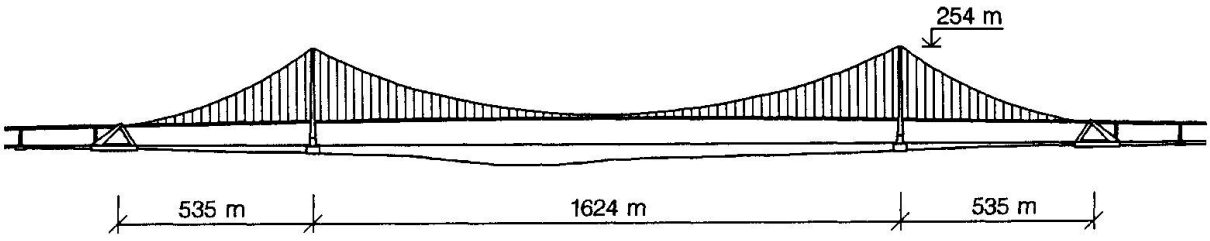

Fig. 1: Elevation of the suspension bridge

2. Pre-spinning Activities.

In order to have balanced horizontal forces on the top of the pylons during spinning of the cables the saddles at the pylons shall be placed offset to their final position. The design value for this offset was 1.24 m at each pylon top. Two possibilities for performing the offset were stated in the tender document: One possibility was by translation of the main saddles on the top of the pylon. Due to the configuration of the top of the concrete pylons, this solution would have required construction of solid platforms to extend the bearing area for the saddles. The other possibility was to directly pull back the top of the pylons towards the anchor blocks and this option was selected by the contractor. This solution was possible due to the slenderness of the pylons, but limitation of the bending stress and risk of cracks in the concrete give some limits in the general use of this the method.

The horizontal force needed to pull back the top of the pylons 1.24 m was calculated to approx. 8,000 KN, based on an E modulus of the concrete of 28,000 MPa corresponding to the figure given in Danish standard. This value includes the effect of creep. Experience on site showed that the short term E modulus of the concrete corresponded to 35,000 MPa.

The pull back cables were fixed at the top of the pylon and the hydraulic tensioning devices were placed on the concrete deck at level +10 m on the anchor block. The first tensioning was performed in April 1996, but due to damages on the pull back cables they were slacked again and retensioned late may 1996, approx. 1.5 month before start of spinning. When the calculated forces were reached, the actual horizontal displacement of the top of the pylons was only approx. 1.0 m compared to the design value of 1.24 m. Increasing of the displacement could be expected due to creep in the concrete, but due to the short time between pull back and spinning, the effect of creep was not fully present, when spinning started. As the pull back cables were damaged by hammering caused by vibrations of the cables, an additional tensioning of the cables, in order to get the design value, was not suitable. This unforeseen situation implied modifications of the initial geometry of the strands taking into consideration the actual displacements of the pylons at start of spinning work. The consequences of these modifications are further described in Section 4.

As soon as the special support structures on the top of the pylons and at the splay saddles were installed, the erection of the catwalks was started. Prefabricated 40 m long rolls of mesh comprising wooden steps and side mesh, were transported to the top of the pylons and rolled down

along the floor strands with assistance of the hauling rope. The floor strands and the mesh panels for both catwalks were erected in 33 working days. The transport of the wheel batteries of the tramway system and of the posts for the lighting system was performed by helicopter. This method was very time saving considering that the offshore work sites at anchor blocks and pylons were only accessible by boat at this time of the construction.

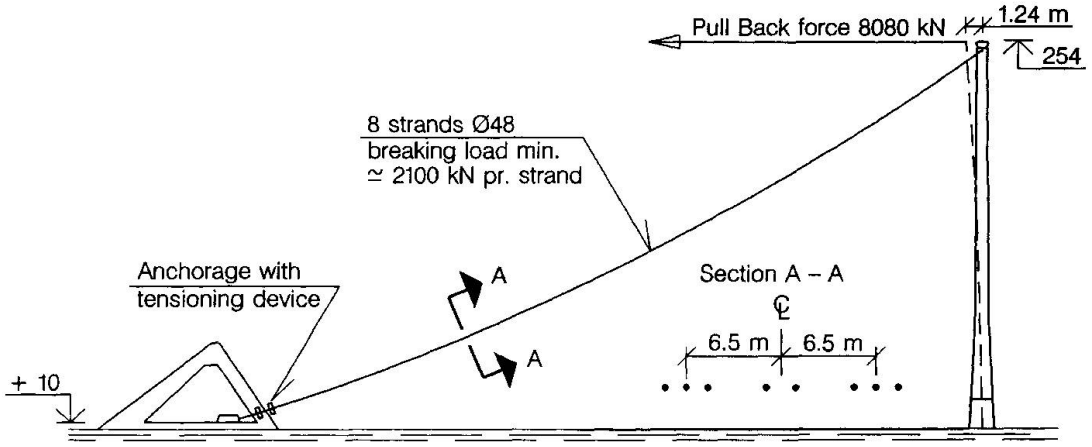

Fig. 2: The pull back system

3. Spinning Works

Each main cable consists of 37 strand of 504 no. of wires giving a total of 18648 no. of wires per cable, corresponding to a weight of 20,000 tonnes for the 2 cables. The spinning works implied the following successive operations: Supply of coils at the reeling unit, reeling and unreeling, spinning of the wires, strand compacting, serving and strand sag adjustment.

1. Supply of coils. All the reeling/unreeling units were located offshore on the eastern anchor block. The coils were transported by lorries on the eastern approach spans in level +57 m and lowered by lift to the anchor block at level +10 m. The average weight of the coils was 800 kg, corresponding to about 4,500 m wire or 1.5 times the length from anchor block to anchor block. The coils were supplied by two different suppliers.

2. Reeling and unreeling of coils. The coils were reeled on drums, each with a capacity of 10 coils. Each reeling/unreeling unit comprises 2 drums. When the wires were reeled on one of the drums from the coils with a tension of 90 kg, the wire on the second drum was unreeled to the spinning wheel. This operation was performed in parallel on all 8 units.

3. Aerial spinning. After a learning period for the personnel and testing of the equipment in full scale on the first strand which was spun with 2 loops only on the spinning wheel, the proper spinning work was performed in 18 set ups. The normal speed of the spinning wheel was 4 m/s with 4 loops of wires on the wheel. The average duration of a complete turn/return trip was 32 min. including time for anchoring the wires around the strand shoes. The global efficiency of the spinning works was 75%, and the 25% down-time was divided into 10 % due to weather conditions and 15 % due to unforeseen problems with the equipment or with handling of the wires. The spinning works began the 6th of July 1996 and were completed the19th of November 1996 giving a total duration of 137 days.

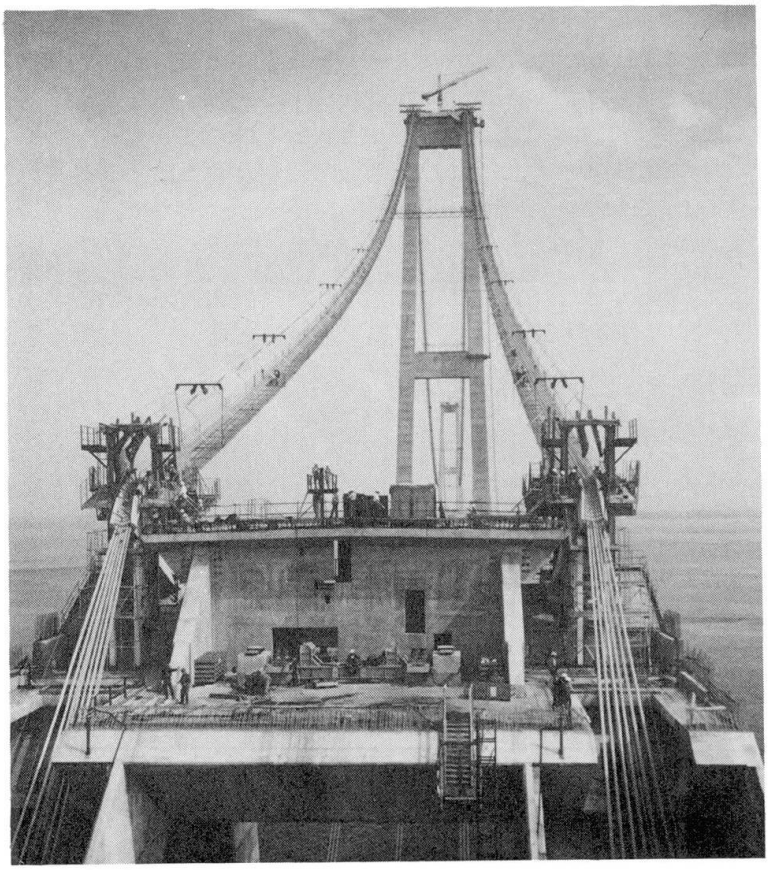

Fig. 3: Catwalk, tramway system and accessories

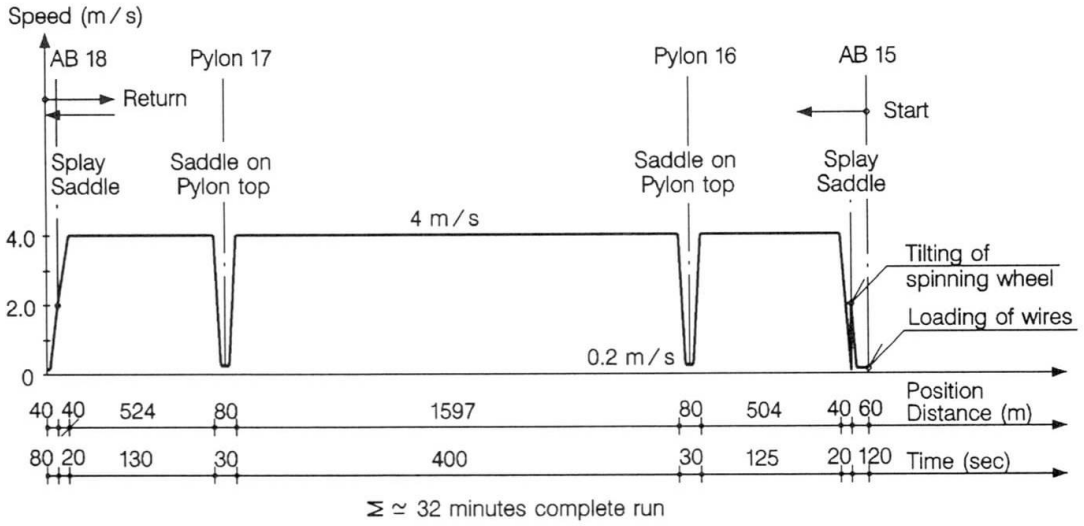

Fig. 4: Typical timechart for one trip of the spinning wheel

4. Sag adjustment. By using " The Low Tension Control" method the single wires are not adjusted during spinning. Adjustments are made on completed strands only. Immediately after the end of the spinning of a strand, the strands are compacted in circular shape and then served. The strands are pulled by jacks at the pylons top and at the anchorages until the strands are free of the cableformers and approx.100 mm above the strands already adjusted. At night time under constant temperature conditions, the strands are lowered into the design

position by slacking the jacks on the pylon top and at anchorages, taking in consideration the calculated cable length and sag, including the actual position of the pylons and the temperature of the strands.

4. Spinning with Reduced Pull Back

As mentioned earlier the full displacement of the pylons was not reached at the time of beginning of spinning. The consequence was an initial unbalance of cable forces at the top of the pylon, and the unbalanced cable forces therefore increased the displacement of the pylons top. A critical point was to be sure that this unbalanced state of forces did not introduce risks for sliding of the first strands in the saddles at pylons, and to demonstrate that the calculated displacement could be reached without additional tensioning of the pull back cables. A set of calculations was made to check this situation using the actual observed conditions as assumptions. The actual displacement of the top of the pylons was recorded periodically during the spinning. Fig. 5 shows that the actual displacement was larger than the assumed one, probably due to creep in the concrete and differential settlement in the foundation. These effects were not included in the calculations. The designed displacement corresponding to the balanced situation was actually reached at the end of spinning.

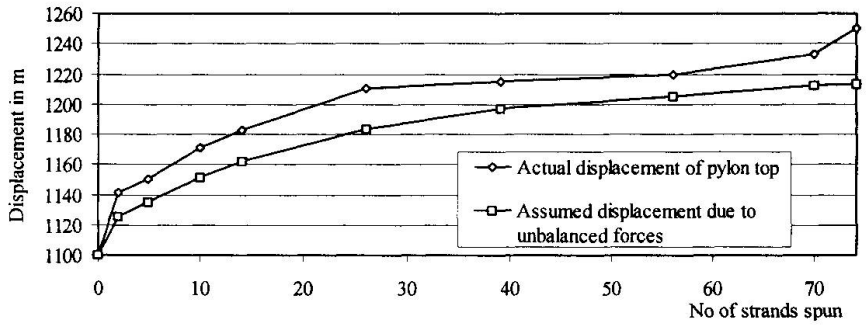

Fig.5: Displacement of pylons during main cable spinning

5. Down-Time due to Adverse Weather Conditions

An assessment of the expected down-time due to adverse weather conditions was carried early in connection with planning of the cable erection. Average down-time was estimated as time where one of the standard criteria in Table 1 from the special conditions was exceeded.

	Wind Speed m/s at +70 m							Precip-itation per day	Tempe-rature	Wind and tempe-rature	Wave height	Ice Baltic Ice Code
Criteria	s<11	11<s<12	12<s<13	13<s<14	14<s<15	15<s<16	16<s	Above 10 mm	Below 5 deg C	Above 15 m/s	Above 1.5 m	Above 4
Standard Efficiency	100%	95%	90%	75%	55%	30%	0%	0%	0%	0%	0%	0%

Table 1: Standard criteria for down-time and standard efficiencies

The result is shown in Fig 6. Simulation on basis of 25 years registered weather data was selected instead of statistical modelling, because it was necessary to use several types of non-independent weather criteria with unknown correlations.

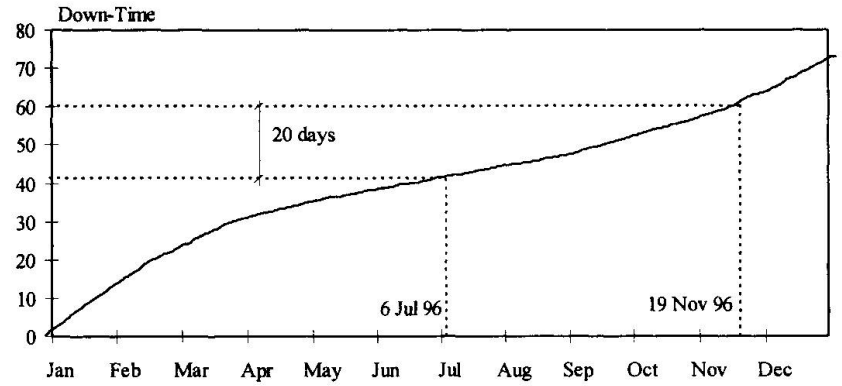

Fig.6: Average accumulated down-time over a year on basis of 25 years weather data

The contractor had foreseen a spinning duration of 147 days, incl. a loss of 16 days due to adverse weather. The spinning was completed after 137 days, incl. a loss of 9 working days due to adverse weather. Completion was 10 days ahead of schedule, 7 of which were won against the weather, in-spite that the weather conditions were worse than average for the 25 years period measured on basis of the standard criteria in Table 1. The contractor has actually recorded 14 calendar days with some weather loss corresponding to a loss of 9 working days. The weather loss was almost entirely due to adverse wind conditions. Other weather conditions did not directly cause delay, but rain can have been an accompanying cause of delay on few days. Temperature and ice conditions are not a problem during this time of the year. The spinning operation was mainly carried out for 21 hours a day and the 3 hours were used for repair and maintenance of equipment.

The estimated down-time was 20 working days, on average, ref. Fig. 6. The standard deviation was 5 days. For the actual spinning period in 1996 the model estimates 27 working days, 19 of which are due to exceeding of the wind criteria, whereas 8 days are due to heavy rains. Reducing the average of 20 days with also 8 days of heavy rain the estimate become 12 working days due to adverse wind conditions.

6. Conclusion

The aerial spinning of the main cables for the Great Belt East Bridge was successfully performed in only137 days in 1996 using " The Low Tension Control" method. When spinning started only a partial offset of the pylon saddles were present. Experience showed that using the unbalanced forces from the strands the full offset value was reached at the end of spinning. This method could be further developed and used in a larger scale in future spinning works for suspension bridges. Adverse wind conditions were the main weather problem. Modelling of down-time was reasonably good, but the model gave a slightly conservative estimate as the spinning contractor was able to work better than the assumed standard efficiencies.

Great Belt East Bridge 1624 m Suspension Bridge Substructure

Erik SKETTRUP
Civil Eng.
Ramboll
Copenhagen, Denmark

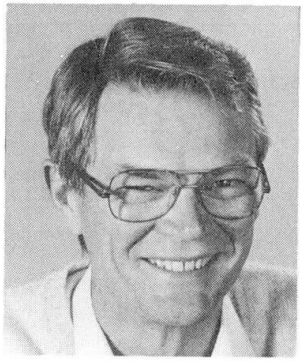

Erik Skettrup, born 1938, received his civil engineering degree form the Technical Univ. in Denmark in 1963. He joined Ramboll in 1988. Member of the Project Management for the Detailed Design of the East Bridge. Chief Adviser, Bridge Dept.

Summary

This paper describes some of the important aspects related to the design and executing of the substructure of the 6.7 km long East Bridge in the Great Belt Link. All caissons for the bridge are performed as prefabricated elements. This construction method appears to have economical and technical advantages because the dimensions of several elements are identical and it is possible to use a very appropriate foundation method on stonebeds. The ship impact has a major influence on the design of the substructure as well as the superstructure.

1. Introduction

This paper describes some of the most interesting technical aspects related to the design and the construction of the substructure to the 6.7 km long East Bridge in the Great Belt Link. The main bridge is a suspension bridge with a main span on 1624 m and two side spans on 535 m. The length of the approach bridges is 2530 m and 1538 m on east and west side of the main bridge. The 19 pier shafts in the approach bridges and all caissons in as well the main bridge as the approach bridges are prefabricated in Kalundborg 30 nautical miles from the bridge site. The design of the East Bridge was performed by CBR, a joint venture between COWI and RAMBØLL Denmark.

2. Design Assumptions

2.1 Safety aspects

The design life for the bridge is 100 years. The design philosophy is based on limit states in accordance with the Danish codes of practice. In the ultimate limit state the required safety level is in principal achieved by means of the partial safety factors indicated in Table 1. The safety factors specified in Eurocodes are indicated in brackets.

Table 1. Partial safety factors

Material	Partial safety factor	Load	Partial safety factor
Concrete	$\gamma_c = 1.9$ (1.50)	Permanent load	$\gamma_G = 1.0$ (1.35)
Reinforcement	$\gamma_s = 1.5$ (1.15)	Variable load	$\gamma_Q = 1.3$ (1.50)

The fundamental differences between the safety factors in the design basis for the East Bridge and the safety factors in the Eurocodes are:

- The ratio γ_Q / γ_G is in Eurocodes = 1.11 and in the design basis for the East Bridge = 1.3
- The safety factor on permanent load is in the design basis = 1.0

The advantages with the safety factors used for the East Bridge are:

- The ratio γ_Q / γ_G = 1.3 in the design basis for the East Bridge ensure a more uniform safety level for different combinations of permanent and variable loads compared with the corresponding ratio in the Eurocodes.
- The partial safety factor γ_G = 1.0 on permanent load in the design basis for the East Bridge make it possible to make geotechnical analyses and analyses of interaction between structure and soil without difficulties. In the Eurocodes these analyses are very complicated because the partial safety factor on permanent load is different from 1.

Fig. 1: East Bridge 1998

2.2 Ship impact

With about 18.000 vessels passing the bridge each year ship impact has been considered as a very important load case. Probabilistically based design criteria have been set to define the required impact resistance of the bridge piers. The influence from ship impact on the piers in the approach bridges depend on the seabed level. The piers in the approach bridges have been designed for impact from vessels from 4,000 DWT near the abutments to 60,000 DWT near the anchor blocks. The anchor blocks and the pylons have been designed for impact from vessels on 250,000 DWT. In all cases the design impact speed was 10 knots.
Local effects from ship impact were analysed by means of the theory of plasticity. In the analysis of global effects of ship impact from the above mentioned vessels limited displacements of the pylons and piers are allowed. By this it is possible to absorb considerable loads from ship impact compared with a purely elastic approach. For the pylons the allowable displacement in the longitudinal direction is 280mm. For the piers the allowable displacements are in the longitudinal direction 500 mm and in the transverse 200 mm.
The bearing capacity of the substructure related to global effects of ship impact was analysed by means of programs ABACUS and SIAS were the interface between soil and structure was assumed having an ideal-elastic-plastic behaviour. In these calculations the load-deformation curves for the ships as well as the time history load aspects during the ship impact was taking into account. The analysis during ship impacts was performed with a complete analysis for each 10^{-4} sec during the impact.
The analysis of the piers in the approach bridges was carried out by taking into account the influence from the superstructure, which in this load case acts as a horizontal support. Though the stiffness of the superstructure is rather low compared with the stiffness of the piers it appeared, that due to the dynamic effect of the ship impact a considerable part of the horizontal force from the impact was transferred to the superstructure. An analysis of ship impact without taking the dynamic effects into consideration would have been completely misleading.
All caissons in the approach bridges are of the same rectangular size. The magnitude of the loads from ship impact on the piers near the navigation channel is significant these piers are therefore protected against ship impact by means of artificial islands.

2.3 Ice Loads

Ice loads on the substructure due to drifting ice are considered as accidental loads, corresponding to a probability of occurrence on 2×10^{-5}.
The design of the substructure is performed based on the ice thickness and strength indicated in Table 2.

Table 2. Ice Thickness and Strength

Probability pr. year	Thickness (m)	Compression Strength (MPa)
0.1	0.42	1.93
0.01	0.63	2.35
0.00002	0.99	2.8

The compression strength indicated in Table 2 is valid for global analysis. The local loads, i.e. loads which are acting on areas smaller than 0.1 m^2, are determined by a crushing strength varying between 12 MPa and 2.8 MPa depending on the size of the contact area.
Compared with ship impact ice loads had only minor influence on the structure.

3. Foundation

The foundation method for all the prefabricated caissons is identical. After excavation to the required level a crushed stone material is placed and screeded at the foundation level, whereupon the caissons are placed on the stonebeds. The caissons are equipped with skirts which penetrates into the stonebeds. The contact between the caissons and the stonebeds is secured by grouting. The underbase grouting was performed after pre-testing and a full scale trial grouting. The characteristic compression strength of the grout was 5 MPa. The grout between the bottom slab and the stonebed ensure a smooth distribution of the stresses between the bottom slab and the stonebed, which is very important in order to reduce the amount of reinforcement in the bottom slab.

Each anchor block has a rectangular form with the length 121.5 m and the width 54.5 m. This base is divided into three parts a front pad of 41.7 m, a centre part of 39.1 m and a rear pad of 40.7 m. Only the front and rear pads are in contact with the stonebeds.

Several different geotechnical analyses were performed in relation to the anchor blocks as reported by T. Feldt (1996). These calculations and the FEM analysis of the anchor blocks proved that the stiffness of especially the centre part of the anchor blocks compared with the assumed stiffness of the soil had a major influence on the position of the reactions from the soil and the stress distribution between the bottom slab and the stonebeds on the rear and front pads of the anchor blocks. The soil conditions had therefore a significant influence on the internal forces in the anchor blocks.

Fig. 2: Anchor Block

4. Anchor blocks. Massifs

The main cables in the suspension bridge are anchored in four concrete massifs in the rear part of the anchor blocks. The width and the height of each massif are approximately 10 m and 30 m respectively. In addition to the non prestressed reinforcement placed in three directions the massifs are from top to bottom prestressed with Macalloy bars in the same direction as the main cables. This prestressing consists of 444 Nos. of bars in each massif corresponding to a pressterssing force on approximately 470 MN.

5. Ballasting of Caissons

All caissons are ballasted with sand or olivine. Olivine is a heavy sand with a high content of silica the dry unit weight when compacted is approx. 24 kN / m^3 .
The pier caissons in the approach bridges were entirely filled with olivine ballast, while the olivine fill in the pier shafts was determined depending on the soil conditions and the horizontal forces mainly from ship impact to be transferred between the caisson and the stonebed.
The anchor blocks are ballasted with olivine in the rear part where the main cables are anchored in the concrete massifs, while the front and centre part of the anchor blocks are ballasted with sand.
The design assumptions in relation to the soil pressure on the walls from the ballast have a significant influence on the internal forces in the anchor blocks. Based on model tests and FEM calculations performed in relation to the design of the West Bridge it was concluded to calculate the soil pressure from the ballast by means of the rest pressure theory because the silo theory seems to be uncertain taking into account the long term behaviour and the properties of the submerged fill.
The knowledge about this item seems to be limited, though it has a significant influence on the structure.

6. Quantities

The quantities of concrete, reinforcement and prestressing steel are indicated in Table 3. The reason for the relatively low amount of reinforcement in the in-situ cast anchor blocks is, that the concrete massifs where the main cables from the suspension bridge are anchored are heavily prestessed with approximately 600 tons of Macalloy bars. Thus it has been possible to reduce the ordinary reinforcement in the 36,000 m^3 concrete massifs to 3,500 tons corresponding to a reinforcement density of 95 kg/m^3 .

Besides the massifs the following elements in the anchor blocks are prestressed, the bottom slab, the slab in level 10m, some of the vertical walls in the centre part of the prefabricated caissons, the walls in the cantilevered splay chamber legs and the cross beam supporting the superstructure.

In the Pylons the bottom slab, the slab in level 21m and the two cross beams are prestressed.

Table 3. Quantities of concrete and reinforcement

Structural element	Quantity		Reinforcement Density kg/m^3	Prestressing Steel tons
	Reinforcement tons	Concrete m^3		
Anchor Blocks Pre-fab Caissons[1)]	6,600	38,000	174	870
Anchor Blocks In-situ[2)]	7,800	65,000	120	750
Pylons Pre-fab Caissons[3)]	3,700	23,500	157	150
Pylons In-situ[4)]	11,700	77,000	152	190
Approach spans 19 Piers and Caissons[5)]	8,300	47,000	177	0

[1)] Dimensions 121.5 x 54.5 m height 16.0 m Foundation level -12.0 m.

[2)] Level of Bearings 53.0 m.

[3)] Dimensions 78.3 x 35.2 m height 20.3 m Foundation level -23.8 m.

[4)] Level of top of pylon leg 254.0 m.

[5)] All piers except one are prefabricated consisting of three elements a caisson, a lower and an upper pier shaft. The foundation levels are from -5.5 m to -12.0 m. The level of the bearings for the superstructure is from 7.6 m to 46.0 m.

7. References

Feld,T. Sørensen, C.S. and Pedersen, F. (1996). *Structure-Foundation Interaction on the Storebælt Link East Bridge. Proc. of the 15th IABSE Congress in Copenhagen pp 809 - 818.*

Study of a New Structural Type for Prestressed Concrete Bridges

Kenji UMEZU
Research Eng.
Sumitomo Constr. Co., Ltd
Tochigi, Japan

Manabu FUJITA
Chief Research Eng.
Sumitomo Constr. Co., Ltd
Tochigi, Japan

Jun YAMAZAKI
Prof.
Nihon Univ.
Nihon, Japan

Summary

In order to achieve a more efficient external tendon layout in prestressed concrete continuous girder bridges, a non-linear analysis was made of a new layout with tendons extending above the girder over the supports as in an extradosed bridge, and below the girder in the span as in a beam string structure. A model group was studied in which the tendon quantity and eccentricity were varied gradually under a constant service load.
The large eccentricity tendon layout allowed the quantity of prestressing tendons to be reduced by 35% as compared to conventional layouts, while maintaining the required flexural capacitys.
Structures with large eccentricity tendon layouts were found to have the following advantages: Economical, and Greater flexural capacity, as advantage is taken of the tension increase in the tendons, and Greater freedom of tendon layout, depending on the required performance.

1. Introduction

Features of extradosed concrete bridges and other large-eccentricity external-tendon prestressed concrete bridges include the ability to use lower girders owing to the large eccentricity of the tendons compared with girder bridges, the ability as a result to reduce the girder weight, and lower stress amplitude due to the live load compared with cable-stay bridges, so that designs can assume higher stress-limit values taking fatigue into account than in designs of cable-stayed bridges. And, the fact that the tower of an extradosed concrete bridge is not very high makes this an attractive design when scenery and environmental conditions are considerations.

Although the advantages of large-eccentricity external-tendon designs are thus becoming clear, numerous aspects of the structure of such designs remain unclear. The authors previously conducted loading experiments using indoor models and nonlinear analyses in an attempt to determine the basic characteristics of large-eccentricity external-tendon prestressed concrete continuous beams, and confirmed that such structures possess sufficient flexural capacity and offer superior economy[1]. In the present study, we performed parameter analyses in order to determine the effects of the prestressing tendon layout and eccentricity on the girder performance for the service load and ultimate load, using a prestressed concrete bridge model with actual-scale spans. Below we report our results.

2. Analysis Model

Existing extradosed concrete bridges employ eccentric towers at central supports, and by increasing the eccentricity of tendons can efficiently deal with the negative flexural moment occurring in the girders. On the other hand, the beam string structure with large tendon eccentricity and with struts placed beneath spans is used to efficiently deal with positive flexural moments. Such large-eccentricity external tendons above supports and below spans serve a similar purpose in that they effectively cancel girder flexural moments. The model studied in this work appears in Fig.1; tendons are placed above and outside girders at supports and in spans, incorporating the structures of both extradosed bridges and beam string bridges in the large-eccentricity tendon model. The model studied was an equal-girder-height box-girder bridge with three continuous spans of 75 m each. Materials used in components are indicated in Table 1. The model design conditions are described below.

(1) All prestressing tendons in the longitudinal direction was present in the form of external tendons. The effective tensile stress of tendons was taken to be 50% of the tensile strength.

(2) From 0.17 to 0.25% of the cross-sectional area of the girder was reinforcing steel, so as to satisfy the condition of a minimum 0.15% steel in the girder.

Table 1. Materials used

		(N/mm²)
Concrete	Design criterion strength	40
PC Strands 12S15.2 SWPR7B	Tensile strength	1860
Reinforcing steel bar SD345	Tensile strength	345

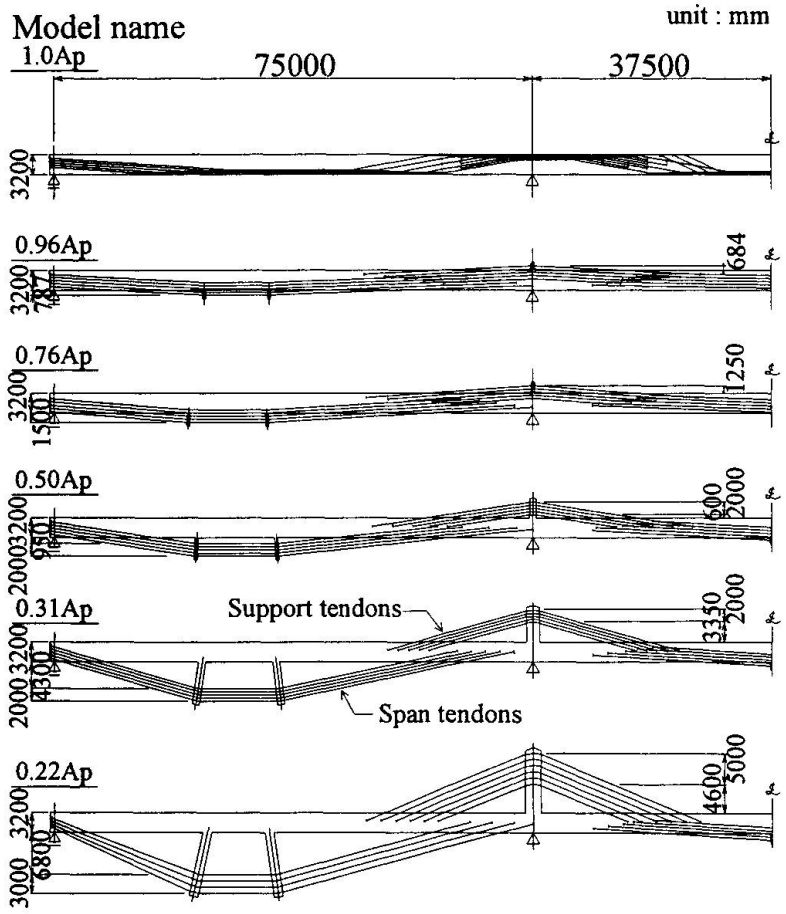

Fig.1 Structure of models studied

(3) In the "1.0 Ap model" the tendon layout is internal, as in the case of internal tendons. However, in analysis the tendons were treated as unbonded tendons, as in the case of external tendons.

(4) The names of the "0.76 Ap" and similar models indicate the Ap ratio with the conventional (1.0 Ap) model of the total cross-sectional area Ap of external tendons in the cross-section at the central support.

In the 0.22 to 0.96 Ap models, the tendons have a concordant layout.

(5) Struts positioned underneath spans are positioned in a direction so as to bisect the inner angle of the deviator. This was done in order to use struts supporting the tendon tension component as axial

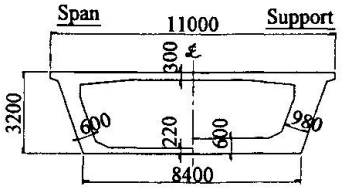

force-predominant materials. In the large-eccentricity model, external tendons were fixed to girders at both ends of cable arrangement intervals, and deviators of towers and deviators of struts, external tendons were kept moveable.

(6) The tendon quantity in these models was laid out so as to satisfy requirements for the allowable stress at the concrete girders for in-service load. The tendon eccentricity in the major cross-section is set such that stress by prestressing forces at the concrete girder's tensioned edge is equal over the entire model. The tensioned edge combined stress at the in-service load appears in Table 2. The relationships between the external tendon total cross-sectional area at the main cross-section and the eccentricity is plotted in Fig. 2.

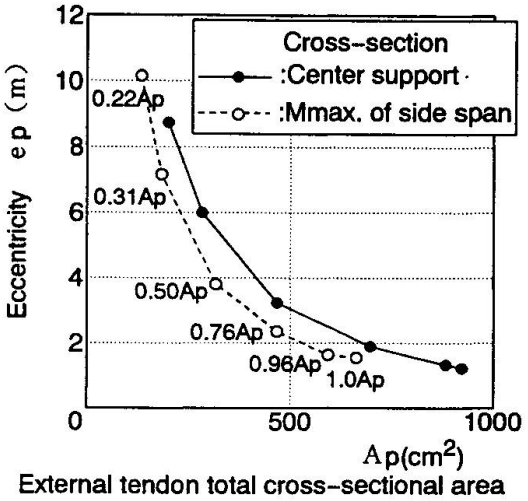

Fig.2 Relationships between total external tendon cross-sectional area and eccentricity in major cross-sections for each model

3. Design by Conventional Method

3.1 Stress amplitudes for in-service loading

Table 3 shows stress amplitudes in tendons occurring in B live loading as determined from linear analysis. The smaller the tendon layout quantity of the model, the greater are the stress amplitudes. Moreover, we see that in all models amplitudes are greater for span tendons than for support tendons. We also note that for the Odawara Blue Way Bridge and Tukuhara Bridge built by Japan Highway Public Corporation, both extradosed concrete bridges the in-service load allowable stress of the tendon tension for which was set at 60% of the tensile strength, the stress amplitudes due to the live load is 37 N/mm ^{2} [2]. It is thought that tendons for which stress amplitudes under a live load are large must be designed with consideration paid to safety with respect to fatigue, including fretting at the deviator.

Table 2. Combined flexural stress of girder cross-section for in-service loading

(N/mm^2)

Model	Mmax of side span		Central support	
	Upper edge	Lower edge	Upper	Lower
1.0Ap	12.0	−1.1	0.4	11.5
0.96Ap	11.2	−1.0	0.1	11.7
0.76Ap	9.0	−1.0	0.0	9.3
0.50Ap	6.3	−0.9	0.0	6.3
0.31Ap	4.1	−1.4	0.0	4.0
0.22Ap	3.6	−1.4	0.0	3.5

allowable stress span : $-1.5 < \sigma < 14$N/mm^2

support : $0 < \sigma < 14$N/mm^2

Table 3. Stress amplitudes in external tendons due to live loads

(N/mm^2)

Model	Support tendon	Span tendon
1.0Ap	7	20
0.96Ap	5	17
0.76Ap	6	21
0.50Ap	11	28
0.31Ap	14	43
0.22Ap	20	54

3.2 Study of conventional designs in ultimate loading

Table 4 shows the flexural failure safety factor under ultimate loading for the conventional model (1.0 Ap). When tendons are regarded as internal bonded tendons in calculations, the safety factor is 1.25 to 1.33; but calculations as external tendons without anticipating an increase in tensile stress an insufficient safety factor of 0.71 to 0.80.

Table 4. Flexural failure safety in ultimate loading

($\times 10^3$kN•m)

Cross-section	Acting moment Md *1	Case assumed to bonded tendon		Case assumed to unbonded tendon *2	
		Resistance Moment Mu	Safety Mu/Md	Resistance Mu	Safety Mu/Md
Mmax of side span	245	318	1.30	175	0.71
Central support	289	385	1.33	229	0.79

*1) Md = 1.7 × (Dead loads + Live loads + Impact) + (the indeterminate forces due to prestressing forces)

*2) calculations as external tendons without anticipating an increase in tensile stress due to deformation of stuctural members

4. Nonlinear Analysis

4.1 Analysis conditions

In analysis for ultimate loading, the "Say-NAP" fiber model program[3] was used, taking the material and geometrical nonlinearity into account. Stress-strain curves for the materials used conformed to the Standard Specification for Design and Construction of Concrete Structures of the Japan Society of Civil Engineers. The concrete tensile strength was taken to be zero.

In analysis, the dead load D and the B live load L in the loaded state (Fig. 3), as well as the impact I, were increased gradually, and the course from in-service loading until material ultimate loading was traced. In the case where the load was gradually increased, the loading shown below was adopted, taking into account the load combination under ultimate loading indicated in the Concrete Bridge Section of Specification for Construction of Road Bridge .

Gradual increase in load,

case : $\gamma \times (D + L + I)$

Where, γ is the load increment coefficient ($\geqq 1.0$).

The load was thus increased gradually, and at all cross-sections of the girder, the point at which the concrete compression edge reached ultimate strain (=0.0035) was taken to be flexural failure, and calculations were halted.

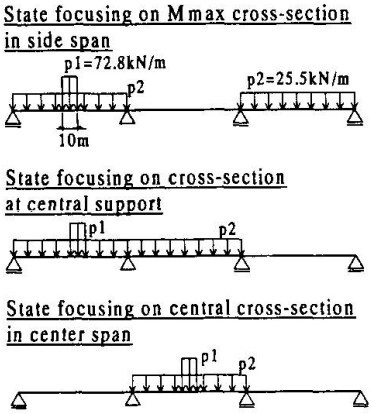

Fig.3 Loading state of Live loads and impact

4.2 Analysis results

(1) Girder deflection and flexural capacity

Figure 4 shows the girder deflection and flexural moment distributions at failure

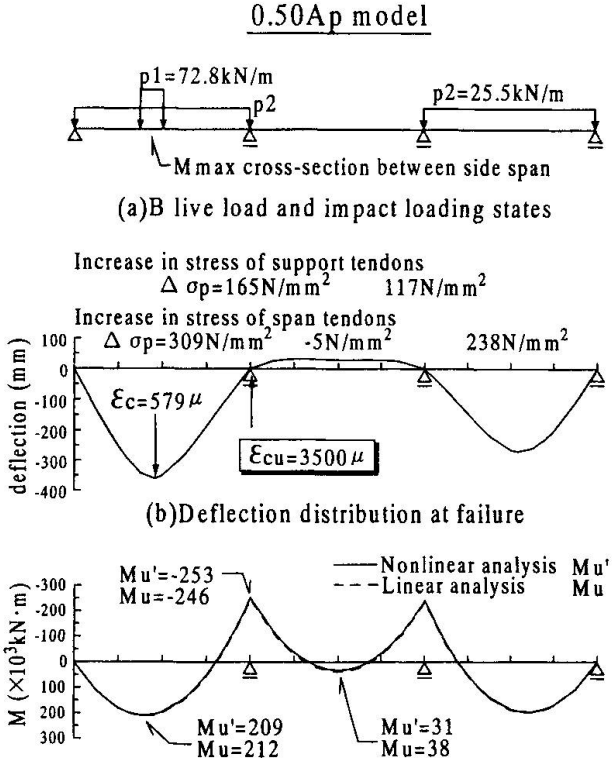

Fig.4 Girder deflection and flexural moment distribution at failure

for the case of live loading, focusing on the Mmax cross-section in side span for the 0.50Ap model. In all loading cases for all models, the failed cross-section was the central support cross-section. This was inferred to occur because the increase in tension is smaller for the support tendons than for the span tendons, so that the flexural capacity of the support cross-section was not increased. In these models, there is not much moment redistribution, and so there was little difference between the flexural moments in the linear and nonlinear analysis.

Figure 5 indicates the relationships between load increment coefficient and girder deflection for each model for the case focusing on the Mmax cross-section in side span; Figure 6 shows the flexural moment (flexural capacity) occurring in the cross-section in question when the center support cross-section undergoes flexural failure in each case. Compared with the conventional model (1.0Ap), nearly all the large-eccentricity models had about the same coefficient γ and flexural capacity at failure and the same deformability as well.

For the present model, which is an entirely external-tendon model, in the case of gradual increase with $\gamma \times$ (D+L+I) flexural failure occurs before reaching γ =1.7; this is because the tendon layout quantity is determined by the required quantity at service load. Analysis to satisfy the requirement for γ is discussed in "5. Study of Tendon Quantity Satisfying Safety Requirements at Ultimate Loading" below.

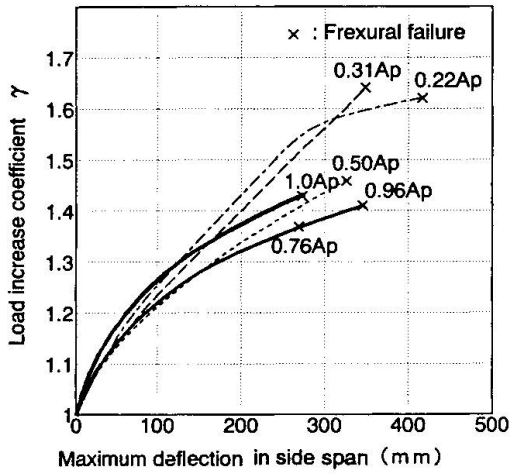

Fig.5 Relationships between load increase coefficient and girder deflection

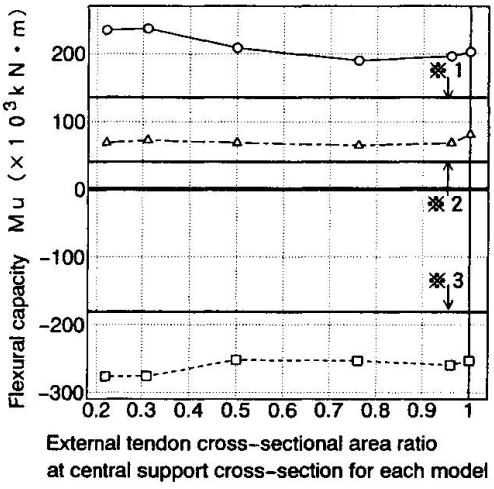

Fig.6 Frexural capacity for each model

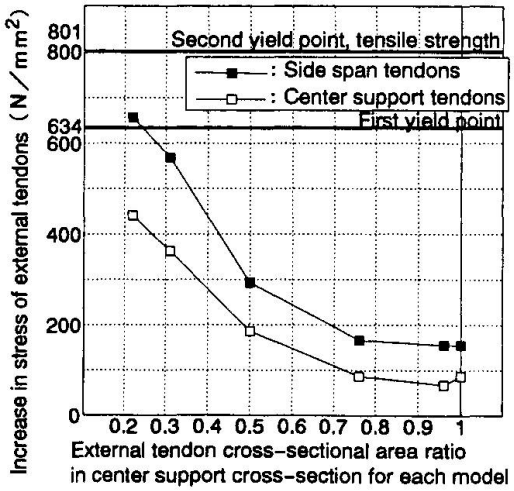

Fig.7 Increase in stress at flexural failure for each model

※ 1 : Side span Mmax cross-section for 1.0 × (D+L+I)
※ 2 : Central cross-section in center span for 1.0 × (D+L+I)
※ 3 : Center support cross section for 1.0 × (D+L+I)
—○— Loading state focusing on Mmax cross-section in side span
--△-- Loading state focusing on central cross-section in center span
---□--Loading state focusing on cross-section at central support

Table 5. Rate of increase of external tendon layout quantity to satisfy safety requirements in final loading

Model	Original tendon layout	Case where tendon layout quantity is increased	
	Loading coefficient γ at failure	Rate of increase of layout quantity	γ
1.0Ap	1.42	×1.25	1.71
0.96Ap	1.39	×1.27	1.71
0.76Ap	1.34	×1.35	1.76
0.50Ap	1.40	×1.30	1.78
0.31Ap	1.54	×1.15	1.74
0.22Ap	1.54	×1.20	1.75

(2) Stress increase in external tendons

Figure 7 shows the increase in stress of the external tendons in each model, from the effective tensile stress point up to flexural failure of the girder. From these results we see that the smaller the tendon layout quantity, the greater is the increase in tendon stress. The stress is from 70 to 440 N/mm ^{2} in the center support tendons passing through the failed cross-section. In the 0.22Ap model, a stress increase extending to the yield point was observed.

5. Study of Tendon Quantity Satisfying Safety Requirements at Ultimate Loading

In the present bridge model, as explained above, safety requirements to prevent flexural failure for load combinations at ultimate loading are not satisfied. In order to satisfy safety requirements for both in-service loading and ultimate loading in this entirely external-tendon model, it is necessary to focus on ultimate loading when setting the tendon layout quantity. In order to improve the girder flexural capacity, the following two approaches are conceivable. (1) Abandon an entirely-external tendon design in favor of a combined internal-external tendon design, with tendons in the longitudinal direction. (2) Increase the external tendon layout quantity. Here we adopted (2) and left the eccentricity of the external tendon group unchanged. Through a nonlinear analysis it was confirmed that the loading coefficient at failure γ is the required value (=1.7); results appear in Table 5. As a result it was found that for each model, the tendon quantity must be increased by 15 to 35%. This relative increase does not vary greatly from one model to another, so that from these study results as well we see that the large-eccentricity model has performance comparable to that of conventional models.

For the example of the 0.50Ap model indicated by shading in Table 5, in order to satisfy safety requirements for service and ultimate loads, the layout tendon quantity must be 0.65Ap (=0.50Ap $\times$ 1.30); but compared with conventional 1.0Ap internal tendon layouts the tendon quantity is decreased by 35%, and can be described as an economical design.

6. Conclusions

The results of this study may be summarized as follows.

(1) The smaller the external tendon layout quantity of a model, it was found, the greater the increase in tension with loading tended to be. For side span tendons in the 0.22Ap model, the yield point was reached at the time of flexural failure of the girder.

(2) Designs in which external tendons layouts have large eccentricities at supports and spans result in increased tension in external tendons due to deformation of structutral members, and so are regarded as an economical bridge design in which the tendon quantity can be reduced while maintaining the required flexural capacity.

(3) Large-eccentricity external tendon designs can be described as structures which afford a high degree of design flexibility and enable freedom in tendon eccentricity and quantity, with due consideration paid to stress amplitudes due to tendon live loads, stress and strain in ultimate loading, and other parameters.

References

1. Umezu,K., Fujita,M., Tamaki,K., Arai,H., Yamazaki,J. "Study on the Ultimate Flexural Strength of 2-Span Continuous Beams Using External Cables" FIP Symposium on Post-Tension Concrete Structures 1996. 9, pp.812 - 819
2. Yamazaki,J., Yamagata,K., Kasuga,A., "Structural Characteristics of Cable-stayed and Extradosed Concrete Bridges" Bridge and Foundation Engineering, Vol.29, No.12, 1995.12, pp.33 - 38
3. Tamaki,K., Arai,H., Itai,E., Yamazaki,J. "Application and Standardization to Externally Prestressed Structures for Non-linear Analysis Program" Proceedings of The 5th Symposium on Developments in Prestressed Concrete, Japan, pp.309 - 314, 1995.10

Poole Harbour Bridge: Innovation in Cable Stayed Bridge Design

Ian P.T. Firth
Partner
Flint & Neill Partnership
London, England

Ian Firth graduated from the Univ. of Bristol in 1979 and obtained a Master's degree in Structural Steel Design at Imperial College in 1982. He has been responsible for many bridge projects with Flint & Neill Partnership, and leads the design team for the Pools Harbour Bridge.

Summary

1. This competition winning design for a multi-span cable stayed bridge was described by the judges as "world class" and has attracted considerable international interest. The bridge contains a number of innovative features, most notably the longitudinal stays connecting the tops of the pylons together and back to the abutments, and these are described in this paper. Environmental factors were paramount, and the design is a sensitive and elegant response to these factors.

Introduction

2. In 1995, the United Kingdom Highways Agency launched an international open design competition for the Poole Harbour Crossing. The need for a crossing had been established many years previously, and the competition was welcomed as part of the Agency's commitment to procuring better quality design in their new bridges and structures. The competition attracted 99 entries, and was won by an international team led by Flint & Neill Partnership which included the Danish architects Dissing+Weitling, engineers Rambøll and Terence O'Rourke who are landscape architects, ecologists and planners based in Bournemouth near to the site.

The Site

3. The shallow waters and extensive mudflats of Poole Harbour are of exceptional nature conservation value, and the scenery and local attractions draw many thousands of tourists each year. This is a highly sensitive Site of Special Scientific Interest with bird and marine life habitats of international significance, and there are many environmental constraints which affect this scheme. However, at the bridge site itself, where it crosses Holes Bay, these factors are less significant than elsewhere in Poole Harbour, and the Environmental Impact Assessments undertaken to date have shown a very positive outcome for the bridge proposal.

4. This low lying estuary, with wide open horizons, requires the bridge to be as transparent as possible to prevent excessive blockage of views. Equally, its alignment with the approach roads enables it to be seen from a distance by approaching motorists, so the visual quality and impact is

of primary importance. These factors led to the desire for maximum slenderness and delicacy in the finished design, and influenced many of the engineering solutions adopted.

5. Water depth is shallow, with peripheral mud flats at low tide and reed beds extending about 180m from the south west shore. This prevents the use of large floating lifting gear, which strongly influences the choice of construction method and thus the design itself. Furthermore, the sediments are known to be contaminated due to earlier industrial activity, so construction methods must be devised to avoid the release of contaminated mud into the water.

6. Careful treatment of the abutments and approaches is necessary, and shoreline footpaths at both ends provide opportunities for landscape and amenity enhancement. At the north east abutment, the plan geometry of the widening roadway and the required roadway level leads to the need for an additional structure, the Triangular Bridge, in place of an embankment at the shoreline, so as to enhance transparency and prevent blockage of the open views across the bay.

Overall Design Concept

7. The bridge is 700m long overall, but the brief called for a clearance of 19m over a navigation channel only 20m wide. Multiple short span solutions were rejected as too intrusive and disruptive, and a long span would have required heavy and dominant pylon or arch structures which are inappropriate in this setting. The most economic span length, which also met the environmental and aesthetic constraints, was found to lie in the 100 - 150m range. Several options were considered with spans in this range, and the final design adopts multiple 142m cable-stayed spans, with A-shaped pylons up to 50m high. (Figure 1)

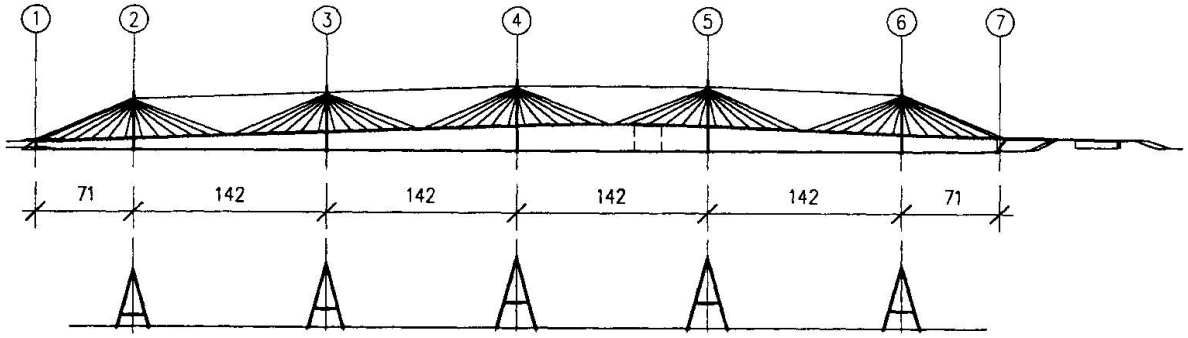

Fig. 1: General Arrangement - Elevation

8. The bridge evokes the imagery of the masts of boats scattered around the bay, with a strong rhythm creating a harmony with the environment, and the cathedral-like driver's eye view along the bridge deck adds excitement to the experience of the crossing, framing the landscape in a memorable way. This is a design with a strong and attractive visual statement, a clear identity and characteristic image, as can clearly be seen in the colour photomontage views.

The Novel Stay System

9. The slenderness of the pylons and deck was maximised in order to achieve the desired transparency and delicacy, and it was this that led to the evolution of the novel stay system.

In multi-span cable stayed bridges, the peak effects arise from patch loading in any one span. The deflection of that span pulls the pylon tops inwards and the adjacent spans lift up because they are not tied down to the ground, unlike a conventional cable-stayed bridge. There is a concentration of curvature in the middle of the adjacent spans and this gives rise to high deck bending moments. (Figure 2) The problem also arises in cross-wind aerodynamic behaviour where vibration modes involve alternate spans moving up and down, concentrating effects again at the midspan positions.

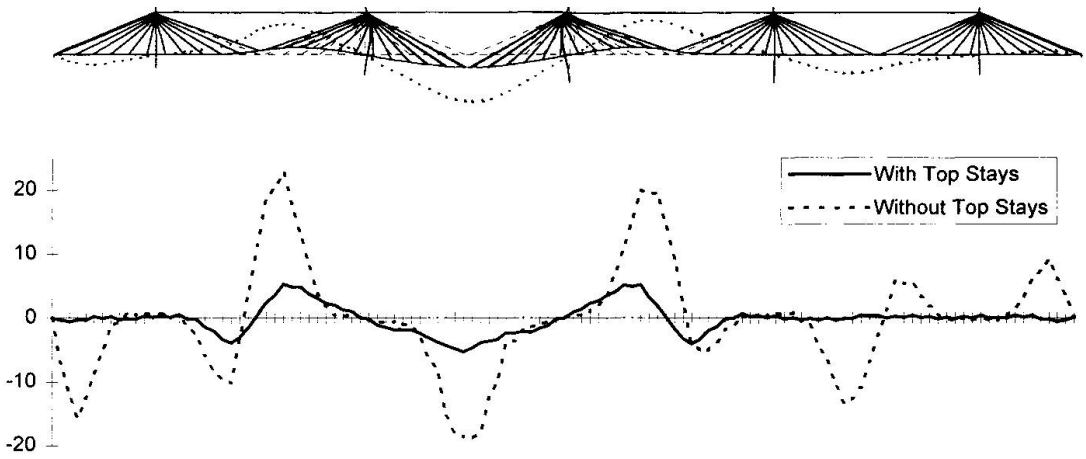

Fig 2: Displacements and Bending Moments (MNm) for live load in Span 3-4.

10. There are various ways of controlling this problem, as proposed by Tang [1], one of which is to tie the tops of the pylons together as adopted here. Other possibilities include crossing over the stays at midspan or tying the tops of each pylon to the base of the adjacent pylons. On the Ting Kau Bridge in Hong Kong, a 4-span cable stayed bridge, the top of the central pylon is tied to the deck at the adjacent tower positions, as described by Bergermann & Schlaich [2]. Both at Ting Kau and in the solutions suggested by Tang, the longitudinal forces arising from these extra stabilising stays are transmitted into the deck as axial compression. At Poole, however, the top stays are anchored back to the abutments, providing in effect a direct tie to stabilise each pylon head, thus adding considerable stiffness to the system and avoiding the extra deck compression.

11. The simple longitudinal tie between the pylon tops is also the best solution from a detailing point of view, since the other options all involve crossing over the stays making the deck edge details clumsy and more complicated. The pylons are not designed with fixed bases, but as a result of anchoring the top stays to the abutments and not the deck, they can all be erected early to permit deck erection to commence at all 5 pylons concurrently.

Articulation

12. The deck is fixed longitudinally to the central pylon only, being free to expand towards each end. Normally this would concentrate all longitudinal forces at this point, but in this case the stay system distributes a significant proportion directly to the abutments. There are no vertical bearings at the pylons, the deck being suspended throughout on the stays to prevent the peak bending effects that otherwise occur at bearing positions. Lateral restraint is provided to the deck at each abutment and each pylon.

Deck Design

13. The high strength Grade 40 reinforced concrete deck comprises two edge beams, carried by the stays at 12.6m centres, with transverse ribs at 3.15m centres supporting a 220mm deck slab. The sloping sides are kept as shallow as possible to enhance the slender appearance, and the edge detail is maintained throughout the length of the bridge without deviation at the pylons. This gives a clean, unified appearance, and facilitates construction. Stay anchorages are contained in pockets within the depth of the edge girder to avoid unsightly protrusions on the soffit. (Figure 3)

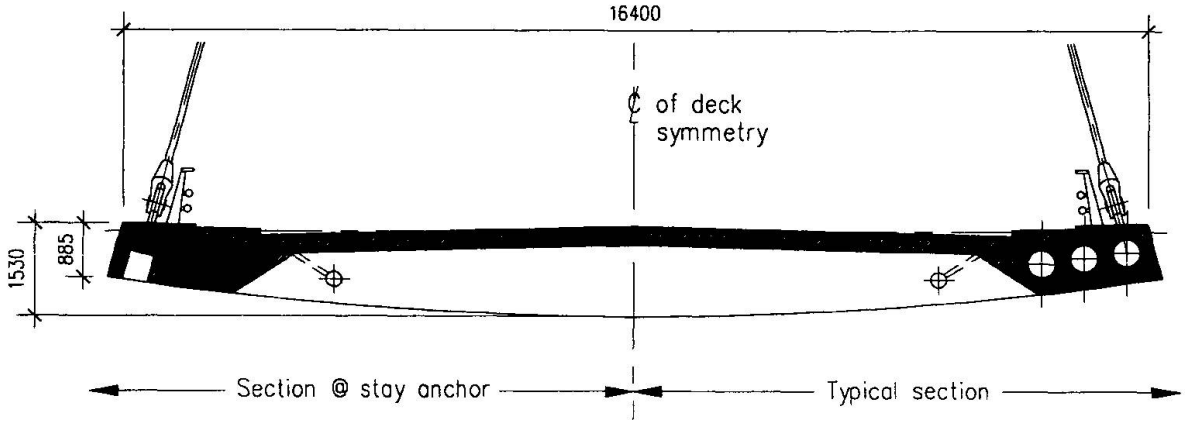

Fig. 3: Typical Deck Cross Section.

Pylon and Stay Design

14. The pylons are simple A-frames with 1.2m diameter high yield steel tubular legs whose wall thickness varies from 35mm to 50mm. A slender tie between the legs is concealed within the depth of the deck girder and supports the lateral bearings. The relative proportions of the A-frames vs. the span evolved through careful consideration of the required roadway width and the pylon heights necessary for an efficient stay system.

15. The stays are galvanised steel wire spiral strands between 85mm and 120mm in diameter, socketed at both ends, and anchored to a lug on the pylon and a cast steel threaded anchor at deck level. Pre-fabricated stays achieve greater slenderness than site-assembled strand bundles, as a result of both their smaller diameter and their less bulky anchorages, and if properly detailed and constructed they also provide the greatest confidence in long term performance. The twin top longitudinal stays have screwed tensioning devices incorporated into the socket anchorage at the pylon head. Individual strand replacement is possible throughout, including the top stays, and the whole system is designed to facilitate future maintenance and achieve a long service life.

Foundations

16. All foundations use open tube steel piles driven into the marine deposits, and the ten individual pylon leg foundations each have three 1.5m diameter raking piles, varying in length from about 20 to 25m. The concrete pile caps use pre-cast ring segments as permanent cofferdams within which the piles are driven and the in-situ connection is constructed. This system ensures that any release of disturbed mud from each work site into the bay is minimised.

Dynamic Behaviour

17. Although the deck is relatively heavy (25 tons/m), it is also relatively stiff due to the stay system and the modest span length, and the A-frame cross section arrangement ensures a high torsional stiffness. As a result, the first vertical bending and torsional modes are well separated, with predicted natural frequencies of 0.3 Hz and 0.7 Hz respectively. Wind tunnel tests have not yet been performed, but significant aerodynamic instability is not anticipated. The twin top stays have a relatively high dead load tension in order to achieve the desired stiffness, and studies have indicated that wind-induced vibration of these is unlikely as a result. They are separated by about 20 diameters so interference and wake buffeting effects are minimal.

Abutments

18. At the north east end, the link to the abutment is provided by the reinforced concrete Triangular Bridge, which has a ribbed soffit to mirror that of the main bridge and is integral with the abutment walls so as to avoid bearings and minimise maintenance requirements. An inverted tripod pier supports the ends of the Triangular Bridge and the main bridge each side of the expansion joint. At the south west end, the bridge terminates in a simple concrete abutment which retains the end of the approach embankment.

19. At the expansion joints, a novel flexible leaf plate design is proposed in place of traditional rockers. These long flat plates bend to accommodate thermal movements while still carrying the imposed vertical loads, thus avoiding rotating pins and minimising maintenance.

Construction

20. Because of insufficient water depth for floating cranes, it envisaged that a temporary jetty will be constructed alongside the bridge extending out from each bank, with a gap of 100m at the navigation channel. The pylons will be assembled on vacant land immediately adjacent to the site and floated or carried into position for lifting by mobile cranes on the jetty. Once all are erected, initially using temporary stays and then finally secured with the top longitudinal stays, deck erection can proceed by conventional balanced cantilever construction. After evaluating the options for pre-casting, it was decided that constructing the deck in-situ in 12.6m bays on travelling formwork was the most economic and avoided the problems associated with joints in pre-cast construction. Temporary stays from the pylons are used to support the end of the travelling form, and the balanced cantilevers are stabilised using temporary props off the jetty. On completion, the jetty will be removed and its temporary piles withdrawn.

Maintenance

21. The design was developed from the outset with minimum maintenance requirements in mind. It is partly for this reason, for example, that a concrete deck was adopted throughout in order to avoid the need for regular painting and the long term problems associated with welded steelwork in fatigue-prone areas. The number of bearings and expansion joints, which are usually high maintenance items, have been minimised, and the north east approach bridges have integral abutments. Innovative maintenance free flexible leaf bearings are used at the expansion joints, so the only moving parts are the sliding PTFE lateral buffers.

22. The steel pylons will require periodic painting, but the use of clean tubular sections with smooth paint surfaces is intentionally maintenance friendly. There are no stiffeners, bolted joints or external corners where dirt and water can collect, and this extends the life of the paint treatment and facilitates effective re-painting considerably.

23. High level access up to about 30m above deck level can be by mobile hydraulic lift, which could be used during off peak periods, without the need for a bridge closure. Excessive pylon heights have been avoided in order to facilitate such maintenance.

Conclusion and System Developments

24. The Poole Harbour Bridge design has developed with a strong emphasis on visual quality, and a desire for slenderness arising from the site characteristics has led to an innovative cable stay system which will be the first of its kind in the world. The modest span length is ideal for such an innovation, but there is no fundamental reason why these ideas cannot be further developed and extended to much longer spans for potential application to very long crossings. The span limit for this particular system arises when the axial stiffness of the top stays becomes too low to provide sufficient restraint to the pylon heads. Aerodynamic effects also become more significant with greater span and would need to be carefully evaluated. The possibility of adopting unequal spans in order to spoil coherent vibration of all spans over the entire length should be examined.

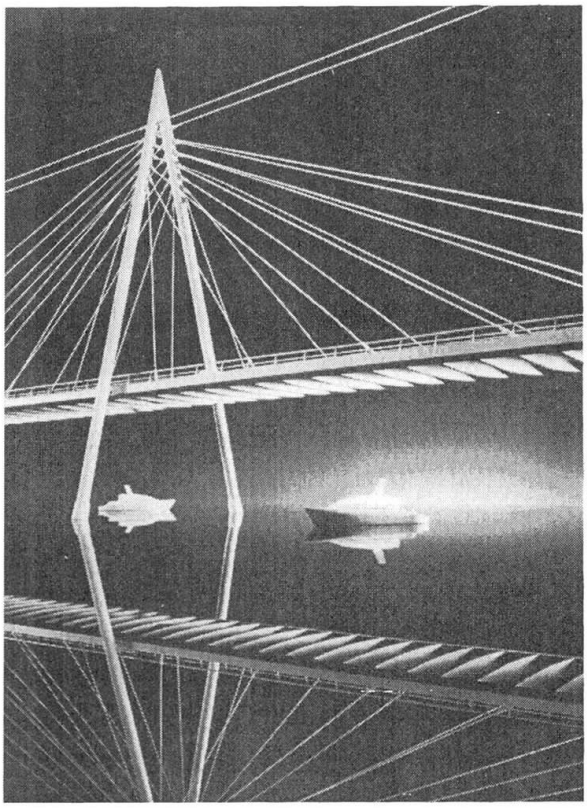

Fig.4: View of 1:100 Physical Model

Acknowledgements

I acknowledge the contribution by the other members of the team, **Dissing+Weitling**, **Rambøll** and **Terence O'Rourke**, and also the valuable assistance of **Amec Civil Engineering** and **Watson Steel** in confirming our construction methods and costs. In addition I am grateful for the images prepared by **Hayes Davidson** using photographs by **Nick Wood** and the physical models made by **Unit 22**.

References

1 Man-Chung **Tang**: Multispan Cable Stayed Bridges. *Bridges into the 21st Century, Hong Kong, October 1995, and also the 15th IABSE Congress, Copenhagen, June 1996.*

2 R. **Bergermann** & M. **Schlaich**: Variety in Cable Stayed Bridge Design (the conceptual design of the Ting Kau bridge). *IASS Symposium on the Conceptual Design of Structures, Stuttgart, October 1996.*

The Exceptional Structure of the Rion Bridge in Greece

Jacques COMBAULT
Scientific Dir.
Dumez-GTM
Nanterre, France

Pierre MORAND
Constr. Mgr
Gefyra Kinopraxia
Nanterre, France

Jaques Combault, born in 1943, obtained his civil eng. degree at the Ecole Centrale de Lyon. Bridge designer for more than 20 years, he has served as Director of the Scientific Dept of Dumez-GTM since 1993.

Pierre Morand born 1956, X76, received his civil eng. degree from Ecole Nationale des Ponts et Chaussées, Paris in 1982.

Summary

The Rion Antirion Bridge will cross the Gulf of Corinth near Patras, in western Greece. An exceptional combination of physical conditions makes the project quite unusual. Upon signature of the contract in December 1997, the final design phase began, including the careful study of the methods of construction to be used.
Although still subject to possible improvements, the conceptual design of the structure is carried out in view of challenging the earthquakes and ensuring the every day serviceability of the link as well. Innovative techniques have been developed to solve the critical problem of high degree seismicity in conjunction with a weak soil.

Introduction

The Rion Antirion crossing consists of a main bridge, measuring 2290 m long and 26.30 m wide, connected to the land by two approaches, respectively 378 m and 252 m long, on each side of the gulf.

The main bridge is located in an exceptional environment which consists of a high water depth, a deep soil strata of weak alluvions (the bedrock being approximately 800 m below the sea bed level) and finally a strong seismic activity with possible slow but important tectonic movements.

If all these difficulties could be considered separately , there would be no problem. However, the conjunction of all these problems leads to a tough design.

As the seismic activity is severe, the soil structure interaction is the center of high forces. As high forces are generated in the weak top layers of the soil, they have to be reinforced and such reinforcement is not an easy task under 60 m of water.

Design features

The seismic conditions to be taken into account are given by the response spectrum at the sea bed level which corresponds to a 2000 year return period. The peak ground acceleration is 0.5 g and the maximum spectral acceleration is equal to 1.2 g on a rather large period range.

As previously mentioned the bridge also has to accommodate possible fault movements which could lead to a 2 m horizontal displacement of one part of the main bridge with regard to the other part, the pylons being simultaneously the subject of small inclinations due to the corresponding rearrangement of the sea bed below the foundations.

In addition to that, the pylons have to withstand the impact of a big tanker (180 000 t) sailing at 16 knots.

Main bridge concept

Taking into account this range of possible disasters, the first thing to do was to adjust the span length with regard to the cost of the supports (pylons) of the main bridge, in order to reduce as much as possible, in terms of global project cost, the number of pylons in the strait.

This lead to an exceptional multi-cable stayed span bridge made of 3 central spans 560 m in length and 2 side spans 305 m long.

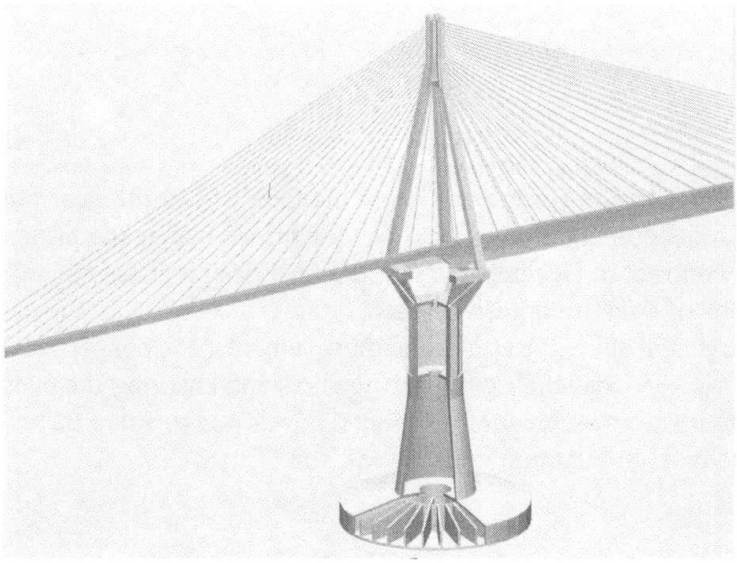

Main Bridge Concept - General view

The corresponding 4 pylons rest on the sea bed through a large concrete substructure foundation, 90 m in diameter, 65 m high, which distribute all the forces to the soil.

Below this substructure, the heterogeneous and weak soil is improved by means of inclusions which consist of 20 mm thick steel pipes, 20 to 30 m long and 2 m in diameter, driven at a regular spacing equal to or less than 7 m.

Initially, these huge foundations supported, through octagonal pylon shafts, pyramidal capitals which were the base of 4 concrete legs converging at the top of the pylons and giving them the appropriate rigidity.

This was absolutely necessary as long as each pylon supported a symmetrical cantilever 510 m long and each cantilever was connected to the adjacent one or to the approaches by a simply supported deck girder 50 m long.

But this concept has been revised as it lead to a tremendous set of bearing and spring dampers under each pylon with characteristics never reached before.

Parametric Studies and Design Improvements (Preliminary Design Phase)

As long as the signature of the contract was delayed by the banks and the bridge is really an enormous undertaking, it was decided to spend about one year to proceed with sophisticated parametric studies in view of optimising the concept and the structure as well.
Careful analyses of the behaviour of the reinforced soil and improvements of this innovative concept lead to give up the initial statical scheme of the main bridge and to definitely move towards a much more efficient structure with a continuous pylon (from sea bed to head) and a continuous deck fully suspended and therefore isolated as much as it can be. This made possible to reduce the height of the deck girders and therefore to reduce also the wind effects on the bridge.

Nevertheless, the main bridge concept is not fully finalised yet, but it is undergoing a spectacular evolution, which takes into account all the aspects of the project economy and which is the result of the close interaction between design and study of realistic construction methods.

Some unusual aspects of construction methods:

Construction of the main bridge is facing a major difficulty in the depth of the seabed, which reaches 65m for central piers. In relation with this, foundation works, including dredging, steel pipes driving but also exceptional works like precision laying of a 8000 m^2 gravel bed, are forming a impressive package requiring unusual skills and equipments.

To achieve this challenging task, offshore technology, with respect to GBS platforms construction and specially designed heavy duty pontoons and vessels, will be extensively called for.

Pier construction:

Piers up to mean sea level are built in two phases:

. the footing, 90 m diameter, 9 m high in the periphery, 13,5 m in the center, is a hollow piece of 65.000 tons of concrete, with an external volume around 72.500 m^3, thus providing a sufficient buoyancy. It will be cast in a dry dock and

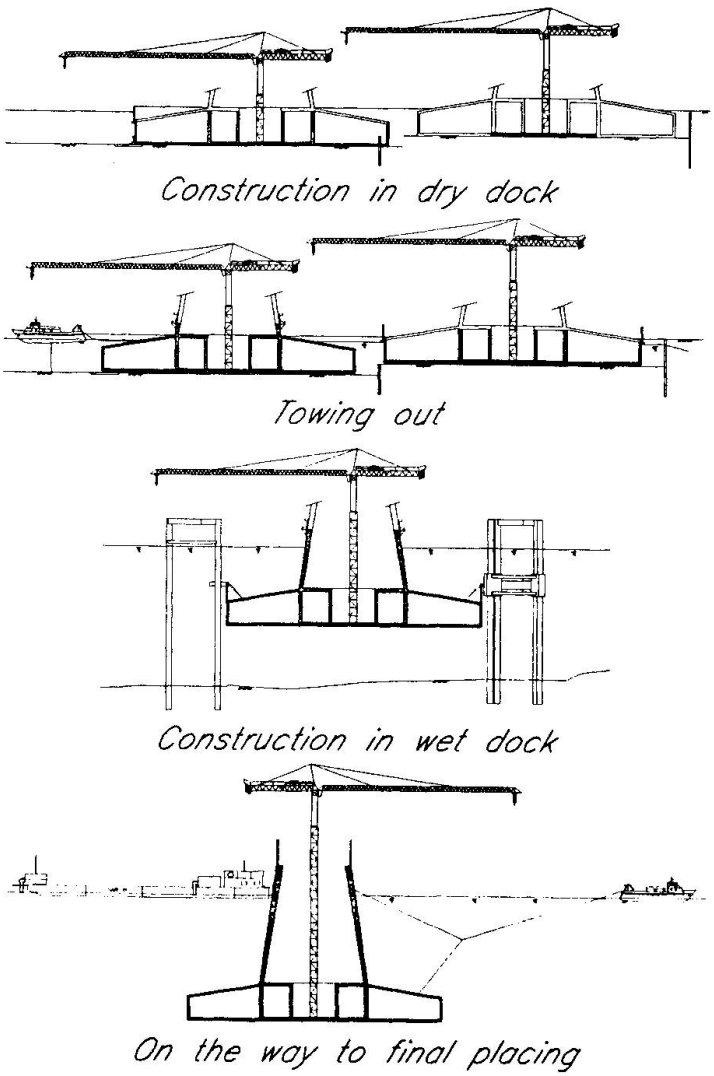

Pylon Base Erection and Placing Stages

floated out once completed. This dry dock is 200 m long by 100 m wide, to allow for simultaneous fabrication of 2 footings. Its closure system is quite unusual: the first footing is built behind the protection of a dyke, but once moved out, the second one, which construction was started backward, is floated in the front place and used as a gate to close the dock.

. the cone, 38 m diameter at the bottom, 26 m at the top, 53 m high for central piers. It will be cast with classical jump forms atop the footing in a wet dock, floating and attached by dolphins or mooring lines, with a final draft of around 50 m.

Once completed, the pier bases will be towed to their final immersion site and sunk on previously prepared foundations. Compartments created in the footing by the radial beams will be used to control trim by differential ballasting. Then the piers will be filled with water (and maybe some sand) to anticipate and speed up settlements. This preloading will be maintained during pier shaft and pier head construction, thus allowing a correction for differential settlements when erecting the pylon.

Foundation works-Tension leg platform :

Foundation works will include dredging to level the seabed, driving the inclusions, and placing the final layer of selected granular materials. Pier n°3 will also require a substitution of the top 5 m clay layers, by dredging, then placing sand and gravel and finally densification by vibroflotation, which technique should also be used to improve sand and gravel top layers found under pier n°4.

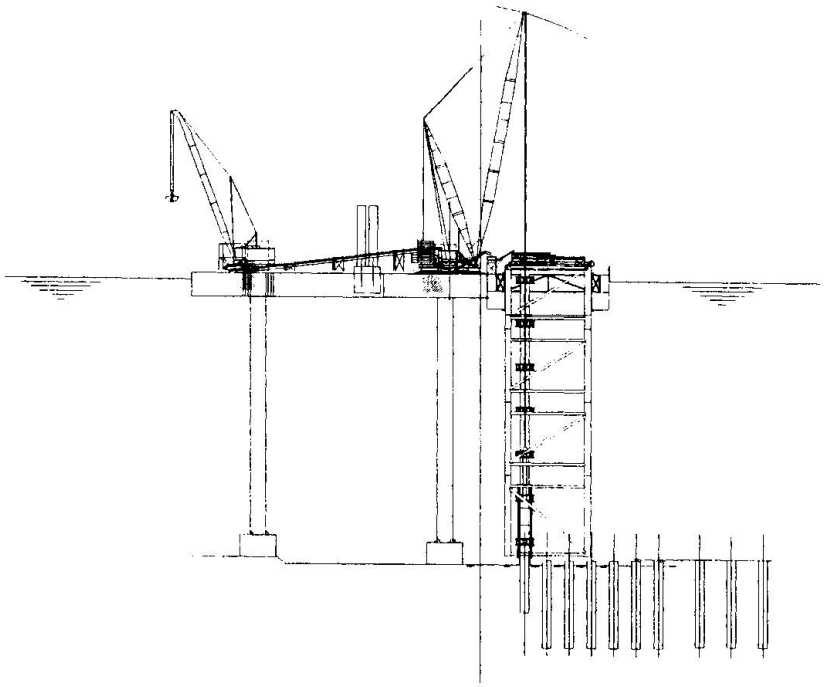

Inclusions driving with the tension leg platform

Tension Leg Platform

Tolerance in altitude for the 8.000 m^2 gravel bed is the most demanding dimensional constraint : between $\pm$ 3 and $\pm$ 5 cm. This can be achieved either with a floating pontoon and a sophisticated placing system able to compensate for sea surface movements, which is the option chosen in the Oresund project between Denmark and Sweden, or a platform providing a stable elevation. A jack-up barge is a possible solution, even with 65 m of water, but soft soil would impose huge spuds at the legs bottom. Thus, the preferred solution is a tension leg platform.

This type of barge is based on active anchorage with dead weights lying on seabed straight under the barge, and chain anchor lines tensioned to force it down in water, so that its elevation will not, to a certain extent, be influenced by sea surface movements and loads handled by cranes disposed on its deck: if sea goes down, or if a load is added, the tension in the chains decreases, but the platform's elevation does not change. A reserve of buoyancy is provided so that by increasing the tension, the anchor weights can be lifted from seabed, and the whole thing can move floating.

This concept provides a better stability than usual barges with 8 mooring lines, without the problems induced to navigation by the huge area where these lines are in the way, and displacements are easy with a cargo barge, quick coupling devices ("docking rollers", a licensed product of GTM group) , DP system and GPS positioning.

For Rion project, the platform should be obtained by retrofitting a jack-up barge used for heavy lift during Second Severn Crossing. Existing jacking houses would be converted to handle anchor chains (typically ∅168mm grade 4). Nominal working tension would be 750 tons each, thus providing 3.000 tons with 4 chains, mobilizing 1.5m of draft for 2.000 m^2 of deck. A Manitowoc 888 ringer, with 600 metric tons capacity, and a weight of 1.000 tons, is considered as main crane, far above the capacity required to handle the 100 tons packages formed by one inclusion and the pile-driver on top of it, but well suited for heavy lifts to be performed during superstructure construction.

All handling operations will be performed from this barge. Then, a catamaran semi-floating pontoon, attached to this stable platform, will provide the transfer system between surface and sea bed: it will support a mobile riser with guides for inclusions and a tremie pipe for gravels, covering around 400 m^2 of seabed. Gravels would be laid in parallel berms, 2 m wide, separated by V shaped cuts around 30 cm deep to provide some flexibility when placing the pier, distributed and leveled by a rectangular open frame at the bottom of the tremie pipe, kept full up to a minimum of 2 m.

Some indications about the schedule:

Contract Effective Date:
- December 24th, 1997

Construction time limit:
- 7 years (December 24th, 2004)

Start of works:
- Dry dock: September 1998
- Foundation works:
  Spring 1999
- Pier n°4 construction:
  January 2000
- Pier n°4 immersion:
  beginning of 2001
- Pier n°4 deck erection:
  mid 2002

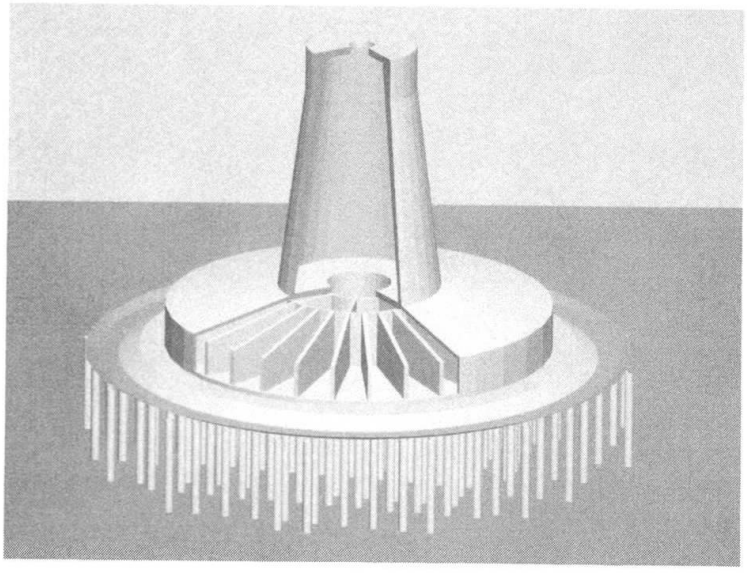

Reinforced soil - Pylon base - Final concept

Leere Seite
Blank page
Page vide

Controlling Methods of Bridge Launching Process

Oleg CHEMERINSKY
Civil Eng.
Giprotransmost J.S. Co
Moscow, Russia

Vadim SELIVERSTOV
Civil Eng.
Giprotransmost J.S. Co
Moscow, Russia

Alexander CHVYREV
Civil Eng.
Volgomost J.S. Co
Saratov, Russia

Vyacheslav AKATOV
Civil Eng.
Volgomost J.S. Co
Saratov, Russia

Jury NAYANOV
Eng. Physicist
Politechnical Univ.
Saratov, Russia

Summary

Over the past two decades the erection of steel and composite bridges by method of incremental launching has become one of the most widely used. To assure the safety of erection process and reliability of the bridge structures during construction, a special attention is paid for controlling of launching process. This paper presents some typical practices related to techniques of erection control and provides some details on means of control implementation applied for bridge construction in Russia.

1. Introduction

Erection of bridges by method of incremental launching comprises site preassembly of steel superstructure from manufactured at specialized shops segments. These segments weigh up to 35 t and normally are 10.5 and 21 m long, they are transported to construction site by railways or highways. During the process of launching the superstructures bear over special sliding devices located on top of piers. The typical features of the Russian erection practice using the method of incremental launching were discussed in detail in ref. [1].

When the erection by method of incremental launching is implemented, the stressed-strained state of bridge structures is persistently changed. During this period the launched superstructure is very sensible to deviations from design assumptions. Typical superstructure cross sections commonly applied in practice are single and two box girders (three box structures are rarely used). Linear weight of such superstructures varies in a range of 7-12 t/m, this normally results in overpier reactions up to 1600-2000 t for spans of 130-160 m. The coefficient of friction between the polished stainless steel of sliding device and antifriction material (e.g. teflon) depends on various factors and is typically within a range of 4-8%. A possible exceedance of safe reaction values or coefficient of friction may cause a loss of load carrying capacity of superstructure or piers or both. Therefore the control of stressed-strained state of superstructures and piers during the launching process is an important aspect.

2. Methods of Control at Launching

2.1 Development of controlling techniques

Generally the methods of control comprise continuous visual inspection of different bridge components and measuring (monitoring) of load effects in the structures by means of various signaling and controlling systems and devices. The following factors are continuously checked: reactions at piers, superstructure pushing-out forces, stresses in superstructure web panels, deviation of pier tops, cantilever end deflection, wind velocity, deviation of superstructure in plan. The construction site is also equipped by telephone and radio communications.

The development of practice for implementation of control during erection included the elaboration of new and improvement of existing individual devices and systems to measure various parameters. The developed modern controlling technique links the individual control of pier and superstructure behaviour into a single system, showing on a computer display of the central command station a global picture of launching process. The work of controlling system has been tested in real conditions of steel superstructure launching for the bridge over the Volga river (v. Pristannoe) and proved its efficiency.

The controlling system comprises a central computer located at a command station, which manages the overall launching process. The information are obtained by means of a set of gauges, forming a network, and transferred to the central computer for data processing, storing and displaying results. A general scheme of controlling system is shown in Fig. 1. A detailed description of the controlling system is given below.

2.2 Background to choice of main parameters for control

During the superstructure launching the stresses and deformations exceeding allowable values may occur. This may turn the elements of bridge structures into a state of failure. Due to inaccuracy of sliding devices installation or superstructure assembly on jig supports, a dangerous overloading of one of the box webs may occur at launching. Even if works are completed within allowable tolerances regulated by standards, total accumulated vertical deviations may reach a significant value of up to 10-15 mm. Such deviations at levels of bearing of adjacent beams located over one pier lead to overloading of one of superstructure webs. Narrow boxes having a large torsion stiffness is the most critical in this case.

Theoretical values of pier reactions, bending moments and shear forces for any superstructure section are calculated using a computer program that models the launching process [1]. The results of computation include values of reactions, bending moments, shear forces, deflections at each stage of launching at superstructure sections chosen by the Designer. Moreover the values of ultimate reactions based on provision of stability for web panels of main beams are also determined. During the process of launching the data on measured values of reactions are transferred to the computer (Fig. 1, 1st group of gauges) and compared to the computed (design) and ultimate values.

In the most loaded superstructure sections (the root of the largest cantilever during launching and main girder joints having site splice kinks), the stresses at web panels adjacent to bottom flanges are measured (Fig. 1, 4th group of gauges).

At certain stages of launching the reactions at piers may reach values comparable to operation condition. The antifriction materials applied for sliding devices have a sufficient magnitude of friction coefficient depending on many factors - air temperature, specific pressure, time of launching interruption and some others. To control the state of piers, the deviations of pier tops are measured, representing a function of their load-carrying capacity (Fig. 1, 2nd group of gauges).

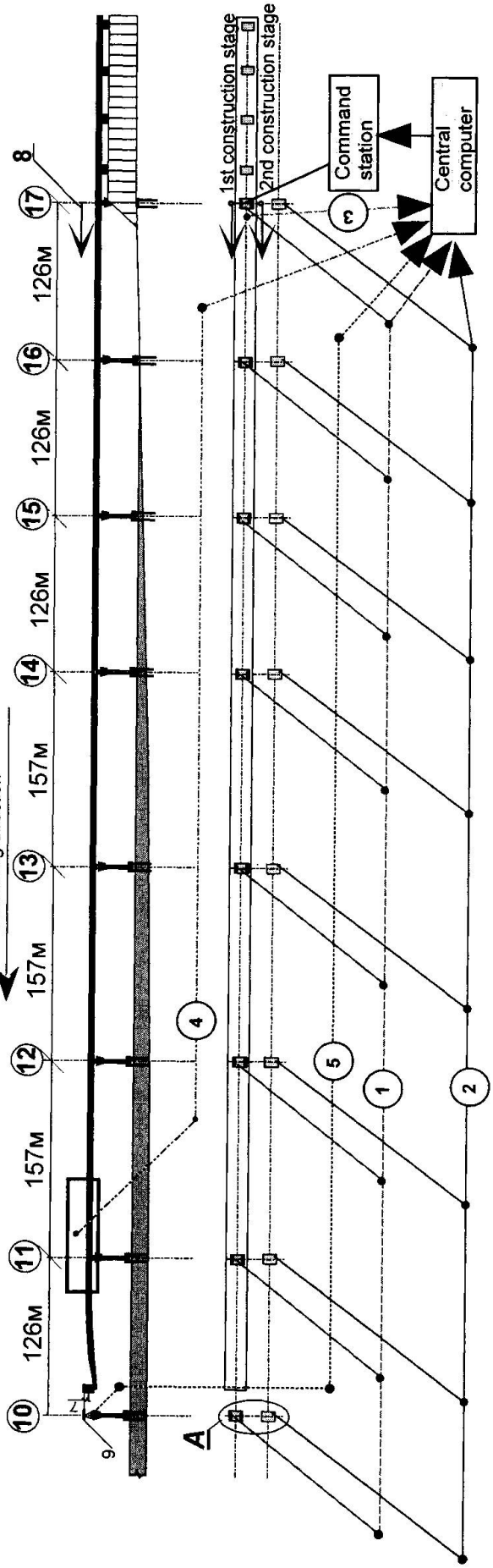

Fig. 1. General scheme of controlling system for bridge launching

① - group of gauges for collection of data on reactions,

② - group of gauges for collection of data on pier top deviations,

③ - group of gauges for collection of data on pushing-out force and length of superstructure movement ,

④ - group of gauges for collection of data on stress values at webs ,

⑤ - group of gauges for collection of data on superstructure cantilever end horizontal and vertical deviations ,

1 -hydraulic jacks of 1000t capacity, 2 - manometer, 3 - pumping station, 4 - laser, 5 - screen scale, 6 - deviation of pier top, 7 - deviation of cantilever end in vertical (deflection) and horizontal directions, 8 - pushing device, 9 - videocamera

Also other parameters, which do not influence on workability of structural elements but provide the successful implementation of erection, are controlled. These are control of value of pushing-out force (Fig. 1, 3rd group of gauges) and control of cantilever end horizontal and vertical deviation (Fig. 1, 5th group of gauges).

2.3 Details about work of controlling system

To maintain the computer controlling system in working condition, and to outline and track the influence of temperature and some other temporary factors, during the intervals of launching, on variability of loaded pier and superstructure behaviour, 24 hours regime of work have been required.

The principles of relevant information interpretation about launching process are discussed below.
A typical monitor screen is shown in Fig. 2. The monitor screen contains a mosaic graphic display consisting of lighted, coloured tiles which interpret the status of all conditions being monitored by the computer system. The screen is divided by 5 windows. The purpose of each window is obvious from Fig. 2.

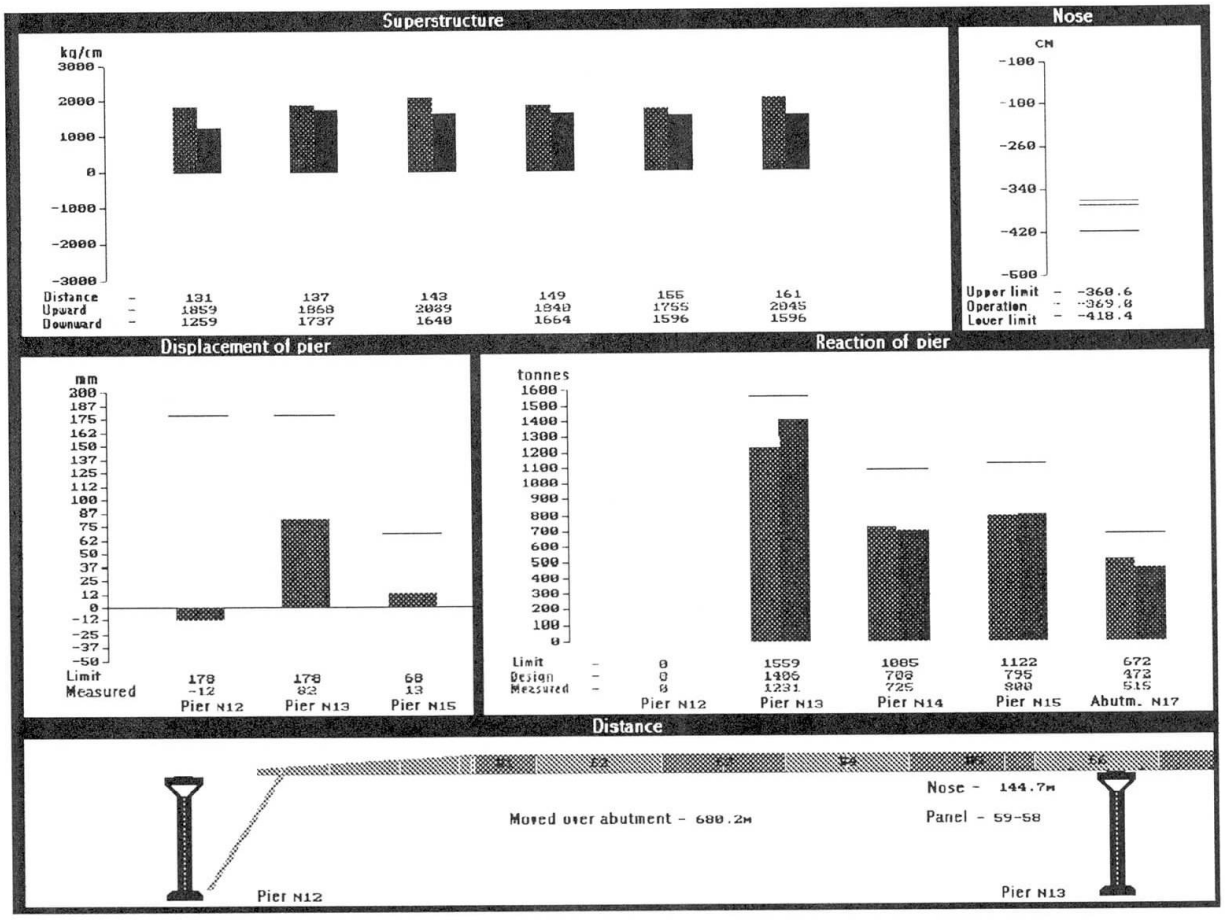

Fig. 2. Typical monitor screen with parameters controlled during launching process

The principle of reaction value control is based on continuous comparison of design (calculated) values to that of measured at each moment of time. This information is presented in window «Reaction of pier». In adjacent window «Displacement of pier» the information on pier top displacement during launching is shown. Next window «Superstructure» demonstrates data on stress values in the superstructure webs. In each window the information is grouped by a single type in a form of histograms and figures. In these three windows the values of ultimate (allow-

able) parameters are input by the Designer. The beginning of dangerous situation is reflected in the computer by turning the colour of histograms into red. If the value is exceeded, an electric signal is given to the command station and the process of launching is automatically stopped to investigate the reasons of fault state beginning.

Window «Nose» provides information on three dimensional position of nose end, characterizing superstructure deflection and deviation in plan. Bottom window «Distance» schematically shows superstructure passing over pier with synchronous reflection how launching proceeds (in real scale of time).

For a typical plot showing how reactions at pier change when launching proceeds see Fig. 3. The values of the design reactions have been obtained by the computer analysis of superstructure launching and measured values - from field measurements. As it is noted from the plot the results are in good agreement with the measured ones. The dispersion is very small.

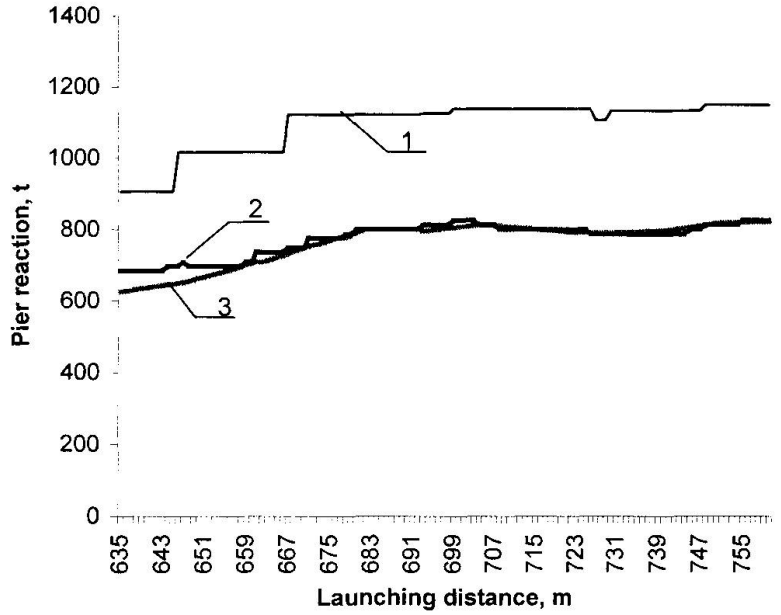

Fig. 3. Typical plot of pier reactions change related to consequent stages of launching. 1 - ultimate reaction values, 2 - design (calculated) reaction values, 3 - measured values of reactions

2.4 Means of parameters measurement

To level the reactions at superstructure webs, hydraulic converters (jacks) are installed under the sliding devices. These jacks are connected into a single hydraulic system over the pier and the information on reactions are taken by means of manometers and special gauges. The measurement accuracy is within a limit of 5 tons.

To control the deviations of piers, laser measurement units are installed on pier tops of the 2nd construction stage and photo receiver - on pier tops of the 1st construction stage. Because of possibility of fault situation quick development (within few seconds), a deviation measuring gauge is questioned by the central computer 10 times a second. The measurement accuracy is not greater than 2 mm.

Stresses at superstructure web are determined by measuring of web deformations using digital indicators with accuracy of 2 μm. By technical reasons the indicators are normally required to be in action for some launching stages only in the most stressed positions of the superstructure.

To determine a position of distant object, a special target is fixed to a nose and videocamera connected to the computer is installed over the pier. Theoretical calculations and experimental results have shown that using this method the position of object (in case of moving) at a distance of up to 100m could be measured with an accuracy of 1 cm.

3. Some notes on safety of bridge structures during erection

Over the duration of erection phase, the bridge structure threatened by certain hazards. During launching the bridge may be exposed to natural hazards such as wind, earthquake etc. Consideration of these aspects is essential for design with respect to safety.

The condition of launching is more critical for wind action than completed bridge, especially with the largest cantilever of superstructure under erection. The current Russian codes concerning bridge construction and erection design stipulate a design of pulling and restraint systems for launching for a wind loading corresponding to a wind speed of up to 13 m/s. This limit of wind speed is based on provision of safety for construction works. However this limit is not likely to be a reasonable approach. Because during launching the allowed wind speed may be exceeded for a certain short period of time and it would be very dangerous to stop overall technological cycle of erection and leave a large free superstructure cantilever. In such a case the launching should normally be continued to reach the pier and fix it in this position. The design specifications are required to establish a relevant procedure to treat the action of such an extreme event.

The analysis of superstructure under the launching conditions for wind interaction usually made for the same value of wind loading as specified for operation condition. Evidently it would be more appropriate to apply a reduced wind speed in erection calculations to allow for the short period at which the relevant structure is at risk. The use of methods based on risk analysis theory is an appropriate tool to establish the reasonable value of load and to elaborate a set of appropriate safety measures for erection of bridges exposed to extreme events.

4. Conclusion

The worked out methods have been tested at a large number of bridge projects. The recently worked out complex controlling system showed its efficiency, this was expressed in timely warning about the development of dangerous situations which might further cause a failure. Using this system of monitoring in the launching process assures reliability for the bridge structures during superstructure erection and therefore reach the goal of cost saving construction.

At the same time it should be noted that the elaboration of controlling system was based on non-contact methods of measuring and transferring the obtained data into figures. This system has some advantages. However it has been noted that the accuracy of measurements was slightly reduced in case of high air humidity. To improve the controlling system further research into means of providing protection to its components for operation independently of level of humidity has been conducted. Also a location of main cable over the superstructure requires continuous pulling during the process of launching which is an inconvenient operation and in addition may affect work of certain part of the system. The results of research will improve the technical parameters and reliability of computer system control for stress-strained state of launched superstructure and bridge piers.

5. References

1. Zhuravov L.N., Chemerinsky O.I., Seliverstov V.A., Launching Steel Bridges in Russia. Structural Engineering International, vol. 6, No. 3, p.p. 183-186. IABSE, Zurich, 1996.

New Building Technology for Prestressed Concrete Structures

Mechislav CHEKANOVICH
Assoc. Prof.
Agricultural Univ.
Kherson, Ukraine

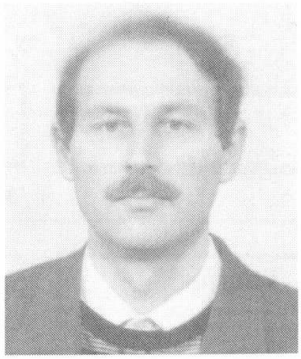

Mechislav Chekanovich, born 1960, received his civil Eng. degree from Kiev Highway Eng. Inst. in 1982 and PhD in Kiev Civil Eng. Institute in 1993.

Summary

The new building technology offered has led us to the possibility of increasing concrete strength in prestressed structures up to 50- 70 per cent, crack resistance being usual. It is achieved due to compressing unset concrete mix during the operation of steel tensioning. A wide range of research and practical studies has shown that the given technology provides necessary steel pretensioning and uniform or predetermined concrete compaction as well as hardening of concrete in a structure.

1. Introduction

Prestressed concrete structures are usually produced according to post-or pretensioning technology [1]. There are a great number of proposals as to the realization of these technologies. The majority of them are well studied, and some of the best ones find their practical application. Almost all these suggestions can be united according to the principle of the steel prestressing transfer, namely onto the hardened strong concrete. The possibilities of manufacturing more effective prestressed reinforced concrete structures in the limited frames of the single principle are in many respects exhausted. Many specialists think it is the reason for slowing down progress in this direction. We need here qualitative transition to new concepts in the sphere of prestressed concrete to have precedents for rapid flourishing of ideas and developments.

2. New technology

The author has offered and put into practice the principle of prestressing transfer onto the freshly placed concrete mix of structures. In this case prestressing is made already at the stage of cement concrete components.

After vibrodynamic compaction, the placed unset mix is under compression of the steel prestressing force, and it hardens under the pressure. All this leads to the concrete mix compaction, the removal of water excess and air from the mix, to eliminating macro- and partly microdefects of the concrete structure, and to restraining destructive

processes during concrete hardening. Steel prestressing is preserved, for after the compaction of the specially proportioned concrete mix, rather a strong and rigid skeleton of solid ingredients is formed, and the stressed steel is then fixed onto this skeleton (fig.1).

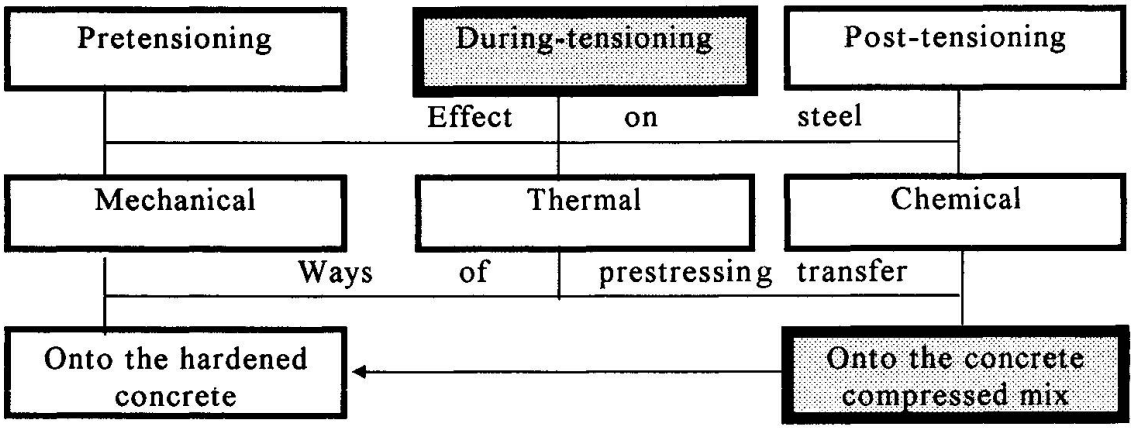

Fig.1. Extended scheme of methods of making prestressing in reinforced concrete structures

It is also possible to partially transfer steel prestressing onto the concrete mix [2]. The realization of the new technology method of concrete mix prestressing became possible after the author had invented original movable forms and devices for full or partial prestress transfer [3].

Considerable increase of the effect of uniform concrete compression, the elimination of undesirable initial stress in reinforcement is possible due to the application of movable steel bars proposed by the author. The bars are made in a special way. During the pretension these elements are shortened within the length of the structure. The concrete contacting the steel is compressed and reaches a high degree of compaction. A high quality contact is provided. Prestressing is transferred onto the concrete.

3. Experimental results

According to the offered presstressing method there have been made experimental beams with rectangular cross section and dimensions of 100x200x2000mm and columns with round cross section (d=250 and l=1500mm). Under comparison in all equal conditions traditional prestressed elements and usual reinforced concrete ones were also produced. The results of beam and column tests are graphically presented on fig. 2.

For the experimental beams with μ=2.2 per cent we have reached the increase of carrying capacity up to 25-34 per cent due to the compression according to the new method. The effect of carrying capacity increase in columns amounted to 75 per cent. It is illustrated graphically on fig.3, where K is the ratio of the carrying

capacity of a reinforced concrete element compressed according to the "during-tensioning" method to the usual one.

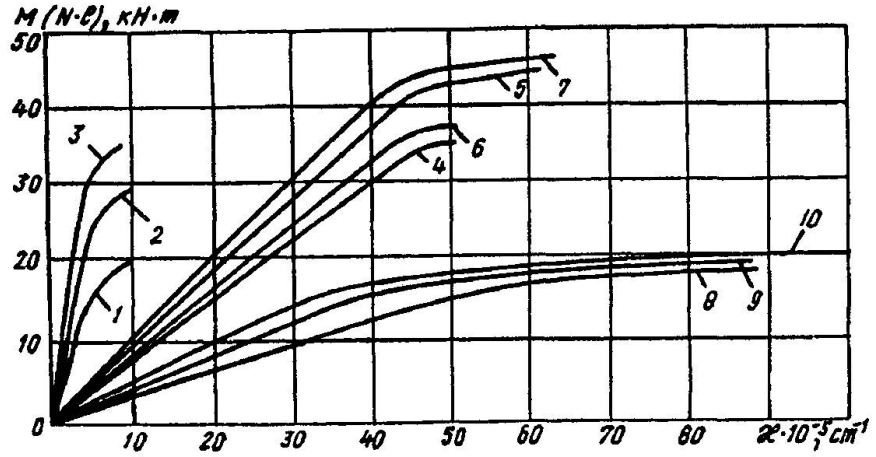

Fig. 2. Typical relationship "load-curvature"

1; 2 and 3 – for the columns with σ_N correspondingly 0; 2 and 4 MPa;
4; 5; 7 – for the beams with μ=2.2% when σ_N is correspondingly 0; 5; 10 MPa, and
6 – according to the "pretensioning" method;
8; 9 and 10 – for the beams with μ=0.063, when σ_N is correspondingly 0; 2 and 4 MPa.

The analysis of the results shows that the losses of steel prestressing caused by the deformations of the compressed mix, shrinkage and concrete creep are less than in traditional structures. The prism strength of concrete after the compression increased up to 2.2 times comparing it with the initial one. The most

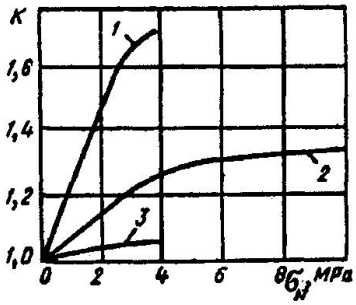

1- for columns;
2- for the beams with μ=2.2%;
3- for the beams with μ=0.6%.

Fig. 3 Diagram "K– σ_N"

intensive strength growth was marked under the pressure value up to 6 MPa. The values of elasticity modulus E_b and relative deformations ε_{bR} increased by 40-50 per cent.

4. Theoretical analysis

According to the research data obtained by the author, to preserve the force of steel prestressing we should use in the offered structures concrete with contacting skeleton location of the grains of strong coarse aggregate after compaction. In

addition, the greater part of the prestressing force is transferred contactingly through thin mortar membranes in a grain-to-grain way (fig. 4.).

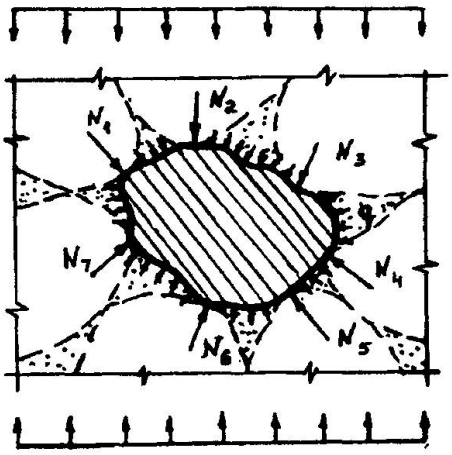

To get a strength formula for prestressed reinforced concrete of a matrix-carcass structure the author has suggested that one should proceed (besides the well-known premises) from the fact that the value of failure loading depends on the crushability of grain mix of coarse aggregate as integral characteristics of its strength. The influence of precompression and dynamic effect on the concrete mix is revealed in compaction, and also in additional loading of the skeleton of coarse aggregate grains.

Fig. 4. Scheme of loading of coarse aggregate grain

Taking into account the above mentioned and proceeding from the well-known premises, there has been obtained the following formula of strength of prestressed concrete with a matrix-carcass structure:

$$R_B^* = \left(K_P \frac{q}{K_c} + K_1 K_2 K_3 (1 + \alpha_1 \ln 98p) R_{mbt} - c\sigma_N \right) \cdot \left(\frac{1}{1 - (1 + \alpha_2 \ln 98p) \frac{E_m}{E_{ag}}} - K_V \frac{V_m}{V_b} \right)$$

Here K_p – index reflecting the change of structure composed of coarse aggregate under crushability (0.2-0.36); q – value of standard loading while defining the crushability of coarse aggregate grains (11.32 MPa); K_c – crushability index of coarse aggregate grains placed as in concrete, i.e. it may be filling, vibrocompaction, dynamic effect with loading; K_1, K_2 and K_3 – correspondent indices of form (1.27-1.55), relief (1.18-1.40) and microrelief (1-1.41) of aggregate grains; p – value of pressure action on the cement-sand mortar; R_{mbt} – tensile strength of the usual uncompressed mortar; $c\sigma_N$ – value of pressure acting on the coarse aggregate; E_m and E_{ag} – elastisity modulus of mortar (matrix) and aggregate material; K_V – compaction index of the mortar.

According to the given formula it is possible to calculate concrete strength under full or partial transfer of the prestressing σ_N on the concrete mix. If the prestressing is relieved after compaction, and it doesn't further load the skeleton of coarse aggregate, the value C is to equate with O. Besides, in this formula the value of the P parametre for the usual uncompressed concrete with skeleton arrangement of coarse aggregate grains equals O.

On fig.5 there are typical plots showing dependence of the index of concrete strength increase on the value of prestressing and the mode of its application. The comparison of analysis dependences with experiments testifies to their being in

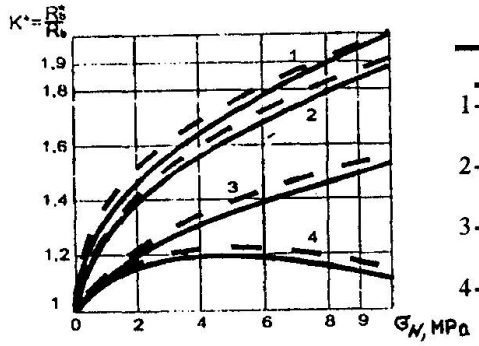

——— - experimental
- - - - - - - - theoretical
1- compressed under dynamic influence and its further relieving;
2- the same operation, under preserving the stress of compression;
3- compression without dynamic influence with its further relieving;
4- the same operation, under preserving the stress of precompression.

Fig.5. Diagram "K-σ_N"

agreement. The given formula shows satisfactory results in practical application. It takes into account the transfer of prestressing onto concrete mix both in cases of its preserving and relieving.

5. Production implementation

The level of research includes production implementation. At present, large 30-ton bridge elements of prestressed concrete made by compressing the unset concrete mix by the force of steel tensioning are successfully used in Ukraine (fig. 6).

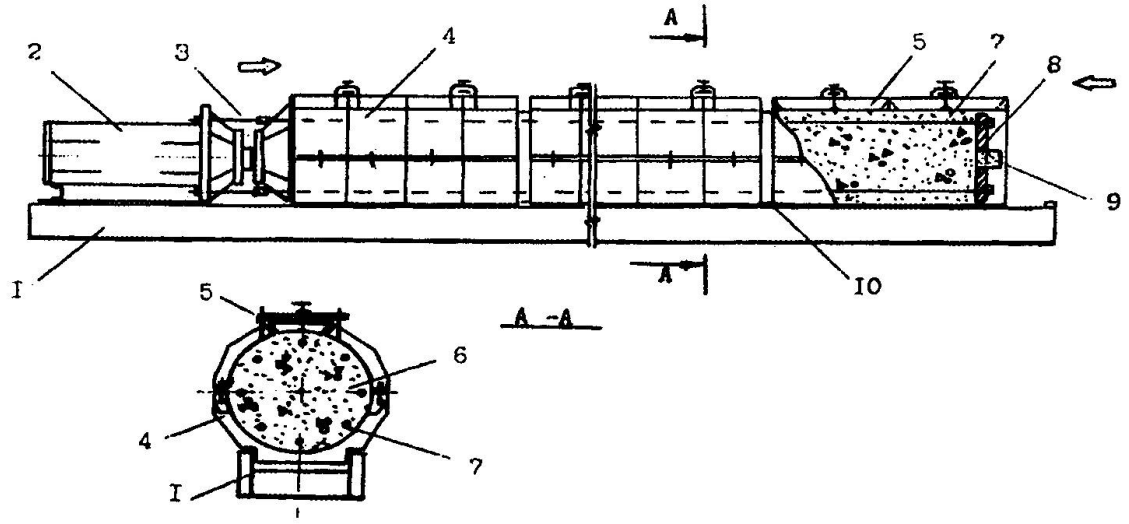

Fig. 6. Scheme of compressing the pillar in the formwork according to the " during- tensioning" method.

1- frame; 2 - tensioning device; 3 - tie-rods; 4 - section formwork; 5 - hole with screw lock; 6 - concrete mix; 7 - bar reinforcement; 8 - movable end: 9 - device for taking concrete samples; 10 - functional joint

Favouring practical application of the above mentioned elements was the device invented by the author, which provides reliable control over the quality of the compressed concrete directly in the product [3]. Service observations of the reinforced concrete pillars produced according to the technology offered in the piers of the trestle part of a large bridge over the river Dnieper in the town Dneprodzerzhinsk (Ukraine) confirmed high quality of the structures compressed according to the "during-tensioning" method.

6. Conclusions

Taking as a basis the experimental research data, we can state that self-organization of concrete structure at the stage of mix prestressing, concrete density, high bond between concrete and steel, preservation of the force of prestressing - all this becomes a guarantee for high strength and quality of the concrete elements offered. Industrial application of prefabricated bridge elements with prestressing onto the concrete mix has proved the expediency of the method proposed.

The current level of the method development allows recommending for the lot production the following reinforced concrete structures: columns and pillars, piers, bulky foundation elements, some beams, thick slabs for briges, airfields and motorroads, curbstones, tram and train ties, poles.

We expect that further experimental research and perfection of the "during-tensioning" method will make it possible to broaden the list of economically expedient compressed reinforced structures, the lot production of the ones compressed according to the new method, and tested in practice, hopefully favouring progress in construction.

REFERENCES

[1] Leonhard F. "Spannbeton" für die Praxis. Wyd.3. Ernst u.Sohn, Berlin-München-Düsseldorf, 1973, p.246

[2] Rasskazow A.O., Čekanovič M.G., "Čiastočne predpäté konštrukcie s prenesenim predpätia na nezatvrdnutú betónovú zmes", Konferncia "Konštrukcie z čiastočne predpätého betónu", Bratislava, 1988, p.58

[3] Chekanovich M., "Prestressed Concrete Structures with Compression of Unset Mix", Kherson: "Prosvita", 1996, 64p.

Best Cross Stay Location for Super Long Span Suspension Bridge

Masahiro YONEDA
Assoc. Prof.
Kinki Univ.
Osaka, Japan

Katsunori OHNO
Eng.
Kawasa Industries Inc.
Tokyo, Japan

YoshihikoTAMAKI
Eng.
Kawada Industries Inc.
Tokyo, Japan

SUMMARY

This paper deals with the best cross stay location for a super long span suspension bridge with a center span of 2,500m. Compound flutter performance is investigated by the direct flutter FEM analysis for 3-D frame model. Both measured aerodynamic forces on the deck and Theodorsen's aerodynamic forces on the flat plate were used for the flutter analysis. From these analytical results, some useful informations for the best cross stay location are obtained in designing a super long span suspension bridge with a center span of 2,500m.

1. Analytical study

The following cases were considered to investigate the effects of cross stays on compound flutter speed:
1) Case-S with a pair of cross stays only on the side spans
2) Case-C with a pair of cross stays only on the center span
3) Case-SC with a pair of cross stays in both the side and center spans

In this paper, it is assumed that a pair of cross stays with each cross sectional area of $0.01m^2$ (Young's modulus of elasticity=$1.4 \times 10^7 tf/m^2$) is effective for compression in analyzing each case mentioned above.

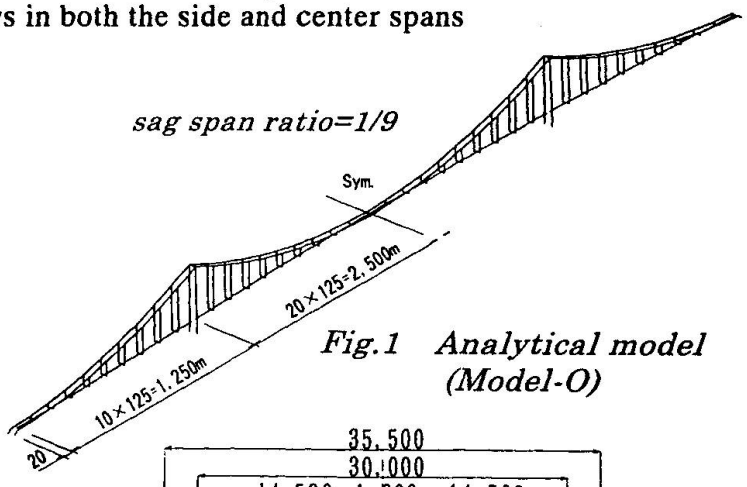

Fig.1 Analytical model (Model-O)

2. Effects of cross stays on flutter performance

Flutter speeds for the cases described above were computed using Model-O which was idealized as three dimensional frame-work (see Fig.1). Both measured aerodynamic forces on streamlined box girder as shown in Fig.2 and Theodorsen's aerodynamic forces on the flat

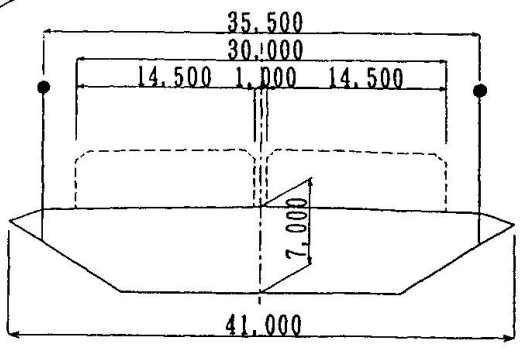

Fig.2 Section of girder

plate were used for the flutter analysis. Figs.3 ~ 5 show the analytical results by the direct flutter FEM analysis method. These analytical results are summarized below.

(1) Greatly reduced compound flutter speed have been observed in some cases when the measured aerodynamic forces on the deck were used for the bridge with a pair of cross stay only on the side spans (see Fig.3).

(2) The best cross stay location on the center span is not nearly dependent on different acting aerodynamic forces, and the maximum flutter speed based on the measured aerodynamic forces by the installation of a pair of cross stays in best position x/L=0.3 is almost equal to the value based on Theodorsen's aerodynamic forces (see Fig.4).

(3) The flutter speed of a bridge with a pair of cross stays on side spans x/L_S=0.5 and on the center span x/L=0.3 respectively due to the measured aerodynamic forces is $V_F \fallingdotseq 59.5$m/s(δ =0.02) which is lower than $V_F \fallingdotseq 62$m/s(δ =0.02) with a pair of cross stays only in side spans, x/L_S=0.5 (see Fig.5). On the other hand, it was obtained from the flutter analysis based on Theodorsen's aerodynamic forces that flutter speed by the installation of cross stays both at x/L_S=0.5 and x/L=0.3 is $V_F \fallingdotseq 75$m/s. Hence, it must be emphasized that the flutter analysis based on Theodorsen's aerodynamic forces is not always sufficient for the streamlined box girder suspension bridges with the cross stay system effective for compression.

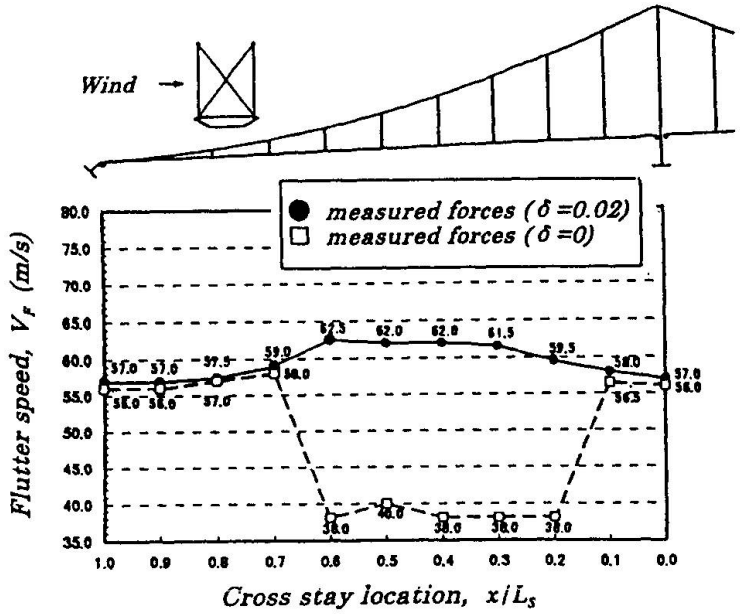

Fig.3 Effects of cross stays on flutter speed (Case-S)

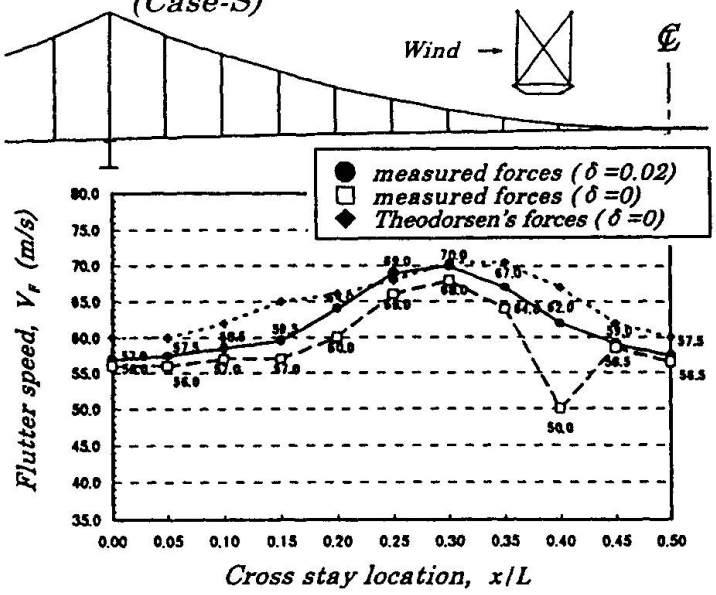

Fig.4 Effects of cross stays on flutter speed (Case-C)

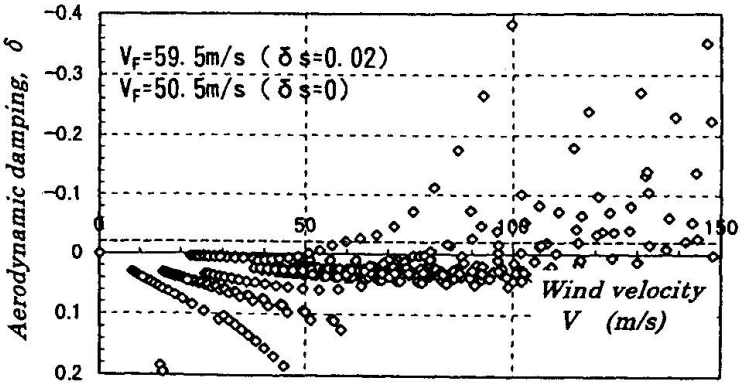

Fig.5 V-δ curve (Case-SC) (cross stays location ; x/L_S =0.5 for side spans, x/L =0.3 for center span)

The Öresund Link: Bridges for Rail and Road Traffic

Anders H. JANSSON
Production Dir.
Sundlink Contractors HB
Malmö, Sweden

Anders Jansson is Production Director and Deputy Project Director for Sundlink Contractors, the joint venture constructing the bridges in the Öresund link. He is employed by Skanska AB, Sweden

Ingvar H. OLOFSSON
Vice President
Skanska Teknik AB
Göteborg, Sweden

Ingvar Olofsson is head of the Departement for Design of Bridges and Civil Engineering Structures within Skanska Teknik AB, a Subsidiary of Skanska AB, Sweden

Summary

The article presents the structural system, design basis and production methods for the 7800 m bridge that forms a part of the Öresund Link between Denmark and Sweden. The bridge is a composite steel-concrete superstructure, supported by reinforced concrete piers and pylons that are directly founded on a limestone substratum. Construction of the two-storey cable-stayed main bridge and the approach bridges is based on extensive prefabrication of very large elements.

General

The Öresund Link presently under construction between Sweden and Denmark, is a 16 km long combined road and rail connection, consisting of a 3750 m immersed concrete tunnel, a 4500 m man-made island and a 7800 m long two-level bridge. The main bridge is a 1092 m long cable stayed bridge, with a 490 m main span and a free height of 57 m. The eastern and western approach bridges are 3014 m and 3739 m in length respectively.

The contract for the bridges was awarded to Sundlink Contractors in November 1995 by the owner, Öresundskonsortiet AB. Sundlink Contractors is a joint venture of Skanska AB from Sweden, Hochtief A.G. from Germany, and Højgaard and Schultz a/s and Monberg & Thorsen A/S, both from Denmark.

Design

The contract agreement is a design and build type. The design is based on the Eurocodes in combination with a Project Application Document (PAD) and specific Design Requirements for the project. These rules define the structural and aesthetic design of the bridges, together with rather detailed contract requirements regarding e.g. statical system, use of materials, shape and

exterior dimensions. The required service lifetime is 100 years, with recognition given to the need to replace specific elements within a shorter time-limit.

The bridge girders are designed as composite steel-concrete units with the concrete roadway on top. The roadway is prestressed in the transverse direction. The railway is located at the bottom level between two steel trusses. On the cable-stayed bridge the railway will run in ballast filled troughs, resting on a closed steel box, thus forming the bottom chord of the trusses. On the approach bridges the railway will run in two parallel concrete troughs, supported at 20 m centres by steel cross girders connected to the bottom chords of the steel trusses. The concrete troughs are continuous between the expansion joints and work in composite action with the steel structure. With continuous lengths as large as 1740 m, design movements of up to 1200 mm have to be accommodated by means of special structures supporting the tracks.

The bridge foundations are formed directly on the limestone substratum and are governed by ice loads and ship impact loads.

As the production of the bridge is based on the concept of combining very large prefabricated elements, a major design task has been to optimise each unit with due regard given to the adopted construction methods, including the manufacturing, transport, handling and joining of the elements.

Construction

The prefabricated production of the substructure elements i.e. the caissons and pier shafts, is executed at a purpose-built yard in Malmö, Sweden, close to the bridge line. The caissons are constructed in a number of steps along two production lines. There are intermediate stations where individual successive casting steps are performed. Each pier shaft on the other hand is made complete at one of ten separate positions in the pier shaft area. After prefabrication, the caissons and pier shafts are lifted, transported and placed in the bridge line by the Heavy Lift Vessel Svanen. The reinforced concrete pylons for the High Bridge are each 203 m in height and are constructed in-situ, using a traditional self-climbing formwork technique.

The foundations for the pylons were prefabricated as cellular caissons in an existing dry dock in Malmö. The 19 000 ton pieces were transported to their final position by a purpose-built catamaran. Also the superstructures of the bridges are prefabricated. The steel girders for the High Bridge are manufactured in 8 sections in Karlskrona, Sweden, some 200 km from Malmö. After painting they are brought by barge to the prefabrication yard in Malmö, where the concrete road deck is cast. Due to the shallow waters which exist in the Öresund, it is possible to erect the main span of the High Bridge in four units by utilising three temporary towers that support the 140 m long sections until the cable stays are erected.

The 49 steel girders for the Approach Bridges are fabricated in Cádiz, Spain, including the casting of the concrete road deck. The 120-140 m long girders are transported, two by two, on ocean-going barges to Malmö, where they are fitted out with the concrete troughs for the railway deck, before being transported to and erected in the bridge line.

The lifting, transporting and placing of all superstructure sections is executed by the HLV Svanen. The construction of the bridges started during late 1996 and will be finished by mid 2000.

Super Long-Span Suspension Bridge with 3-Chord Truss and 3 Cables

Yoshiaki NAKAYAMA
Senior Consult. Eng.
Advanced Technology
Yokohama, Japan

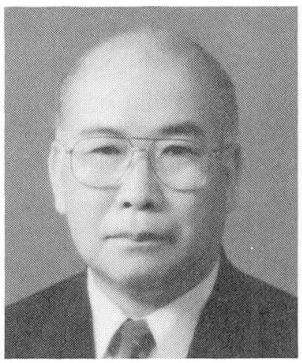

Yoshiaki Nakayama, born 1928, received his degree of Dr. Eng. from the Univ. of Osaka in 1985. He was engaged in designing of bridge in Yokogawa Bridge Works Ltd for 10 years and then worked for Nippon Kikan K.K. on the design and development of bridge and maritime civil structures for 26 years.

Summary

A suspension bridge with a three-chord-member stiffening truss girder and three main cables was proposed as a super long-span suspension bridge with improved wind stability. The stiffening truss girder of the bridge has a triangular cross section. Each chord member is suspended directly from each main cable locating right above it. The sag ratio is slightly varied between the center main cable and the side main cables. As a result, the torsional rigidity and the structural damping capacity of the bridge can be increased and, therefore, the wind stability is expected to be improved. The basic concept and the structure of the bridge are presented.

1. Principle and Mechanism for Improving Wind Stability

1.1 Damping of the First Antisymmetric Torsional Oscillation by Center Main Cable

Among the various oscillation modes of a free-hanged single main cable, the oscillation on vertical plane with a node at around a center of the span hardly needs energy and, then, hardly causes damping. In the case of conventional bridges without sufficient torsional rigidity in their bodies, a torsional oscillation of the stiffening truss girder caused by aerodynamic forces, in combination with such a oscillation of the main cable, easily generates the first antisymmetric torsional oscillation. In order to avoid this catastrophic oscillation, the mode of the main cable oscillation has to be suppressed by increasing energy for the oscillation. In the proposed bridge, the shear center is located in the comparatively lower portion of the stiffening truss girder cross section. If the first antisymmetric torsional oscillation is generated and the horizontal displacement of the third chord member is supposed to be δ_T, the deformation of the chord member in a horizontal direction can be illustrated as Fig. 1-C. Since the chord member is connected to the main cable by hangers, the deformation of the chord member is propagated to the main cable through the hangers. However, the main cable can not easily be deformed horizontally because the large tension is applied to the cable. Therefore, the deformation of the chord member is strongly constrained. This effect is comparable to that of increasing the torsional rigidity of the stiffening truss girder. As a result, the torsional oscillation generated in the bridge can rapidly be damped.

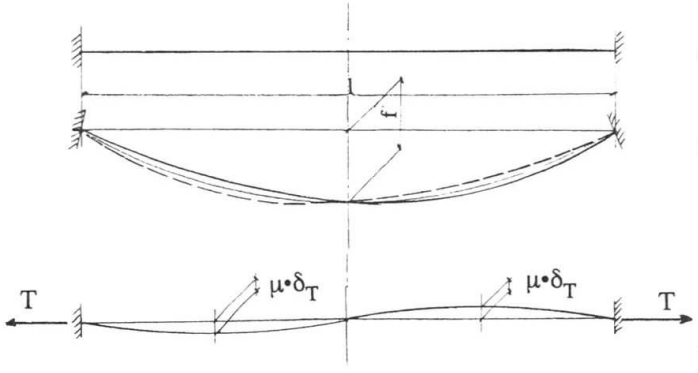

Fig. 1. Deformation of center main cable.

1.2 Damping Capacity against Bending Oscillation

Natural frequency is different between the center main cable and the side main cables because of the different cable tension and sag ratio. Therefore, for example, when the first antisymmetric oscillation is generated in the side main cables, the absorption of the oscillation by another oscillation system including the center main cable can be expected to occur. As a result, the oscillation energy is not accumulated and the action to disturb the oscillation is generated due to the difference in the phase of oscillation, and, then, the divergence of the oscillation, that is the flutter, can be avoided.

2. Outline of Bridge Structure

The cross section of the proposed stiffening truss girder is shown in Fig. 2. The rigid triangular frames (sway bracings) on a vertical plane are required to be installed at intervals of 50 m to connect the three main cables with the stiffening truss girder. This type of structure can easily be established with recent structural engineering technologies. All the truss girder members including frames have sufficient capacity to absorb the aerodynamic oscillation energy and sufficient torsional and bending rigidity because of the increased elastic deformation due to their extended length as compared to the conventional bridge members. These long members need to have a circular cross section in order to resist wind pressures and buckling by compression forces. As for the technologies for fatigue resistance of the bridge to pulsating forces by wind, they have already been well established through experiences in constructions of maritime structures.

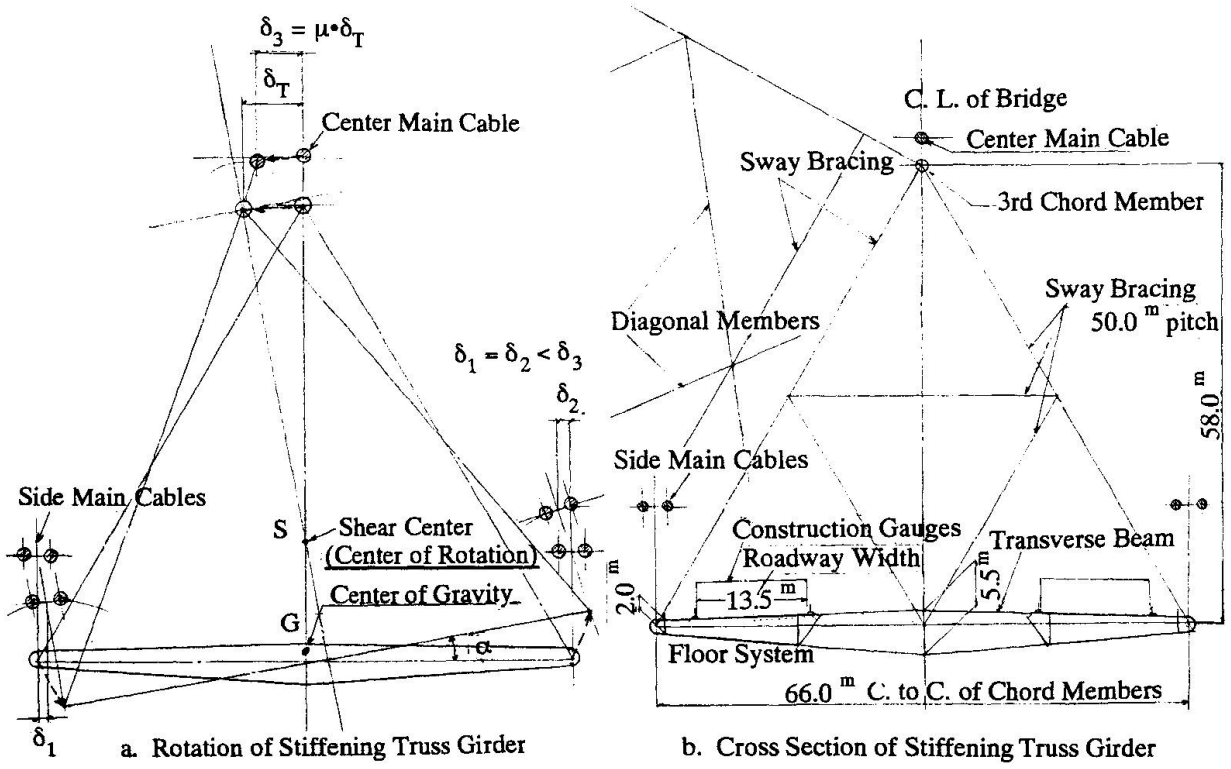

Fig. 2. Cross section of stiffening truss girder.

Aerodynamic Stability of Suspension Bridge with Open Grating Deck

Katsunori OHNO
Eng.
Kawada Industries Inc.
Osaka, Japan

Masahiro YONEDA
Assoc. Prof.
Kinki Univ.
Osaka, Japan

Yoshihiko TAMAKI
Eng.
Kawada Industries Inc.
Osaka, Japan

Kimio KIMURA
Eng.
Kawada Industries Inc.
Osaka, Japan

Shin-ichi MIYACHI
Eng.
Kawada Industries Inc.
Osaka, Japan

Summary

This paper deals with the aerodynamic stability of super long span streamlined box girder suspension bridge with open grating deck. Two dimensional wind tunnel tests were carried out in order to understand differences in the aerodynamic stability of structures with the different types of grating (wire net or thin perforated plate), and the porosity of these sections. It was shown from wind tunnel test results that the open grating method was effective to improve the characteristics of both the vortex-induced and the compound flutter oscillations.

1. Assumed Suspension Bridge and Wind Tunnel Tests

The effects of grating types and their porosity on aerodynamic stability were examined through wind tunnel tests of section models. Considering a super long span suspension bridge which has center span length of 2500m with two side spans of 1250m each (Fig.1), the cross section of girder and the structural characteristics are shown in Fig.2 and Table Ⅰ. Table Ⅱ shows the test cases in this study, where AD is the basic case (without openings), W1L1 is the case in which the parts W1 and L1 are completely open as shown in Fig.2 and Table Ⅱ. Other cases shown in Table Ⅱ, W1L1/50G through W1L1/70H are with gratings installed. The porosity of grating is shown by numerals, and letters G and H signified either wire net or thin perforated plate.

2. Wind Tunnel Test Results

2.1 Characteristics of Vortex-induced Oscillation

Fig.3 shows relationships between amplitude of vortex-induced oscillation and angle of attack. In Fig.3, when the angle of attack was 0 degree, with the model configuration W1L1, both the vertical and the torsional vortex-induced oscillations took place, where the maximum vertical amplitude was 100mm, and torsional amplitude was 1.7 degrees. And, the Test case AD demonstrated a vertical vortex-induced oscillation with the maximum amplitude of 500mm at the angle of attack of -3 degrees. At the same angle of attack, the Test case W1L1 showed the maximum of the torsional vortex-induced oscillation of 2.1 degrees. On the other hand, in each case of open gratings, no vortex-induced oscillation was observed at these angles of attack. The open grating method made it possible to suppress the vortex-induced oscillation which appeared in the fully opened case (W1L1) or the fully closed case (AD). However, when the angle of attack was +3 degrees, the torsional vortex-induced oscillation was observed in all cases.

2.2 Characteristics of Compound Flutter

Fig.4 shows relationships between critical wind speed of flutter and angle of attack. Here, the compound flutter speed for all cases of G-series was found to be approximately twice that of AD at the angle of attack of -3 degrees. However, with H-series, it was found that the compound flutter speed varied with the cases tested. In W1L1/50H (the case with porosity of 50%) the compound flutter speed was 90m/s, but the compound flutter speed decreased to approximately 50m/s for W1L1/70H. When the angle of attack was 0 degree, the compound flutter speed varied with each case in both G-series and H-series. In these cases, the compound flutter speeds for W1L1/50G and W1L1/50H were 80m/s and 90m/s, and it could be said that if the porosity of grating was approximately 50%, the aerodynamic stability seemed to be improved best. At the angle of attack of +3 degrees, the compound flutter speed was approximately 40～50m/s in all cases.

3. Concluding Remarks

In this study, concluding remarks are as follows;

(1) The open grating method made it possible to suppress the vortex-induced oscillation which appeared in the fully opened case (W1L1) or the fully closed case (AD) when the angle of attack was -3 or 0 degree.

(2) The aerodynamic stability was improved if the porosity of grating was approximately 50% when the angle of attack was -3 or 0 degree.

(3) It is necessary to study the countermeasures to improve the aerodynamic stability when angle of attack is +3 degrees.

Finally, this paper is offered to examine technical questions in carrying out the project " Aerodynamic Investigation and Research Regarding the Economical Super Long Span Suspension Bridge". We wish to thank the members involved with this project (Public Works Research Institute, Honshu-Shikoku Bridge Authority, Public Works Research Center and 8 companies for steel bridge in Japan including Kawada Industries, Inc.).

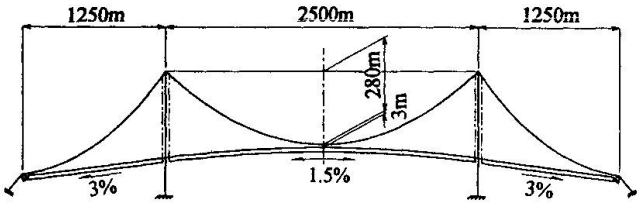

Fig.1 Assumed suspension bridge

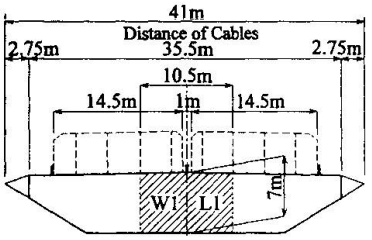

Fig.2 Cross section of girder

Table I Structural characteristics

Span		1250m+2500m+1250m
Sag Ratio		1/9
Distance of cables		35.5m
Allowable stress of cables		100 kgf/mm^2
Dead Weight	Cable	11.0 tf/m/Br.
	Girder	24.0 tf/m/Br.
	Total	35.0 tf/m/Br.
Stiffness of Girder	Vertical	12.0 m^4/Br.
	Horizontal	160.0 m^4/Br.
	Torsional	28.0 m^4/Br.
Polar Moment of Inertia	Cable	350 tf•s^2•m/m/Br.
	Girder	340 tf•s^2•m/m/Br.
	Total	690 tf•s^2•m/m/Br.

Table II Test cases

Case	Pattern
AD	WIND
W1L1	WIND W1 L1
W1L1/50G* W1L1/50H*	WIND W1 L1 ϕ=50%
W1L1/60G W1L1/60H	WIND W1 L1 ϕ=60%
W1L1/70G W1L1/70H	WIND W1 L1 ϕ=70%

* G : wire net
* H : thin perforated plate

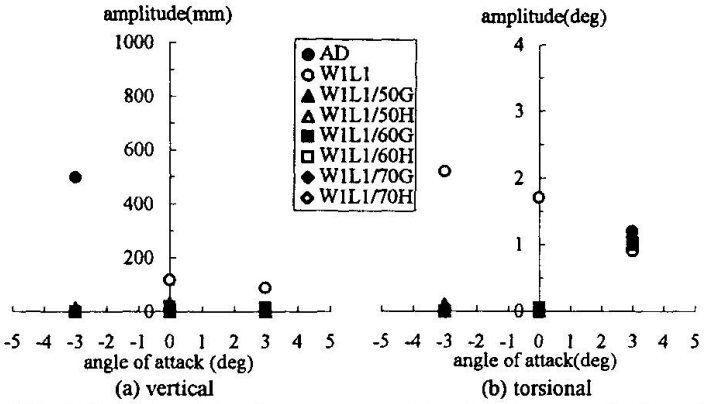

Fig.3 Relationships between amplitude of vortex-induced oscillation and angle of attack

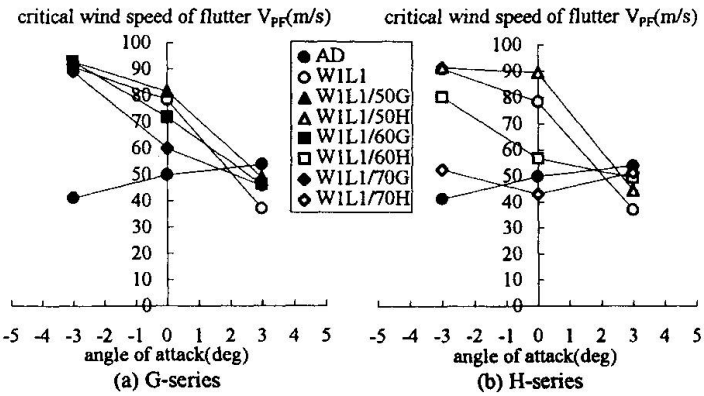

Fig.4 Relationships between critical wind speed of flutter and angle of attack

Jiangyin Yangtze Highway Bridge: Foundations' Construction

Shi Zhong ZHOU
Director
Yangtze Bridge Construction Dept
Jiangyin, China

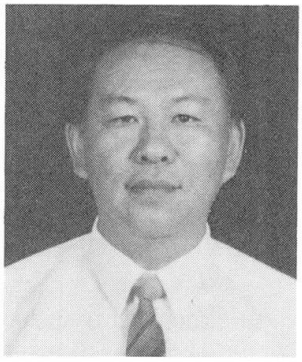

Shi Zhong Zhou, born 1943, graduated from Ocean & River Univ. in 1965. Now he is the head of Yangtze Bridge Construction Dept and Yangtze Bridge Company.

Summary

Jiangyin Yangtze Highway Bridge will stride over Yangtze River in central part of Jiangsu Province,forming a common crossing for two national trunk lines. Construction commenced in November 1994. Till September of 1997, substructure of the Bridge has been completed mainly. Contractor of superstructure entered work-site in October the same year. We anticipate the Bridge will complete in September 1999 and open to traffic after one month.

1.Brief description

Navigation runs very busy in the lower reaches of Yangtze and the Bridge will cross the narrowest part, considering stability of current and flood, the option of suspension bridge has been selected. Southern tower sets at the bank and northern one at flood land, that avoids hitting of ships. Main span is 1385m, clearance will keep 50m in height for seagoing vessels passing through.

Suspension bridge will be arranged as 336.5m+1385m+309.4m. Main span is a steel box girder with wind noses at both sides. Anchored spands are continuous prestressed concrete box girders. The deck is designed for expressway in dual direction,three lanes each, its width is 29.5m. According to Chinese Standard, designed life load complies with Super-20 and Trailer-300. With regard to the factor of multilane deduction, load means 40KN/m for six-lane deck. Pedestrian load of 3.15KN/m acts on inspection sidewalk, which is formed by wind noses. Wind speed of 40.8m/s and VI degrees intensity of earthquake are designed.

Cable of the Bridge will consist of parallel galvanized steel wires which diameter is 5.35mm each, tensile strength must be over 1600Mpa. Cable in main span will be 864mm in diameter and 1/10.5 of dip/span ratio. Hangers will be made of parallel galvannized steel wires too, arranged at intervals of 16m.

Steel box girder of main span is designed only 3m high, its section looks quite flat.,

however, enough safety of air dynamics will be secured. All surfaces of steel box girder are orthotropic. Top board is 12mm in thickness, web and bottom plate is 10mm. Asphalt concrete in thickness of 48mm will be surfacing of steel deck. These make steel deck lighter and lead decrement of the horizontal tensile force acting at anchoranges. Especially, northern anchorage founded on soil, the designer tries to decrease its burden. Southern tower foundation falls on sandstone layer inclined towards the river, 24 drilling piles diameter 3m each inserted into the rock will transfer force from tower to deeper stratum for security. Southern anchorage situates on the hill. Because of developed rock joint, a gravity reinforced concrete anchorage inlays into rock. Its inclined toothlike footing prevents from sliding and decreased the volume of concreting in construction.

In zone of northern tower and anchorage, thickness of overburden is 80m-120m. Soil there formed in latest period is in low solidity and saturated, as the depth increasing, it changes from loosen sand clay to powder sand then to medium and coarse sand with gravel. Limdstone layer appears deeper than 80m. Northern tower founded on 96 drilling piles, each one is 2m in diameter and longer than 85m. Before piling work commenced, a lot of tests concerning technology had been done. Thus insured the foundation construction successful.

Both northern and southern towers are hollowed double shaft with 3 prestressed concrete portal beams. Each tower finished in 7 monthes and concreted 19000m^3.

2.Construction of caisson foundation

Geological condition of northern anchorage is unfavourable. Rock layer embeds down to 100m from ground surface. The anchorage bears 550MN horizontal force. Final selection is a gravity anchorage with open caisson foundation to satisfy the requitement of stability and less deflecton. Layer of medium and coarse sand with gravel is chosen to be bearing stratum. Dimension of the reinforced concrete caisson is 69m $\times$ 51m, divided into 6 $\times$ 6=36 cells, sinking depth is 58m.

Simple to say,construction method of caisson is concreting the caisson into horizontal sigments and to sink one by one. Lower 30m of caisson was sunk in open air. Under ground water was pumped away through well pipes arranged arround the caisson, descending water table lower than the caisson bottom. Water guns and sand pumps were used to cut and transfer the soil out. When edged footig cut soil down to more than 30m, excavation proceeded under water, soil inside was taken out by air jets. As it fell down to the depth 1m higher than designed elevation, with help of air curtain surrounded outside walls, caisson set into its final position. The final deviation and inclination are much less than that required by Contract Technical Specification. In period of 20 monthes, there were 200 thousand m^3 of soil excavated out of northern anchorage foundation. Because the caisson does not set on rock, to restrict its horizontal and vertical deflection is significant. In consequent construction, surveying for caisson foundation must be continued. When superstructure is being erected, suitable adjustment has to be added to offset the deviation of anchorage foundation.

Ten Years' Maintenance of Seto Ohashi Bridges

Masahiko YASHUDA
Gen. Mgr, 2nd Maintenance Dept
Honshu-Shikoku Bridge Authority
Okayama, Japan

Masahiko Yasuda, born 1945, received his civil eng. degree from Kyoto Univ. in 1968 and PhD in 1994.

Motoi OKUDA
Civil Eng., 2nd Maintenance Dept
Honshu-Shikoku Bridge Authority
Okayama, Japan

Motoi Okuda, born 1953, received his civil eng. degree from Hokkaido Univ. in 1976.

Tsuyoshi MATSUMOTO
Civil Eng., 2nd Maintenance Dept
Honshu-Shikoku Bridge Authority
Okayama, Japan

Tsuyoshi Matsumoto, born 1954, received his civil eng. degree from Kyoto Univ. in 1978.

Summary

On April 10th, 1998, the Seto Ohashi Bridge celebrated its tenth anniversary since its opening. During these ten years, some problems which were due to the initial defects were found. In this paper, the inspection of these bridges is introduced first then some of these problems are reported. These are, the corrosion of main cables of suspension bridges, the damages of cables of cable-stayed bridges due to vibrations, the accident of an inclination of one link type expansion joint, the noise problem of same joints, the noise problem of rolling leaf expansion joints and the noise problem of end links of the Shimotsui-Seto Bridge.

1. Inspection

The inspection can roughly be divided into three types. They are the fundamental inspection, the emergency inspection and the close examination. Except for patrol inspections, bridges are closely eye-inspected and hand-inspected once a year utilizing inspection ways and inspection vehicles. This is the fundamental inspection. The emergency inspection is carried out after earthquakes, strong winds, or other abnormal conditions to confirm the bridge conditions. The vertical alignments of the bridges, the sags of the main cables of the suspension bridges, the inclination of towers, the tensile force of the cable-band bolts and so on are inspected one year and three years after the completion and once every three years afterwards. This is the close examination.

2. Findings of the inspection and their repairs

In 1992, main cables of the suspension bridges were inspected and some corrosions were found. Since then main cables were being treated to remove stains. Recently it is decided to protect main cables by blowing dry air into the main cables. At present, this work is in progress.

Two rows of vibration control ropes, which connect cables each other laterally, are installed on the cables of the cable-stayed bridges. In May 1994, it was found that one of these ropes had been cut due to the vibration. The broken ropes were exchanged immediately and all other vibration ropes were examined afterwards. Some ropes, which had larger damages, were exchanged.

The cables are fixed inside of the upper codes of the truss bridge deck. The angular bend buffers of cables are installed just above the upper codes. In June 1995, some damages of the buffers of the Hitsuishi-jima Bridge was found. The epoxy resin fillers were broken, the polyethylene tubes of the cables were broken and the polyurethane resin filler inside of the polyethylene tubes spilled out. Other buffers were examined afterwards and some damaged buffers were also found. These damages were caused by the

vibration of the two parallel cables due to the wake galloping. At present, the method of repair works of these damages are being considered.

The cable-stayed bridges and truss bridges of the Seto Ohashi Bridge employ the link expansion joints for the road way. These expansion joints had noise problems in 1988, when the bridge opened, so the noise reduction countermeasures were carried out but this could not be a fundamental solution. From 1993, the structure of fingers which consisted of many individual steel bars, which was the source of noise, has been changed to one structure. That is, all fingers are cast as one piece. Also the pin joints have been changed to the rubber joints. This improvement work continued until 1997, when all of the link expansion joints were exchanged to the new structure.

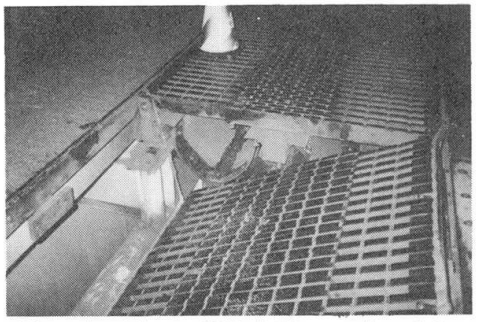

Fig.1 Accident of Link Expansion Joint

On May 3rd 1994, there was an accident that one of the link expansion joints of the Iwaguro-jima Bridge inclined and one car was damaged. This accident was due to the fact that the nuts of bolts of the universal joint which connected the expansion joint and the bridge deck loosened and fell. Consequently one end of the joint fell and the whole joint inclined. To prevent same accidents, expansion joint stoppers are installed and cotter pins are applied on all bolts which connect expansion joints and bridge decks. This improvement was finished in March 1995.

Three suspension bridges of the Seto Ohashi Bridge employ the rolling leaf expansion joints for the road way. These expansion joints also had noise problems after the opening of the Seto Ohashi Bridge. To suppress these noises, various countermeasures were adopted for these joints, until April 1989.

The ends of stiffening truss girders of the three suspension bridges of the Seto Ohashi Bridge are supported upward by end links vertically from beneath the girder. The maximum reaction force of the end link of the Shimotsui-Seto Bridge is 2558 ton, which is about twice larger than other two suspension bridges because this bridge has extended side spans which are not suspended from the main cables. From June 1993, these end links began to make large noises when heavier freight trains passed through the bridge. In January to February 1994, the noise source was closely investigated using the acoustic emission method. It was found that the noise source was the center of the semispherical boss of the lower pivot structure of the end links. The pivot structure consists of a semispherical boss which is embedded on a concrete abutment and a concave semispherical cover which is placed at the end of the link beam and over the boss. It was inferred that the movement of a pivot was not large enough to diffuse solid lubricant embedded in the concave cover, consequently a stick slip phenomenon of metal surfaces occurred and noises were emitted. To prevent this stick slip phenomenon, a hole was bored on a concave cover to reach the center of a boss and liquid lubricant was pressured into the surfaces. This countermeasure worked well and the noise problem was solved. All of the end links of the Shimotsui-Seto Bridge was repaired by this method until 1997.

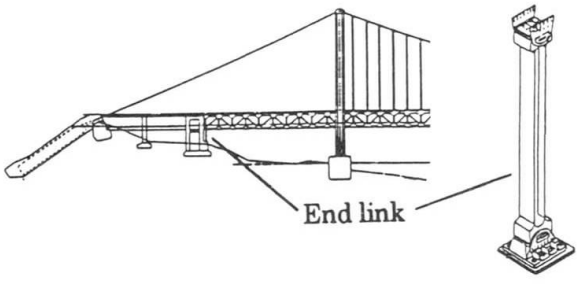

Fig.2 End link of the Shimotsui-Seto Bridge

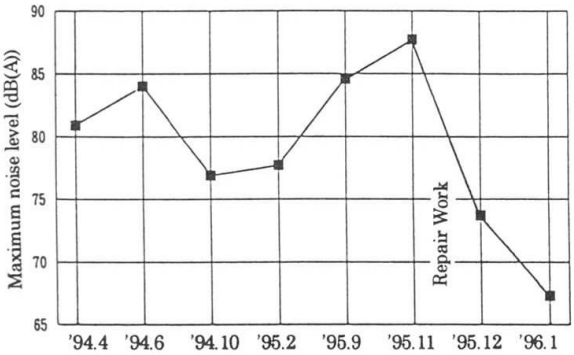

Fig.3 Noise reduction of end link

Erection of Long-Span Suspension Bridges by Direct Hoisting Method

Jun-ichi HIRAYAMA
Dir., Eng. Dept
Honshu-Shikoku Bridge Auth.
Kobe, Japan

Shinichiro ITO
Mgr, Eng. Section
Honshu-Shikoku Bridge Auth.
Imabari, Japan

Yoshihiro ASAKURA
Chief Research Eng.
Public Works Research Institute
Tsukuba, Japan

Summary

Direct hoisting method is necessary for erection of box type girders. But it is hard work at straits, because it receive heavy forces by tidal current and obstruct navigation. This paper presents the useful equipments for this method, that is, self-positioning barge and automatic coupling. They shorten the actual duration at hoisting work of the Kurushima bridges.

1. Development of Direct Hoisting Method

In consideration of safety and the influence on economic activities caused by tugboat fleets that obstruct navigation in the areas around erection sites, many truss type girders have been adopted in Japan. However box type girders have the advantage of low fabrication and erection costs. They have gradually gained favor because of this, and because their simple form eases maintenance. But, there has been only one erection method :lifting from directly to installation point. It is hoped that box type girders will be accepted for future long-span bridge construction due to lower costs and shorter construction periods.
The Kurushima Straits are narrow sea lanes with swift tidal currents. The Kurushima Bridges will be built there using box type stiffening girders. In the old direct hoisting method, a deck barge with a girder block was anchored against sea currents with cables. But, due to the prolonged construction period, the wide area of sea lane involved, and the number of accidents that have occurred in the past in the Kurushima Straits, the cable anchoring method will not be adopted. Instead HSBA has developed an erection method whereby the block is hoisted directly by a cargo deck barge which has Dynamic Positioning System (D.P.S.). In addition we also developed the equipment for joining the girder block's "Quick Joint", in a way that saves critical time (Fig. 1). By the developments the duration of hoisting work of Kurushima Bridges took only about 30 min. The duration of the barge positioning also took only about 10 min.

2. Carrying Cargo Deck with D.P.S.

The control method of a cargo deck barge with D.P.S. is to balance tidal forces, wave forces, and wind forces against the force of barge's four thrusters. The goal position of the barge is maintained by measuring and counteracting deviations with the D.P.S. This closed-loop control system minimizes deviation from the goal position by calculating both rotational drift and positional offset. The deviations is solved by calculating the real-time coordinates of the barge. The coordinates are calculated by measuring the distance between two fixed station on land and the traveling station on the barge ,that is, triangulation, and the direction of the barge by gyrocompass. Fixed station and traveling station search each other by its automatic pursuit device. Fixed station transmits distance data to traveling station by light waves.

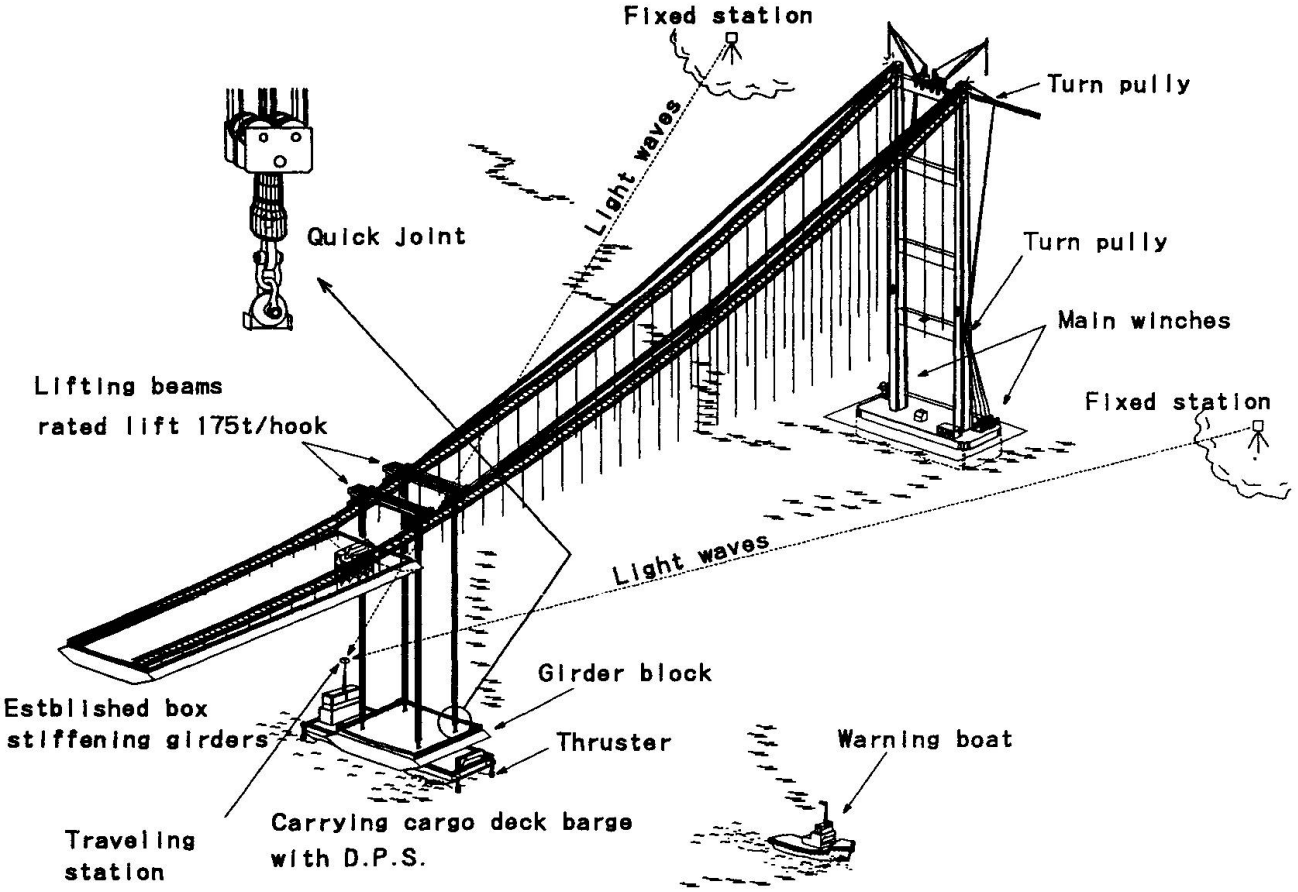

Fig. 1 Direct hoisting method of Kurushima Bridges

3. Quick Joint

Quick Joint is equipment of automatic coupling for hoisting a girder block. it is composed of a pencil plug and a socket. The tension winches on the lifting beams stand the plugs by pulling leading rope that installed on the point. The main winches of lifting beam lower the sockets and they are guided to the plugs by the leading rope (Fig. 2). The plugs push up the inside slide rings of the sockets . they finish pushing and the slide rings return by springs. As the result the plug and the socket is joined firmly by wedge effect.

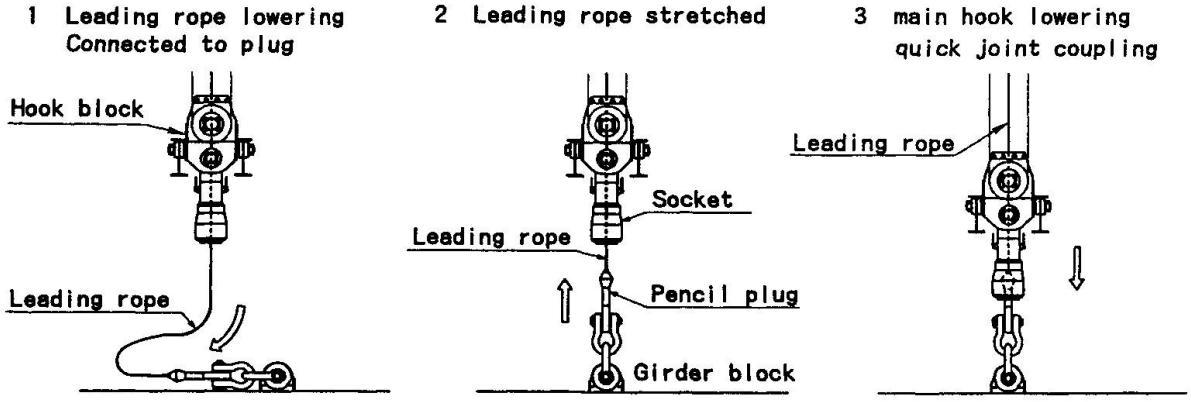

Fig. 2 Movement of joining Quick Joint

Anti-Washout Concrete and Highly Workable Concrete

Masahiro HAYASHI
Civil Eng., Third Design Div.
Honshu-Shikoku Bridge Authority
Kobe, Japan

Masahiro Hayashi was born in 1965. He graduated from Civil Eng. Dept of Osaka Univ. in 1990.

Toshimi MORITANI
Mgr, Third Design Div.
Honshu-Shikoku Bridge Authority
Kobe, Japan

Toshimi Moritani was born in 1950. He graduated from Civil Eng. Dept of Gifu Univ. in 1973.

Toshihiro KURIHARA
Dep. Mgr, Third Design Div.
Honshu-Shikoku Bridge Authority
Kobe, Japan

Toshihiro Kurihara was born in 1953. He graduated from Civil Eng. Dept of Oita National College of Technology in 1974.

Atsushi GOTO
Civil Eng., Third Design Div.
Honshu-Shikoku Bridge Authority
Kobe, Japan

Atsushi Goto was born in 1964. He graduated form Civil Eng Dept of Gifu National College of Technology in 1984.

Summary

The foundations of the Akashi Kaikyo Bridge are enormous concrete structures, and the natural conditions under which they had to be constructed were without precedent. A special anti-washout concrete and highly-workable concrete were developed and used, respectively, for the main tower foundations constructed in the Akashi Strait and the anchorages on either shore.

1. Development and Use of Anti-washout Concrete

The two main-tower foundations were constructed in currents of up to 4 m/sec. by the laying-down caisson method. Anti-washout concrete was cast into the caissons. This type of concrete was first introduced into Japan between 1975 and 1984, and is made by adding an underwater anti-washout admixture and a superplasticizer to ordinary concrete. This provides it with excellent anti-washout properties as well as self-leveling characteristics. With a total of 264,000 m^3 of concrete needing to be cast in 30 operations, or about 9,000 m^3 per casting, for the main-tower foundations (2P and 3P), it was necessary to develop a new method of casting such massive amounts of concrete at speeds far in excess of conventional capabilities. Regarding the quality of the concrete, the challenges faced were (i) to minimize strength loss while retaining an adequate anti-washout property and flowability for many hours even after flowing through a long placing system; (ii) to look into reducing cement content, using low-heat cement, and using a precooling facility to prevent thermal cracking; and (iii) to calculate the lateral pressure that would act on the steel caissons (which functioned as forms) and study methods of controlling the pressure. After overcoming these challenges, concrete casting for the 2P and 3P foundations was successfully completed in October and December, 1990, respectively.

2. Development and Use of Highly-Workable Concrete

The arrangement of steel reinforcement, structural steel, and anchor frames securing the main suspension bridge cables is extremely complex, and difficulties were anticipated in casting good-quality concrete into the two anchorages, 1A and 4A. To achieve adequate quality control in pouring large quantities of concrete into sections with dense arrangements of steel, the authority developed a highly-workable concrete using low-heat generating cement. This low-heat generating concrete is highly flowable and has desegregation and good filling properties.

There are various methods that can be used to make concrete more flowable. In this case, because a special plant was to be built for the purpose and as a result of economic considerations, it was decided to secure flowability and the desegregation property by adding an AE water reducing agent while at the same time replacing some of the aggregate with a fine limestone powder to increase the powder content.

The introduction of this highly-workable concrete made it possible to cast 140,000 m^3 of concrete into anchorage 1A (on the Kobe side) in just 18 months and 240,000 m^3 into anchorage 4A (on the Awaji side) in 31 months. Use of this concrete achieved a labor-saving of about 30-40% in the casting work. This effort demonstrates that highly-workable concrete using low-heat cement can effectively reduce construction periods, offer manpower savings, and ensure good quality.

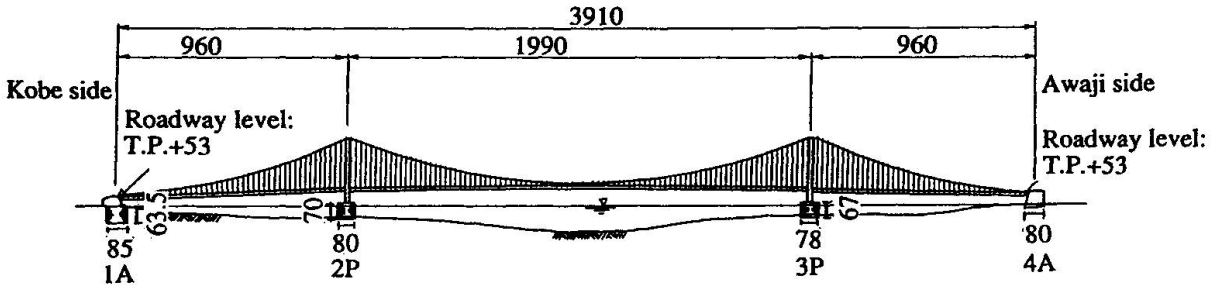

T.P.: Mean sea level of Tokyo Bay

Fig. 1 Elevation of Akashi Kaikyo Bridge

Table 1 Concrete volume (unit: m^3)

	1A	2P	3P	4A
Underwater anti-washout concrete	-	260,000	240,000	-
Highly-workable concrete	140,000	-	-	240,000
Others	380,000*1	90,000*2	80,000*2	-

*1 Concrete for RCC and earth-retaining wall

*2 Non-underwater concrete

Construction Work under Low-Frequency Horizontal Motions

Katsutoshi OHDO
Research Official
National Inst. of Industrial Safety
Tokyo, Japan

Katsutoshi Ohdo, born 1965, received his civil eng. degree from Nagoya Univ. in 1988. He is currently a research official at the National Institute of Industrial Safety.

Hisao NAGATA
Senior Research Official
National Inst. of Industrial Safety
Tokyo, Japan

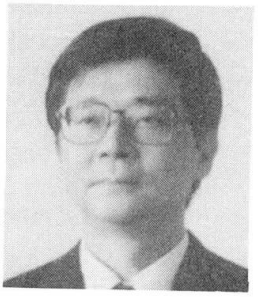

Hisao Nagata, born 1948, granted PhD from Yokohama National Univ. in 1992. He is currently a senior research official at the National Institute of Industrial Safety.

Summary

According to an investigation of construction sites in Japan, approximately 40% of construction workers on high-rise structures experienced excessive low-frequency horizontal vibration due to wind. In this study, critical limits of continuous tasks such as welding works and straight line drawings were experimentally investigated. From the results obtained, it was found that the critical acceleration for experimental tasks of straight line drawings and simulated tasks of welding works increased in proportion to frequency between 0.5 and 2.0 Hz. However, under the level of 0.5 Hz, inverse proportion was shown. The experimental results differ from the international standards of ISO 6897.

1. Introduction

In the construction of tall structures such as bridge pylons and buildings, weather has a strong influence on work efficiency and safety. The influence of weather on the construction of 14 tall bridge pylons and buildings sites in Japan was investigated by questionnaires to workers. One result from the questionnaires, shown in fig. 1, reveals about 40% of the workers experienced excessive low-frequency horizontal vibration during work, with bridge construction being especially demanding due to wind-induced sways. Bridge pylons under construction are likely to vibrate at wind speeds less than 10 m/s, which is a widely used criterion for suspension of construction work in Japan. In fact, on one construction site, the welding workers felt it difficult to work due to wind-induced sways. Even with these problems, no criteria or standards on limits of construction work under low-frequency horizontal motions have been made.

2. Methods

Critical task limits of construction work under horizontal motions were experimentally investigated by an original device which generates sway, vibration or linear acceleration, and is shown in fig. 2. Low-frequency sine-formed vibrations were given to each subject by the device, and the critical acceleration of straight line drawing tasks, simulated welding tasks or holding limits of human standing posture was investigated. A total of 15 young males, 15 females, and 5 welding workers participated in the series of experiments.

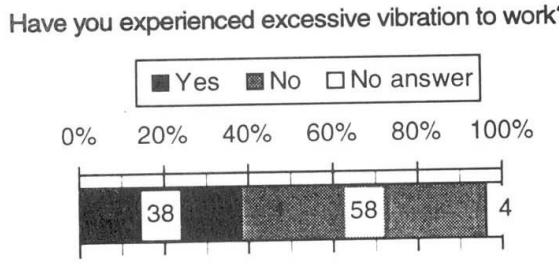

Fig. 1 : Result from questionnaires concerning vibration due to wind

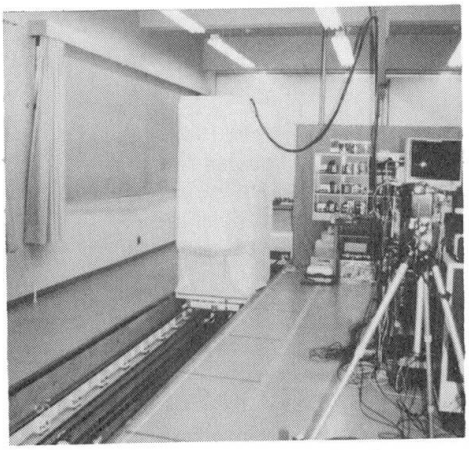

Fig. 2 : Experimental device which generates horizontal motions or vibrations

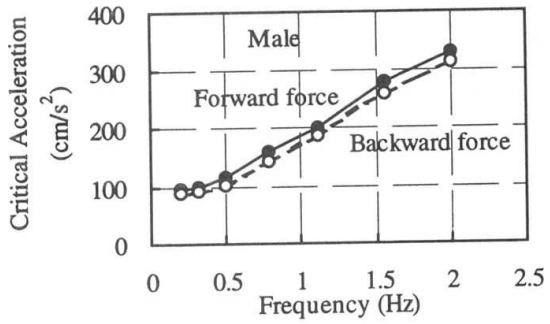

Fig. 3 : Limits for holding human standing posture for males

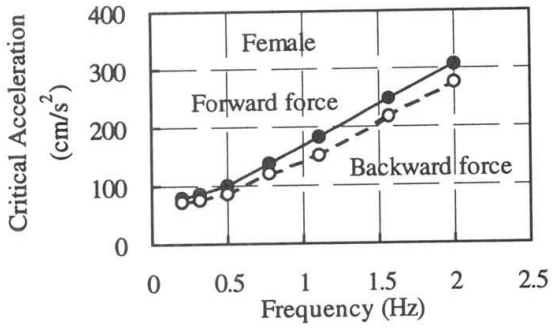

Fig. 4 : Limits for holding human standing posture for females

3. Results

3.1 Critical limits for holding human standing posture

Fig. 3 and fig. 4 show experimental results of critical acceleration for holding human standing posture. It was found that the values for male subjects were larger than the values for female subjects. Considering critical values for holding human standing posture, subjects were likely to lose balance under backward forces. The critical acceleration increased in proportion to frequency, which ranged from 0.5 to 2.0 Hz. However, under 0.5 Hz the critical values tended to keep constant.

3.2 Critical limits of welding tasks

Fig. 5 shows the critical acceleration of straight line drawing tasks performed by male subjects. Limits of welding tasks were verified by five welding workers, as shown in fig. 5. It was found that the relation between the values for straight line drawing tasks and for welding tasks showed similar tendencies and these values were at similar levels. Both critical accelerations increased in proportion to frequency between 0.5 and 2.0 Hz. However, they were in inverse proportion to the frequency under 0.5 Hz. These results show different tendencies from the international standards of ISO 6897 of the guidelines to evaluate the response of occupants of off-shore structures to low-frequency horizontal motion, as shown in fig. 5.

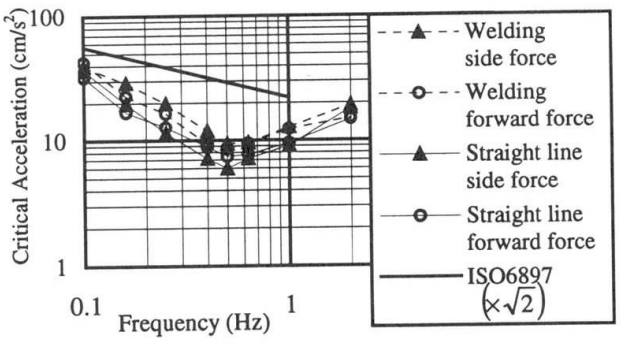

Fig. 5 : Limits of straight line drawing or welding tasks

Tsugaru Strait Bridge

Yukitake SHIOI
Prof.
Inst. of Technology
Hachinohe, Japan

Akira HASEGAWA
Prof.
Inst. of Technology
Hachinohe, Japan

Haruo YOSHIKOSHI
President
Tohoku Constr. Assoc.
Sendai, Japan

Hideo TAKAHASHI
Dir., Sendai Branch
CTI Eng. Co. Ltd
Sendai, Japan

Summary

The Tsugaru Strait Bridge is proposed over the Tsugaru Strait, with the distance of 19km and the greatest depth of 270m,between Honsyu and Hokkaido in Japan. The Bridge is planned with 1 continuous suspension bridge with 2 spans of 4,000m in the center, to secure the international navigation route, and 2 suspnsion bridges with 2,000m central span on both sides. To realize these bridges, a suspension system with a combination of 3 main cables and sub-cables, 2 separated steel decks, cable stayed prestressed concrete decks, jacket piers with inclined legs and joint anchorages between 2 suspension bridges are proposed. Through these measures, such benefits as reduction of cable tension, wind stability, possibility of re-erection, minimizing displacements of tower tops and decks for seismic force, reducing preparatory works, cancellation of tractions at the anchorages etc. can be obtained. The Tsugaru Strait Bridge shall be the new goal of bridge engineering in Japan, after the Akasi Strait Bridge.

1.Situation of the Bridge site

The 4 main islands in Japan are connected with some highway bridges except Hokkaido, where exists Seikan Railway Tunnel as shown in fig.1. Hokkaido with the population of 5.7 million and the area of 77 thousand km^2 desires to be linked to Honsyu with a highway bridge over the Tsugaru Strait for the development of industries by more reliable and free-moving transportation. The Strait has distances of 19 km and the greatest water depths of 140 m and 270 m along two favourable routes. The bridge is advantageous over the tunnel in points of ventilation, disaster prevention, preferable sight, maintainance costs, better trafficability, etc. However, very long spans are requested due to the international navigation course where many large-scaled vessels and submarines are passing. Furthermore the natural conditions of this region are severe with strong wind, great earthquakes, cold and snowy climat, etc.

2.Design of the Bridge

In order to solve these problems, we propose a combination of a continuous suspension bridge with 2 spans of 4.000 m in the center, and 2 suspension bridges in scale of Akasi Strait Bridge on both sides (see fig.2). This continuous suspension system has 3 main cables hanging 2 separated steel decks, cable stayed portions with concrete decks, ellipse steel-concrete tower columns in A shape, footings in shell structure, jacket foundations with inclined legs, shown in fig. 3-7, and joint anchorages. A sub-cable pulls the main cable at a midway point to the end of the cable stayed portion and has to be designed in state of no compression by live loads. In order to keep long life of this valuable Bridge, 3 cables and 2 decks system makes it possible to replace when the superstructure wears.

The near parts to the tower are precast concrete decks hanged by stayed cables and other parts are hexagon steel box girders with heating inside against freezing. The long span continuous steel girders are sustained on Warren trusses hanged from 3 main cables. The space between girders shall contribute stability against strong wind. The tower consists of steel structure at the upper part to decrease its weight and steel-concrete composit structure at the lower to endure very strong reaction. The pier and the footing are designed as shell structure of reinforeced concrete to keep rigidity and to reduce weight. The jacket acts as a working platform for piling and becomes a foundation together with piles inside of legs. The inclined legs give inverse rotation of footing to horizontal forces and cosequently the displacements of the tower top and the decks become small. The joint anchorage between the central and the side suspension bridges has the minimum dimensions required, by cancellation of each tension.

3.Computer analysis

The results from calculation for the structures in fig.2-7 show tension of 80 thousand tf in the main cable (200kgf/mm^2), tension of 20 thousand tf in the sub-cable, vertical force of 350 thousand tf at the

tower and so on. Based on these results, we get fig.8 which shows that the unit weight of the Bridge with the center span of 4.000 m is corresponding to the suspension bridge with 2.500 m and is 95% of total load. This proposal is one of many possible cases. We must make more case studies for each dimensions to save the construction cost and to improve the functions of the Bridge, when completed.

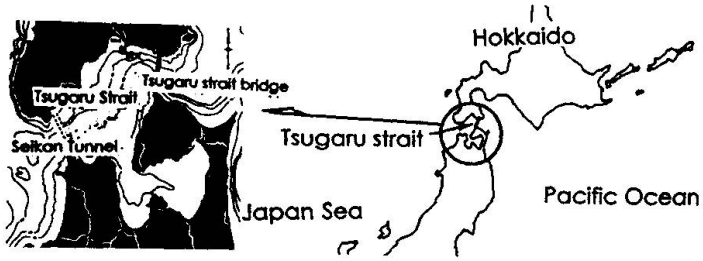

Fig.1 Location of the Tsugaru Strait Bridge

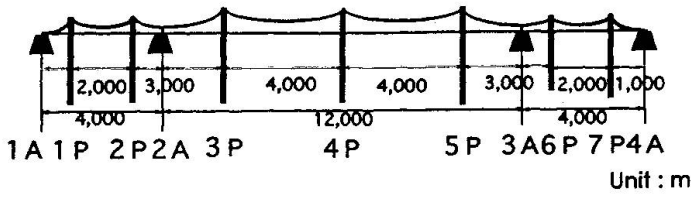

Fig.2 Skeleton of the Bridge

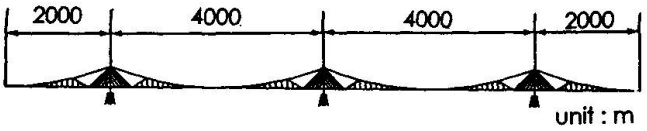

Fig.3 Tower & cables of continuous suspension bridge

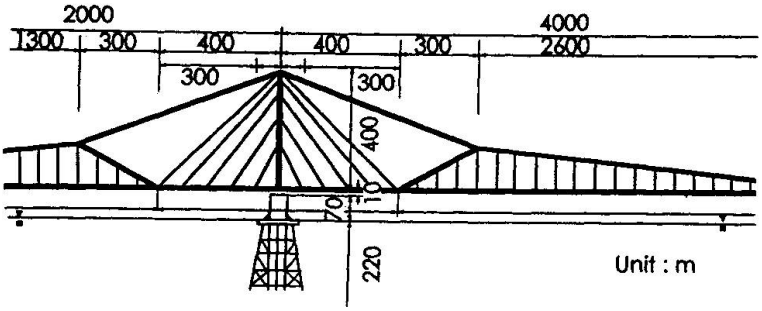

Fig 4 Detail of cables of cable-stayed & suspension portions

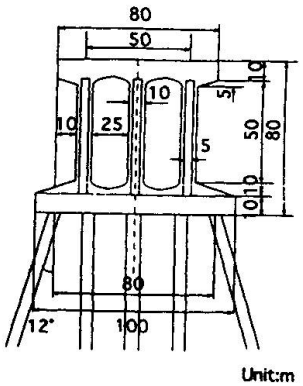

Fig.7 Pier & footing in shell structure

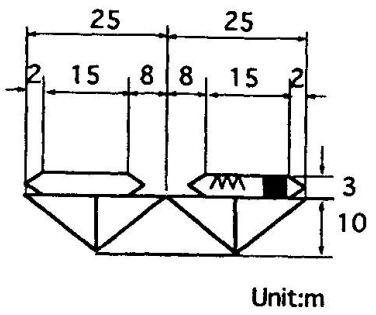

Fig.5 Warren truss & steel decks

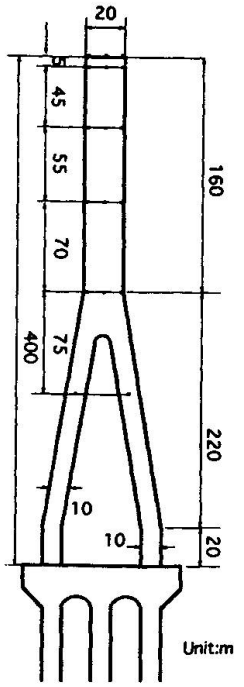

Fig.6 Main tower

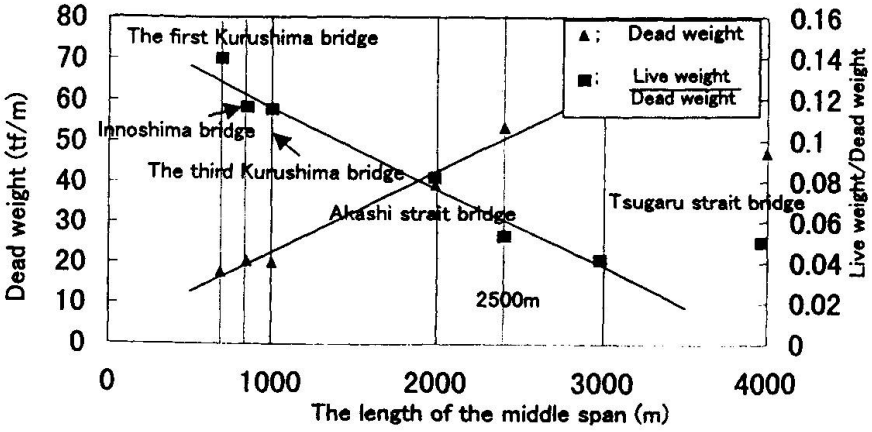

Fig.8 Relation between weights & central span length

New System for Aerodynamic Stability of Suspension Bridge

Toshihiro YOSHIMURA
Civil Eng.
Chodai Co. Ltd
Tsukuba, Japan

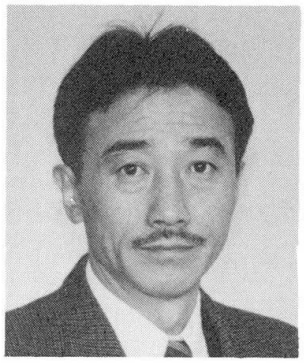

Toshihiro Yoshimura has experience in design and construction of major bridges at Honshu-Shikoku in Japan. He is currently a resident engineer for construction management of Yongjon Grand Bridge in Korea.

Summary

Aerodynamic stability is one of major issues to be considered in designing long span bridge with more than 3,000 meter of cable span length.

In this paper an attempt is made to discuss the use of cable formers for the system with four main cables, each of which is located at certain distance from others cables. The effectiveness of the new system for 3 span suspension bridge as well as 5 spans suspention bridge was examined by means of dynamic analysis.

It was found that the new system shall improve the torsional rigity of suspension bridge and also increase the frequency of the torsional vibration.

1. Concept of the New System

Strait-crossing bridges with more than 3,000 meter of span length are now being planned all over the world. Among them include Messina Crossing (Italy),Gibraltar Strait (Spain-Morocco) and Tugaru Strait (Japan). These longer span bridges, if implemented, will encounter the difficulty in maintaining the stability against drag forces.

The Key to solve this problem is to use main cables and let the torsional strength have an effect on the drag resistance, in order to improve the torsional rigidity of the suspension bridge. The feature of torsional vibration is explained by the forces which drag the right and left cables in the opposite direction. Therefore keeping the constant distance of cables was estimated to increase the frequency of torsional vibration (See Fig.1).

2. Result of the Vibration Analysis

In this paper cable formers were set up to keep the constant distance of cables and height of the cables. The initial finding is that cable formers were effective to increase the aerodynamic stability. After the vibration analysis, the effects of the new system are summarized as follows;

1) Installation of cable formers increased the freqency of torsional vibration(See Fig.2)
2) Difference of the height improved the efficiency
3) New system increased the torsional rigidy, up to the same level as that of the stiffenning girder(See Fig.3)

Applying the Selberg's equation, it was found that the critical wind velocity for flutter can be increased more than 20% by using this system, without increasing additional weights of stiffenning girder.

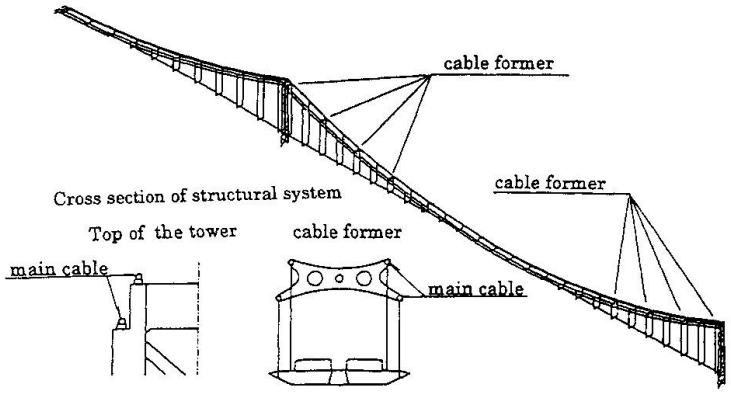

Fig.1 Illustration of the New System

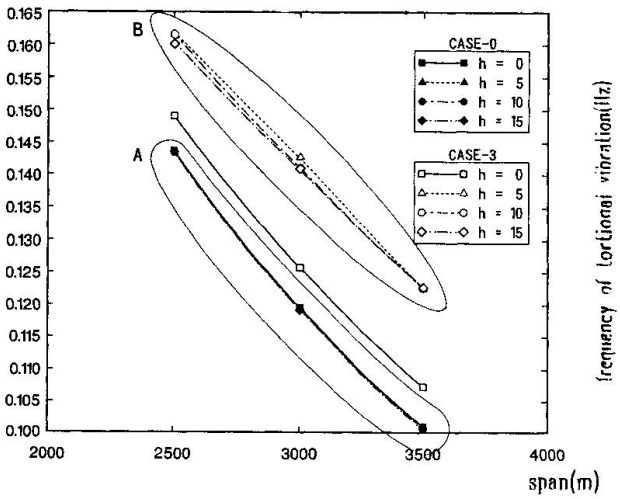

Fig.2 Influence of span-length on torsional vibration

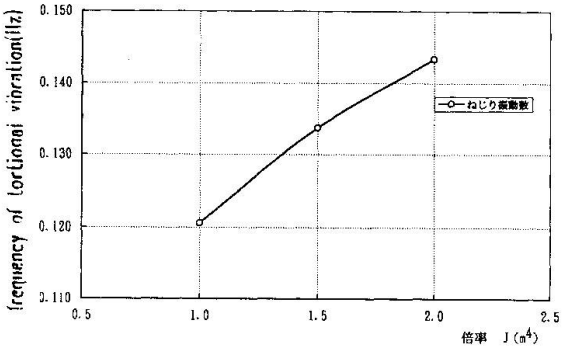

Fig.3 Magnification of tortional rigidy to stiffenning girder

Seismic and Safety Design Criteria for Expansion Joints

Christian FURRER
Civil Eng.
mageba sa, Huber + Suhner Group
Bülach, Switzerland

Christian Furrer is graduated Civil Eng. from the Swiss Federal Institute of Techn. in Zurich, Switzerland. He is in charge of S.E.Asian Business, as well as Research and Dev. at mageba sa.

Martin RENK
Civil Eng.
mageba sa, Huber + Suhner Group
Bülach, Switzerland

Martin Renk is a graduated Civil Eng. from the Swiss Federal Institute of Techn. in Zurich, Switzerland. He is head of the mabega sales dept and Member of CEN TC 167 Committee for Structural Bearings.

Summary

Bridge design has changed in the last years: Spans are becoming longer, loads are increasing and seismic design has become more and more important. This has an influence on the design and manufacturing of numerous parts of the bridge. Expansion joints and bearings are unique and require special solutions to fulfil the high demands and safety standards. The challenging design of these mechanisms requires advanced technology to take care of large movements in all directions, combined with high vertical and horizontal loads due to these increased dead loads, earthquake loads and accidental traffic loads e.g. braking ,skidding.

Seismic Design Criteria for Expansion Joints

Bridges are often the lifelines of infrastructure. If an earthquake causes major damage in cities or regions with such lifelines, it is important, that they stay intact. A key element of bridges are expansion joints. If an earthquake destroys or damages an expansion joint, the bridge can become impassable. Therefore expansion joints have to be designed earthquake resistant. Modern modular expansion as described below joints fulfil this requirement. They can adapt movements and rotations in all 3 directions and around all 3 axes. The lamella joints are built in modules, which are highly adaptable to the needs of the bridge designer. For large longitudinal movements the length of the joists and joistboxes can be designed accordingly. Joistboxes with a trapezoid shape can allow big transverse movements. Similar design is possible for big vertical movements. Such expansion joints have already been built with longitudinal movements of ±1000 mm and transverse movements of ±250 mm.

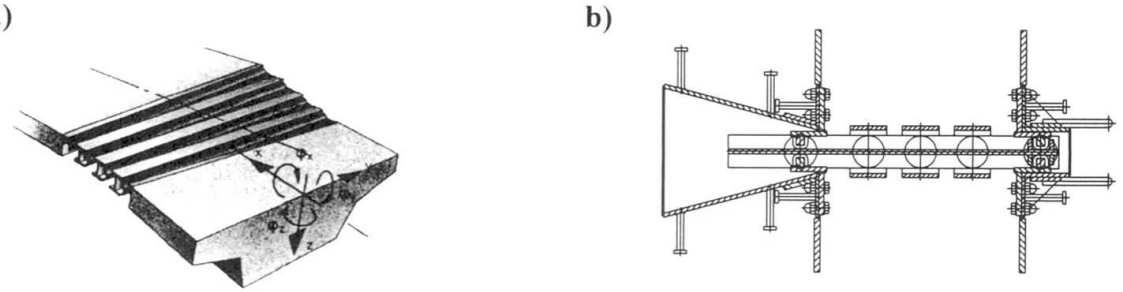

Fig. 1:Modern modular expansion joint
a) unrestrained movements and rotations in all 3 directions and around all 3 axes.
b) trapezoid shape of joist boxes for big transverse movements.

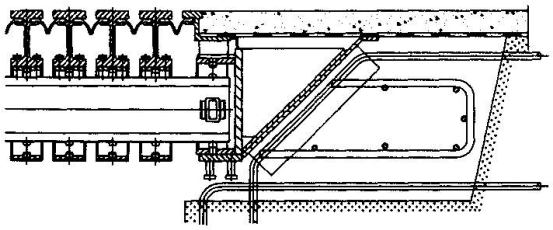

Expansion joints with fuse boxes prevent damage to the adjacent structures and are an economic solution, if small damage on joints are acceptable and if it is not a design requirement, that the joint is passable at any time after an earthquake.

Fig. 2: Fuse box of LR-Joint; Tagus Bridge.

With modern lamella joints it is possible to fulfil almost all technical needs and still find economic solutions. In order to obtain the most suitable solution, close contact between the bridge designer and the joint manufacturer at an early design stage is very important.

Safety Aspects of Expansion Joint Road Surface

Large modular expansion joints for extremely long span bridge structures require a special safety concept to ensure secure roll-over of all kind of traffic, while ensure safe transmission of braking force but preventing skidding of vehicles on the joint. The fully opened expansion joint at Tsing Ma Bridge or at Jangyin Yangtse River Bridge forms a 4.0m wide metallic structure (see Figure 3), consisting of about 50% gaps and 50% metallic lamellas.

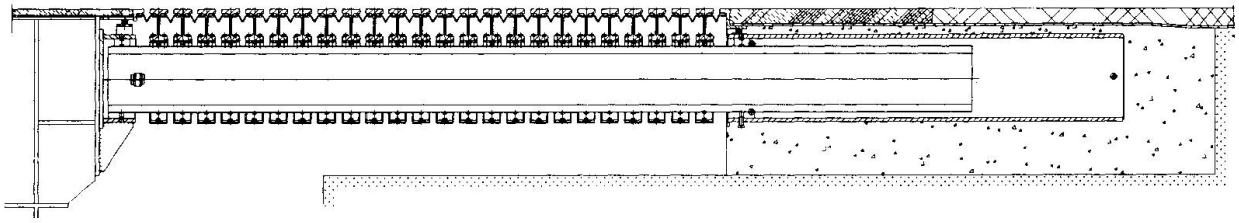

Fig.3: 25 gap modular expansion joint for Tsing Ma Bridge at Honk Kong; length up to 4 m.

While smaller expansion joints require only coating for corrosion protection very large modular expansion joints require special treatment of the metallic lamella surfaces. A friction coefficient of μ =0,5 must be assured for a service lifetime under all weather conditions, and neither pollution nor excessive radiation from sunlight should reduce the long-term quality of the special anti-skidding coating. The coating is a special surface treatment, proven and robust enough to guarantee minimal friction coefficient μ =0,5 for service lifetime under the most adverse traffic and weather conditions.
The horizontal load transmission system for braking forces, introduced by the traffic, has to be investigated and specially designed for large modular expansion joints. As well as other gap control and steering systems, the flexible controlling device has a reinforced water tight sealing strip as a special gap limiting feature. The horizontal braking forces are transferred and damped by the combined action of the sealing strip and the elastic steering system to the edge profiles. The new sealing strip was developed and tested at various occasions and has proven its key role in the safety concept and the design of the joint. The reinforced water sealing strip profile is strong enough to tie back the horizontal forces into the adjacent structures.
Special anti-skidding coating of the road surface of the modular expansion joint combined with the comprehensive horizontal load transmitting and gap limiting system can assure safe driving on very large expansion joints at any time.

Super Long-Span Bridge with 2-Box and 1-Box Combined Girder

Kazushi OGAWA
Senior Mgr, Bridge Eng. Dept
Kawasaki Heavy Ind. Ltd
Akashi, Hyogo, Japan

Hideki SHIMODOI
Mgr, Bridge Eng. Dept
Kawasaki Heavy Ind. Ltd
Akashi, Hyogo, Japan

Chiaki NOGAMI
Eng., Bridge Eng. Dept
Kawasaki Heavy Ind. Ltd
Akashi, Hyogo, Japan

Summary

In the super-long span suspension bridge, it becomes serious how to make the bridge aerodynamically stable in economical ways. This paper investigates application of the 2-box and 1-box combined girder to the super-long span suspension bridge, in which the 1-box girder is used at the tower part and the 2-box girder at the other part. The 2-box girder opened between boxes improves aerodynamic stability and the 1-box girder prevents the deck width from increasing the space of pylon. In the study the newly developed suspension bridge with the 2-box and 1-box combined girder shows better aerodynamic characteristics on flutter than the usual suspension bridge with the 1-box girder.

1. Description of super-long span bridge with 2-box/1-box combined girder

A conceptual view of the newly developed suspension bridge having a main span of 2,500m is shown in Fig.1. Areas of the 1-box girder and the 2-box girder are indicated in Fig.2. Cross sections of 1-box girder and 2-box girder are shown in Fig.3. The space between cables is 7m, adjusted to the open width of the 2-box girder. Hangers suspend the 1-box girder obliquely and the 2-box girder vertically. The total mass of the girder and cables in the 2-box/1-box combined girder is 37.9t/m, which is only 1.1 times heavier than that in the 1-box girder. According to the dynamic analyses of the super-long span bridge with the three dimensional finite element method, the 17th mode corresponds to the 1st torsional vibration, in which torsional displacement prevails. The 1st torsional frequency is 0.155Hz.

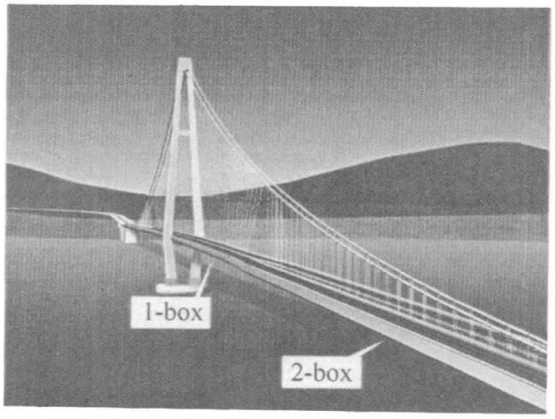

Fig. 1 Image of super-long span bridge

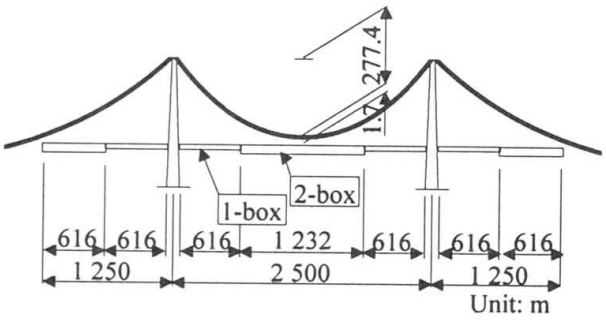

Fig. 2 Areas of 2-box girder and 1-box girder

2. Aerodynamic characteristics of super-long span bridges

Distortion of the super-long span suspension bridge in wind was analyzed with the large deformation finite element method. Fig.4 shows torsional displacement of the girder at the center of the main span due to wind forces. In the original 2-box and 1-box combined girder, unbearable large torsional displacement is induced in the high wind velocity of over 70m/s. Using the modified section in the 2-box girder to abbreviate pitching moment of the steady aerodynamic force on the girder, torsional displacement can be decreased less than that of the suspension bridge with the 1-box girder only.

The flutter phenomena on the bridge were analyzed with the multi-mode flutter analyses, considering the first 30 modes. The aerodynamic forces on the girder were induced from the wind tunnel test with the two dimensional deck model. Fig.5 shows results of flutter analyses on the super-long span suspension bridge at the wind attack angle of 0°. The flutter velocity in the 2-box/1-box combined girder, 67m/s, is higher than that in the 1-box girder, 50m/s. Applying the modified section to the 2-box girder, it can be improved to 80m/s. If torsional displacement of the girder due to wind is considered in the flutter analyses, the flutter velocity can be estimated at 90m/s. Thus combination of the 2-box girder and 1-box girder can improve flutter stability of the super-long span suspension bridge notably.

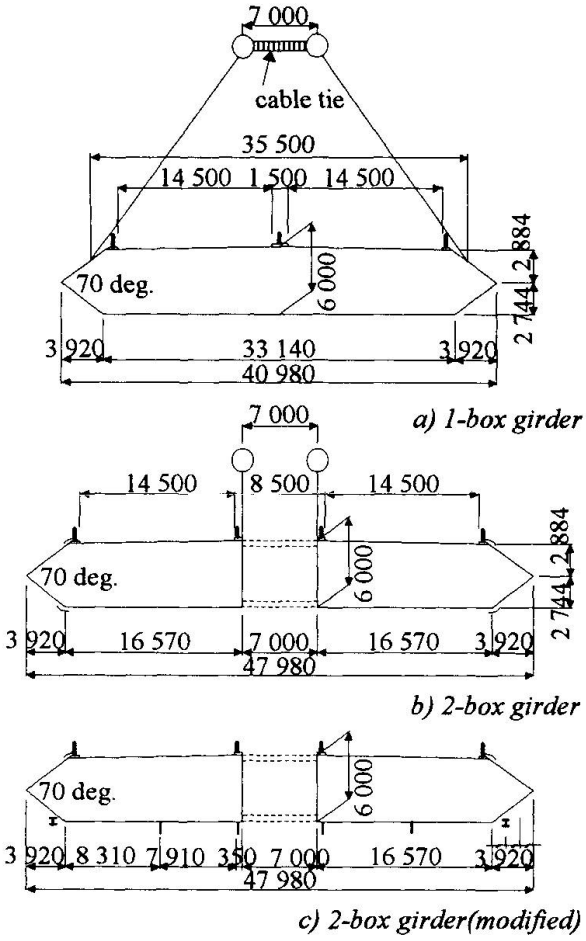

Fig. 3 Stiffening girder section

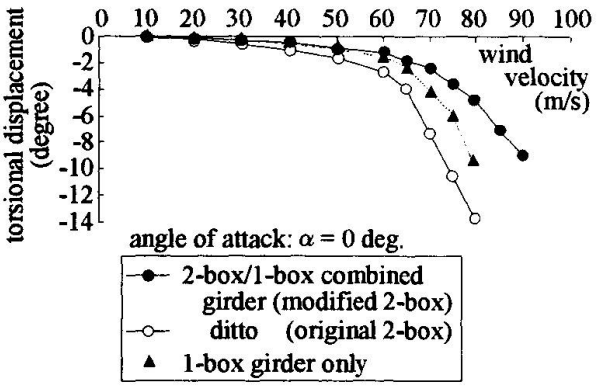

Fig. 4 Torsional displacement of girder due to wind forces

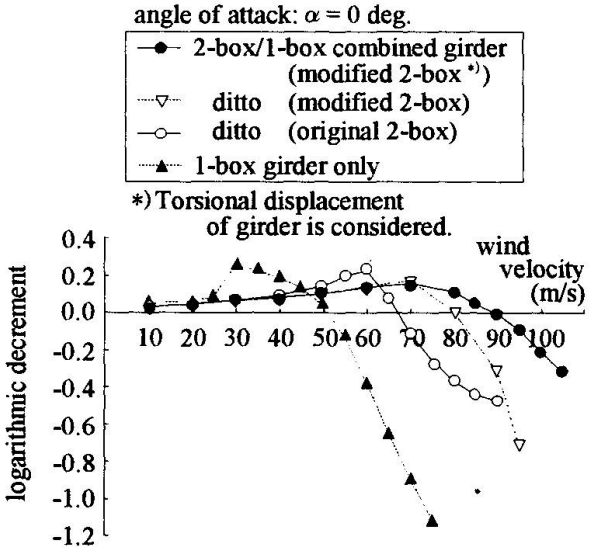

Fig. 5 Flutter response of super-long span bridges

Planning and Construction of the First Cable-Stayed Bridge in Indonesia

Honorius RACHMANTIO
President Dir.
PT Karya Titan - PT Profes CWT
Jakarta, Indonesia

Honorius Rahmantion, born in 1937, received his eng. degree in Metallurgy from the Techn. Univ. in Aachen, Germany and his Doctor's degree from Berlin Techn. Univ. Currently he is President Director of PT. Karya Titan, a General Eng. Contractor and PT. Profes Cipta Wahana Teknik dealing in Constr. Management.

Summary

The first long span bridge in Indonesia was built, three decades ago, crossing the broad Musi River in Sumatra. Recently, another two new bridges have been constructed and open to traffic. These include the 918m long multi-span steel suspension bridge over the Barito River in Kalimantan, and the 642m long cable stayed bridge , linking two islands in the Batam area.

This paper will examine the planning for, and the construction methods used in the construction of Indonesia's first cable stayed bridge, the Batam-Tonton Bridge.

Special attention will be given to the Construction Engineering developed for the erection of the cable stay superstructure, and the design of the pylon foundations.

1. Planning for Construction

Unlike most other bridge construction, cable stayed bridges require intensive input before and during the construction phase. Critical at each stage is the control of the deck alignment and stress state within the deck and stay cables. A critical issue was the understanding of how the partially completed structure would behave at any time during the construction.

Prior to construction, the Client and Construction Management (PT Profes) recognized this fact, making the Contractor responsible for the determination and monitoring of forces and deflections in the permanent structure, and for it's intermediate static and dynamic stability during construction.

This was provided in the form of a "Construction Engineering Package" , which includes a detailed deck construction sequence, together with a step-by-step confirmation of the strength and serviceability of the structure for wind and gravity loads, as well as the effects of creep, shrinkage and temperature at each construction stage.

Monitoring of this construction engineering during construction, was then carried out on site by the Contractor and Construction Management.

2. Construction

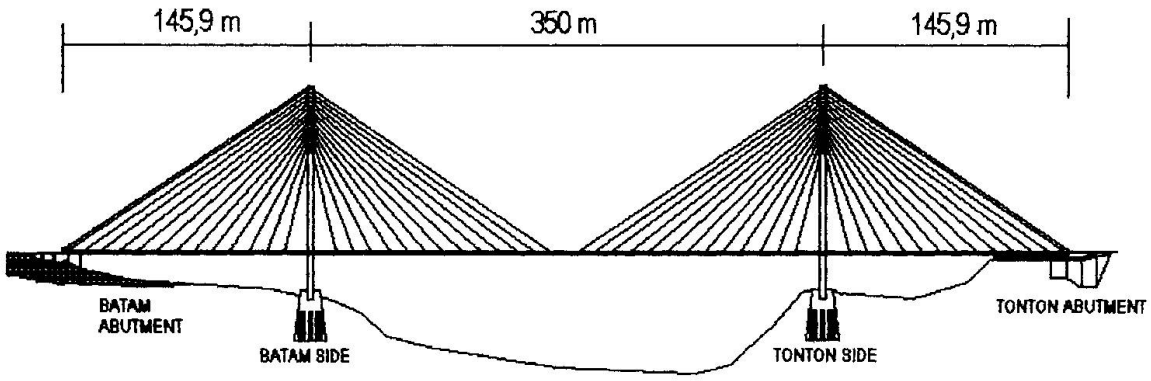

2.1 Pylon Foundation

The foundation was based on two pile groups, each consisting of 30 bored piles, 1.5m in diameter, with average depths of 38 m to 40 m. Contract Level was determined based on rock sockets, with minimum lengths of 2.2 m, and end-bearing capacities of 2 MPa. In addition, static load tests were carried out on two piles, to confirm the load carrying capacity (1,100 tones per pile) of the as-build piles.

2.1 Pylon

The pylon was constructed two parts - the pylon legs and the pylon head. 45 MPa strength concrete was used for the pylon legs, and 50 MPa for the pylon head. The legs of the pylon, which are hollow in section and inclined at 82 3' 44", were constructed in 4m high sections, using a pair of jump forms. The cycle time for the first section was 19 days, which was reduced to an average of 6 days for the last 18 sections. At the head of the pylon, the two jump forms were joined together, and jumped vertically as a single unit.

2.2 Deck

Each deck segment is 21.5m wide, 12.0m in length, weighs approx. 500 tones and is supported by one cable in each edge beam. The construction was based on the cantilever method starting from each pylon. The side span segments were constructed on Kingshore scaffolding, and the main span segments with a 310 ton steel form traveler. Initially, the Pier Table (28.4m of deck immediately below the pylon head), was constructed on Kingshore scaffolding. The first two side span segments were then constructed, and the steel form traveler installed on the main span side of the Pier Table. The typical deck segment erection cycle then commenced, with pouring of the side span segment, pouring of the main span segment, Installation and stressing of the stay cable and launching of the traveler.

The first cycle was completed in 26 days, which was reduced to 13 days in a relatively short time. This excellent production rate was due mainly to the efficient field coordination of the organizing team, and the quick and effective adaptation of all workforce on site.

On completion of the side span segments, the 4 out-of-balance, main span segments were construction, and balanced by the backstay cables. The 2 form travelers will then approach each other at the middle of the main span, to execute the closure procedure.

Cable-Stayed Bridge with a Single Pylon in the Czech Republic

Milan KOMINEK
Civil Eng.
CityPlan Ltd
Prague, Czech Republic

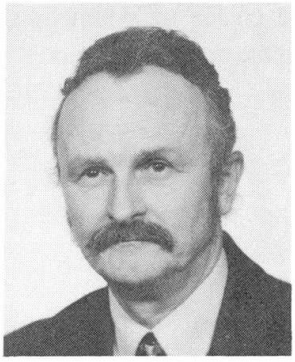

Milan Kominek, born in 1947, received his civil eng. degree from the Czech Techn. Univ. in Pragues in 1970. He is currently the head of the bridge and transportation dept. of CityPlan Ltd.

Summary

Ústí nad Labem is a city with 100.000 residents. It is located about 100 km north of Prague, the capital of the Czech Republic. The Labe (Elbe) is the largest river in the country and separates the city into two parts. The only road bridge is an old arch bridge in poor condition. It was the only bridge for 30 km around Ústí across the Labe. Any disruption of the bridge's function could lead to a state of emergency in the whole region. Since this situation was no longer acceptable, in 1993 city officials decided to build a new bridge. The Czech Commercial Bank provided a financing scheme that made the City of Ústí nad Labem the first large-scale municipal infrastructure investor in the Czech Republic after WWII. The City Council and the Department of Urban Development made a conscious choice in favour of a dominant shape and made the necessary funds available. The new bridge will be completed and ready to use in June of 1998.

1. Philosophy of the Solution

One of the most important aspects for city representatives when they began to consider the construction of a new bridge was its aesthetic impact. The only possible location for the new bridge was right up against the Marian Rock, which with its huge mass led to the idea of the maximum lightening of the bridge and the ramps below the Marian Rock and to the relocation of all structurally necessary masses on the opposite river bank. This decision was further supported by the terrain configuration, the shallowness of the river bed and geological formations at the Strekov side of the river, which was ideal for the pylon location. Together with the complicated traffic situation on the right (Strekov) side, the above conditions led the authors of the project, Milan Komínek and Roman Koucký, to the idea of shaping the bridge as an asymmetrical suspended construction without counter suspension in the shortened back span and with the system of the couple of suspension planes in the main span. The idea of the back span without suspensions had an impact on the pylon's design, because it was obvious that the pylon's shape must logically follow the course of internal forces, to take over bending stress and to eliminate the negative reaction in the end support as much as possible. The concept that was followed from the beginning was the idea of the shortened back span where the pylon is a part of this bridge as the stabilizing part of the structure and from which the curve of the main suspended span originated and spanned the river. This fixed part of the bridge was considered from the beginning an important condition for the method of construction to serve after its erection as the base from which the remaining superstructure of the main span would be constructed because the only available space for the building yards was on the right (Strekov) bank.

The new cable-stayed bridge has a single inclined pylon with two planes of 15 cables in a modified harp arrangement supporting the suspended deck, with a main span of 123,3 m, with no back stay.

2. Technical Solution and Construction

The shape of the pylon is designed to transfer the load of the main suspended span by its flexural rigidity with the help of the parapet beams of the back span into which the system of the perpendicular girders is fixed. In the cross-section, the use of the pylon led to the choice of symmetrical twins of the vertical masses, converging due to the anchoring of the suspenders in the upper part of the structure.

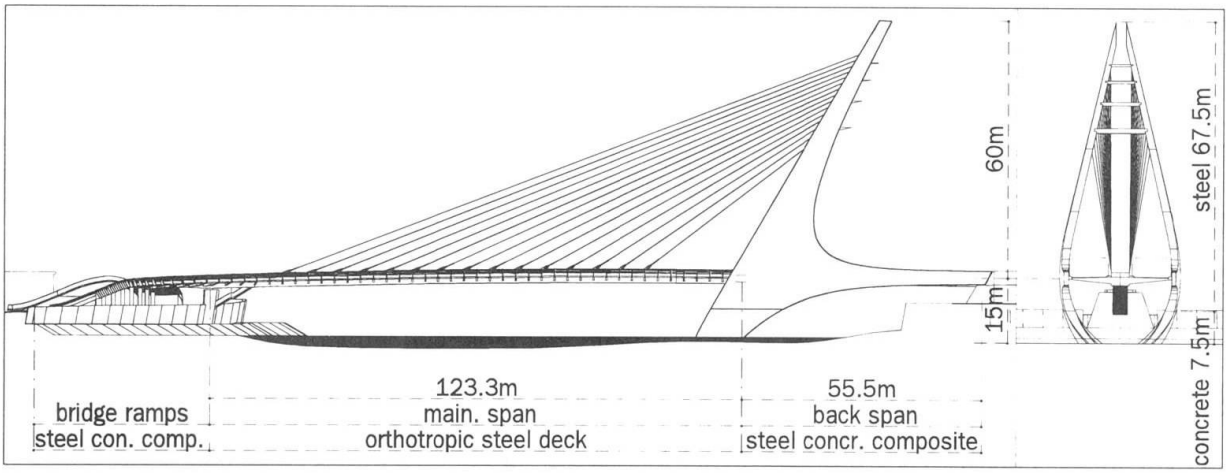

Fig. 1 Longitudinal view and cross-view-section

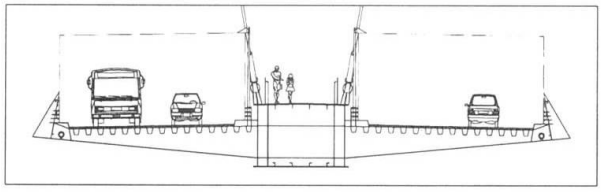

Fig. 2 Main span cross section

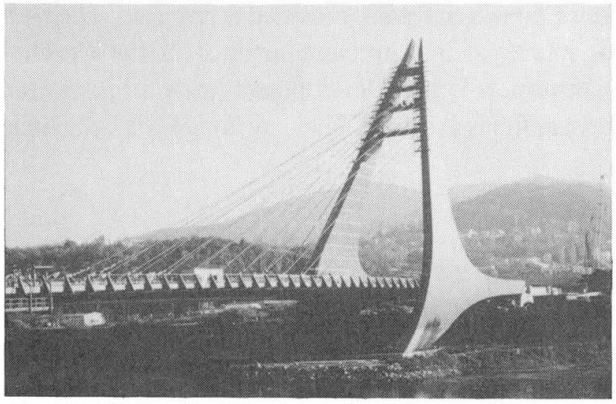

Fig. 3 Overall view from the Marian Rock

Fig. 4 Overall view toward the Marian Rock

This upper part is also reinforced by cross beams in the shape of wings. Both walls of the pylon further envelop the horizontal load-bearing structure with additional cross-reinforcement at the level of the bridge deck and both walls converge again below the deck and are anchored into the foundation.

The horizontal load-bearing structure of the main span was designed as a very light one-chambered beam with a height of 3,0 m and a width of 4,2 m, with the 10,95 m consoles in the lower part that is carrying the 4-lane roadway. The upper part of the main girder (in the middle section of the cross-section) is designed to carry pedestrian and bicycle traffic. This design used to its advantage the necessary structural height of the main beam and at the same time used the space between the suspenders (4,2 m pitch). The suspender pitch is for static purposes designed to solve the construction stress in the cross direction including torsion. The concept and design of the bridge is the result of the very intensive cooperation between the bridge engineer Milan Komínek, the architect Roman Koucký, and traffic engineer Jiří Landa. The construction drawings are the teamwork of the above mentioned engineers, as well as others. The whole project was made possible by the sustained effort of the city officials to provide their city with the infrastructure for the world of the 21 st century.

Cable Mounted Bridges: a New Approach in Construction of Long Bridges

Mansour ZIYAEIFAR
Post doctoral fellow
Chiba Univ.
Chiba, Japan

Hiroshi NOGUCHI
Prof.
Chiba Univ.
Chiba, Japan

Peter NDORU LOMODI
Ph.D. Student
Chiba Univ.
Chiba, Japan

Summary

Design and construction of bridges across deep valleys have always been a challenge for engineers. Construction process of these structures usually requires interference and access to the valley, incurring large cost and causing potential damage to the environmentally delicate regions. In this paper a technique is proposed to keep the valley's underneath unobstructed and to reduce the cost of the bridge. In this method, each prefabricated longitudinal segment of the bridge would be consecutively mounted on a system of cable-set across the valley and it will be placed on its final position by a wrench mechanism. Construction cables in this approach are arranged to be used later as the main pre-stressing tendons for the bridge. The cost of the structure in this method is reduced not only because of the cost effective constructional procedure but due to the effective use of structural materials in the bridge system.

1. Main concept

In cable mounted bridges, a system of cables across the valley is used to support the construction process from the above. This cable-set is mainly composed of two or more horizontal (or inclined) parallel cables, stretched from one side of the valley to the other. The deck of the bridge consists of longitudinal prefabricated segments. Each of these them, mounted on a special cart, will be pulled along the cable-set by a simple wrench mechanism located on the opposite side of the valley. When all segments are in their final position, the anchorage of supporting cables from the valley will be transferred to the deck of the bridge and pre-stresses all the segments together. In the construction procedure there could be some other supporting cables to stabilize the process of construction but they are considered as temporary and minor components of the system. Fig.1 illustrates the process of construction while Fig.2 shows a panoramic view of a completed bridge.

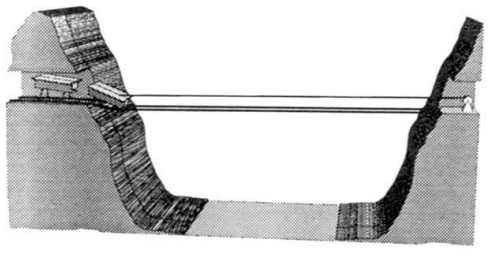

Fig. 1 - Construction process

2. Construction procedure

Construction begins by installing a set of tightly stretched cables across the valley. The tilt and height of every pre-fabricated longitudinal segment of the bridge must be set accordingly (based on a preliminary calculation regarding the final position of each segment and deformation of cable-set at that position). When the last segment of the bridge enters onto the cable system, all the segments are positioned consecutively with a small apparent misalignment with respect to each other. In order to construct the deck of the bridge, an accurate alignment of all the bridge's segments in a horizontal line is required. Since pre-

setting of tilt and height of the carts can not guarantee an accurate alignment between bridge's segments, the adjustment mechanism implemented in each cart system must be used to reposition each segment and to reach to a precise alignment between all segments of the bridge. Figure 3. Shows one example of an adjustable cart. In such a simple mechanism, a person walking on top of the deck will be able to easily adjust the height and tilt of each segment of the bridge.

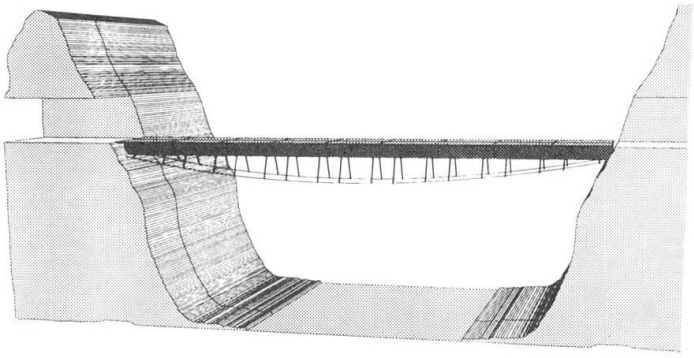

Fig. 2 - An artistic view of a completed bridge.

To establish connectivity between all segments of the deck system a few pre-stressing tendons is required. These tendons passes through all segments of the bridge and provides a small pre-stressing force on the deck and connects all the segments together. At this phase, if by a sophisticated mechanism and/or procedure, the anchorage of cables to the valley transfers to the deck of the bridge, there would be a large axial force on the deck which effectively pre-stresses all the segments together. Having a large axial force on the bridge provides enough bending moment capacity to the deck to resist the effects of live loads. The bridge system at this point is considered as a classic example of a post-tensioned bridges.

3. Advantages

In this approach there is no need for heavy equipment in the construction process. The construction procedure is also faster than other techniques because of the use of prefabricated segments and the routine process of installation of each segment on the cable-set. Another important feature in this approach is the fact that, most of the construction components of the bridge system can be used as permanent parts of the bridge. The cable-set will be used directly as the main post tensioning tendons for the bridge and components of the cart system can be used as permanent parts of the bridge system. This technique can also be applied to multi-span bridges without any major modifications.

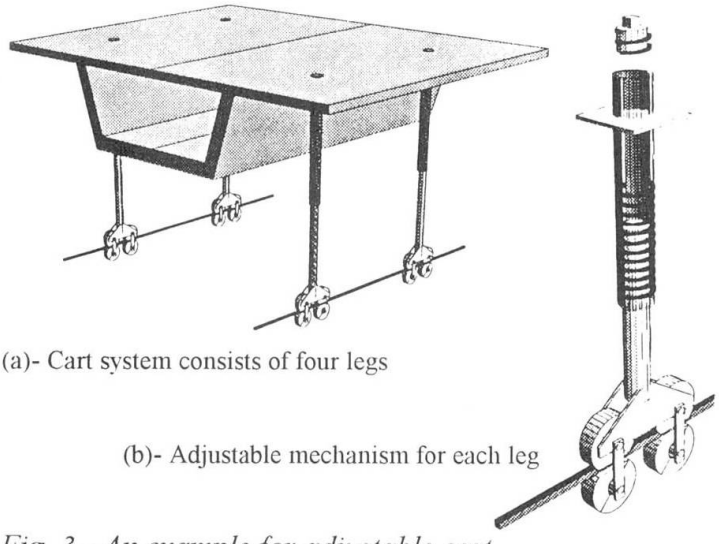

(a)- Cart system consists of four legs

(b)- Adjustable mechanism for each leg

Fig. 3 - An example for adjustable cart

Cable mounted approach although is considered predominately as a cost saving construction method, but it also offers some structural benefits. In this approach there will not be any dead load bending moment in the deck of the bridge and all the dead loads in the system is carried by tension in cable-set and compression on the deck of the bridge (i.e., in the most efficient way, truss action).

3. Technical notes

In the process of construction any unbalanced load in the cable set (also on the deck of the bridge) may cause unprecedented forces, not sustainable by the bridge system. Therefore tensile force in the cable system must be carefully monitored and continually adjusted during the construction procedure. The anchorage of cable-set to the valley during construction is another major concern in this technique. It is obvious that the magnitude of tensile force in cables is enormous and transferring this force to the valley needs careful preperation.

Static Issues in Long-Span Suspension Bridge Design

Giulio NICOLOSI
Prof.
Univ. Federico II
Napoli, Italy

Aldo RAITHEL
Prof.
Univ. Federico II
Napoli, Italy

Paolo CLEMENTE
Research Structural Eng.
ENEA - C.R. Casaccia
Roma, Italy

Summary

A terrific increase of the maximum span length of a suspension bridge has occurred in the last years. First the 1624 *m* Great Belt East Bridge in Denmark, and then the 2000 *m* Akashi Kaikyo Bridge in Japan, were completed. A 3300 *m* span has been proposed to cross the Messina Strait. The feasibility of longer spans is related to the implementation of new high-strength light-weight materials. As a matter of fact, as spans become longer, cables become heavier. Therefore a high percentage of the cable stress is related to its own self-weight. Furthermore the stiffening contribution of the deck on the structural behaviour becomes negligible. In this paper the main aspects of the very long-span suspension bridge behaviour under static loads are discussed.

1. Analysis of the Structural Behaviour

The terrific increase of the bridge span requires the basic concepts of the structural behaviour to be revised, also under static loads. The preliminary design can be carried out by referring to the unstiffened cable, ignoring the contribution of the girder stiffness. Suppose that the geometrical shape is fixed and so is the parameter $k = f/\ell * cos\alpha_m$, f being the height, ℓ the span and α_m the maximum value of the slope angle α, with respect to the horizontal. The self-weight of the cable can be supposed to be uniformly distributed and equal to $w_c = \gamma_c * A_c * L_c/\ell = \gamma * A_c$, A_c being the cable cross-sectional area, γ_c the cable weight per unit volume and L_c the cable length. The structure is also subject to a uniform permanent load w_p. So the total dead load is:

$$w = w_p + \gamma A_c$$

As usual, two kinds of travelling loads are considered: a slight vehicular load p_1 uniformly distributed on the main span and a uniform railway load p_2 coming to the main span, whose maximum length is $c_2\ell$ ($c_2<1$). The maximum value H_{max} of the horizontal component of the cable tension occurs when p_2 is placed symmetrically around mid-span. With reference to this load condition, by equalling the maximum stress in the cable with the allowable one, the limit value of the span, i.e. the span at which the cable will just support itself, can be deduced

$$\ell_{lim} = 8k \cdot (\sigma/\gamma)/(1+\beta)$$

where $\beta=[w_p+p_1+p_2*(1-(1-c_2)^2)]/\gamma A_c$ is the ratio between the permanent-plus-live load and the self-weight of the cable. The limit span increases linearly with σ/γ and with k, while the influence of β is more significant. In Fig. 1 the diagram of ℓ_{lim} versus σ/γ is plotted for different values of β and k=1. For a fixed ℓ, the previous equation allow to find out the cross sectional area A_c of the cable

$$A_c = \left(w_p + p_1 + p_2\left(1-\left(1-c_2\right)^2\right)\right) \Big/ \left(8k\,\sigma/\ell - \gamma\right)$$

and therefore it is very useful in the preliminary design.
A numerical investigation was carried out. The main span was supposed to be simply supported at the pylons. The following realistic values of the loads were assumed: $w_p = 250$ *kN/m*, $p_1 = 20$ *kN/m*, $p_2 = 300$ *kN/m* with $c_2 = 750$ *m*. The cable material was characterised by the allowable stress $\sigma = 850$ *MPa*, the weight per unit volume $\gamma_c = 0.078$ *MN/m*^{3}, and the Young's modulus E_c=180000 *MPa*. Values of ℓ ranging from 1000 *m* to 3500 *m* were considered, keeping $k = 0.1$. The cable cross-section was designed by using the previous relation. Then the analysis of the stiffened cable was carried out for different values of the girder bending stiffness. The tension H and then the equilibrium configuration of the suspension bridge were found by using an

iteration procedure, that leads to the same results, i.e. with the same approximation, of the deflection theory (Nicolosi et al. 1998).
In Fig. 2 the diagrams of the maximum vertical displacement v versus ℓ, for different values of the girder bending stiffness EI [$MN*m^2$], are plotted. In the case of $EI = 0$ the displacement v increases up to its maximum value at $\ell = 2800$ m, this span value being related to the length of load p_2 (750 m). For $\ell > 2800$ m the vertical displacement v decreases. This maximum is reached for higher values of the span when the girder stiffness gets higher. The curves tend to be closer to each other when the span increases, i.e., the vertical displacement is independent of the girder stiffness when ℓ becomes very high. This behaviour is due to the increase of w_c. In fact, when the span gets higher w_c gets higher too, and a large percentage of the cable capacity is required to carry its own self-weight. Stresses in the cable due to live load are very low and so are the displacements. As obvious, for usual spans a noticeable reduction of the displacement is obtained if the girder bending stiffness is high. The maximum displacement occurs always at 0.27 ℓ. The corresponding horizontal tension H, obtained with the same load condition is also plotted in Fig. 2 (dashed line). It is only slightly lower than the maximum value of the horizontal component of the cable tension (continuous line), which occurs when p_2 is placed symmetrically around mid-span. The girder stiffness has no significant influence on the maximum tension. Therefore the values of the diagram are relative to the unstiffened cable ($EI = 0$).

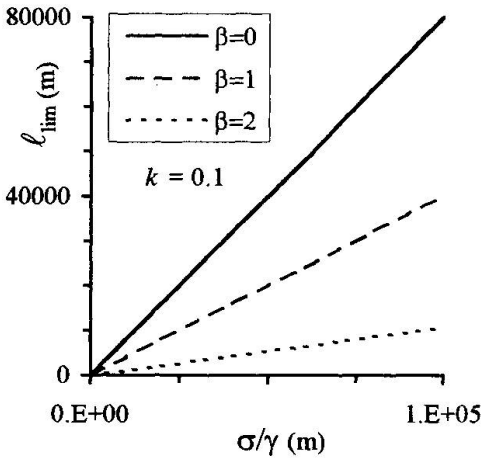

Fig. 1 Limit span versus σ/γ

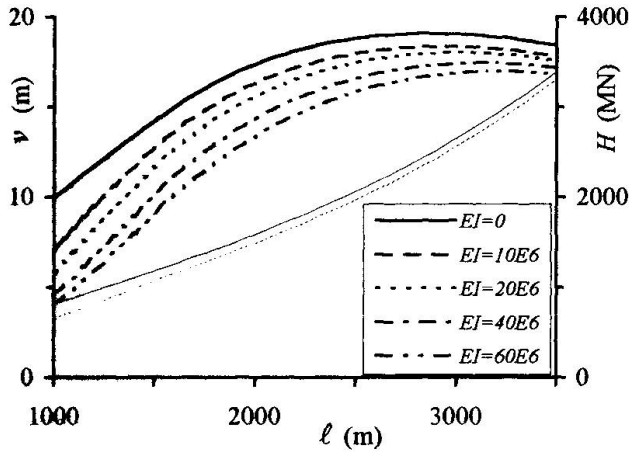

Fig. 2 Maximum displacement and horizontal tension versus ℓ

2. Conclusions

In very long-span suspension bridges the contribution of the stiffening girder is negligible and the structure behaves like an unstiffened cable. The limit span of a suspension bridge is obviously related to the material characteristics. The numerical results shown in this paper are relative to steel cables, but they can be easily generalised to other materials. Materials, characterised by low values of σ/γ_c, represent the future of the long-span structures, but they are too expensive at the present time. In particular, carbon fibre composite cables seem to be very good because of their high strength and their very low unit weight, but may have a lower Young's modulus. The aerodynamic behaviour of light cables is also to be investigated. Use of new structural types is advisable in order to span longer distances in the future.

References

Nicolosi G., Raithel A. and Clemente P. (1998). "Structural behaviour of very-long span suspension bridges." *To be published.*

Ultimate Behavior and Strength of Long-Span Suspension Bridges

Xu XIE
Research Assoc.
Saitama Univ.
Urawa, Japan

Hiroki YAMAGUCHI
Prof.
Saitama Univ.
Urawa, Japan

Masatsugu NAGAI
Prof.
Nagaoka Univ. of Technology
Nagaoka, Japan

Summary

This paper presents elasto-plastic finite displacement analysis of long span suspension bridges, in which inelastic behavior of main cables is taken into account. In this analysis, inelastic behavior of all the members such as girder, towers, main cables and hangers are taken into account simultaneously. A 3000-meter suspension bridge model is employed and the effect of the safety factor for the main cables on the elasto-plastic behavior of the bridge is studied.

1. Introduction

In recent years, various types of suspension bridges with main span of around 3000 meters have been studied by many researchers. The main aim of these researches is to develop economical systems that ensure the safety against flutter instability. However, static ultimate strength of long-span suspension bridges has not been made clear. In this paper, 3-D elasto-plastic large displacement analysis is carried out to investigate the ultimate strength of long-span suspension bridges. Especially, the effect of the safety factor for main cables on the ultimate behavior and strength is studied.

2. Bridge model and load case

In this study, a 3000-meter suspension bridge is dealt with. Fig.1 shows a side-view of the bridge and a front-view of the tower. Preliminary designed cross-sectional properties of the model are listed in Table 1. The area of the main cable and hangers are determined based on the criteria $\sigma_D + \sigma_L < \sigma_u/\gamma$, where σ_D, σ_L and σ_u are the stress caused by dead load, that by live load and ultimate stress, respectively. The safety factor γ of hanger is assumed to be 2.5. The safety factor of the main cable is taken as a parameter, and is varied from 1.8 to 2.0. On the other hand, we assume that the girder and the tower are made of elastic perfect-plastic material, and the cables are made of the material with bilinear constitutive relation. The yield point of the girder and the tower is 235 200KN/m^2 and 450 800KN/m^2, respectively. The yield point and ultimate stress of the main cable are 1.372×10^6KN/m^2 and 1.6464×10^6KN/m^2. Those of the hanger are 1.1662×10^6KN/m^2 and 1.421×10^6KN/m^2. In this study, the distributed load αw_G applied to the girder is considered. Where, α means the ratio of the vertical load to the dead load w_G of the girder. In the initial state, α is zero.

3. Results and discussions

Figs.2 to 5 show the horizontal displacement at the top of the tower, the bending moment at the bottom of the tower and bending moment at the girder where initial yielding in the cross-section occurred. It can been seen that, the displacement and the bending moment of the tower depends on the stiffness of the main cable. However, the behavior of the girder is nearly the same. When the stress of the hangers reaches the yield point, the deflection and the bending moment of the girder increase rapidly regardless of the safety factor. The load, which causes the initial yield in the hanger, is smaller than that in the main cable, even though the safety factor of the hanger is lager than that of the main cable. On the other hand, when the load coefficient reaches 1.95, the tension of partial hanger elements increased up to ultimate strength.

Table 1 Cross-sectional properties of the girder (Unit: m, m^2 or m^4)

Member	Cross-sectional area	In-plane moment of inertia of area	Out-of-plane moment of inertia of area	St. Venante torsion constant
Girder	1.4912	14.547	181.55	26.503
Tower	3.9360-8.2960	48.791-105.87	59.549-264.74	52.998-151.83
Main cable and Hanger	1.019-1.232 m^2 /(one main cable), 0.01164 m^2 /(one hanger)			

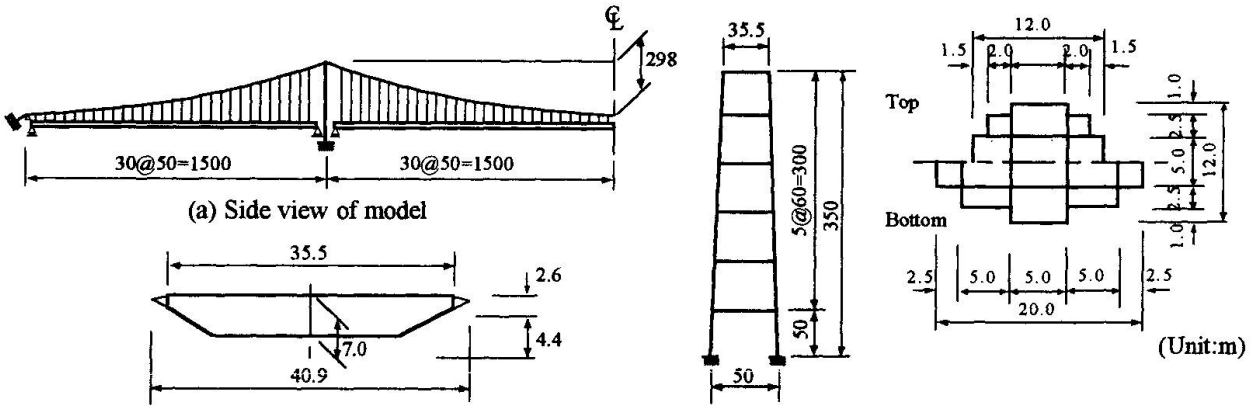

(a) Side view of model

(b) Cross section of the girder

(c) Front view of the tower

(d) Cross section of the tower

Fig.1 Model of suspension bridge

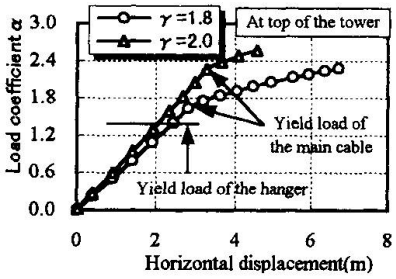

Fig.2 Horizontal displacement of the tower

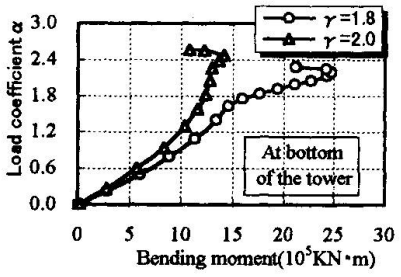

Fig.3 Bending moment of the tower

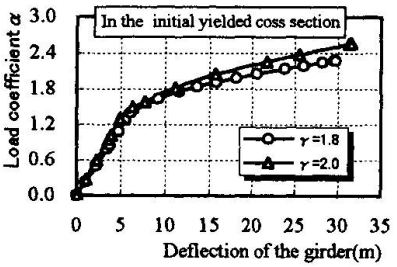

Fig.4 Deflection of the girder

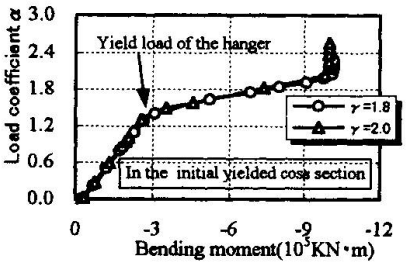

Fig.5 Bending moment of the girder

4. Concluding remarks

In this paper, the effect of the safety factor for the main cable on ultimate behavior is investigated. The main results obtained from this study are summarized as follows.

1) The ultimate behavior of the tower depends on the factor of safety of the main cable. When the yield occurs in the main cable, the stiffness becomes to be flexible. However, the effect of the safety factor of the main cable is not remarkable for the ultimate behavior of the girder. The displacement and bending moment increase when the stress of the hanger comes into yield range.

2) In this case, even the factor of safety of the hanger is larger than that of main cables, but earlier yield phenomenon occurred in the hanger.

3) From this study, it can be seen that the effect of the main cable is important for analysis of the tower.

Design of the Road/Railway Bridge across the Oeresund

Anton PETERSEN
Technical Mgr, Bridges
COWI
Lyngby, Denmark

Lars HAUGE
Chief Engineer, Bridges
COWI
Lyngby, Denmark

Summery

The 7,7 km long Øresund Bridge is the major part of the Øresund link between Denmark and Sweden. The bridge is designed with a two level girder for combined road and railway traffic. The span lengths vary from 120m to 140m for the approach bridges to 490m for the cable-stayed part which crosses the navigation channel. This poster focuses on three main features in the detailed design.

1 Pylon foundation

The 203.5m high pylons for the cable-stayed bridge are placed close to the navigation channel, and thus the design of the lower part of the pylons and the caissons has been governed by ship impact. The design requirements describe two types of ship impact: Sideways collision and HOB (Head on Bow) collision. For both types the impact load corresponds to a 295m ship in ballast (85000 tonnes displacement). The corresponding max. impact forces are 560 MN and 438 MN, respectively. For the pylon caissons the dimensions were governed by sideways collision.

The analysis has been carried out as a linear elastic time history analysis on the Global IBDAS model which is also used for the overall design of the bridge. In the chart below the variation of the shear force in the bottom of the caisson together with the applied ship impact force are shown. The dynamic amplification is found to be 1.16. The bearing and displacement capacities were verified by quasi push-over analysis using a 2-D elasto-plastic finite element model.

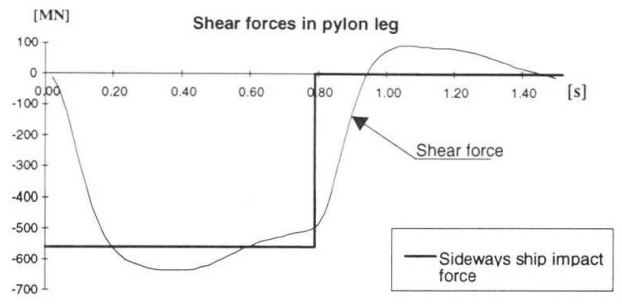

Fig. 1 : Dynamic shear force at level -17 m.

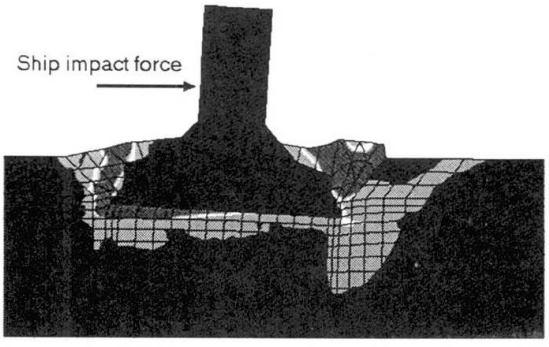

Fig. 2 : Plastic zone development

2 Corrosion protection

The maintenance strategy for the bridge is based on more than 100 years of operation with maintenance costs as low as possible. Therefore, the layout of the truss girders has been based on closed box sections with smooth external surfaces suitable for painting and future maintenance. They will be protected by a 390 microns dry film thickness epoxy based paint system. All internal surfaces will stay unpainted, and the corrosion protection will be based on dehumidification of the inside air by circulating dry air inside the box elements. The dehumidification units for the approach bridges will be placed in the cross beams, and inside the box girder for the railway at the cable-stayed bridge. With dehumidification an environmental friendly and overall cost saving system has been achieved taking in mind that the internal steel area is approx. 490,000 m^2 compared to a 300,000 m^2 external painted area. The principle for dehumidification of the truss girders is shown in fig 3.

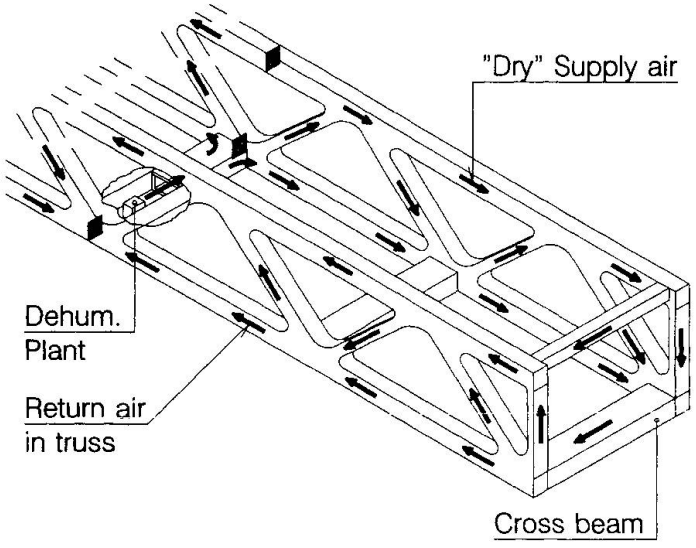

Fig. 3: Dehumidification system

3 High Strength Steel

High strength steel has been used extensively for the two level composite truss girders. In the 6,7 km long approach bridges the railway is carried by concrete troughs, spanning 20m between steel cross beams. The design of the 1,5m high and 2,5m wide cross beams is governed by fatigue, and steel grade S355N (EN10113-2) was found to be most favourable for the cross beams. For the truss girders the design was governed either by the Ultimate or the Accidental Limit State (ULS/ALS). By substituting the traditional grade S355N steel by steel grade S460M (EN10113-3) it was possible to reduce the amount of steel by approx. 15 percent for the approach bridges. For the cable-stayed bridge Steel Grade S420M has been used for the main part of the structure. For the heavy, compact and very stiff Øresund bridge girder the application of high strength steel has shown to be cost-effective.

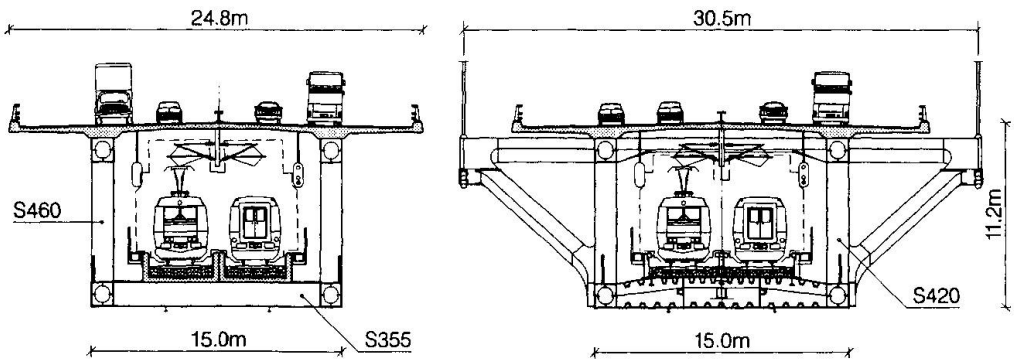

Fig. 4: Cross section of approach and high bridge, respectively